METHODS IN MOLECULAR BIOLOGY™

Series Editor
John M. Walker
School of Life Sciences
University of Hertfordshire
Hatfield, Hertfordshire, AL10 9AB, UK

For other titles published in this series, go to
www.springer.com/series/7651

Cell-Based Microarrays

Methods and Protocols

Edited by

Ella Palmer

Quantitative Systems Biology, Faculty of Medicine,
MRC Clinical Sciences Centre, Imperial College London,
London, UK

Humana Press

Editor
Ella Palmer
Quantitative Systems Biology
Faculty of Medicine
MRC Clinical Sciences Centre
Imperial College London
Du Cane Road
W12 ONN London
Hammersmith Hospital Campus
London, UK
e.l.palmer.01@cantab.net

ISSN 1064-3745 e-ISSN 1940-6029
ISBN 978-1-61737-969-7 e-ISBN 978-1-61737-970-3
DOI 10.1007/978-1-61737-970-3
Springer New York Dordrecht Heidelberg London

Printed on acid-free paper

Humana Press is part of Springer Science+Business Media (www.springer.com)

Preface

Cell-based microarrays are a technique first described by the Sabatini group in 2001. They detail the printing of cDNA or siRNAs in a vector construct onto a coated glass slide using a robotic microarrayer. The vector constructs are transfected in defined areas within cells grown over the surface of the slide or microplate. These cell-based microarrays can be used for a variety of high-throughput, downstream functional assays.

Since their development in 2001, they have advanced significantly, and this book, intended for molecular biologists, geneticists, immunologists, and biochemists, covers many aspects of their evolution.

Chapter 1 gives a detailed overview of the whole subject area, including a discussion of the first paper describing the technique and detailed descriptions of the current work in overexpression, RNAi, antibody, and small-molecule cell-based microarrays. The overview also covers the adaptation of cell-based microarrays for a variety of cell types, advances in array surface chemistry and transfection efficiencies, and imaging of cell-based microarrays.

Chapters 2, **3**, **4**, **5**, and **6** describe protocols for overexpression arrays and downstream functional assays. In **Chapters 2** and **3**, Lai et al. and Palmer et al. provide clear protocols for array printing and transfection with standard HEK23T cells. In **Chapter 4**, Redmond et al. describe the use of a novel fluorescent reporter, and in **Chapters 5** and **6**, Hu et al. provide a protocol for high-throughput sub-cellular localization, and Erfle et al. include a protocol for high-throughput organelle imaging.

In **Chapter 7**, Niu et al. provide a protocol for a different cell type to standard mammalian cells: yeast cells (also see **Chapter 11** for blood cells).

Chapter 8 discusses a protocol for shRNAs using adenoviruses, and, in **Chapters 8** and **9**, Konrad et al. and Volkmer et al. both discuss the protocols for infectious disease research.

In **Chapters 10** and **11**, Lin et al. and Roupioz et al. provide protocols for antibody arrays and describe their use with different cell types such as blood.

Chapters 12, **13**, **14**, and **15** discuss protocols for increasing transfection efficiencies on cell-based microarrays. Yamaguchi et al and Hook et al, in **Chapters 12** and **13**, provide protocols for different slide coatings (also discussed in **Chapter 8**). Pernagallo et al., in **Chapter 14**, discuss the use of polymer arrays for functional tissue modelling, and Kato et al., in **Chapter 15**, discuss the use of electroporation to increase transfection efficiency.

In **Chapter 16**, Damoiseaux et al. provide a protocol discussing the development of cell-based array technology by use of microfluidic image cytometry for the analysis of small diagnostic samples with few cells.

Together, the chapters provide an easy-to-use, up-to-date, and comprehensive set of protocols on every aspect of cell-based microarrays.

Ella Palmer

Contents

Preface . . . . . *v*

Contributors . . . . . *ix*

1. Cell-Based Microarrays: Overview 1
Ella Palmer

2. Cell-Based Co-transfection Microarrays for Use with HEK293T Cells on a Poly D-Lysine-Coated Polystyrene Microplate 13
Meenal Soni and Fang Lai

3. Large-Scale Cell-Based Microarrays and Their Use with HEK293T Cells and Downstream Apoptotic Assays 27
Ella Palmer and Tom C. Freeman

4. A Novel Fluorescent Transcriptional Reporter for Cell-Based Microarray Assays 41
Tanya M. Redmond and Michael D. Uhler

5. High-Throughput Subcellular Protein Localization Using Transfected-Cell Arrays 53
Yuhui Hu and Michal Janitz

6. Cell Arrays for the Measurement of Organelle Dynamics in Living Cells 73
Holger Erfle, Tautvydas Lisauskas, Christoph Claas, Jürgen Reymann, and Vytaute Starkuviene

7. High-Throughput Immunofluorescence Microscopy Using Yeast Spheroplast Cell-Based Microarrays 83
Wei Niu, G. Traver Hart, and Edward M. Marcotte

8. Cell-Based Microarrays of Infectious Adenovirus Encoding Short Hairpin RNA (shRNA) 97
Hansjürgen Volkmer and Frank Weise

9. Reverse Transfected Cell Microarrays in Infectious Disease Research 107
Andreas Konrad, Ramona Jochmann, Elisabeth Kuhn, Elisabeth Naschberger, Priya Chudasama, and Michael Stürzl

10. Transfected Cell Microarrays for the Expression of Membrane-Displayed Single-Chain Antibodies 119
Baochuan Lin and James B. Delehanty

11. Blood Cell Capture on Antibody Microarrays and Monitoring of the Cell Capture Using Surface Plasmon Resonance Imaging 139
Yoann Roupioz, Sarah Milgram, André Roget, and Thierry Livache

12. Immobilized Culture and Transfection Microarray of Non-adherent Cells 151
Satoshi Yamaguchi, Erika Matsunuma, and Teruyuki Nagamune

13. Plasma Polymer and PEG-Based Coatings for DNA, Protein and Cell Microarrays 159
Andrew L. Hook, Nicolas H. Voelcker, and Helmut Thissen

14. Polymer Microarrays for Cellular High-Content Screening 171
Salvatore Pernagallo and Juan J. Diaz-Mochon

15. High-Throughput Analyses of Gene Functions on a Cell Chip by Electroporation 181
Koichi Kato and Hiroo Iwata

16. Microfluidic Image Cytometry 191
Ken-ichiro Kamei, Jing Sun, Hsian-Rong Tseng, and Robert Damoiseaux

Subject Index 207

Contributors

PRIYA CHUDASAMA • *Division of Molecular and Experimental Surgery, Department of Surgery, University Medical Center Erlangen, Erlangen, Germany*

CHRISTOPH CLAAS • *BioQuant, University of Heidelberg, Heidelberg, Germany*

ROBERT DAMOISEAUX • *Molecular Screening Shared Resource, David Geffen School of Medicine, University of California, Los Angeles, CA, USA*

JAMES B. DELEHANTY • *United States Naval Research Laboratory, Center for Bio/Molecular Science and Engineering, Washington, DC, USA*

JUAN J. DIAZ-MOCHON • *School of Chemistry, University of Edinburgh, Edinburgh, UK*

HOLGER ERFLE • *BioQuant, University of Heidelberg, Heidelberg, Germany*

TOM C. FREEMAN • *Division of Genetics and Genomics, University of Edinburgh, Roslin BioCentre, Midlothian, UK*

G. TRAVER HART • *Department of Chemistry and Biochemistry, Center for Systems and Synthetic Biology, Institute for Cellular and Molecular Biology, University of Texas at Austin, Austin, TX, USA*

ANDREW L. HOOK • *Laboratory of Biophysics and Surface Analysis, University of Nottingham, Nottingham, UK*

YUHUI HU • *The Berlin Institute for Medical Systems Biology, Max Delbrück Center for Molecular Medicine (MDC), Berlin-Buch, Germany*

HIROO IWATA • *Institute for Frontier Medical Sciences, Kyoto University, Kyoto, Japan*

MICHAL JANITZ • *School of Biotechnology and Biomolecular Sciences, University of New South Wales, Sydney NSW, Australia*

RAMONA JOCHMANN • *Division of Molecular and Experimental Surgery, Department of Surgery, University Medical Center Erlangen, Erlangen, Germany*

KEN-ICHIRO KAMEI • *Department of Molecular & Medical Pharmacology, David Geffen School of Medicine, University of California, Los Angeles, CA, USA*

KOICHI KATO • *Institute for Frontier Medical Sciences, Kyoto University, Kyoto, Japan*

ANDREAS KONRAD • *Division of Molecular and Experimental Surgery, Department of Surgery, University Medical Center Erlangen, Erlangen, Germany*

ELISABETH KUHN • *Division of Molecular and Experimental Surgery, Department of Surgery, University Medical Center Erlangen, Erlangen, Germany*

FANG LAI • *Science and Technology Division Corning Inc, Corning, NY, USA*

BAOCHUAN LIN • *United States Naval Research Laboratory, Center for Bio/Molecular Science and Engineering, Washington, DC, USA*

TAUTVYDAS LISAUSKAS • *BioQuant, University of Heidelberg, Heidelberg, Germany*

THIERRY LIVACHE • *CREAB Group, SPrAM-UMR 5819 (CEA-CNRS-UJF), INAC/CEA-Grenoble, Grenoble, France*

EDWARD M. MARCOTTE • *Department of Chemistry and Biochemistry, Center for Systems and Synthetic Biology, Institute for Cellular and Molecular Biology, University of Texas at Austin, Austin, TX, USA*

ERIKA MATSUNUMA • *Department of Chemistry and Biotechnology, Graduate School of Engineering, The University of Tokyo, Tokyo, Japan*

Sarah Milgram • *CREAB Group, SPrAM-UMR 5819 (CEA-CNRS-UJF), INAC/CEA-Grenoble, Grenoble, France*
Teruyuki Nagamune • *Departments of Chemistry & Biotechnology and Bioengineering, Graduate School of Engineering, and Center for NanoBio Integration (CNBI), The University of Tokyo, Tokyo, Japan*
Elisabeth Naschberger • *Division of Molecular and Experimental Surgery, Department of Surgery, University Medical Center Erlangen, Erlangen, Germany*
Wei Niu • *Department of Genetics, Yale University, New Haven, CT, USA*
Ella Palmer • *Clinical Sciences Centre, Hammersmith Hospital, London, UK*
Salvatore Pernagallo • *School of Chemistry, University of Edinburgh, Edinburgh, UK*
Tanya M. Redmond • *Molecular, Behavioral Neuroscience Institute, University of Michigan, Ann Arbor, MI, USA*
Jürgen Reymann • *BioQuant, University of Heidelberg, Heidelberg, Germany*
André Roget • *CREAB Group, SPrAM-UMR 5819 (CEA-CNRS-UJF), INAC/CEA-Grenoble, Grenoble, France*
Yoann Roupioz • *CREAB Group, SPrAM-UMR 5819 (CEA-CNRS-UJF), INAC/CEA-Grenoble, Grenoble, France*
Meenal Soni • *Science and Technology Division Corning Inc., Corning, NY, USA*
Vytaute Starkuviene • *BioQuant, University of Heidelberg, Heidelberg, Germany*
Michael Stürzl • *Division of Molecular and Experimental Surgery, Department of Surgery, University Medical Center Erlangen, Erlangen, Germany*
Jing Sun • *Department of Molecular & Medical Pharmacology, David Geffen School of Medicine, University of California, Los Angeles, CA, USA*
Helmut Thissen • *CSIRO Molecular and Health Technologies, Clayton, VIC, Australia*
Hsian-Rong Tseng • *Department of Molecular & Medical Pharmacology, David Geffen School of Medicine, University of California, Los Angeles, CA, USA*
Michael D. Uhler • *Molecular, Behavioral Neuroscience Institute, University of Michigan, Ann Arbor, MI, USA*
Nicolas H. Voelcker • *Flinders University, Bedford Park, SA, Australia*
Hansjürgen Volkmer • *Natural and Medical Sciences Institute, University of Tübingen, Reutlingen, Germany*
Frank Weise • *Natural and Medical Sciences Institute, University of Tübingen, Reutlingen, Germany*
Satoshi Yamaguchi • *Department of Chemistry and Biotechnology, Graduate School of Engineering, The University of Tokyo, Tokyo, Japan*

Chapter 1

Cell-Based Microarrays: Overview

Ella Palmer

Abstract

Cell-based microarrays were first described by Ziauddin and Sabatini in 2001 as a novel method for performing high-throughput screens of gene function. They reported a technique whereby expression vectors containing the open reading frame (ORF) of human genes were printed onto glass microscope slides to form a microarray. Transfection reagents were added pre- or post-spotting and cells grown over the surface of the array. They demonstrated that cells growing in the immediate vicinity of the expression vectors underwent 'reverse transfection' and that subsequent alterations in cell function could then be detected by secondary assays performed on the array. Subsequent publications have adapted the technique to a variety of applications and have also shown that the approach works when arrays are fabricated using siRNAs and compounds. The potential of this method for performing analyses of gene function and identification of novel therapeutic agents has now been clearly demonstrated. Current efforts are focused on improving and harnessing this technology for high-throughput screening applications.

Key words: Cell-based microarray, reverse transfection, RNAi, siRNA.

1. Introduction

The utility of the microarray format was first effectively demonstrated for gene expression profiling (1, 2). The availability of whole genome sequences, a growing catalogue of genes, better equipment, resources and the increased analytical power of bioinformatic tools, has fuelled the development and application of microarrays for gene expression analysis. As a result, high-throughput, semi-quantitative analyses of gene expression using this platform are now routine in many laboratories. The desirable characteristics of the microarray format platform also led to a diversification in the use of microarray technology in areas other than the study of gene expression. Over the last years, many variations of the microarray format have evolved, including arrays for performing comparative genomic hybridisations (3, 4),

E. Palmer (ed.), *Cell-Based Microarrays*, Methods in Molecular Biology 706,
DOI 10.1007/978-1-61737-970-3_1,

genotyping (5, 6) and DNA methylation (7), as well as for detecting DNA–protein (8), protein–protein (9, 10), carbohydrate–protein (11) and receptor–ligand interactions (12). Also in the last few years, extensive collections of full-length cDNA resources have been created for key model species such as C. elegans (13) and D. melanogaster (14) and genome-wide clone sets are also comprehensive for human and mouse (16–18). Likewise, genome-wide RNAi reagents are also available for a range of species (19–21), paving the way for cell-based microarray technology. *See* **Fig. 1.1** for an overview of the cell-based transfection methodology.

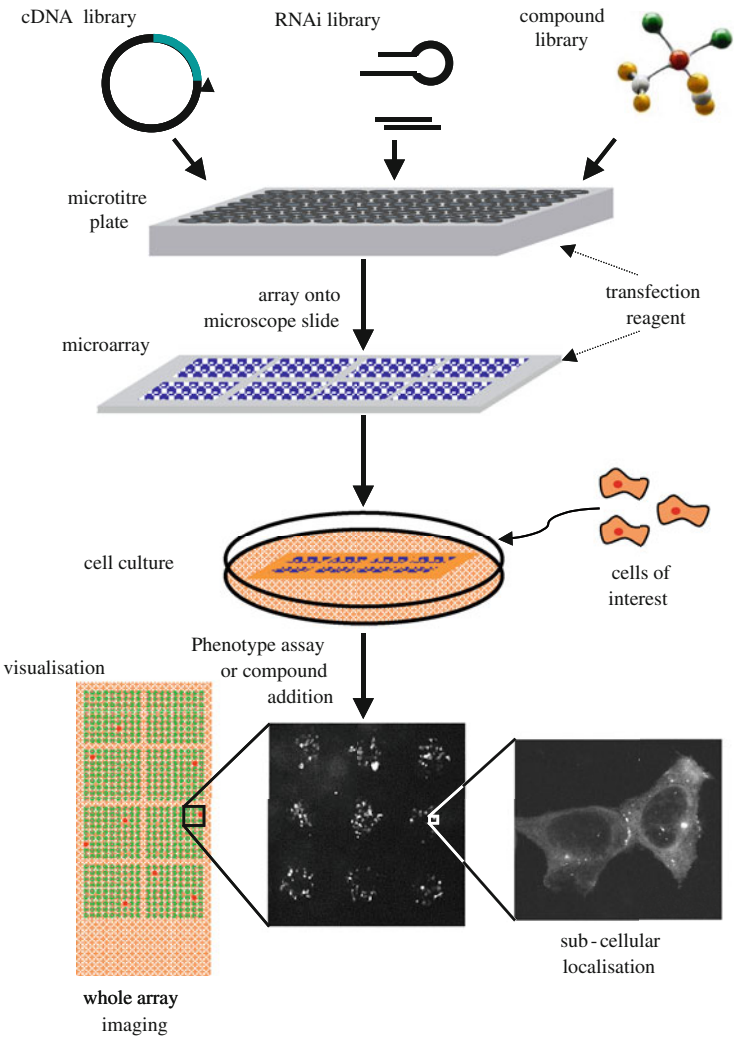

Fig. 1.1. Cell-based microarray methodology. Plasmids are prepared from cDNA or RNAi clone expression libraries, alternatively compound libraries can be used directly. Transfection reagent used to transport DNA/RNA into the cell can be either added directly to the plates prior to printing or used to treat the array just prior to cell culture. For compound screening, a surface chemistry must be used that is compatible with the retention and controlled release of the compounds. After printing, microarrays are cultured with cells until a confluent monolayer covers the surface of the slide. If reagents are tagged, transfection events can be visualised at the slide or cellular level, or the cells stained to detect cells with altered phenotype.

2. Developments in Cell-Based Microarrays

2.1. Contents and Conclusions of the First Cell-Based Microarray Paper

The first paper describing cell-based microarrays powerfully illustrated the salient features of the technology (22). In initial studies, the Sabatini group printed 192 genes in a V5-epitope-tagged expression vector. The arrays were probed with Cy3-labelled anti-V5 antibody as a transfection control and then with Cy3-labelled anti-phosphotyrosine antibody. Six genes were found to have increased phosphotyrosine activity, five of which were known tyrosine kinase proteins and the sixth gene encoded a protein of unknown function. The cells were also observed for abnormal morphologies, the apoptosis-inducing protein, TNFRSF10B was associated with cells that appeared fragmented and was positive for the TdT-mediated dUTP nick-end labelling reaction. As well, cells growing over the cell surface protein CD36, were found to be in close contact. Sub-cellular localisation studies were also performed on the arrays, many matched localisations that had already been described for the proteins and sub-cellular localisations were also demonstrated for proteins that had not been studied previously. The authors concluded that the advantages of the cell-based microarray technology were that the proteins were translated within the environment of a mammalian cell and were therefore likely to fold correctly and undergo molecular interactions similar to the native protein. Furthermore, the assays were quick compared to other over-expression strategies; the signal was concentrated in small well-defined areas and the arrays could be used to screen live cells. Finally, the arrays were compact, easy to handle, economical and in principle the entire set of human genes could be printed on a small number of slides.

2.2. Downstream Functional Assay-Based Microarrays

2.2.1. Over-Expression Cell-Based Microarrays

Over-expression arrays of cDNAs expressing the gene of choice, as published by the Sabatini group, were the first format of cell-based microarrays, prior to the development of RNAi, and a number of groups still use arrays in this format for functional studies.

In initial studies, Webb et al. co-transfected expression vectors containing the serum response element (SRE) reporter (which activates MAPK and JNK pathways) coupled to GFP with five known upstream activators of SRE. Each of the five SRE activators generated patches of cells with a significantly higher GFP signal than the control vector demonstrating that members of

signalling pathway initiation can be determined using cell-based transfection microarrays (23). Mishina et al. demonstrated that cell-based transfection arrays could be used to identify novel therapeutic targets. G-protein coupled receptors (GPCRs) have a role in mediating signalling in cellular metabolism and are therefore prime candidates for drug targets. Nine hundred GPCRs were printed onto a 96-well plate. GPCR agonists and a fluorescent calcium indicator dye were added and 15 positive interactions were discovered (24). In studies using the cAMP-response element (CRE) activated by cAMP-dependent protein kinase (PKA) coupled to GFP, GFP levels were also used to detect genes important in activating this pathway (25).

Since the initial studies, Yamauchi et al., using the vascular endothelial growth factor receptor (FLK1) promoter attached to GFP on mouse embryonic stem cells lines and expressing a combination of transcription factors relevant to differentiation, demonstrated that the level of GFP was an indicator of differentiation, and they discovered a number of potent activators of differentiation (26). Hu et al. have undertaken a high-throughput screen of the sub-cellular localisation of genes on chromosome 21 using organelle markers (27).

Various studies on apoptosis have been undertaken; Ziauddin and Sabatini used a nick-mediated TUNEL assay to identify any pro-apoptotic effects of over-expression (22), and in a study by Palmer et al., TUNEL and caspase 3 assays were used to determine pro-apoptotic genes (28); Mannherz et al. also undertook a screen for pro-apoptotic genes using EYFP attached to the genes as a readout for apoptotic bodies (29).

2.2.2. RNAi Cell-Based Microarrays

RNA interference (RNAi) is an enormously powerful tool for investigating gene function. The process was first discovered in *Caenorhabditis elegans* (30); it was demonstrated that double stranded RNA (dsRNA) can direct the silencing of gene targets in a sequence-specific manner. In invertebrates such as *C. elegans* and *Drosophila melanogaster* (31), when long dsRNA is introduced into their cells it is processed by a dsRNA-specific endonuclease, Dicer (32), into short interfering RNAs (siRNAs) 21–24 nucleotides in length. siRNAs are then incorporated into an RNA-induced silencing complex (RISC) which cleaves mRNAs homologous to the dsRNA originally introduced (33, 34). In mammalian cells, dsRNAs longer than 30 bp trigger the antiviral/interferon pathways, which result in global shutdown of protein synthesis (35). RNAi-mediated gene silencing is however possible in mammalian cells either by delivery of chemically synthesised short (less than 30 bp) double stranded siRNA molecules (36) or by expression of short hairpin RNAs (shRNAs) bearing fold-back stem–loop structures (37).

In initial studies on Drosophila cells, Sabatini's group developed a prototype microarray with 384 different dsRNAs against the majority of tyrosine kinases annotated in the *D. melanogaster* genome and all predicted serine/threonine protein phosphatases. The nucleus and actin were stained and the arrays scanned using automated microscopy and image analysis software, which quantified the number and size of nuclei in cells growing over each dsRNA spot. Forty-four RNAis were identified that resulted in features with at least two standard deviations below the mean number of nuclei as compared to control dsRNA. These, therefore, represented genes likely to be essential for normal cell proliferation, survival or adhesion. The group also found that it was possible to knockdown two genes simultaneously, which opened up the possibility of performing large-scale screens for synthetic or epistatic genetic relationships (38).

Since then, several groups have described RNAi studies in mammalian cells coupled with cell-based microarray technology. A commonly used positive control is to co-transfect GFP expression vectors with vectors containing siRNAs or shRNAs targeting GFP and demonstrate decreased GFP expression (39, 40). Silva et al. printed an array of eight different shRNAs to EG5, a gene involved in spindle formation. Using cells expressing a tubulin–GFP fusion protein, they were able to show that cells growing over two of the shRNAs had spindle defects (41). Erfle et al. optimised a two-step procedure, where the transfection reagent and siRNA are mixed before being printed onto the array. They used siRNAs to knockdown the expression of three genes in the secretory pathway, *COP1*, *GM130* and *Sec31*, and also used a marker assay to show that the *COP1* gene was dysfunctional (42). A further group developed a cell-based array system for screening RNAi reagents, as not all siRNAs/shRNAs selected for targeting a gene result in efficient gene silencing. They printed MyoD, Lamin A/C and P53 siRNAs, and shRNAs onto a slide and then added cells plus expression vectors containing the target gene attached to GFP for visualisation. They were able to gauge the efficacy with which the siRNA and shRNA knocked down the target gene by measuring the levels of GFP fluorescence (43).

More recently, with the availability of genome-wide RNAi reagents for a range of species (19–21), a number of groups have reported high-throughput RNAi screens using cell-based micorarrays.

Neumann et al. in studies led by Pepperkok, developed an array-automated platform for high-content RNAi screening using time-lapse fluorescence microscopy of live HeLa cells expressing histone–GFP to determine chromosome segregation and structure using siRNA (44–46). More recently, Walter et al. have

described a high-throughput RNAi screen of chromosome phenotypes (47).

2.2.3. Antibody Cell-Based Microarrays

A variation on the theme of over-expression arrays was the development of antibody cell-based microarrays. The potential to screen single-chain antibody fragments using cell-based microarrays was first demonstrated by Delehanty et al. They expressed a wild-type fluorescein antibody fragment and three mutants on HEK293T cell membranes on a cell-based microarray and demonstrated that fluorescein had a higher affinity for the wild-type fluorescein antibody fragment than the antibody mutants (48). Suranati et al. and Roupioz et al. have demonstrated the use of antibody arrays for the detection of blood cells, in particular lymphocytes on cell-based micorarrays (49, 50).

2.2.4. Drug Screening on Cell-Based Microarrays

The groups of Sabatini and Stockwell have explored the possibility of combining RNAi and compound screens on cell-based microarrays. To facilitate the retention and slow diffusion of arrayed compounds, they first printed discs of a polymer matrix onto the slide. They then printed 70 known active compounds in triplicate at three concentrations on top of the polymer discs. Seven siRNAs that knocked down proteins involved in cell death, P53, PTEN, MDM2, EGFR, TSC2, BCL2 and BRCA1 were transfected into the cells growing over the bioactive compounds. Clusters of cells associated with three of the compounds were observed to change in density, indicating that the drugs were counteracting the effect of the genes that had been knocked down (51).

2.3. Adaptation of Cell-Based Microarrays for a Variety of Cell Types

The initial studies on cell-based microarrays were carried out in HEK293T cells, as they are an easy to transfect cell line. However, the Sabatini group sought to circumvent this issue by printing lentiviruses onto arrays. Lentiviruses have a high take-up rate in a variety of cells including primary cells, and the group showed that lentiviruses pseudotyped as vesicular stomatitis virus glycoprotein were taken up by primary human BJ fibroblasts and primary mouse dendritic cells as well as HeLa, A549, HEK-293T and DU145 cells (52).

Other groups also developed systems for less easy to transfect cells. Oehmig et al. demonstrated the use of adenovirus for cell-based microarrays; the transfection step is not necessary when using adenovirus and this enables less easily transfected cells to take up the gene of interest. The group demonstrated the approach by the transfection of primary human umbilical vein cells (HUVEC) (53).

Narayanaswamy et al. demonstrated the use of cell-based microarrays with yeast cells; they applied 4,800 yeast deletion

strains to arrays to establish genes controlling the response of yeast cells to mating pheromone (54).

Kato et al. coated the surface of a glass culture dish with a cell membrane anchoring reagent, biocompatible anchor for membrane (BAM), with an oleyl chain as a lipid anchor. They demonstrated that non-adherent human erythroleukemic K562 cells and liposomes could attach to the BAM (55, 56). Another approach by Yoshikawa et al. was to use surface-deposited fibronectin on the surface of the microarray, which enhanced transfection efficiency and allowed transfection of primary human mesenchymal stem cells (57).

2.4. Advances in Array Surface Chemistry and Transfection Efficiencies

A number of groups have tried to improve transfection efficiency on cell-based arrays. One group has developed slides with cationic polymers on the surface, so that cells can be added without the need for a transfection reagent (58). A further group developed a surface transfection and expression protocol (STEP) with recombinant proteins designed to enhance transfection when in a complex with expression vector DNAs prior to spotting on glass slides (25). Kato et al., as previously mentioned, coated the surface of a glass culture dish with a biocompatible anchor for membrane (BAM) (59). In a further study by the same group, Kato et al. demonstrated that a liposome:plasmid expressing GFP mix spotted onto the BAM surface was capable of transfecting cells. They showed that an RNAi to GFP caused the knockdown of GFP in a non-adherent K562 cell line stably expressing GFP (60). Delehanty et al. compared glass slides coated with different substrates to determine which gave the best transfection efficiencies. They compared polystyrene, two types of aminosilane coating and two types of polylysine-coated slides. They concluded that spot size was proportional to substrate hydrophobicity, i.e. the polylysine slides were the least hydrophobic and had the largest spot size. However, the transfection rates were highest with the most hydrophobic coating and polystyrene and lowest on the polylysine slides (61). Yamauchi et al. used micro-patterned, self-assembled monolayers (SAM) of alkanethiols formed on a gold-evaporated glass plate for cell-based microarrays. They demonstrated that by repeating layers of plasmid DNA and liposome:plasmid DNA mixes, improved transfection efficiencies could be achieved (62). How et al. have described the efficient formation of complexes between plasmid DNA and dendrimers on cell-based microarrays that transfect efficiently into the cell after the addition of lipoplexes (63). Isalan et al. achieved transfection in a variety of cell lines in a cell-based microarray format using magnetically defined positions and PCR product-coated paramagnetic beads (64). To increase transfection efficiency further, Yamauchi et al. described an electroporation method in which electric pulses were used to detach plasmids from the microarray surface to introduce

them into cells grown on the microarray (65). More recently the Iwata group have developed this method for siRNA (66) and have also prolonged the durability of the electroporation microarrays by adding saccharides to nucleic acids (67).

Another approach by Yoshikawa et al. was to use surface-deposited fibronectin on the surface of the microarray, which enhanced transfection efficiency (57).

Hook et al. described a high-density poly (ethylene glycol) coating on glass slides with phenylazide-modified polymers and irradiation by UV to result in cross-linking of the polymer spots to the surface and printing of plasmids for strong attachment; they demonstrated that this coating provides a very adherent substrate for DNA, protein and cell-based arrays (68).

Pernagallo et al. have investigated the use of polymer arrays which allow non-adherent cell lines to adhere and proliferate; they demonstrated that K562 human erythroleukemic cells, which normally grow in suspension, adhered and proliferated on several different polymers coated on slides for cell-based microarrays (69).

2.5. Imaging of Cell-Based Microarrays

High-throughput imaging systems are necessary to systematically record cell-based microarray readouts for fixed and live imaging, and methods are being developed for cell-based microarrays and the Pepperkok group is the forefront of the development of high-throughput RNAi screens (44–47).

A cell image analysis software called CellProfiler has been developed and is freely available to allow automatic quantitative measurements to be made from thousands of images (70).

3. Conclusions

Cell-based microarrays are very powerful analysis tools. Their utility in exploring gene function through both over- and knock-down expression studies has now been clearly demonstrated due to libraries of siRNA and cDNAs for different organisms becoming comprehensive. Robust methods for attachment of cDNA to glass slides have been implemented, transfection techniques have been improved through electroporation and adeno- and lentivirus work allowing a variety of different types of cells such as non-adherent stem cells to be analysed in a high-throughput fashion. Automated platforms for cell imaging have been developed and image software is freely available. The compact format of cell-based arrays and the ability to carry out thousands of independent assays in parallel with the minimum reagent requirements make the cell-based microarray approach a very attractive proposition where routine high-throughput screening is required.

Acknowledgments

Adapted from Pharmacogenomics (2005), *6*(5), 527–534 with permission of Future Medicine Ltd.

References

1. DeRisi, J., Iyer, V., Brown, P. (1997) Exploring the metabolic and genetic control of gene expression on a genomic scale. *Science 278*, 680–686.
2. Wodicka, L., Dong, H., Mittmann, M., Ho, M., Lockhart, D. (1997) Genome-wide expression monitoring in Saccharomyces cerevisiae. *Nat Biotechnol 15*, 1359–1367.
3. Pinkel, D., Segraves, R., Sudar, D., Clark, S., Poole, I., Kowbel, D., Collins, C., Kuo, W., Chen, C., Zhai, Y., Dairkee, S., et al. (1998) High resolution analysis of DNA copy number variation using comparative genomic hybridization to microarrays. *Nat Genet* 20, 207–211.
4. Pollack, J., Perou, C., Alizadeh, A., Eisen, M., Pergamenschikov, A., Williams, C., Jeffrey, S., Botstein, D., Brown, P. (1999) Genome-wide analysis of DNA copy-number changes using cDNA microarrays. *Nat Genet* 23, 41–46.
5. Hacia, J., Fan, J., Ryder, O., Jin, L., Edgemon, K., Ghandour, G., Mayer, R., Sun, B., Hsie, L., Robbins, C., Brody, L., et al. (1999) Determination of ancestral alleles for human single-nucleotide polymorphisms using high-density oligonucleotide arrays. *Nat Genet* 22, 164–167.
6. Mei, R., Galipeau, P., Prass, C., Berno, A., Ghandour, G., Patil, N., Wolff, R., Chee, M., Reid, B., Lockhart, D. (2000) Genome-wide detection of allelic imbalance using human SNPs and high-density DNA arrays. *Genome Res* 10, 1126–1137.
7. Shi, M. H., Maier, S., Nimmrich, I., Yan, P. S., Caldwell, C. W., Olek, A., Huang, T. H. (2003) Oligonucleotide-based microarray for DNA methylation analysis: principles and applications. *J Cel Biochem* 88, 138–43.
8. Ren, B., Robert, F., Wyrick, J., Aparicio, O., Jennings, E., Simon, I., Zeitlinger, J., Schreiber, J., Hannett, N., Kanin, E. (2000) Genome-wide location and function of DNA binding proteins. *Science* 290, 2306–2309.
9. Pavlickova, P., Schneider, E., Hug, H. (2004) Advances in recombinant antibody microarrays. *Clin Chim Acta* 343, 17–35.
10. Uetz, P. (2001) Two-hybrid arrays. *Curr Opin Chem Biol* 6, 57–62.
11. Fukui, S., Feizi, T., Galustian, C., Lawson, A., Chai, W. (2002) Oligosaccharide microarrays for high-throughput detection and specificity assignments of carbohydrate-protein interactions. *Nat Biotechnol* 20, 1011–1017.
12. MacBeath, G., Koehler, A. N., Schreiber, S. L. (1999) Printing small molecules as microarrays and detecting protein-ligand interactions en masse. *J Am Chem Soc* 121, 7967–7968.
13. Lamesch, P., Milstein, S., Hao, T., Rosenberg, J., Li, N., Sequerra, R., Bosak, S., Doucette-Stamm, L., Vandenhaute, J., Hill, D., Vidal, M. (2004) C. Elegans ORFeome version 3.1: increasing the coverage of ORFeome resources with improved gene predictions. *Genome Res* 14, 2064–2069.
14. Stapleton, M., Carlson, J., Brokstein, P., Yu, C., Champe, M., George, R., Guarin, H., Kronmiller, B., Pacleb, J., Park, S., Wan, K., Rubin, G., Celniker, S. (2002) A drosophila full-length cDNA resource. *Genome Biol* 3, RESEARCH0080.
15. Brizuela, L., Richardson, A., Marsischky, G., Labaer, J. (2002) The FLEXGene repository: exploiting the fruits of the genome projects by creating a needed resource to face the challenges of the post-genomic era. *Arch Med Res* 33, 318–324.
16. Mewes, H., Amid, C., Arnold, R., Frishman, D., Güldener, U., Mannhaupt, G., Münsterkötter, M., Pagel, P., Strack, N., Stümpflen, V., Warfsmann, J., Ruepp, A. (2004) MIPS: analysis and annotation of proteins from whole genomes. *Nucleic Acids Res* 32, D41–D44.
17. Strausberg, R., Feingold, E., Grouse, L., Derge, J., Klausner, R., Collins, F., Wagner, L., Shenmen, C., Schuler, G., Altschul, S., et al. (2002) Generation and initial analysis of more than 15,000 full-length human and mouse cDNA sequences. *Proc Natl Acad Sci USA* 99, 16899–16903.
18. Temple, G., Gerhard, D., Rasooly, R., Feingold, E., Good, P., Robinson, C., Mandich, A., Derge, J., Lewis, J., Shoaf, D., et al. (2009) The completion of the mammalian

gene collection (MGC). *Genome Res* 19, 2324–2333.
19. Berns, K., Hijmans, E., Mullenders, J., Brummelkamp, T., Velds, A., Heimerikx, M., Kerkhoven, R., Madiredjo, M., Nijkamp, W., Weigelt, B., et al. (2004) A large-scale RNAi screen in human cells identifies new components of the p53 pathway. *Nature* 428, 431–437.
20. Kamath, R., Fraser, A., Dong, Y., Poulin, G., Durbin, R., Gotta, M., Kanapin, A., Le Bot, N., Moreno, S., Sohrmann, M., et al. (2003) Systematic functional analysis of the Caenorhabditis elegans genome using RNAi. *Nature* 421, 231–237.
21. Paddison, P. J., Silva, J. M., Conklin, D. S., Schlabach, M., Li, M., Aruleba, S., Balija, V., O'Shaughnessy, A., Gnoj, L., Scobie, K., Chang, K., Westbrook, T., et al. (2004) A resource for large-scale RNA-interference-based screens in mammals. *Nature* 428, 427–431.
22. Ziauddin, J., Sabatini, D. (2001) Microarrays of cells expressing defined cDNAs. *Nature* 411, 107–110.
23. Webb, B., Díaz, B., Martin, G., Lai, F. (2003) A reporter system for reverse transfection cell arrays. *J Biomol Screen* 8, 620–623.
24. Mishina, Y., Wilson, C., Bruett, L., Smith, J., Stoop-Myer, C., Jong, S., Amaral, L., Pedersen, R., Lyman, S., Myer, V., Kreider, B., Thompson, C. (2004) Multiplex GPCR assay in reverse transfection cell microarrays. *J Biomol Screen* 9, 196–207.
25. Redmond, T., Ren, X., Kubish, G., Atkins, S., Low, S., Uhler, M. (2004) Microarray transfection analysis of transcriptional regulation by cAMP-dependent protein kinase. *Mol Cell Proteomics* 3, 770–779.
26. Yamauchi, F., Okada, M., Kato, K., Jakt, L., Iwata, H. (2007) Array-based functional screening for genes that regulate vascular endothelial differentiation of flk1-positive progenitors derived from embryonic stem cells. *Biochim Biophys Acta* 1770, 1085–1097.
27. Hu, Y., Warnatz, H., Vanhecke, D., Wagner, F., Fiebitz, A., Thamm, S., Kahlem, P., Lehrach, H., Yaspo, M., Janitz, M. (2006) Cell array-based intracellular localization screening reveals novel functional features of human chromosome 21 proteins. *BMC Genomics* 7, 155.
28. Palmer, E., Miller, A., Freeman, T. (2006) Identification and characterisation of human apoptosis inducing proteins using cell-based transfection microarrays and expression analysis. *BMC Genomics* 7, 145.
29. Mannherz, O., Mertens, D., Hahn, M., Lichter, P. (2006) Functional screening for proapoptotic genes by reverse transfection cell array technology. *Genomics* 87, 665–672.
30. Fire, A., Xu, S., Montgomery, M. K., Kostas, S. A., Driver, S. E., Mello, C. C. (1998) Potent and specific genetic interference by double-stranded RNA in *caenorhabditis elegans. Nature* 391, 806–811.
31. Elbashir, S. M., Martinez, J., Patkaniowska, A., Lendeckel, W., Tuschl, T. (2001) Functional anatomy of siRNAs for mediating efficient RNAi in *drosophila melanogaster* embryo lysate. *EMBO J* 20, 6877–6888.
32. Hammond, S. M., Bernstein, E., Beach, D., Hannon, G. J. (2000) An RNA-directed nuclease mediates post-transcriptional gene silencing in drosophila cells. *Nature* 404, 293–296.
33. Huppi, K., Martin, S., Caplen, N. (2005) Defining and assaying RNAi in mammalian cells. *Mol Cell* 17, 1–10.
34. Stevenson, M. (2004) Therapeutic potential of RNA interference. *N Engl J Med* 351, 1772–1777.
35. Gil, J., Esteban, M. (2000) Induction of apoptosis by the dsRNA-dependent protein kinase (PKR): mechanism of action. *Apoptosis* 5, 107–114.
36. Elbashir, S. M., Lendeckel, W., Tuschl, T. (2000) RNA interference is mediated by 21- and 22-nucleotide RNAs. *Gen Dev* 15, 188–200.
37. Brummelkamp, T., Bernards, R., Agami, R. (2002) A system for stable expression of short interfering RNAs in mammalian cells. *Science* 296, 550–553.
38. Wheeler, D., Bailey, S., Guertin, D., Carpenter, A., Higgins, C., Sabatini, D. (2004) RNAi living-cell microarrays for loss-of-function screens in drosophila melanogaster cells. *Nat Methods* 1, 127–132.
39. Baghdoyan, S., Roupioz, Y., Pitaval, A., Castel, D., Khomyakova, E., Papine, A., Soussaline, F., Gidrol, X. (2004) Quantitative analysis of highly parallel transfection in cell microarrays. *Nucleic Acids Res* 32, e77.
40. Mousses, S., Caplen, N., Cornelison, R., Weaver, D., Basik, M., Hautaniemi, S., Elkahloun, A., Lotufo, R., Choudary, A., Dougherty, E., et al. (2003) RNAi microarray analysis in cultured mammalian cells. *Genome Res* 13, 2341–2347.
41. Silva, J., Mizuno, H., Brady, A., Lucito, R., Hannon, G. (2004) RNA interference microarrays: high-throughput loss-of-function genetics in mammalian cells. *Proc Natl Acad Sci USA* 101, 6548–6552.

42. Erfle, H., Simpson, J., Bastiaens, P., Pepperkok, R. (2004) SiRNA cell arrays for high-content screening microscopy. *Biotechniques* 37, 454–458.
43. Kumar, R., Conklin, D., Mittal, V. (2003) High-throughput selection of effective RNAi probes for gene silencing. *Genome Res* 13, 2333–2340.
44. Erfle, H., Neumann, B., Liebel, U., Rogers, P., Held, M., Walter, T., Ellenberg, J., Pepperkok, R. (2007) Reverse transfection on cell arrays for high content screening microscopy. *Nat Protoc* 2, 392–399.
45. Neumann, B., Held, M., Liebel, U., Erfle, H., Rogers, P., Pepperkok, R., Ellenberg, J. (2006) High-throughput RNAi screening by time-lapse imaging of live human cells. *Nat Methods* 3, 385–390.
46. Simpson, J., Cetin, C., Erfle, H., Joggerst, B., Liebel, U., Ellenberg, J., Pepperkok, R. (2007) An RNAi screening platform to identify secretion machinery in mammalian cells. *J Biotechnol* 129, 352–365.
47. Walter, T., Held, M., Neumann, B., Hériché, J., Conrad, C., Pepperkok, R., Ellenberg, J. (2009) Automatic identification and clustering of chromosome phenotypes in a genome wide RNAi screen by time-lapse imaging. *J Struct Biol* 170, 1–9.
48. Delehanty, J., Shaffer, K., Lin, B. (2004) Transfected cell microarrays for the expression of membrane-displayed single-chain antibodies. *Anal Chem* 76, 7323–7328.
49. Roupioz, Y., Berthet-Duroure, N., Leïchlé, T., Pourciel, J., Mailley, P., Cortes, S., Villiers, M., Marche, P., Livache, T., Nicu, L. (2009) Individual blood-cell capture and 2d organization on microarrays. *Small* 5, 1493–1497.
50. Suraniti, E., Sollier, E., Calemczuk, R., Livache, T., Marche, P., Villiers, M., Roupioz, Y. (2007) Real-time detection of lymphocytes binding on an antibody chip using SPR imaging. *Lab Chip* 7, 1206–1208.
51. Bailey, S., Sabatini, D., Stockwell, B. (2004) Microarrays of small molecules embedded in biodegradable polymers for use in mammalian cell-based screens. *Proc Natl Acad Sci USA* 101, 16144–16149.
52. Bailey, S., Ali, S., Carpenter, A., Higgins, C., Sabatini, D. (2006) Microarrays of lentiviruses for gene function screens in immortalized and primary cells. *Nat Methods* 3, 117–122.
53. Oehmig, A., Klotzbücher, A., Thomas, M., Weise, F., Hagner, U., Brundiers, R., Waldherr, D., Lingnau, A., Knappik, A., Kubbutat, M., et al. (2008) A novel reverse transduction adenoviral array for the functional analysis of shRNA libraries. *BMC Genomics* 9, 441.
54. Narayanaswamy, R., Niu, W., Scouras, A., Hart, G., Davies, J., Ellington, A., Iyer, V., Marcotte, E. (2006) Systematic profiling of cellular phenotypes with spotted cell microarrays reveals mating-pheromone response genes. *Genome Biol* 7, R6.
55. Kato, K., Umezawa, K., Funeriu, D., Miyake, M., Miyake, J., Nagamune, T. (2003) Immobilized culture of nonadherent cells on an oleyl poly (ethylene glycol) ether-modified surface. *Biotechniques* 35, 1014–1018.
56. Kato, K., Umezawa, K., Miyake, M., Miyake, J., Nagamune, T. (2004) Transfection microarray of nonadherent cells on an oleyl poly (ethylene glycol) ether-modified glass slide. *Biotechniques* 37, 444–448.
57. Yoshikawa, T., Uchimura, E., Kishi, M., Funeriu, D., Miyake, M., Miyake, J. (2004) Transfection microarray of human mesenchymal stem cells and on-chip siRNA gene knockdown. *J Control Release* 96, 227–232.
58. Chang, F., Lee, C., Chen, M., Kuo, C., Chiang, U., Hang, C., Roffler, S. (2004) Surfection: a new platform for transfected cell arrays. *Nucleic Acids Res* 32, e33.
59. Kato, K., Umezawa, K., Funeriu, D. P., Miyake, M., Miyake, J., Nagamune, T. (2003) Immobilized culture of nonadherent cells on an oleyl poly (ethylene glycol) ether-modified surface. *Biotechniques* 35, 1014–1021.
60. Kato, K., Umezawa, K., Miyake, M., Miyake, J., Nagamune, T. (2004) Transfection microarray of nonadherent cells on an aleyl poly (ethylene glycol) ether-modified glass slide. *Biotechniques* 37, 444–452.
61. Delehanty, J., Shaffer, K., Lin, B. (2004) A comparison of microscope slide substrates for use in transfected cell microarrays. *Biosens Bioelectron* 20, 773–779.
62. Yamauchi, F., Kato, K., Iwata, H. (2004) Micropatterned, self-assembled monolayers for fabrication of transfected cell microarrays. *Biochim Biophys Acta* 1672, 138–147.
63. How, S., Yingyongnarongkul, B., Fara, M., Díaz-Mochón, J., Mittoo, S., Bradley, M. (2004) Polyplexes and lipoplexes for mammalian gene delivery: from traditional to microarray screening. *Comb Chem High Throughput Screen* 7, 423–430.
64. Isalan, M., Santori, M., Gonzalez, C., Serrano, L. (2005) Localized transfection on arrays of magnetic beads coated with PCR products. *Nat Methods* 2, 113–118.
65. Yamauchi, F., Kato, K., Iwata, H. (2004) Spatially and temporally controlled gene

transfer by electroporation into adherent cells on plasmid DNA-loaded electrodes. *Nucleic Acids Res* 32, e187.
66. Fujimoto, H., Kato, K., Iwata, H. (2008) Electroporation microarray for parallel transfer of small interfering RNA into mammalian cells. *Anal Bioanal Chem* 392, 1309–1316.
67. Fujimoto, H., Kato, K., Iwata, H. (2009) Prolonged durability of electroporation microarrays as a result of addition of saccharides to nucleic acids. *Anal Bioanal Chem* 393, 607–614.
68. Hook, A., Thissen, H., Voelcker, N. (2009) Advanced substrate fabrication for cell microarrays. *Biomacromolecules* 10, 573–79.
69. Tourniaire, G., Diaz-Mochon, J., Bradley, M. (2009) Fingerprinting polymer microarrays. *Comb Chem High Throughput Screen* 12, 690–696.
70. Carpenter, A., Jones, T., Lamprecht, M., Clarke, C., Kang, I., Friman, O., Guertin, D., Chang, J., Lindquist, R., Moffat, J., et al. (2006) CellProfiler: image analysis software for identifying and quantifying cell phenotypes. *Genome Biol* 7, R100.

Chapter 2

Cell-Based Co-transfection Microarrays for Use with HEK293T Cells on a Poly D-Lysine-Coated Polystyrene Microplate

Meenal Soni and Fang Lai

Abstract

Analysis of the human genome sequence has identified thousands of putative genes with unknown function; therefore, a new tool allowing for rapid identification of gene functions is needed. Reverse transfection microarray technology, which turns a DNA microarray into a cell-based microarray, has emerged for simultaneously studying the function of many genes. Since the initial demonstration in 2001, many variations have surfaced, making the technology more versatile for a broad range of applications. We have developed a protocol to make ready-to-transfect DNA microarrays in a 96-well microplate for co-transfection of two plasmids into HEK293T cells. This cell-based microarray in a microplate may be used for screening hundreds of analytes against multiple protein targets in parallel, providing a powerful tool for functional genomics and drug discovery.

Key words: Reverse transfection, surface-mediated transfection, co-transfection, cell microarray, microplate, GFP, LacZ.

1. Introduction

Reverse transfection microarray technology first developed by Ziauddin and Sabatini is a powerful tool for bridging genomics with proteomics (1). The technology involves three basic steps to turn a DNA microarray into a cell-based microarray. First, a DNA microarray is fabricated, in which each microspot contains a plasmid DNA capable of expressing a gene of interest. Second, the DNA microarray is treated with transfection reagents. Third, adherent cells are grown on the treated DNA microarray.

E. Palmer (ed.), *Cell-Based Microarrays*, Methods in Molecular Biology 706,
DOI 10.1007/978-1-61737-970-3_2,

Due to surface-mediated transfection enabled by the presence of transfection reagents, the cells on top of a microspot take up the plasmid DNA and express the protein encoded by it, producing a localized patch of transfected cells, a cell microspot. This cell-based microarray with the number of cell microspots corresponding to the number of DNA microspots can be used to simultaneously study the function of dozens or hundreds of genes. Recently, the technology has been extended for turning a microarray of siRNA, virus, or even chemical compounds into a cell-based microarray for many cellular and biological applications (2–4).

Over the years, many modifications have been made. To circumvent the need for extensive post-transfection processing of the cell-based microarray to detect protein activity, we have developed a reporter system using green fluorescent protein (GFP) for direct readout (5). In this system, two plasmids, one for a target protein and the other for GFP which can be turned on only when the target protein is active, are printed within a single microspot and can be co-transfected. Since the presence of GFP, which is readily visualized by an imaging system, is the indicator of the activity of the target protein, the cell-based microarray assay is substantially simplified through elimination of fixing and permealizing cells, as well as immunostaining with multiple antibodies.

Although γ-aminopropylsilane (GAPS)-coated glass (Corning Incorporated, Lowell, MA) and poly-D-lysine (PDL)-coated glass or polystyrene (PS) surfaces are suitable for reverse transfection, efforts have been made to create a ready-to-transfect surface so that the second step, treatment with transfection reagents, may be eliminated. In 2000, before the publication of reverse transfection, Zheng et al. reported that immobilizing a plasmid DNA on polyethyleimine (PEI) attached to a polymer film made of poly(epsilon-CBZ-L-lysine) (PCBZL) mixed with poly(D,L-lactic-co-glycolic) or poly(L-lactic acid) could enable surface-mediated transfection (6). In 2008, two reports described the use of PEI-plasmid complexes immobilized on self-assembled monolayers (SAMs) of ethylene glycol (EG) and carboxylic acid-terminated alkanethiols or on small intestinal sub-mucosa (SIS) for improved transfection efficiency (7, 8). Similarly, calcium-phosphate (Ca-P)–DNA co-precipitates on or encapsulated in fast-degrading polymer was also found to be adequate for transfection of HEK293, HeLa, and NIH 3T3 cells (9). Most recently, Oyane et al. reported that including a cell adhesion molecule such as laminin or fibronectin in a DNA-apatite composite layer enhanced transfection efficiency (10). Moreover, fibrin-based hydrogel embedded with lipofectamine–plasmid lipoplexes was shown to be useful for transfection of cells on top of the gel (2D) and within the gel (3D) (11).

While potentially useful, the feasibility of applying aforementioned methods to making cell-based microarrays has not yet been demonstrated.

Using a PDL-coated PS microplate, we have developed a method to print plasmid mixed with transfection reagents (effectene) and gelatin into a DNA microarray for reverse transfection (12). This ready-to-transfect DNA microarray could be stored at 4°C for up to 1 year without significant loss of transfection efficiency. While our paper was still in press, another group reported a similar method but on poly (vinyl alcohol) (PVA) surface pre-patterned with sodium hypochlorite (NaOCl) (13).

A growing list of adherent cells with different tissue or species origin such as A549, cos7, and Drosophila cells has been successfully used for reverse transfection. Human embryonic kidney 293T (HEK293T), a cell line derived from transforming HEK293 cells with SV40 large T gene, is one of the most widely used cell lines. The fast-growing HEK293T cells, with a doubling time of 16–20 h, are relatively easy to transfect with 40–80% of transfection efficiency.

The transfection efficiency is affected by multiple factors, including cell type, the size, purity, and amount of plasmid DNA, transfection reagents, as well as transfection formats (surface mediated vs. solution based). The last two factors have been systematically examined (14, 15). On a particular surface with a given cell type, optimizing transfection conditions are often necessary to achieve high transfection efficiency. In this chapter, using a two-plasmid model (one for GFP and one for LacZ), we have described a detailed protocol for making a ready-to-transfect DNA microarray in a 96-well microplate and optimal co-transfection of HEK293T cells for creating a cell-based microarray for two-color assays.

2. Materials

2.1. Microarray Fabrication

1. phMGFP, plasmid containing the gene for green fluorescent protein (GFP) (Promega, Madison, WI). Store at –20°C.
2. pcDNA3.1/V5-His/lacZ, plasmid containing the gene for LacZ, and its vector phRL-SV40 (Invitrogen Co., Carlsbad, CA). Store at –20°C.
3. Gelatin, 12% (w/v) in deionized (DI) water. Store at 4°C. Prepare working solution by mixing 10 μl of 12% gelatin with 90 μl of DI water to make final concentration of 1.2%, and store at 4°C up to 1 month.

4. Poly-D-lysine (PDL)-coated microplates (Corning Incorporated, Lowell, MA). Store at 4°C.
5. 384-well plate reservoir (Corning Incorporated, Lowell, MA).
6. Effectene transfection reagent kit, including EC buffer, enhancer, and effectene (Qiagen, Valencia, CA). Store at 4°C.
7. 1.5 M Sucrose in DI water (Invitrogen Co., Carlsbad, CA). Store at 4°C.
8. Chipmaker Micro Spotting Pin CMP10B (Arrayit Corporation, former Telechem International, Inc., Sunnyvale, CA).

2.2. HEK293T Cell Culture

1. Human embryonic kidney cell line HEK293T (GenHunter, Nashvil, TN).
2. Fetal calf serum (FCS). Store at –20°C.
3. Pen Strep: 10,000 units/ml penicillin, streptomycin 10,000 μg/ml. Store at –20°C.
4. Dulbecco's modified eagle medium (DMEM). Store at 4°C.
5. Complete medium: DMEM 500 ml, FCS 10% (v/v), Pen Strep 1% (v/v) (final concentration of penicillin 100 units/ml and streptomycin 100 μg/ml). Store at 4°C for up to 6 months.
6. Trypsin–EDTA: 0.025% (w/v) trypsin and 0.01% (w/v) EDTA (ethylenediaminetetraacetic acid in a phosphate buffer salt solution with 5 mM glucose) (Invitrogen Co., Carlsbad, CA). Store at 4°C.
7. Phosphate buffered saline (PBS). Store at 4°C.
8. Dimethylsulfate (DMSO).
9. Tissue-culture-treated (TCT) flasks, T-75, and T-150.
10. 15- and 50-ml centrifuge tubes.

2.3. Cell Microarray Assay

1. 0.2% Triton X-100: prepare a working solution, 0.2 ml triton X-100, 99.8 ml PBS.
2. Ten percent goat serum (Invitrogen Co., Carlsbad, CA): prepare a working (blocking) solution, 1 ml goat serum, 9 ml PBS.
3. Primary antibody, anti-Lac Z mouse IgG (Santa Cruz Biotechnology, Santa Cruz, CA).
4. Secondary antibody, Cy3-labeled goat anti-mouse IgG (Jackson ImmunoResearch Laboratories, West Grove, PA).
5. Ninety-six-well microplate aluminum sealing tape (Corning Incorporated, Lowell, MA).

3. Methods

3.1. Transformation and Bacterial Culture

If starting with a plasmid preparation, it is necessary to make a bacterial clone for replicating the plasmid via transformation. Many companies sell *Escherichia coli* competent cells accompanied with a detailed protocol for transformation. We have used the *E. coli* HB101 competent cells from Invitrogen (Carlsbad, CA) for cloning purpose.

3.2. Plasmid Amplification and Purification

A plasmid is amplified in a 200-ml bacterial culture. It is isolated and purified with an alkaline method using a QIAGEN Plasmid *Plus* Maxi kit according to the manufacturer's protocol (QIAGEN Inc., Valencia, CA).

3.3. Microarray Sample Preparation

1. Add 1 μl each of the phMGFP (250 ng/μl) and the pcDNA3.1/V5-His/lacZ (250 ng/μl) plasmid DNAs (250 ng each) to 9.5 μl EC buffer to a final volume of 11.5 μl (*see* **Note 1**).
2. Add 2 μl of enhancer, 1.2 μl of 1.5 M sucrose, and 2 μl of effectene to a total volume of 16.7 μl. The DNA concentration is ~30 ng/μl (*see* **Note 2**).
3. Incubate the above mix at room temperature for 15 min to allow the formation of DNA and transfection reagent complexes.
4. Add 12 μl of 1.2% gelatin to make a final DNA concentration of ~18 ng/μl with each plasmid at 9 ng/μl.
5. Load all 28.7 μl of the sample (mixture of plasmid DNA, transfection reagents, and gelatin) in a well of a 384-well microplate until use. Although it is desirable to use the sample for printing right away, it may be kept at room temperature for up to 2 h without any noticeable effect.

3.4. Microarray Fabrication

1. Prior to sample preparation, turn on the PixSys 5,500 printer (Cartesian Technologies, Irvine, CA), set relative humidity (RH) to 70%, and let it warm up for 1 h.
2. Prior to printing, turn on warm DI water (45–50°C) circulator and vacuum pump. Warm water helps to clean the quill pin thoroughly, but is optional.
3. Place the 384-well microplate carrying the sample onto the source plate holder.
4. Pre-warm a 96-well PDL-coated microplate for 10 min to room temperature, and place it onto a sample plate holder.
5. Place a clean 3×4-inch glass slide onto a slide holder.

6. Place a CMP10B pin onto the pinhead. With the CMP10B pin, the diameter of a microspot is ~365 μm. With a 600 μm center-to-center spot distance, a microarray containing up to 36 microspots (6×6) may be printed in each well. If printing three replicate microspots per sample, then up to 12 samples can fit into one well.
7. Print microarrays at the bottom of individual wells of the 96-well PDL-coated microplate using the following program:
   a. Move the pin to water bath, rinse it, and vacuum dry it for 1 s each; repeat the pin wash cycle four times.
   b. Move the pin to source plate, dip it into the sample for 3 s to ensure that the quill (slit) is fully filled (0.6 μl).
   c. Move the pin to the glass slide and blot 20 dots to remove excess sample outside of the pin.
   d. Move the pin to a well of the 96-well PDL-coated microplate and print three replicate microspots at the bottom; move it to next well to print three microspots; and so forth until the first four columns of 32 wells are printed (with a total of 96 microspots).
   e. Repeat Steps "a" through "d" twice until the entire plate is printed with a total of 288 microspots per sample.
   f. Repeat Steps "a" through "e" to print second sample until all the samples are printed. Up to 12 samples may be printed in one 96-well PDL-coated microplate.
8. Dry the printed microarray plate in a desicator for 1 h at room temperature. The humidity in the desicator should be <20%.
9. Cover the dried microplate with a lid, wrap with a piece of parafilm, and store in a desicator at 4°C till use. The printed microarrays are stable for up to 1 year under this storage condition.

3.5. HEK293T Cell Preparation

1. Pre-warm complete medium (DMEM with 10% FCS and 1% Pen Strep) in a 37°C water bath for 15–30 min. The pre-warmed complete medium is used in all subsequent steps.
2. Take out a frozen vial of HEK293T cells from a liquid nitrogen tank (typically contains $2–4\times10^6$ cells), while holding it, immediately place the vial in 37°C water, and gently swirl it until the liquid inside of the vial is completely thawed.
3. Take the vial out from water and spray it thoroughly with 70% ethanol to sterilize the surface, and place it in a laminar flow hood. All of the following steps are done in the hood.
4. Carefully open the vial and transfer all the cells inside to a T-75 flask filled with 20 ml of complete medium.

5. Place the T-75 flask into a CO_2 (5%) incubator set at 37°C with 95% humidity to let cells attach and grow overnight.
6. Take the T-75 flask out from the CO_2 incubator, gently aspirate off the used medium to completely remove DMSO contained in the frozen vial, and add 20 ml of fresh complete medium.
7. Put the T-75 flask into the CO_2 (5%) incubator set at 37°C with 95% humidity, and continue to grow cells until the cells reach 80–90% confluency ($\sim 5–11 \times 10^4$ cells/cm^2) by visual inspection under a microscope. It typically takes 1–2 days to yield $\sim 4–8 \times 10^6$ cells per flask depending on the number of viable cells at beginning. It is important to avoid letting cells reach 100% confluency as many cells start to die or become unhealthy.
8. Aspirate off the medium and gently wash the cells with 5 ml of PBS to remove trypsin inhibitors that may come from serum in the medium.
9. Aspirate off the PBS and trypsinize the cells with 1 ml of trypsin–EDTA for 2–3 min at room temperature. The cells can be readily detached from the surface by gently tapping the flask. Do not shake the flask vigorously and make sure that cells do not sit in trypsin–EDTA for >10 min.
10. Add 5 ml of complete medium to the flask to stop trypsinization, break cell clumps by gently pipetting up and down several times without making bubbles, and transfer all the cells to a 15-ml centrifuge tube.
11. Centrifuge at $\sim 1{,}000 \times g$ for 3 min to pellet cells (3,000 rpm in Baxter Scientific Centrifuge Model 2742 Biofuge 17, Heraeus Sepatech, Germany). Gently pour off supernatant to remove trypsin–EDTA, and resuspend the cells in 6 ml of complete medium.
12. The resulting cells may be (i) used for reverse transfection if $<4–8 \times 10^6$ cells are needed, (ii) further propagated for a large scale reverse transfection, (iii) split (1:10 or 1:20) for maintenance up to 10 passages, and (iv) propagated for making more frozen vials.
13. To directly use the cells for reverse transfection, proceed to Step 18 for cell count.
14. To propagate cells for a large scale reverse transfection, add 1 ml of the cells ($\sim 7–13 \times 10^5$ cells) into each of five T-75 flasks filled with 20 ml of complete medium (*see* **Note 3**).
15. Culture cells in a CO_2 (5%) incubator set at 37°C with 95% humidity overnight to let cells attach and grow.
16. Change the medium the next day, and then every other day until the cells reach 80–90% confluency by visual inspection under a microscope.

17. Harvest cells by repeating Steps 8–11 and transfer the resulting 6 ml of cells from each T-75 flask to a 50-ml centrifuge tube (pool all the cells from multiple flasks into one centrifuge tube).
18. Take 50 μl of the cell suspension for cell count using a Beckman-Coulter Cell Counter (Fullerton, CA) following manufacturer's instructions (*see* **Note 4**). The cells are now ready for reverse transfection (proceed to **Section 3.6**).
19. For cell passage, add 1 ml of the cells from Step 11 into a T-75 flask filled with 20 ml complete medium and repeat Step 15–16 until cells reach 80–90% confluency. To keep HEK293T cells healthy, which is critical for efficient reverse transfection, it is recommended to use the cells within 10 passages.
20. For making a large quantity of frozen vials of cell stock at passage #1, add 5 ml of the cells from Step 11 into a T-150 flask filled with 40 ml of complete medium, and repeat Step 15–16 until cells reach 80–90%. Trypsinize the cells with 6 ml Trypsin–EDTA for 3–5 min, add 30 ml of complete medium, and count cells. Pellet cells and re-suspend the cells in freezing medium (85% DMEM, 10% CFS, 5% DMSO) at 2–4×10^6 cells/ml (as described in Step 8–11). Aliquot the cells at 1 ml per vial, store them at –80°C overnight, and then transfer them to the vapor phase of a liquid nitrogen tank for long-term storage.

3.6. Reverse Transfection

1. Centrifuge the cells from Step 17 (in **Section 3.5**) at ~1,000×*g* for 5 min, and aspirate off the medium.
2. Re-suspend the cells gently in an appropriate volume of complete medium to make final concentration of 7×10^5 cells/ml based on the total cell number obtained from Step 18 (in **Section 3.5**).
3. Use an automatic pipettor to add 100 μl of the cells into each well of a 96-well printed microarray plate (7×10^4 cells/well). Make sure that there are no air bubbles trapped in the bottom of individual wells, specifically between the cells and the surface. If there is a bubble, remove it immediately by pipetting out the cells and gently adding them back into the well. Having no barriers for cells to attach to the surface is crucial for the success of reverse tranfection.
4. Incubate the plate in a CO_2 (5%) incubator set at 37°C with 95% humidity overnight. With exogenous GFP expression, patches of transfected cells are first detected after 16–24 h. To ensure maximum transgene expression, cell microarrays are usually assayed after 48 h.

3.7. Cell Microarray Assay

1. Remove media with a pipette carefully and gently to avoid dislodging cells as transfected HEK293T cells usually become less adherent and easily detached. To prevent cells from drying, it is recommended to work with no more than eight wells at a time when doing the assay manually.
2. Wash each well with 100 μl of PBS twice.
3. Add 100 μl of 4% (v/v) formaldehyde in PBS carefully and slowly down the wall.
4. Incubate for 10 min at room temperature; wash once with 100 μl PBS.
5. Add 100 μl of 0.2% Triton X-100 very carefully down the wall.
6. Incubate for 5 min at room temperature. This is a permeabilizing agent and therefore a difficult step since there is a high chance that cells may be washed off.
7. Add 100 μl of blocking solution (10% goat serum in PBS) to each well and incubate for 15 min at room temperature.
8. Dilute primary antibody, anti-LacZ mouse IgG, in PBS (usually between 1:20 and 1:500), and add 100 μl of the diluted primary antibody in each well.
9. Incubate for 1 h at room temperature for detecting an exogenous protein. The time needed for detecting endogenous proteins may be longer (up to 2 h).
10. Remove the primary antibody and carefully wash three times with 100 μl of PBS.
11. Dilute fluorescently labeled secondary antibody, Cy3-labeled goat anti-mouse IgG, in PBS (usually 1:500), and add 100 μl of the diluted secondary antibody in each well.
12. Incubate for 1 h in the dark.
13. Remove the secondary antibody and carefully wash three times with 100 μl of PBS.
14. Cells can be stored with foil covering over the microplate at 4°C until ready to image.

3.8. Cell Microarray Imaging and Data Analysis

1. Carefully flip the microplate on a piece of paper towel to drain all the liquid in the wells, and seal the wells with a piece of microplate sealing tape.
2. Scan the microplate for GFP signals with a 488-nm laser and a 532-nm filter (488 nm_{ex}/535 nm_{em}) at a PMT gain of 190, and LacZ signals (labeled with Cy3) with a 532-nm laser and a 590-nm filter (532 nm_{ex}/590 nm_{em}) at PMT gain of 210 in a Tecan LS400 fluorescent scanner (Research Triangle Park, NC).

3. The images may be analyzed with Array Pro Analyzer (provided by Tecan). Individual cell microspots are circled, and relative fluorescent units (RFU) within a circle are measured (*see* **Note 5**). The data output is exported to Excel, further calculated for average signal intensity of three replicate spots and standard deviation, and graphed (*see* **Note 6**).

4. Notes

1. Affected by purity and size, the optimal DNA amount for high transfection efficiency varies from plasmid to plasmid, and sometimes even from prep to prep. For a given plasmid DNA prep, it is highly recommended to test a range of quantities first to determine the optimal amount. We typically tested the range of 100–1,000 ng, translating to 3.5–35 ng/μl after mixing with transfection reagents to a total volume of 28.7 μl. With a given phMEGF plasmid DNA prep, the effect of DNA amount is shown as an example in **Fig. 2.1**. The highest transfection efficiency is achieved with 250 ng (8.7 ng/μl). For co-transfection, similar tests are done by varying amounts of the two plasmids in a two-way titration (e.g., 100, 250, 500, and 750 ng) to determine the optimal amount and ratio of the two plasmids. For the combination of phMGFP plasmid and pcDNA3.1/V5-His/lacZ plasmid, we have found that a 1:1 ratio (250 ng each) works the best (12).
2. Effectene is a nonliposomal lipid reagent and has been routinely used for solution-based transfection. In an effort to optimize surface-mediated transfection in a ready-to-transfect format, i.e., printing DNA together with transfection reagents, varying amounts of enhancer (4–8 μl) and effectene (2–4 μl) in the final DNA-transfection reagent mix have been tested. The difference seems negligible at least for the phMGFP plasmid and HEK293T cells as shown in **Fig. 2.2**. Lipofectamine 2000 from Invitrogen has also been shown to work (data not shown).
3. The way to propagate cells for reverse transfection can be very flexible in terms of the number and the size of flasks or Petri dishes and the ratio of cells to medium (1:20–5:20) used; all depend on the timing and the scale for the next reverse transfection experiment. One may use the following information as guidelines. When HEK293T cells are cultured in complete medium, approximately $4–8\times10^6$ cells ($7–13\times10^5$ cells/ml in a total volume of 6 ml) may be harvested from a 80–90% confluent T-75

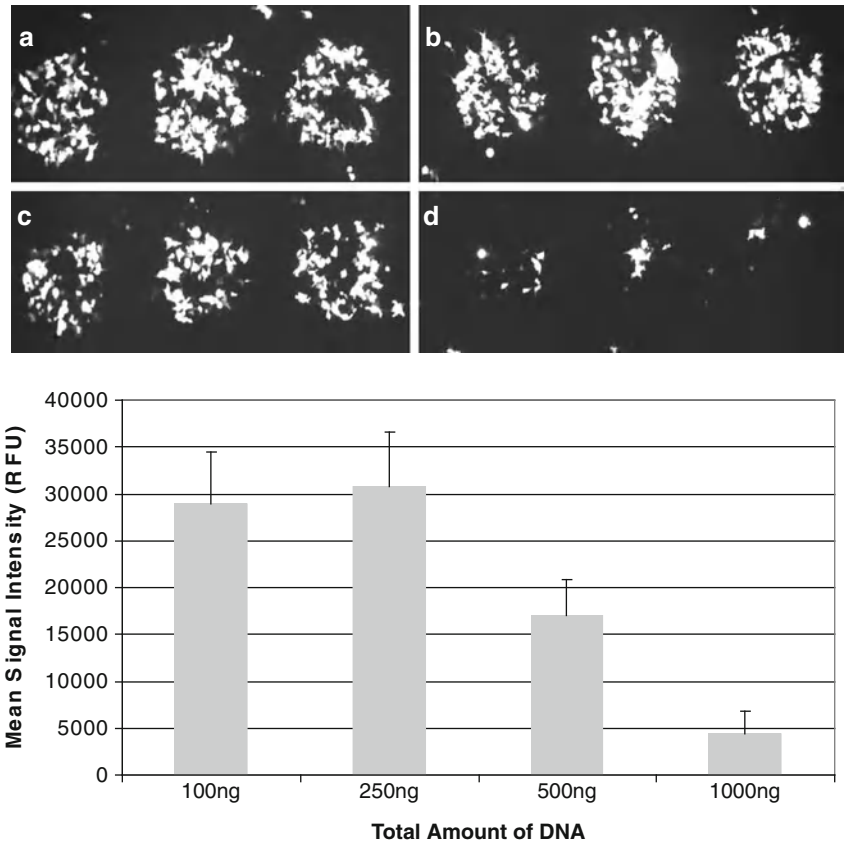

Fig. 2.1. Effect of DNA amounts on reverse tranfection efficiency. *Top* is the image of a HEK293T cell microarray expressing GFP excited at 488 nm and captured at 535 nm with a Tecan scanner. HEK293T cells were transfected with different amounts of phMGFP plasmid DNA, 100 ng (*a*), 250 ng (*b*), 500 ng, (*c*) or 1,000 ng (*d*) each mixed with transfection reagents and printed in triplicate spots. At the *bottom* is the histogram showing the average relative fluorescent units (RFU) of three cell microspots resulting from the reverse transfection with the amount of DNA indicated at the *bottom*.

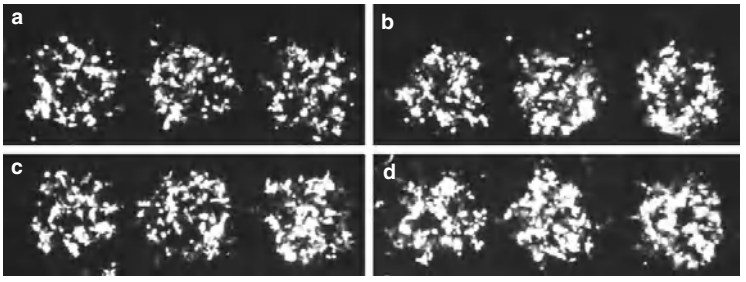

Fig. 2.2. Optimization of transfection reagents. Shown is the image, excited at 488 nm and captured at 535 nm with a Tecan scanner, of a HEK293T cell microarray expressing GFP generated by mixing 250 ng of phMGFP plasmid DNA with various amounts of enhancer and effectene. The combinations tested were (*a*) 4 μl enhancer + 2 μl effectene, (*b*) 4 μl enhancer + 4 μl effectene, (*c*) 8 μl enhancer + 2 μl effectene, and (*d*) 8 μl enhancer + 4 μl effectene.

flask ($5–11\times10^4$ cells/cm^2). If splitting at 1:20 (1 ml cells in 20 ml medium) ratio in a T-75 flask ($7–13\times10^5$ cells, $\sim9–17\times10^3$ cells/cm^2), it takes 4–5 days to reach 80–90% confluency.

4. We have used a cell counter to count cells for convenience and minimizing human error. The downside of this method is that there is no information regarding the percent of viable cells, an important indicator of the cell quality for reverse transfection. The problem may be circumvented by not using overly confluent cells (>90%). Conventional hemacytometer can also be used for cell count. Using trypan blue staining for viable cell count is desirable but not necessary.
5. Any microarray imaging system equipped with proper lasers and filters can be used for imaging cell-based microarray. Since the resolution of a microarray imaging system is typically at 5–10 microns per pixel, one can collect only average signal from multiple transfected cells within a microspot, demanding high transfection efficiency for sufficient signals. Moreover, the shape of individual cell microspots is often irregular, and signals within a microspot are blotchy; therefore, defining a microspot area can be tricky and often leads to big spot to spot variations.
6. We have also used the Discovery-1 automatic fluorescence microscope (Molecular Devices Co., Sunnyvale, CA) at 2× or 10× images and Zeiss Axiovert 135 microscope (Carl Zeiss, Thornwood, NY) at 2.5× or 20× objectives for imaging cell-based microarrays. Both imaging systems offer single cell resolution. Coupled with MetaMorph software, fluorescent signals from individual transfected cells can be measured and quantified, which is especially helpful for calculating co-transfection efficiency.

Acknowledgments

We would like to thank Brian L. Webb for his pivotal role in developing the technology and Janie Causer for her excellent support in printing DNA microarrays.

References

1. Ziauddin, J., Sabatini, D. M. (2001) Microarrays of cells expressing defined cDNAs. *Nature* 411, 107–110.
2. Wheeler, D. B., Bailey, S. N., Guertin, D. A., Carpenter, A. E., Higgins, C. O., Sabatini, D. M. (2004) RNAi living-cell microarrays for loss-of-function screens in drosophila melanogaster cells. *Nat Methods* 1, 127–132.
3. Bailey, S. N., Ali, S. M., Carpenter, A. E., Higgins, C. O., Sabatini, D. M. (2006) Microarrys of lentiviruses for gene function

screens in immortalized and primary cells. *Nat Methods* 3, 117–122.
4. Bailey, S. N., Sabatini, D. M., Stckwell, B. R. (2004) Microarrays of small molecules embedded in biodegradable polymers for use in mammalian cell-based screens. *Proc Natl Acad Sci USA* 101, 16144–16149.
5. Webb, B. L., Díaz, B., Marttin, G. S., Lai, F. (2003) A report system for transfection cell arrays. *J Biomol Screen* 8, 620–623.
6. Zheng, J., Manuel, W. S., Hornsby, P. J. (2000) Transfection of cells mediated by biodegradable polymer materials with surface-bound polyethyleneimine. *Biotechnol Prog* 16, 254–257.
7. Pannier, A. K., Wieland, J. A., Shea, L. D. (2008) Surface polyethylene glycol enhances substrate-mediated gene delivery by non-specifically immobilized complexes. *Acta Biomater* 4, 26–39.
8. Tseng, S. J., Chuang, C. J., Tang, S. C. (2008) Electrostatic immobilization of DNA polyplexes on small intestinal submucosa for tissue substrate-mediated transfection. *Acta Biomater* 4, 799–807.
9. Zhang, Q., Zhao, D., Zhang, X. Z., Cheng, S. X., Zhuo, R. X. (2009) Calcium phosphate/DNA co-precipitates encapsulated fast-degrading polymer lims for substrate-mediated gene delivery. *J Biomed Mater Res B Appl Biomater*, 91B, 172–180.
10. Oyane, A., Murayama, M., Yamazaki, A., Sogo, Y., Ito, A., Tsurushima, H. (2010) Fibronectin-DNA-apatite composite layer for highly efficient and area-specific gene transfer. *Biomed Mater Res A*, 92A, 1038–1047.
11. Lei, P., Padmashali, R. M., Andreadis, S. T. (2009) Cell-controlled and spatially arrayed gene delivery from fibrin hydrogel. *Biomaterials* 30, 3790–3799.
12. Walczak, W., Pipalia, N. H., Soni, M., Faruqi, A. F., Ralph, H., Maxfield, F. R., Webb, B. L. (2006) Parallel analysis of v-src mutant protein using reverse transfection cell arrays. *Comb Chem High Throughput Screen* 9, 711–718.
13. Peterbauer, T., Heitz, J., Olbrich, M., Hering, S. (2006) Simple and versatile methods for transfection of arrays of live mammalian cells. *Lab Chip* 6, 857–863.
14. Kneuer, C., Ehrhardt, C., Bakowsky, H., Kumar, M. N., Oberle, V., Lehr, C. M., Hoekstra, D., Bakowsky, U. (2006) The influence of physicochemical parameters on the efficacy of non-viral DNA transfection complexes: a comparative study. *J Nanosci Nanotechnol* 6, 2776–2782.
15. Bengali, Z., Rea, J. C., Gibly, R. F., Shea, L. D. (2009) Efficacy of immobilized polyplexes and lipoplexes for substrate-mediated gene delivery. *Biotechnol Bioeng* 102, 1679–1691.

Chapter 3

Large-Scale Cell-Based Microarrays and Their Use with HEK293T Cells and Downstream Apoptotic Assays

Ella Palmer and Tom C. Freeman

Abstract

Cell-based microarrays are a powerful technology platform for performing high-throughput screens of gene function. The approach entails printing expression vectors containing either genes or shRNAs onto a glass microscope slide or 384-well microtitre plate to form an array. These vectors are then packaged in lipid-based transfection reagent, cells grown over the top of the array are transfected and the arrays can then be examined for alterations in cellular function as manifested in localised changes to the cells biochemistry or morphology. We have used this technology for two purposes: to study the sub-cellular localisation of proteins and to perform a large-scale screen for genes that when over-expressed lead to apoptotic cell death. Here we have provided detailed protocols for the large-scale screen and discuss some of the issues associated with this technology.

Key words: Reverse transfection, cell-based arrays, high-throughput screens, MGC collection.

1. Introduction

Cell-based microarray technology was first described by Ziauddin and Sabatini in 2001 (1) for use in performing high-throughput over-expression studies. The technique as originally published entailed printing full-length ORFs of genes inserted into an expression vector onto a glass microscope slide to form a microarray. The arrays were then treated with transfection reagent and cells grown over the top of the array until confluent. Cells growing in the vicinity of the spots of packaged genes were shown to be transfected and the encoded protein over-expressed. Arrays

E. Palmer (ed.), *Cell-Based Microarrays*, Methods in Molecular Biology 706,
DOI 10.1007/978-1-61737-970-3_3,

can then be examined for alterations in cellular function, as manifested in localised changes to the cells' biochemistry or morphology. If the expression vector contains a 'tag', then the sub-cellular localisation of the protein can also be analysed (1, 2). Due to the techniques' potential for high-throughput analyses and economy of reagents, a number of groups have since developed the basic ideas behind cell-based microarrays for a variety of applications. These applications include the discovery of new members of signalling pathways (3) to identify G protein coupled receptor (GPCR) targets (4) and to screen single-chain antibody fragments (5) for promoter analyses (6) and for RNAi screens (7, 8).

Whilst in principle cell-based microarrays provide a powerful platform for performing high-throughput transfection screens, few studies had shown the use of large-scale arrays and analyses tended to focus on the over-expression of a relatively small number of genes. One factor that had limited the use of the technology was the availability of suitable clone sets that contain tagged full-length ORFs in mammalian expression vectors, as described in the original paper (1). Such clone collections are now available from commercial sources, but for most their use is prohibited by their expense and restrictions on their use. In a previous study (2), we explored the use of GFP-tagged genes in Gateway expression vectors in the fabrication of cell-based arrays. Whilst this work demonstrated the utility of using tagged clones in visualising the sub-cellular localisation of the transfected protein, it also highlighted certain limitations with this approach. For example, apart from the considerable expense and time involved in sub-cloning genes into the Gateway cloning system, there is the possibility of introducing errors into the ORF during the initial PCR of the cDNA insert. We also demonstrated that tagging a gene can cause the protein to mislocalise and therefore disrupt the function of the native protein.

For the protocol presented here, we therefore elected to use untagged human cDNA clones from the mammalian gene collection (MGC) (9) for the construction of a cell-based microarray capable of screening a large number of genes, thus avoiding the problems that a large tag can cause to the folding of the protein. This protocol describes a truly high-throughput screening method utilising some of the MGCs non-redundant set of over 17,000 sequence verified, full-length ORF human clones. We constructed a cell-based microarray containing plasmid DNA from 1,959 of these clones in the expression vector pCMV-SPORT6, with each clone printed in quadruplicate. Seven Gateway GFP-tagged genes were printed as transfection controls, and an empty GFP vector (pEGFP-C1) was also printed to act as a transfection control and to provide a positional address for the untagged MGC clones (10). *See* **Fig. 3.1** for an overview of the procedure.

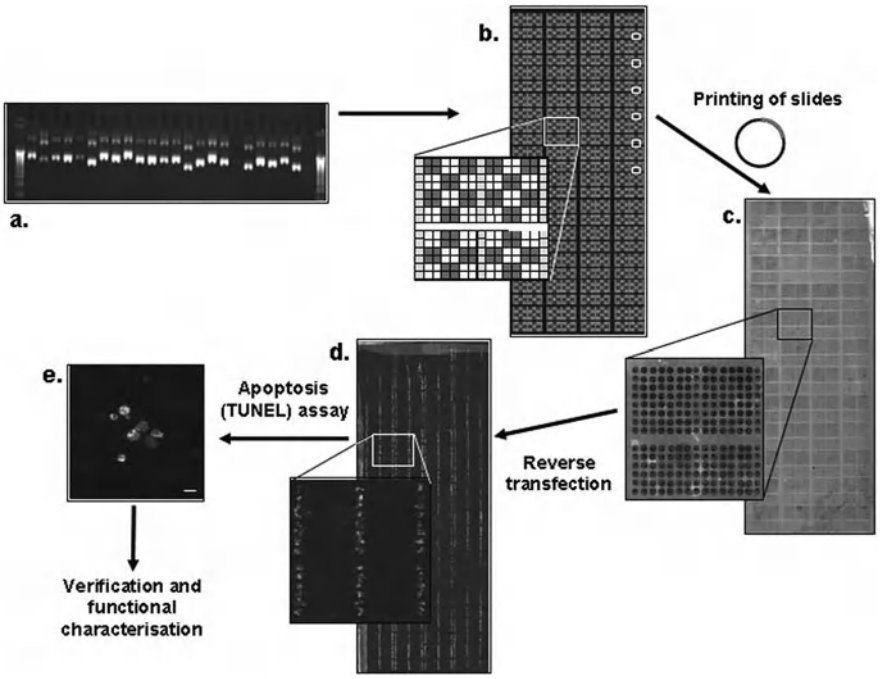

Fig. 3.1. Overview of the design and use of the large-scale cell-based microarray for over-expression studies. (**a**) Representative agarose gel image of plasmids prepared from 2,976 MGC (IRAT) clones. (**b**) Array was designed such that each clone was printed in quadruplicate (*grey* and *white squares*) surrounded by columns of GFP vector (*white columns*). The position of GFP-tagged positive control genes is shown by small white boxes. (**c**) 1,959 plasmids in 0.3% gelatin were printed onto a glass slide to form an array with 9,888 features. The image is of an array scanned directly after printing (Agilent microarray scanner). (**d**) An array cultured with HEK293T cells and scanned with a fluorescent imager (GE Healthcare, Typhoon) to show lines of GFP-positive cells. (**e**) Arrays were subjected to a functional assay to detect changes in the cell after over-expression of proteins. The image is of TUNEL positive cells; scale bar = 10 μm.

2. Materials

2.1. Preparation of IRAT Working Plates and Millipore 96-Well Miniprep

1. IRAT stock plates: 1–21 and 36–45 (Geneservice, Cambridge).
2. Flat-bottomed 96-well plate (Corning).
3. MultiScreen$_{96}$ PLASMID plate kit (Millipore).
4. Plastic sealing plate (Elkay, Basingstoke, UK).
5. 2× TY medium: 16 g tryptone, 10 g yeast extract, 5 g sodium chloride, H_2O to 1 l. Adjust pH to 7.0. Autoclave. Store at 25°C.
6. Glycerol/ampicillin medium: 250 ml 100 μg/ml ampicillin (50 mg/ml), 4 ml glycerol (8%), 496 ml 2× TY medium. Use immediately.
7. 50 μg/ml Ampicillin medium: 500 μl 100 μg/ml ampicillin, 1 l 2× TY medium (*see* **Section 2.1**). Use immediately.

8. 1 M Glucose: 18 g glucose, 100 ml H_2O. Filter (0.2 mm). Store at 25°C.
9. 10 M NaOH: 4 g NaOH, 100 ml H_2O. Store at 25°C.
10. 0.25 M Na_2EDTA: 9.3 g Na_2EDTA, 70 ml H_2O. Adjust to pH 8 with 10 M NaOH and add H_2O to 100 ml. Store at 25°C.
11. 1 M Tris–HCl: 12.1 g Tris base, 80 ml H_2O. Adjust to pH 8 with HCl and add H_2O to 100 ml. Store at 25°C.
12. GTE: 30 ml 1 M glucose (30 mM), 120 ml 0.25 M Na_2EDTA (30 mM), 15 ml 1 M. Tris–HCl pH 8 (15 mM) and 829 ml H_2O. Store at 25°C.
13. 10 mg/ml RNase: 10 mg RNase (Sigma), 10 ml H_2O. Aliquot 1 ml into tubes. Store at –20°C.
14. GTE/RNase: (70 ml for four 96-well plates), 69.6 ml GTE and 400 ml 10 mg/ml Rnase. Use immediately.
15. NaOH/SDS: (70 ml for four 96-well plates), 28 ml 0.5 M NaOH (0.2 M), 3.5 ml 20%. SDS (1%) (Sigma), 35 ml H_2O. Use immediately.
16. 5 M KoAc: 98.1 g KoAc, 200 ml H_2O. Store at 25°C.
17. KoAc/acetic acid: (70 ml for four 96-well plates) 50.4 ml KoAc, 9.8 ml glacial acetic acid, 9.8 ml H_2O. Use immediately.

2.2. PCR to Check ORF Sizes from IRAT Working Plate Clones and Agarose Gel Electrophoresis

1. P6: 5′ ATTTAGGTGACACTATAG 3′, T7: 5′ TAATACGACTCACTATAGGG 3′.
2. Qiaquick PCR purification kit (Qiagen).
3. 10× TBE: 100 g Tris, 55 g boric acid, 9.3 g EDTA to 1 l of H_2O. Store at 25°C.
4. 1× TBE: 10 ml 10× TBE, 90 ml H_2O. Store at 25°C.
5. Ethidium bromide (Sigma).
6. DNA Hyper ladder IV (Bioline, London, UK).
7. 6× Orange G loading buffer: 0.25 g Orange G, 30 g glycerol, 1× TBE to 100 ml. Store at 25°C.

2.3. DNA Quantification and Re-arraying IRAT Plates

1. Picogreen dsDNA Quantitation Kit (Molecular probes).
2. Black flat-bottomed black plate (Corning).
3. 1× TE buffer: (for one 96-well plate) 6 ml 20× TE buffer, 54 ml H_2O. Store at 25°C.
4. 2 μg/ml Stock DNA: 2 μl 100 μg/ml DNA, 50 μl 1× TE buffer. Store at 25°C.
5. 2,000 ng/ml Standard curve DNA: 30 μl 2 μg/ml stock DNA, 1,470 μl 1× TE buffer.

6. 200 ng/ml Standard curve DNA: 100 μl 2,000 ng/ml stock DNA, 900 μl 1× TE buffer.
7. 20 ng/ml Standard curve DNA: 10 μl 2,000 ng/ml stock DNA, 990 μl 1× TE buffer.
8. 2 ng/ml Standard curve DNA: 1 μl 2,000 ng/ml stock DNA, 999 μl 1× TE buffer.
9. Internal control stock (ICS): 20 μl 50 μg/ml human fetal liver genomic DNA (Biochain, Hayward, California, USA), 480 μl 1× TE buffer.
10. 400 ng/ml Internal control: 200 μl 2 μg/ml ICS, 800 μl 1× TE buffer.
11. 40 ng/ml Internal control: 20 μl 2 μg/ml ICS, 980 μl 1× TE buffer.
12. Picogreen: (for one 96-well plate): 27.5 μl picogreen, 5,472.5 μl 1× TE buffer. Cover with silver foil, use immediately. Store all standard curve and ICS solutions at –20°C.
13. Cytofluor 4,000 and Cytofluor software (Applied Biosystems, Warrington, UK)
14. Cytocalc (Applied Biosystems).
15. Heated vacuum centrifuge (Eppendorf).

2.4. Control Plasmid Preparation

1. pEGFP-C1 vector (Clontech).
2. Plasmid midi prep kit (Qiagen).
3. pENTR/D-TOPO kit (Invitrogen).
4. pcDNA-DEST47 vector (Invitrogen).
5. LR Clonase enzyme kit (Invitrogen).
6. Primers for control genes/clones:

```
CXADR F 5′ CACCATGGCGCTCCTGCTGTGC R 5′
TACTATAGACCCATCCTTGCT 3′
MARKL1 F 5′ CACCATGGCAGCTCTGCGCCAG R 5′
GAGCTCGAGGTCGTTGGA 3′
IL17BR F 5′ CACCATGTCGCTCGTGCTGCTA R 5′
CAAGGAGCAGCAGCCATC 3′
TNFRSF10B F 5′ CACCATGGAACAACGGGGACAG R 5′
GGACATGGCAGAGTCTGCA 3′
CDK9 F 5′ CACCATGGCGAAGCAGTACGAC R 5′
GAAGACGCGCTCAAACTCC 3′
TGIF F 5′ CACCATGAAAGGCAAGAAAGGT R 5′
AGCTGTAAGTTTTGCCTGAAG 3′
NFIB F 5′ CACCATGATGTATTCTCCCATC R 5′
GCCCAGGTACCAGGACTG 3′
M13 F 5′ GTAAAACGACGGCCAG 3′
T7  F 5′ TAATACGACTCACTATAGGG 3′
```

2.5. Cell Passage and Freezing and Thawing Cells

1. Culture medium: 50 ml FCS, 100 U/ml penicillin, 100 mg/ml streptomycin, 500 ml DMEM with 0.11 g/l NA PYR with pyroxidine (Invitrogen). Store at 4°C.
2. Freezing medium: 1.5 ml DMSO, 8.5 ml FCS. Mix and place on ice for 10 min before use.

2.6. Printing Cell-Based Microarrays, Cell Addition to the Arrays and Transfection

1. Polylysine slides (Sigma).
2. 0.3% Gelatin solution: 0.15 g gelatin, 50 ml H_2O. Dissolve in a 60°C water bath for 15 min, cool to 37°C, filter (0.45 mm). Store at 4°C.
3. Biorobotics MicroGrid II Microarrayer (Biorobotics) with a 48-pin head (Quill pins 2,500; Biorobotics)
4. Effectene transfection reagent kit (Qiagen).
5. 10×10 cm square dish (Falcon).
6. DNA microarrayer scanner (Agilent Technologies).
7. Tiff splitter A5.1.1.1 (Agilent Technologies).
8. Image Analysis A.5.1.1 (Agilent Technologies).

2.7. Fluorescent Assays, Cell Visualisation and Counting Positive Cell Fluorescence

1. 1% and 3.8% paraformaldehyde: 38% paraformaldehyde diluted with PBS (Sigma).
2. Apoptag Apoptosis Detection System kit protocol (Flowgen).
3. Cleaved caspase-3 (Asp175) antibody with fluorescein conjugate (Cell Signalling Technology).
4. DAPI mounting medium (Vector).
5. Glass slide coverslip (Agilent).
6. Typhoon scanner (Amersham Biosciences).
7. Eclipse E800 microscope (Nikon) with a confocal attachment (BioRad).

3. Methods

3.1. Preparation of IRAT Working Plates and Millipore 96-Well Miniprep

1. IRAT stock plates stored at –70°C were thawed. 250 μl glycerol/ampicillin medium was added to each well of fresh flat-bottomed 96-well plates, and 1 μl of the stock plates was pipetted in. The plates were wrapped in cling film, incubated at 37°C overnight and stored at –20°C. *See* **Note 1**.
2. IRAT plates were purified in quadruplicate as the kit.
3. Briefly, fill four 2 ml deep well blocks per IRAT plate with 1 ml of 50 μg/ml ampicillin medium.

4. Pipette 10 μl of the working plate clone into the deep well block and incubate for 26 h at 37°C at 320 rpm.
5. Cover the blocks with a plastic sealing plate and centrifuge for 5 min at 15,000×*g*.
6. Pour off the supernatant and turn the block over on tissue for 5 min. Add 175 μl of GTE/RNAse and vortex the block.
7. Add 175 μl NaOH/SDS and 175 ml of KoAc/acetic to the deep well block and vortex.
8. Place the PLASMID MANUPSD50 plate into the bottom of the vacuum manifold.
9. Remove 200 ml of lysate from the bottom of the deep well block, leaving the cell debris behind and add to a HV MAHVN4550 lysate clearing plate.
10. Place the HV plate on top of the vacuum manifold and apply vacuum until all the solution has filtered through to the PLASMID plate.
11. Discard the HV plate. Place a waste collection plate at the bottom of the vacuum manifold in place of the PLASMID plate and place the PLASMID plate on top of the vacuum manifold. Apply vacuum until all the solution has filtered through.
12. Add 200 ml of H_2O to the PLASMID plate and apply vacuum until all the H_2O has filtered through. Add 50 ml of H_2O and leave the PLASMID plate at room temperature for 30 min.
13. Transfer the plasmid dissolved in H_2O from the PLASMID plate to a clean flat-bottomed 96-well plate, combine the four plates containing purified plasmid for each IRAT plate and store at –20°C.

3.2. PCR to Check ORF Sizes from IRAT Working Plate Clones and Agarose Gel Electrophoresis

1. Add 2.5 μl 10× buffer, 0.75 μl 10 mM dNTPs, 0.5 μl 50 mM $MgSO_4$, 0.3 μl *Taq* DNA polymerase, 0.75 μl 100 ng/μl SP6, 0.75 ml, 100 ng/μl T7, 2 μl Plasmid DNA and 17.45 μl of H_2O.
2. Set up a PCR reaction at 94°C for 2 min, then 30 cycles of 94°C for 1 min, 60°C for 2 min 72°C for 7 min and then 72°C for 10 min. *See* **Note 2**.
3. PCR products were purified as described in the Qiaquick PCR purification kit. The size of the PCR products was confirmed with agarose gel electrophoresis.
4. 1 g of agarose was added to 100 ml 1× TBE, heated in the microwave until clear and then cooled to 37°C.
5. 25 μl of 2 μg/ml ethidium bromide per 100 ml was added, mixed, poured into gel plates and left to set for 1 h.

6. Mix 1 μl of PCR product, 1 μl of 6× Orange G loading buffer and 8 μl of water.
7. Mix 5 μl of DNA Hyper ladder IV, 1 μl of 6× Orange G loading buffer and 4 μl of water.
8. Load samples onto the gel and elecrophorese for 1 h at 100 volts.

3.3. DNA Quantification and Re-arraying IRAT Plates

1. Add 499 μl 1× TE buffer to a 96-deep-well block and add 1 μl of purified plasmid DNA to the 1× TE buffer and mix.
2. Add 50 μl 1× TE, 50 μl of the standard curve dilutions, 50 μl of the internal control dilutions (duplicate) and 50 μl (single) of the diluted plasmid DNA to a 96-well flat-bottomed black plate.
3. Add 50 μl of the picogreen dilution to the sample, standard curve dilutions and internal control dilutions in the 96-well flat-bottomed black plate, mix and incubate at room temperature for 5 min.
4. The Cytofluor 4,000 and Cytofluor software were used to measure the fluorescence. The manual mode, three reads per well, excitation 485/20, excitation 530/25 and a gain of 70 were selected.
5. Data were analysed with Cytocalc. The blank 1× TE samples were subtracted from the standard curve and samples and graphs were drawn with a deviation of 1 to check that the standard curve was a straight line and there were no outliers.
6. Cytocalc displays the sample concentrations in ng/ml; these readings were divided by 1,000 as the samples were diluted 1,000 fold, i.e. ng/ml was changed to ng/μl.
7. Adjust the concentrations to the 200 ng/ml internal control, e.g. if the 200 ng/ml control has a value of 135.5 ng/ml, then this is 67.8% of 200 ng/ml; therefore, the plasmid-DNA readings are divided by 67.8 and multiplied by 100.
8. IRAT plasmids with concentrations over 2 μg were sorted and plated into fresh 96-well flat-bottomed plates. The DNA was dried via a heated vacuum centrifuge, H_2O was added back as follows and the plates stored at –20°C. 2–4.9 μg 10 μl H_2O, 5–9.9 μg 20 μl H_2O, 10–14.9 μg 30 μl H_2O, 15–19.9 μg 40 μl H_2O, 20–24.9 μg 50 μl H_2O, 25–29.9 μg 60 μl H_2O, 30–34.9 μg 70 μl H_2O, 35–39.9 μg 80 μl H_2O, 40 μg and over 90 μl H_2O. *See* **Note 3**.

3.4. Control Plasmids

Any fluorescent control plasmids can be used; control plasmids are particularly crucial with this assay as the IRAT pCMV-SPORT6 expression vectors cannot be visualised. We used pEGFP-C1, a

C-terminal-tagged GFP with a promoter for expression. pEGFP-C1 vector was transformed in DH5alpha cells following a standard protocol and a plasmid midi prep undertaken.

We also used CXADR 1, MARKL1 1, TGIF 1, CDK9 2, NFIB 2, IL17BR 1 and TNFRSF10B genes in the C-terminal GFP expression vector pcDNA-DEST47 (11). These were cloned according to manufacturer's instructions. Primer design is crucial to the success of Gateway cloning and briefly the following procedure is undertaken.

1. Design the forward primers with a CACC overhang in front of the ATG start site to facilitate insertion of the gene into the entry vector pENTR/D-TOPO and keep 18 bp after the start site.
2. Design the reverse primers with 18 bp before the stop codon and remove the stop codon to ensure C-terminal fusion expression of GFP.
3. Check the reverse to ensure that there is no CACC at the 3′ end; otherwise the correct orientation will not be maintained.
4. Calculate the melting temperature (T_m) of the primers. A matching T_m of 55–60°C for the primer pairs is ideal, but if the T_m is not within this range, it can be adjusted by adding or removing bases where possible.
5. Check the primers for complementarity.
6. Prepare PCR reaction: 2.5 μl 10× amplification buffer, 0.75 ml 10 mM dNTPs 0.5 μl 50 mM $MgSO_4$, 0.5 μl, 100 ng/ml (F/R primers), 0.3 μl *Pfx* polymerase 16.95 μl H_2O.
7. Undertake PCR at 94°C 2 min, then 30 cycles of 94°C for 1 min, 60°C for 2 min, 72°C for 7 min and 72°C 10 min. *See* **Note 2**.
8. Purify the PCR products using Qiaquick PCR purification kit.
9. Confirm DNA concentrations and undertake agarose gel electrophoresis as in **Section 3.2**.
10. Transfer PCR products into pENTR/D-TOPO vectors as outlined in the kit.
11. Make a glycerol stock – add 850 μl of the overnight-LB culture to 150 μl of glycerol, transfer to a 1.5-ml tube and store at –70°C.
12. PCR or sequence to confirm entry of PCR products into pENTR/D-TOPO using the M13 forward primer and the reverse ORF-specific primer. PCR: 2 μl 10× buffer, 0.5 μl 10 mM dNTP, 1 μl plasmid DNA, 0.2 μl *Taq* polymerase, 1 μl 100 ng/μl F and R primer and 14.3 μl H_2O.

13. Undertake PCR at 94°C for 15 min, 30 cycles of 94°C for 1 min, 60°C for 2 min, 72°C for 7 min and then 72°C 10 min.
14. Confirm PCR product sizes with agarose gel electrophoresis as given in **Section 3.2**.
15. The pENTR/d-topo and pcDNA-DEST47 vectors were combined as the LR clonase enyzme kit (Invitrogen).
16. Undertake PCR to confirm that the genes have inserted correctly as in **Section 3.2**, using the T7 forward primer and the ORF-specific reverse primer.
17. Confirm PCR product sizes with agarose gel electrophoresis as in **Section 3.2**.

3.5. Cell Passage and Freezing and Thawing Cells

1. Grow and maintain human embryonic kidney (HEK293T) cells in culture medium in a T75 flask at 37°C and 5% CO_2.
2. Once confluent, remove the culture medium and add 2 ml of trypsin–EDTA, swirl over the surface of the cells and remove.
3. Add 1 ml of trypsin–EDTA to the flask, tap to detach the cells and leave for 2 min.
4. Add 9 ml of culture medium and mix the cells thoroughly by pipetting up and down for 10 times and add 1 ml to two fresh flasks containing 14 ml of culture medium.
5. After 20 passages, a fresh aliquot of cells was thawed out. Freezing and thawing cells:
6. Follow steps 1–4, **Section 3.5**, but add to a 15-ml tube and centrifuge at 13,000×*g* for 5 min.
7. Remove the supernatant, flick the pellet to mix and leave on ice for 10–30 min.
8. Add 1 ml of freezing medium to the cells and transfer to a freezing ampoule on ice.
9. Place the ampoules in a freezing container and leave at –70°C for 3 days, then store in liquid nitrogen until required.
10. Defrost cells by hand and tip into 30 ml culture medium in a T75 flask. *See* **Note 4**.

3.6. Printing Cell-Based Microarrays, Cell Addition to the Arrays and Transfection

See **Fig. 3.1** for array layout. Using the printing conditions below, the spot size on the microarrys is 140 μm with a 30-μm gap between each spot and a 170-μm gap between each sub-grid. 48 15×15 sub-grids can be printed. As IRAT plasmid clone transfections cannot be visualised due to the lack of any tag in the pCMV-SPORT6 vector, the array is designed with three columns of pEGFP-C1 plasmid either side and in the middle of

each sub-grid to act as transfection controls. MARKL1, IL17BR, CDK9, TNFRSF10B, NFIB, TGIF and CXADR in Gateway GFP C-terminal destination vectors were also included on the array as transfection controls because they had transfected well previously and showed distinct sub-cellular staining (11). A row in the middle of each sub-grid was left empty and together with the pEGFP-C1, aided orientation when observing the reverse transfection array through a confocal microscope. After the controls were taken into account, there was space for each IRAT plasmid to be printed four times. We printed 1,959 plasmids and our array had 9,888 features.

1. It is preferable to experiment with printing conditions using Cy3 in 0.3% gelatin first. *See* **Note 5**.
2. 1 μg IRAT plasmids, pEGFP-C1 vector and CXADR, MARKL1, IL17BR, TNFRSF10B, CDK9, TGIF and NFIB in the pcDNA-DEST47 vector were made up to 30 μl with 0.3% gelatin and transferred into 384-well plates. *See* **Note 6**.
3. Print clones onto polylysine slides using a Biorobotics MicroGrid II Microarrayer with a 48-pin head. Program the microarrayer to print 16 single pre-spots, 12 spots with a 25-ms dwell with two 7 s, 60°C wash and dries between picking up clones. It is preferable to print a large run, e.g. 100 arrays over 5 days to prevent repeat thawing and freezing of the re-array IRAT plates.
4. Determine if the DNA has printed correctly by scanning arrays with Cy3 and Cy5 lasers on a DNA microarrayer scanner, split the resultant.tif files using Tiff splitter A5.1.1.1 and view with the software program Image Analysis A.5.1.1. Each spot was ~140 μm in diameter. Arrays were stored desiccated at 4°C. *See* **Note 7**.

Cell addition:

5. Count Confluent HEK293T cells with a haemocytometer, add 1×10^7 HEK293T cells to a T75 flask and make up to 15 ml with culture medium. Incubate at 37°C, 5% CO_2 for 24 h.
6. Before cell addition, vortex and incubate 16 μl enhancer and 150 μl EC buffer per slide at RT for 5 min.
7. Add 25 μl effectene and vortex. Pipette the transfection reagent solution onto one end of the slide. Cut a plastic piece of film; cut to the size of the slide and carefully place onto the slide. Incubate at RT for 20 min. *See* **Note 8**.
8. Add 1×10^7 cells per array to a 50-ml tube, make up to 20 ml with culture medium and invert to mix.
9. The arrays were placed in a square dish. Carefully pour the HEK293T cells onto the array avoiding direct contact with

the printed areas and incubate the dish at 37°C, 5% CO^2 until the cells are confluent – about 40 h.

3.7. Fluorescent Assays, Cell Visualisation and Counting Positive Cell Fluorescence

We used two apoptotic assays, but any fluorescent assays can be used on the arrays.

1. Fix the cells with 1% paraformaldehyde for 10 min for the TUNEL assay or 3.8% paraformaldehyde for 20 min for the CASP3 assay.
2. Follow the protocol for the TUNEL and CASP3 assays. *See* **Note 9**.

Cell visualisation and counting positive cell fluorescence:

3. Apply a drop of mounting medium containing DAPI stain to a glass slide coverslip and lower onto the cell-based microarray. Primarily visualise fluorescence using a Typhoon scanner (*see* **Note 10**) with a resolution of 50 μm to determine if transfection has occurred.
4. This level of resolution is not high enough to analyse the transfection events on the arrays; therefore, use an Eclipse E800 microscope (Nikon) with a confocal attachment (Bio-Rad). *See* **Note 11** to analyse the arrays at ×10 magnification. At this magnification, the GFP positive controls can be used as a positional tool.
5. Positives were recorded as a quadruplicate clone patch with one or more fluorescent cells. Each microarray was scored twice and the genes were ranked in Excel according to the number of positives. Slides were stored at 4°C. *See* **Note 12**.
6. Positive genes from the assays were transfected in six-well plates to check whether they were true positives.

3.8. Statistical Analysis of Transfection Assays

1. Calculate the distribution of probabilities based on constant probability.

Divide the number of measurable array positions for each plasmid by the probability distribution and calculate the number of positives expected by chance and compare to the actual number observed on the arrays.

2. Calculate the sensitivity of the arrays using the equation true positive (TP)/(TP + false negative (FN)). Calculate the TP as the number of positives in the six-well assay follow-up experiments. Calculate FN as the number of known genes on the array known to elicit the assay response but were not found to be positive.
3. Use the equation TP/TP+false positive (FP) to calculate the positive predictive value of the arrays. Calculate FP as the number of genes found to be positive in half of more of

the arrays, but in the follow-up, six-well plate assay was not found to be positive.

4. Notes

1. IRAT plates 22–35 were not purified as the ORFs were not in an expression vector.
2. If reactions failed, they were repeated with an annealing temperature of 55°C.
3. It was not desirable to print a cell-based microarray directly from the purified plasmid plates as the plasmids had varying concentrations. It was estimated that 2 μg of each plasmid was necessary to prepare 200 cell-based microarrays. In our hands two-thirds had yields over 2 μg. Therefore, the clones were sorted into concentration ranges, re-arrayed into 21 new plates and all the plasmid concentrations were adjusted to 0.5 μg/ml.
4. HEK293T cells can cope with fairly extreme conditions and do not need to be treated as carefully as other cell types.
5. To optimise the printing of the cell-based microarrays, 0.3% gelatin with Cy3 was prepared. It was found that 15×15 sub-grids were achievable without the spots running into one another. In some of the test runs, the gelatin was drying, clogging the pin and causing unacceptable printing failure rates. This problem was circumvented by implementing 60°C washes to ensure that the gelatin did not solidify.
6. Different concentrations of gelatin were experimented with, but 0.3% was found to be more stable than 0.2%. The Sabatini protocol recommends that the gelatin percentage should not fall below 0.17%; therefore, with the higher gelatin percentage more dilute DNA samples could be printed.
7. Any scanner and software can be used which is capable of taking images of the arrays.
8. It was established by us that clear plastic film (parafilm) could be used in place of the hybriwell from the Sabatini protocol; this has the advantage that no air bubbles form and that it could be cut exactly to size allowing more features on the array.

9. Use parafilm that is cut to the size of the array for antibody incubation.
10. Any fluorescent flat bed scanner can be used.
11. Any confocal microscope can be used.
12. Manual analysis of the data can be time consuming and laborious; therefore, automatic imaging tools can be utilised.

References

1. Ziauddin, J., Sabatini, D. M. (2001) Microarrays of cells expressing defined cDNAs. *Nature* 411, 107–110.
2. Palmer, E., Freeman, T. (2004) Investigation into the use of C- and N-terminal GFP fusion proteins for subcellular localization studies using reverse transfection microarrays. *Comp Funct Genomics* 5, 324–353.
3. Webb, B. L., Diaz, B., Martin, G. S., Lai, F. (2003) A reporter system for reverse transfection cell arrays. *J Biomol Screen* 8, 620–623.
4. Mishina, Y. M., Wilson, C. J., Bruett, L., Smith, J. J., Stoop-Myer, C., Jong, S., Amaral, L. P., Pederson, R., Lyman, S. K., Myer, V. E., Kreider, B. L., et al. (2004) Multiplex GPCR assay in reverse transfection cell microarrays. *J Biomol Screen* 9, 196–207.
5. Delehanty, J. B., Shaffer, K. M., Lin, B. (2004) Transfected cell microarrays for the expression of membrane-displayed single-chain antibodies. *Anal Chem* 76, 7323–7328.
6. Yamauchi, F., Okada, M., Kato, K., Jakt, L., Iwata, H. (2007) Array-based functional screening for genes that regulate vascular endothelial differentiation of flk1-positive progenitors derived from embryonic stem cells. *Biochim Biophys Acta* 1770, 1085–1097.
7. Kumar, R., Conklin, D. S., Mittal, V. (2003) High-throughput selection of effective RNAi probes for gene silencing. *Genome Res* 13, 2333–2340.
8. Mousses, S., Caplen, N. J., Cornelison, R., Weaver, D., Basik, M., Hautaniemi, S., Elkahloun, A. G., Lotufo, R. A., Choudary, A., Dougherty, R. E. (2003) RNAi microarray analysis in cultured mammalian cells. *Genome Res* 13, 2341–2347.
9. Temple, G., Gerhard, D., Rasooly, R., Feingold, E., Good, P., Robinson, C., Mandich, A., Derge, J., Lewis, J., Shoaf, D., et al. (2009) The completion of the mammalian gene collection (MGC). *Genome Res* 19, 2324–2333.
10. Palmer, E., Miller, A., Freeman, T. (2006) Identification and characterisation of human apoptosis inducing proteins using cell-based transfection microarrays and expression analysis. *BMC Genomics* 7, 145.
11. Palmer, E., Freeman, T. (2004) Investigation into the use of C- and N-terminal GFP fusion proteins for subcellular localization studies using reverse transfection microarrays. *Comp Funct Genom* 5, 342–353.

Chapter 4

A Novel Fluorescent Transcriptional Reporter for Cell-Based Microarray Assays

Tanya M. Redmond and Michael D. Uhler

Abstract

Cell-based microarrays have been used for a wide variety of assays including gain-of-function, loss-of-function and compound screening. Many of these assays have employed fluorescent proteins as reporters. These fluorescent reporter proteins can be monitored in living cells but have low sensitivity of detection compared to enzymatic reporters. Here we have described a novel transcriptional reporter assay using the alkaline phosphatase reporter enzyme and a fluorescent substrate (ELF-97) to screen for gain-of-function mutations in the type-I cGMP-dependent protein kinase (PRKG1). We have identified a constitutively active mutant of this enzyme in which a conserved Glu at position 81 was mutated to Lys.

Key words: Microarrays, alkaline phosphatase, reporter genes, transfection, protein kinase.

1. Introduction

In the first published description of cell-based microarray transfection, Ziauddin and Sabatini described the process of reverse transfection for the characterization of changes in cellular phenotype as determined by radioligand and antibody binding (1). We developed the process of surface transfection and expression protocol (STEP), which employs recombinant proteins containing viral protein sequences such as the adenoviral penton protein to enhance the breadth of cell types that could be used in cell-based microarray studies (2). Our original use of STEP for the study of transcriptional regulation (3) as well as studies by other groups (4, 5) have employed fluorescent proteins such as EGFP as transcriptional reporters. While the use of

E. Palmer (ed.), *Cell-Based Microarrays*, Methods in Molecular Biology 706,
DOI 10.1007/978-1-61737-970-3_4,

fluorescent proteins has the advantage of continuous monitoring of the same population of transfected cells over time, the use of enzymatic reporters offers increased sensitivity to changes in transcriptional reporter activity. We have recently developed the alkaline phosphatase (AP) reporter for studies of transcriptional regulation in cell-based microarrays and have described the methods related to these studies here.

The AP substrate 2-(5′-chloro-2-phosphoryloxyphenyl)-6-chloro-4(3H)-quinazolinone, or ELF (*E*nzyme-*L*abeled *F*luorescence)-97 phosphate, forms a bright green–yellow precipitate in solution after removal of the phosphate moiety (6). We first compared the sensitivity of EGFP and a mouse placental AP expression vector in cell-based microarray transfection studies (**Fig. 4.1**). Similar exposure times demonstrated that for comparable CMV promoter constructs in HEK-293 cells, ELF-97 detection of AP activity was approximately 10 times more sensitive than EGFP (compare **Fig. 4.1a, b**). More quantitative studies in HEK-293 cells demonstrated that the fluorescent signal of CMV-AP6-transfected cells could easily become limited by ELF-97 substrate availability. Staining with 2% ELF-97 showed signal saturation at approximately 10% CMV-AP6 reporter DNA, whereas staining with 20% ELF-97 showed saturation when approximately 40% of the transfected DNA was CMV-AP6 (**Fig. 4.1c**). In contrast to HEK-293 cells, COS cells are typical of many cells which show a low endogenous phosphatase activity seen when only control vector is transfected (**Fig. 4.1d**). However, even in these COS cells, the AP reporter expression is more sensitive than the EGFP reporter (**Fig. 4.1d**).

In order to test the practical efficacy of the AP reporter system, we first constructed an AP reporter that encoded an AP protein stably attached to the extracellular surface of the transfected cell, since the placental AP protein is attached to the cell surface through a glycosyl phosphatidylinositol linkage which is readily cleaved by phospholipase D activities (7). Therefore, we generated an expression vector in which the coding region of the placental AP enzyme was fused to the transmembrane domain of the PDGF receptor to create the CRE-SEAPteth reporter vector. This vector also has tandem cAMP response elements (CREs)

Fig. 4.1. Characterization of AP/ELF-97 staining of transfected cells in cell-based microarrays. (**a**) A fluorescent micrograph of HEK-293 cells over a spot containing a STEP complex with CMV-EGFP DNA. (**b**) A fluorescent micrograph of cells over a spot containing a STEP complex with pCMV-AP6 plasmid DNA. (**c**) Quantitation of fluorescence signal from HEK-293 cells transfected with CMV-EGFP or CMV-AP6 followed by staining with either 20% ELF-97 or 2% ELF-97. (**d**) Quantitation of fluorescence signal from HEK-293 cells transfected with varying amounts of CMV-EGFP or CMV-AP6, followed by staining with either 20% ELF-97 or 2% ELF-97.

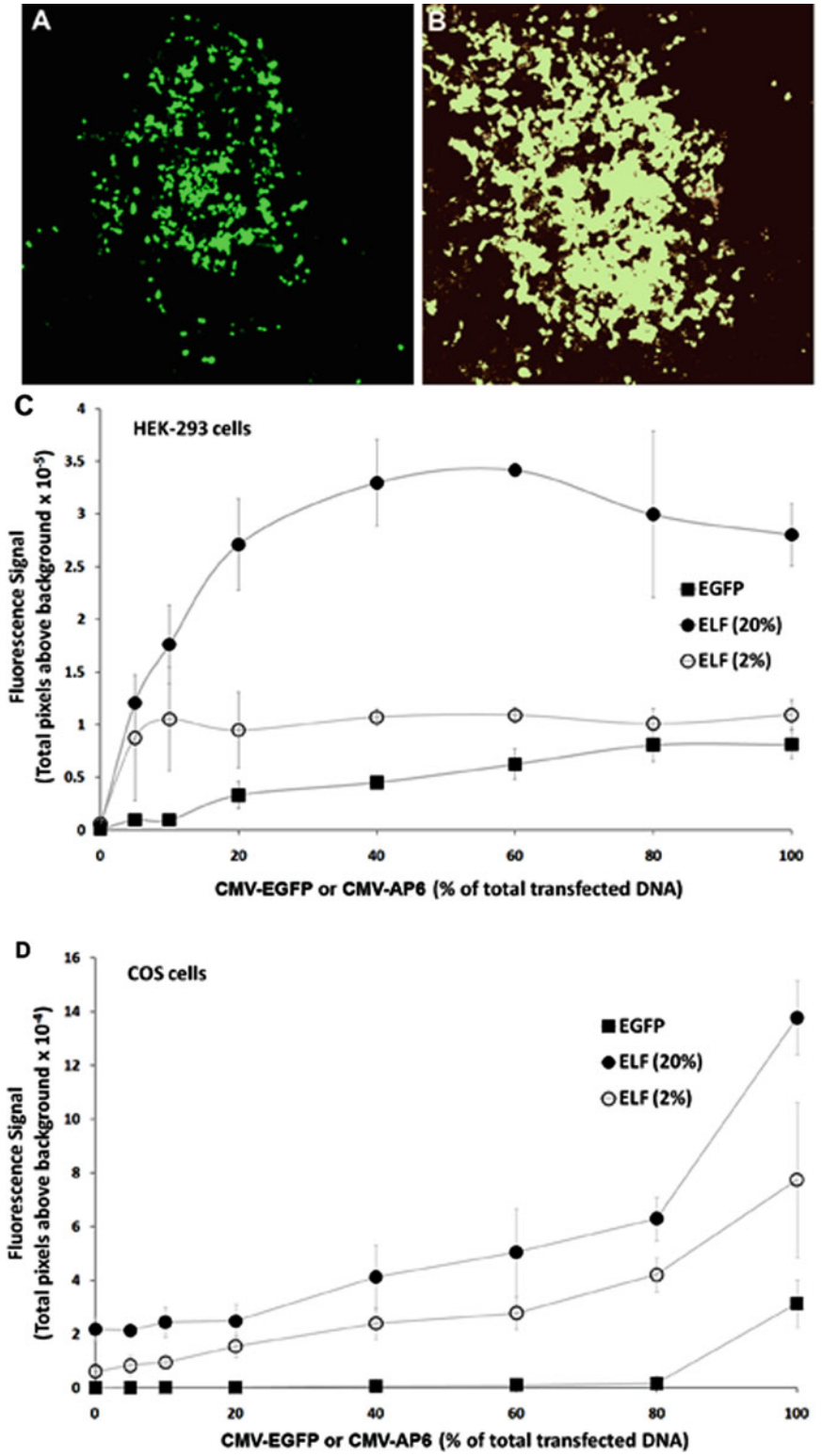

Fig. 4.1. (continued)

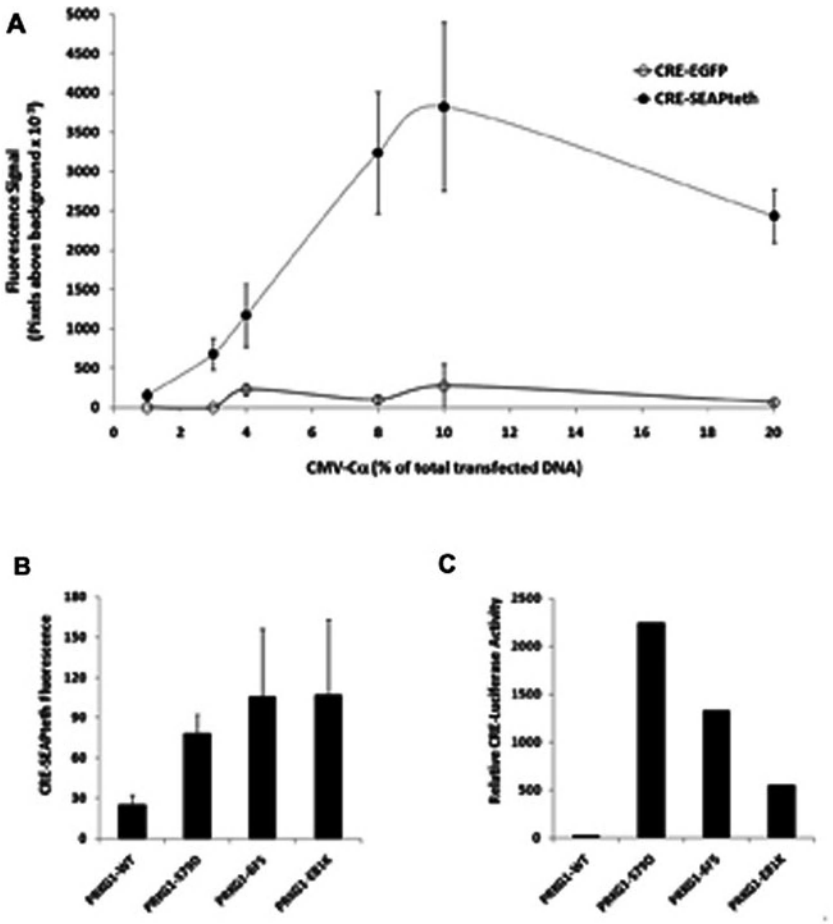

Fig. 4.2. Characterization of regulation of a tethered AP reporter in STEP-based microarray transfection for use in structure/function studies of PRKG1. (**a**) Regulation of either the CRE-EGFP or the CRE-SEAPteth reporter by varying concentrations of expression vector encoding a constitutively active protein kinase (CMV-Ca) in HEK-293 cells. (**b**) CRE-SEAPteth fluorescence of HEK-293 cells co-transfected with either wild-type PRKG-1, the constitutively active Ser70Asp mutant of PRKG1, the compound mutant 6F5 identified by STEP screening using AP/ELF-97, and the single point mutant PRKG-1 Glu81Lys. (**c**) Solution co-transfection of a CRE-responsive luciferase construct (HCG-luciferase) with either wild-type PRKG-1, the constitutively active Ser70Asp mutant of PRKG1, the compound mutant 6F5 identified by STEP screening using AP/ELF-97 and the single point mutant PRKG-1 Glu81Lys.

upstream the SEAP-teth reporter so that the reporter expression is elevated following CREB protein phosphorylation by either cAMP- or cGMP-dependent protein kinases.

As shown in **Fig. 4.2a**, HEK-293 cells transfected with the CRE-SEAPteth reporter vector showed induction of ELF-97-stained AP activity upon co-expression with an expression vector encoding a constitutively active PKA catalytic subunit (CMV-Ca). The fluorescent signal from the CRE-SEAPteth reporter was 10–250-fold more sensitive than an analogous CRE-EGFP reporter (**Fig. 4.2a**). We then used the CRE-SEAPteth to screen a small mutational library (106 different compound mutants) of

the type-I cGMP-dependent protein kinase for novel constitutively active mutants of this kinase. The constitutively Ser79Asp mutant previously characterized (8) was used as a positive control for the cell-based screening. One of the 106 clones (designated 6F5) screened showed significant constitutive activity when co-transfected with the CRE-SEAPteth reporter. Because of the extensive mutagenesis, this mutated expression vector contained five distinct mutations: Glu81Lys, Asn188Ile, Phe211Ile, Ser245Asn, and Glu254Asp. Further STEP transfection characterization of single point mutants using the CRE-SEAPteth reporter demonstrated that the Glu81Lys mutant was responsible for the majority of the constitutive activity demonstrated by this mutant (**Fig. 4.2b**). The constitutive activity of this Glu81Lys mutant was then confirmed in classical solution transfection protocols (**Fig. 4.2c**). It is of interest to note that the Glu81 residue is found within the same conserved pseudosubstrate domain of PRKG1 as the Ser79 previously characterized (8). Our findings suggest that not only is the use of ELF-97 for cell-based microarray transfection more sensitive than fluorescent protein reporter systems but also that cell-based array studies of protein structure and function are feasible using the AP/ELF-97 reporter system.

2. Materials

2.1. Cell Culture and Luciferase Assay

1. Dulbecco's modified eagle's medium (DMEM) (Invitrogen) supplemented with 10% fetal calf serum (FCS; HyClone, Ogden, UT) and 5% penicillin/streptomycin (Invitrogen).
2. Trypsin–EDTA 1×; 0.05% trypsin, 0.2 g/l EDTA (HyClone, Ogden, UT).
3. 60-mm cell culture dishes, tissue-culture-treated polystyrene (BD-Falcon).
4. Lipofectamine (Invitrogen).
5. Dual Luciferase Assay Kit (Promega).
6. Ninety-six-well assay plates: flat bottom, non-treated, black with clear bottom, non-sterile, polystyrene (Costar).

2.2. STEP Transfection and Imaging

1. MicroGrid II Compact (BioRobotics), fitted with solid 0.7-mm pins (Apogent).
2. ArrayWorx'e', a white light CCD scanner (Applied Precision, Issaquiah, WA) fitted with GFP filter set (Chroma, 480/520, Rockingham, VT).
3. STEP array analysis was collected with Digital Genome software (Applied Precision, Issaquah, WA).

4. Pre-cleaned white poly-L-lysine-coated microscope slides (Electron Microscopy Sciences, Hatfield, PA).
5. 384-well V-bottomed plates with covers (Genetix, Boston, MA).
6. Quadriperm plates, four-well chambered tissue culture plates (Viva Science, Littleton, MA).
7. The CMV-AP6 construct was generated using oligonucleotides containing BglII recognition sites to amplify the coding region of the mouse placental alkaline phosphatase cDNA (9) and subcloning of this fragment into CMV.Neo (10).
8. The CRE-SEAPteth construct was generated by PCR with oligonucleotides containing XbaI and FseI sites to amplify the DNA encoding the PDGF receptor transmembrane domain from the pHOOK1 plasmid and subcloning of this fragment into XbaI and FseI digested pCRE-SEAP (Promega).

2.3. ELF-97 Staining

1. ELF-97 (Invitrogen), diluted to 20 or 2% in 100 mM Tris, pH 8.3.
2. Liquid Blocker Super Pap Pen (Sigma-Aldrich).
3. Pre-cleaned white poly-L-lysine-coated microscope slides, gridded (Electron Microscopy Sciences, Hatfield, PA).
4. Paraformaldehyde (Fisher): A 3.7% (w/v) freshly prepared each experiment in 1× DPBS + calcium + magnesium (HyClone, Waltham, MA).

2.4. Mutagenesis and Cloning

1. Primers were generated to the 5′ and 3′ end of PRKG1 using Lasergene and ordered from Invitrogen. The 5′ primer is AGGCGTGTACGGTGGGAGGTCTA and the 3′ primer is ATGTTATTGCCGCAGAAGCT.
2. Genemorph II Random Mutagenesis Kit (Stratagene).
3. pGemT–Easy (Promega).
4. Standard, stackable, sterile, polysterne petri dishes (Fisher Scientific).

3. Methods

3.1. Preparing STEP Complexes

1. All DNAs were kept at 0.12 mg/ml concentration. For the dilutions of CMV-AP6 or CMV-EGFP, the total DNA was balanced with the parental vector CMV-Neo. First, the individual plasmids were prepared at 0.12 mg/ml in separate

tubes and then mixtures were prepared from these stocks for STEP complex formation.

2. A solution of 25% sucrose was made with dH_2O and filtered with a 0.2-μm filter. Sucrose was found to aid in the drying of the complexes so that the STEP complex was evenly spread across the surface of the spot.
3. STEP complexes were made by pipetting each of these components in the following order: 1 μl of 25% sucrose, 3 μl of diluted DNA, 3 μl of 0.02 μg/μl penton protein, and 3 μl of Lipofectamine 2000 (*see* **Notes 1** and **2**). The complex solution was then mixed by pipetting and incubated at room temperature for 10 min.

3.2. Automated Spotting of STEP Complexes

1. Complexes were spotted to slides in two different ways. Usually for more than 20 samples, a MicroGrid II Compact spotter was used.
2. Ten microlitre of the sample was loaded into a 384-well V-bottomed plate from Genetix. The plate was briefly centrifuged (400×*g*) before loading into the MicroGrid II Compact.
3. The spotter was programmed so that solid 0.7-mm pins dipped twice in the sample plate before depositing the sample on to poly-L-lysine slides with a 1-s dwell time under relative humidity conditions of 65–75% (*see* **Note 3**). The slides were spotted a total of three times in the same area to increase the total sample deposited on the slide. Spots were spaced 1.8 mm apart on the slide and at least 7 mm from the edge of the glass slide.
4. Slides were placed in the Quadraperm plates and allowed to dry for 2 h in a tissue culture flow hood. The lids of the plates were left off of the plates during this drying time (*see* **Note 4**).

3.3. Spotting the Complexes via Hand Spotting

1. Hand spotting was typically used if there were fewer samples. An advantage to hand spotting is that much more sample is deposited to the slide, which can aid in transfection of some cell types. However, hand-spotted slides cannot be rigorously quantified due to significant differences in spot size. Slides that were used for hand spotting are stamped with an 8×8 grid which allows for easy identification of the location of all the samples.
2. Using a 2.5-μl Eppendorf pipet, 1 μl of sample is pipetted up. The tip is then removed by hand. When this is done, the sample moves up the tip slightly but by flicking the tip downward, the sample will come down to the edge of the tip.

3. The tip was touched to the surface of the slide, which deposited a small amount of sample onto the slide. Typically, 1 μl of sample makes 10 spots of complex on the slide before needing to reload the pipet tip.
4. Slides were dried on the lab bench top for 1 h at room temperature, uncovered.

3.4. Plating of Cells to Spotted Slides

1. HEK-293T and COS cells were trypsinized and resuspended in a volume of DMEM containing 10% FCS and 5% penicillin/streptomycin that was sufficient for drop-wise adding of 1 ml of the resuspension to the top of each slide. Carefully, the slides were placed in the tissue culture incubator for 2 h while the cells attached to the slide (*see* **Note 5**).
2. After this incubation, 9 ml of additional media was added to the wells of the Quadraperm plate.
3. Cells were typically assayed 48 h after plating on to the slides.

3.5. ELF-97 Staining

1. HEK-293 or COS cells were grown on glass slides using sterile technique. However, the staining procedure was completed under non-sterile conditions on the lab bench top. The slides were removed from the Quadraperm plates with tweezers and rinsed in 1×DPBS twice.
2. Excess DPBS was drained from the slides by touching a corner of the slide to a Kim Wipe.
3. A PAP pen was used to create a barrier around the edge of the slide (*see* **Note 6**). This prevents the ELF-97 stain from draining off the slide during the staining procedure. The slides were placed in a Quadraperm plate for the staining procedure.
4. A 20 or 2% solution of Elf-97 was made in 100 mM Tris, pH 8.3 solution. This solution was added drop-wise to the slide and incubated on the cells at room temperature for 10 min (*see* **Note 7**). During the incubation, the slides were covered with aluminum foil to prevent photobleaching. Typically, between 800 μl and 1 ml, total volume of stain was placed within the hydrophobic barrier to stain each slide.
5. The slides were dipped once in 1×DPBS to remove the stain.
6. After this staining, the cells were fixed in freshly prepared 3.7% paraformaldehyde for 10 min at room temperature (*see* **Note 8**). Again, the plates are covered with aluminum foil during this incubation.
7. Slides were placed back in the Quadraperm plates, which contain 1×PBS, for imaging.

8. Slides were rinsed in dH_2O and stored dry at room temperature in the dark.

3.6. Microscopic Imaging and Quantitation

1. Imaging of the ELF-97-stained cells was completed immediately following the staining procedure.
2. Cells were viewed using an inverted fluorescent microscope using a cube specific for the 365/530 nm wavelength of ELF-97.
3. A Cool Snap HQ camera was used to capture the images. Images taken for EGFP are 10-fold higher in length of time than those of the ELF-97. Typical exposure times for EGFP are 3–4 s, whereas ELF-97 exposure times are 0.3–0.4 s.
4. Spot images were opened in MCID Basic 7.0 software.
5. Circular markers were used to select the entire area of a typical spot. This same-sized circular marker was used to quantify all of the images from the experiment.
6. Data analysis was collected under the "Study" tab, choosing "Grain Count," followed by "Scan Area" and finally setting the threshold of what the user felt was true-positive cells under "Density Levels."
7. Numerical values were collected and averaged for "Mean Grain Area." Either standard deviations or standard error of the mean was calculated.

3.7. Scanner Imaging and Quantitation

1. Mutations were screened using the Arrayworx'e', white light CCD scanner, fitted with a GFP filter set.
2. The *.mwbr file from the MicroGrid II which contains the identity of all the spots on the arrayed slide was imported to the ArrayWorx'e' scanner. This was created from a *.csv file created in Excel.
3. The Digital Genome software was used to scan and analyze the arrayed slides. The slides were inserted in to the scanner slot with the cell surface facing down.
4. Once the slide was scanned inside Digital Genome, the *.mwbr file was loaded. Spot Detection Settings was turned on and images were loaded.
5. An array of circles appeared over the image as designated by the *.mwbr file. From the Image tab, selection of "Enable Spot Movement" allowed for manual alignment of the grid file over the image to account for cell migration during the transfection.
6. Once aligned, all of the spots were selected for analysis by highlighting them and the intensity values of the spots were determined. These data were exported as a *.txt file which

was later converted to an Excel file for averaging the pixel intensities of the spots.

3.8. Mutagenesis of PRKG1

1. An expression vector encoding PRKG1 (8) was mutagenized using the GeneMorph II Random Mutagenesis Kit from Stratagene. Primers were designed around the coding region of PRKG1 between the BglII and XhoI sites of the mouse PRKG1 cDNA corresponding to the region coding for the regulatory domain of the kinase.
2. PCR was carried out with mutazyme II with an annealing temperature of 57°C and for a total of 40 cycles.
3. We found that to sufficiently mutagenize the PRKG1 coding region, we needed to amplify the PCR fragment two additional times before we saw five to eight mutations per our 1.1 kb region of interest. To do this, we used the amplified fragment from the first round of mutagenesis as template for the second round of mutagenesis. The second amplified fragment was used as template for the third round of mutagenesis. The original PCR temperatures were used for all rounds of mutagenesis.
4. After the third round of PCR mutagenesis, a library of amplified fragments were made in pGemT-Easy.
5. The mutagenized region was removed from the pGemT-Easy vector with a Bgl II and Xho I double digest. This resulting fragment was subcloned into the parental CMV-PRKG1 vector.
6. The resulting expression vectors were electroporated into XL1-Blue *Escherichia coli* and plated onto LB plates containing 0.5 mg/ml ampicillin.
7. Clones were picked from these plates and grown up in 96-well plates. These clones were then screened via PCR for the presence of insert by using the same primers that were used to do the mutagenesis.
8. Those clones that contained amplified fragment were screened via STEP transfection for their activity with CRE-d2EGFP or CRE-SEAPteth.

3.9. Solution Transfection

1. To prepare cells for transfection with Lipofectamine, HEK-293 cells were passed on to 60-mm dishes and allowed to adhere for 3 h in a 37°C incubator with 5% CO_2 in 10% FCS DMEM containing 5% penicillin/streptomycin.
2. A solution of 4 μg DNA (45% mutant PRKG1 kinase DNA, +50% HCG-luciferase+5% CMV Renilla–Luciferase) was first diluted with 150 μl of serum-free DMEM. In a separate tube, 30 μl of Lipofectamine was diluted in 150 μl of serum-free DMEM. The contents of the above tubes were mixed

and incubated at room temperature for 30 min while DNA and Lipofectamine complexes formed.

3. Growth media was removed from the HEK-293 cells and replaced with 1.2 ml of serum-free media.
4. The incubating DNA Lipofectamine complexes were diluted with 0.9 ml serum-free media and added drop-wise to the cells.
5. This was incubated at 37°C in serum-free media for 3 h before 2.4 ml complete media containing 20% FCS was added back to the plates.
6. The cells were collected 48 h after the transfection.
7. Firefly and Renilla–Luciferase activities were determined in cell extracts using the passive lysis buffer and reagents from the Dual Luciferase Assay System (Promega). The luciferase activity was collected on a FLUOstar OPTIMA plate reader.

4. Notes

1. Glycerol is another drying aid which can be used for STEP complexes. We found that including 10% glycerol to the STEP complex increases the transfection efficiency of the cell although occasionally this also caused the spots to spread on the slide.
2. Penton protein transfection efficiency varied between purification batches and the most effective penton protein concentration should be optimized for each penton protein preparation (2).
3. Environmental conditions change the manner in which the spots will dry on the slides. Changes to percentage of sucrose as well as the percent humidity used for complex spotting may be required for optimal transfection in order to compensate for lower ambient humidity.
4. Spotted slides were generally used immediately after drying, but it is possible to store spotted slides in Quadraperm plates at –20°C, wrapped in parafilm, for up to 6 months.
5. Cells should be exponentially growing when plated onto STEP complexes.
6. Some commercially available PAP pens are toxic to living cells.
7. Cleavage of the ELF-97 substrate happens very quickly and thus it is easy to saturate the fluorescent signal. Time courses should be preformed to optimize each cell type to be transfected.

8. Cells detach easily during ELF-97 staining. We found that staining the cells before they were fixed vastly improved our ability to keep cells attached to the slide during the staining process. However, it is also possible to fix the cells before staining with ELF-97. In addition, using 1×DPBS, rather than 1×PBS significantly reduces the loss of cells.

References

1. Ziauddin, J., Sabatini, D. M. (2001) Microarrays of cells expressing defined cDNAs. *Nature* 411(6833), 107–110.
2. Redmond, T. M., et al. (2004) Microarray transfection analysis of transcriptional regulation by cAMP-dependent protein kinase. *Mol Cell Proteomics* 3(8), 770–779.
3. Ren, X., Uhler, M. D. (2009) Microarray transfection analysis of conserved genomic sequences from three immediate early genes. *Genomics* 93(2), 159–168.
4. Tian, L., et al. (2007) Screening for novel human genes associated with CRE pathway activation with cell microarray. *Genomics* 90(1), 28–34.
5. Webb, B. L., et al. (2003) A reporter system for reverse transfection cell arrays. *J Biomol Screen* 8(6), 620–623.
6. Cox, W. G., Singer, V. L. (1999) A high-resolution, fluorescence-based method for localization of endogenous alkaline phosphatase activity. *J Histochem Cytochem* 47(11), 1443–1456.
7. Metz, C. N., et al. (1991) Production of the glycosylphosphatidylinositol-specific phospholipase D by the islets of langerhans. *J Biol Chem* 266(27), 17733–17736.
8. Collins, S. P., Uhler, M. D. (1999) Cyclic AMP- and cyclic GMP-dependent protein kinases differ in their regulation of cyclic AMP response element-dependent gene transcription. *J Biol Chem* 274(13), 8391–8404.
9. Brown, N. A., Stofko, R. E., Uhler, M. D. (1990) Induction of alkaline phosphatase in mouse L cells by overexpression of the catalytic subunit of cAMP-dependent protein kinase. *J Biol Chem* 265(22), 13181–13189.
10. Huggenvik, J. I., et al. (1991) Regulation of the human enkephalin promoter by two isoforms of the catalytic subunit of cyclic adenosine 3′,5′-monophosphate-dependent protein kinase. *Mol Endocrinol* 5(7), 921–930.

Chapter 5

High-Throughput Subcellular Protein Localization Using Transfected-Cell Arrays

Yuhui Hu and Michal Janitz

Abstract

Knowledge of protein localization within the cellular environment is critical for understanding the function of the protein and its regulatory networks. Protein localization data, however, have traditionally been accumulated from single or small-scale experiments. Transfected-cell arrays (TCAs) represent a robust alternative for the high-throughput analysis of gene/protein functions in mammalian cells. For protein localization studies, TCAs not only allow for the transfection and expression of over 1,000 genes in a single experiment but also make it feasible for simultaneous co-localization analyses of different subcellular compartments. In this chapter, we have described a protein co-localization protocol using transfected human cell arrays for a large set of cellular compartments, including the nucleus, ER, Golgi apparatus, mitochondrion, lysosome, peroxisome, and the microtubules, intermediate filaments and actin filaments. The application of these "organelle-co-localized cell arrays" facilitates the precise determination of the localizations of numerous recombinant proteins in a single experiment, making it currently the most efficient technique for high-throughput protein co-localization screening.

Key words: Transfected-cell array, protein localization, organelle counterstaining, reverse transfection, confocal immunofluorescence, His_6-tag.

1. Introduction

The subcellular localization of a protein can provide important information about its function within the cell. Eukaryotic cells, in particular mammalian cells, are characterized by a high degree of compartmentalization. Most protein activities can be assigned to particular cellular compartments. Categorizing proteins by subcellular localization is therefore one of the essential goals for

E. Palmer (ed.), *Cell-Based Microarrays*, Methods in Molecular Biology 706,
DOI 10.1007/978-1-61737-970-3_5,

functional genomic annotations. Protein localization experiments have been traditionally confined to only one or a few particular genes of interest. In the past, without labeling the concrete subcellular organelles, the classification of protein localization sites was often based solely on the empirical determination of subcellular structures through their morphology. For the precise identification of intracellular compartments and thus the location of studied proteins, a labeling strategy specific to each cellular organelle should be carried out in each localization experiment. This type of "protein/organelle co-localization" study is particularly difficult to perform on a large number of proteins with conventional transfection platforms, such as those using microwell plates.

Transfected-cell arrays offer a robust platform for protein co-localization studies (1). The principle of the TCA technique is based on the transfection of a set of DNA or RNA molecules that are immobilized on a solid surface in a microarray format into mammalian cells. Only the cells growing on top of the spotted nucleotides become transfected, creating spots of localized transfection within a lawn of non-transfected cells (2). Using an appropriate tagging strategy, e.g., a His_6-tagged vector (*see* **Note 1**), the localization of up to 1,000 different proteins can be monitored in one experiment by immunofluorescent labeling with anti-His antibodies. Simultaneously, organelle-specific antibodies and dyes are used to counterstain the cellular compartments with different fluorophores. The fluorescence overlap between recombinant proteins and organelle-specific markers allows for the objective determination of localization sites. A combination of the organelle-counterstaining strategy with the transfected-cell array technique makes it currently the most efficient technique for high-throughput protein co-localization screening (3).

2. Materials

2.1. Cell Culture

1. Human embryonic kidney HEK293T/17 cells (ATCC®, CRL-11268).
2. Dulbecco's modified eagle's medium (DMEM) (Gibco Invitrogen) was supplemented with 10% fetal bovine serum (Biochrom AG, Berlin, Germany), 2 mM L-glutamine (Gibco Invitrogen), and 50 units/ml penicillin and 50 μg/ml streptomycin (Gibco Invitrogen).

2.2. Array Printing

1. Gamma-amino propyl silane (GAPS) slides (Corning).
2. Standard microscopy slides, 76 × 26 × 1 mm (Menzel-Glaeser, Germany).

3. Poly-L-lysine (Sigma).
4. Vectabond solution: 350 ml acetone and 7 ml Vectabond™ (VECTOR Laboratories).
5. Virtek Chipwriter robotic arrayer (Virtek, Toronto, Canada).
6. Stealth micro spotting pins (SMP4) (Telechem International, Sunnyvale, CA).
7. Piezo Dispenser sciFlexarrayer S5 (Scienion, Germany).
8. Plastic pipetting tip for manual spotting (SAFESEAL tips PREMIUM XL, 10 µl; Biozym, Germany).
9. 384-Well plates, "V" shape (Genetix Limited, UK).
10. Nalgene vacuum desiccator with a 250-mm stopcock (VWR).

2.3. Reverse Transfection

1. Effectene Transfection Reagent Kit containing EC buffer, Enhancer, and Effectene (Qiagen, Hilden, Germany).
2. QuardriPERM plates (Greiner bio-one, Frickenhausen, Germany).
3. HybriWell™ Sealing, 40 × 22 × 0.25 mm (#HBW2240, Schleicher & Schuell, Grace Bio-labs).
4. Petri dish, 100 $mm^2 \times 15$ mm thick (Falcon®, Becton Dickinson, Germany).
5. Conical tube, 50 ml (Falcon®, Becton Dickinson).
6. Vortex Genie 2 (VWR, Darmstadt, Germany).
7. Cell culture dishes, 100 × 20 and 150 × 20 mm (TPP, Zurich, Switzerland).
8. Primary and secondary antibodies used for counterstaining procedures are listed in **Tables 5.1** and **5.2**.

2.4. General Materials

1. Mammalian expression vectors with a His_6-tag at the N-terminus of the protein-coding sequence that allows for efficient transfection and expression of recombinant proteins of interest, such as the full open reading frame of chromosome 21 proteins that are cloned into the pDEST™26 plasmid (Invitrogen) following the Gateway™ Technology (Invitrogen) (3, 4).
2. The 0.2 and 0.05% (w/v) gelatin solutions are prepared as follows: dissolve gelatin powder (Sigma, Germany) in sterile MilliQ water by gently swirling mixture for 15 min in a 60°C water bath. Cool the 0.2% gelatin solution at room temperature, and, while still warm (~37–40°C), filter it through a 0.45-µm cellular acetate (CA) membrane.

Table 5.1
Primary antibodies and counter-stains used in this study

Antibodies and counterstains	Source	Supplier	Cat. no.
Anti-adaptin-γ (clone 88)	Mouse IgG1	BD Biosciences Pharmingen	610385
Anti-calreticulin	Rabbit polyclonal IgG	Abcam, Cambridge, UK	ab4
Anti-catalase	Rabbit polyclonal IgG	Abcam, Cambridge, UK	ab1877
Anti-LAMP2	Mouse monoclonal IgG1	Developmental Studies Hybridoma Bank, Iowa City, IA, USA	H4B4
Anti-PDI (clone 1D3)	Mouse IgG1	Stressgen, San Diego, CA	SPA-891
Anti-prohibitin	Rabbit polyclonal IgG	Abcam, Cambridge, UK	ab2996
Anti-tubulin (clone DM 1A)	Mouse IgG1	Sigma, Missouri, USA	T 9026
Anti-vimentin (clone J144)	Mouse IgM	ABR Affinity BioReagents, Golden, CO, USA	MA3-745
DAPI	–	Sigma	D-8417
Lectin GS-II from *Griffonia simplicifolia*, AlexaFluor488 conjugate	–	Molecular Probes; Invitrogen	L-21415
Rhodamine–phalloidin	–	Molecular Probes; Invitrogen	R-415
Anti-His tag antibody	Mouse monoclonal IgG1	DPC Biermann	SM1693P
Anti-His tag antibody	Goat polyclonal IgG	Abcam, Cambridge, UK	ab9136
Anti-His (C-term) antibody	Mouse monoclonal IgG2b	Invitrogen	R930-25
Anti-His G antibody	Mouse monoclonal IgG2a	Invitrogen	R940-25
Penta•His AlexaFluor 488 antibody	Mouse monoclonal IgG1	Qiagen	35310
Penta•His AlexaFluor 555 antibody	Mouse monoclonal IgG1	Qiagen	35350
Penta•His antibody	Mouse monoclonal IgG1	Qiagen	Kit 34698
RGS•His antibody	Mouse monoclonal IgG1	Qiagen	Kit 34698
Tetra•His antibody	Mouse monoclonal IgG1	Qiagen	Kit 34698

DAPI, 4, 6-diamidino-2-phenylindole; LAMP2, lysosome-associated membrane glycoprotein 2 (precursor); PDI, protein disulfide isomerase.

Store the aliquots of filtered gelatin solution at 4°C until use. For 0.05% gelatin solution, dilute 0.2% gelatin solution with sterile water to a final concentration of 0.05%.

3. Effectene Transfection Reagent Kit containing EC buffer, Enhancer, and Effectene (Qiagen).
4. EC buffer (from Effectene Transfection Kit) containing 0.2–0.4 M sucrose (Invitrogen).
5. Paraformaldehyde, formaldehyde (Merck).

Table 5.2
Secondary antibodies used for protein co-localization and cell death detection

Antibodies and counterstains	Source	Supplier	Cat. No.
AlexaFluor488-anti-mouse IgG (H+L)	Goat F(ab′)2	Molecular Probes; Invitrogen	A-11017
AlexaFluor568-anti-mouse IgG (H+L)	Goat F(ab′)2	Molecular Probes; Invitrogen	A-11019
AlexaFluor488-anti-rabbit IgG (H+L)	Donkey	Molecular Probes; Invitrogen	A-21206
AlexaFluor555-anti-rabbit IgG (H+L)	Goat F(ab′)2	Molecular Probes; Invitrogen	A-21430

6. Triton X-100 (Sigma).
7. Saponin (Carl Roth GmbH., Karlsruhe, Germany).
8. Bovine serum albumin (BSA) (PAA Laboratories).
9. Blocking solution: 5.0% BSA in PBS.
10. Antibody dilution solution: 0.5% BSA in PBS.
11. Mounting reagent-1: Prolong Gold Antifade Reagent (Molecular Probes).
12. Mounting reagent-2: Fluoromount-G (Southern Biothechnology).
13. The filter sets used for image acquisition with BioCCD scanning were listed in **Table 5.3**.

Table 5.3
The filter sets used for image acquisition with BioCCD scanning system

Fluorescence	Excitation filter	Emission filter
AlexaFluor 488	470/30	510/20
AlexaFluor 568, AlexaFluor 555	565/20	596/14

3. Methods

The success of DNA and protein microarrays has motivated researchers to miniaturize cell-based functional studies in a high-density array format. The transfected-cell array (TCA) combines the DNA or RNA microarray platform with cellular biology

techniques such as cell transfection and detection assays to achieve high-throughput functional analyses in mammalian cells. Briefly, the process of a TCA can be divided into the following three distinct steps: (i) DNA or RNA microarray preparation, (ii) reverse transfection of cells, and (iii) functional detection assay (**Fig. 5.1**) (5).

In the process of preparing microarrays for TCA, expression vectors containing the open reading frames (ORFs) are printed on commercial glass slides, as previously described by Ziauddin and Sabatini (6). For DNA spotting on cell arrays, the robotic arrayers used to manufacture classical DNA microarrays can be used. The design of cell arrays does not differ from the classical DNA or protein microarray, and the same robotic arrayer software

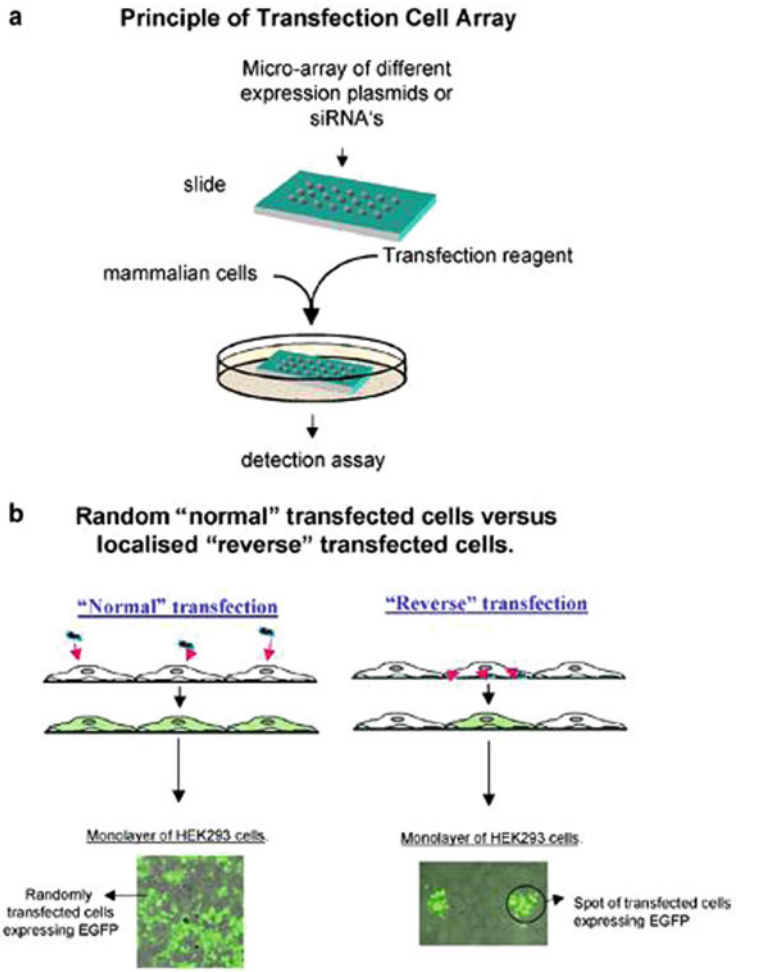

Fig. 5.1. TCA technology combines the microarray technique with living cells (**a**). Reverse transfection allows for multiple, spatially separated transfections of nucleic acids in a single experiment (**b**). Adapted by permission from Macmillan Publishers Ltd: Oncogene, 2004.

can be used to arrange the spots on the slide. The preparation of DNA samples for cell arrays differs, however, from the sample preparation for traditional DNA or protein microarrays, where spotted probes are used for hybridization (*see* **Note 2**). In cell arrays, the expression vectors cannot be permanently immobilized on the solid surface because they have to be subsequently transfected into the cells growing on top of the array. Therefore, DNA samples are prepared in gelatin solution to equilibrate the adherence of nucleotides on the glass slide before transfection and the release of molecules into the cells during transfection.

In the second step of TCA experiments, adherent cells are added on top of the arrayed slide to form a cell monolayer that covers the spotted nucleic acids. This step has been named "reverse transfection" by Ziauddin and Sabatini. The cells are transfected by the nucleic acids that are immobilized underneath rather than by the nucleic acids that are added from the top, as in normal transfection. Along with the release of DNA from the solid surface, only the cells growing on top of the DNA or RNA spots take the nucleotide molecules up and become transfected. Consequently, in contrast to normal transfection, where transfection events occur throughout the entire cell layer, reverse transfection takes place in spatially separated groups of cells and allows for the investigation of multiple targets in a single experiment (**Fig. 5.1b**). The arrayed DNA spots must be incubated with suitable transfection reagents before the addition of cells on top of the slides.

Depending on the purpose of the experiment, a variety of assays can be carried out on either living or fixed cells to monitor the effects of protein overexpression or gene silencing. Some changes in cellular morphology, such as cell death, can be directly inspected under the light microscope. Most phenotypic effects, however, have to be detected using specific cell-based bioassays. These comprise fluorometric, colorimetric, and luminescent assays, which monitor the apoptosis, cell proliferation and signaling, and individual protein features. The most common method used for TCA is based on the detection of fluorescence emitted from fluorophores (e.g., Cy3, Cy5, or Alexa dyes) coupled to cellular components by antibodies or, alternatively, through non-immunological labeling. For signal acquisition, fluorescent microscopy and fluorescence-based scanners are used in most of cases. Standard microarray-based software can also be used for image analysis, including identifying and quantifying the signal recorded on cell arrays.

For protein localization, in our own study, open reading frames of the human chromosome 21 (Chr.21) proteins were cloned into an expression vector with a His_6-tag at the N-terminus of the protein coding sequence (3) (*see* **Note 3**). This plasmid construct architecture allows for simultaneous

transfection, expression, and detection (using anti-His-tag antibodies) of recombinant proteins across the cell array. Likewise, by applying appropriate organelle markers, cells covering the array can be counterstained to identify cellular compartments. The capacity to investigate hundreds of proteins in a single-cell array experiment currently makes the TCA approach the most efficient technique for high-throughput co-localization screening.

Transfected-cell arrays are prepared in the following three steps: (i) probe (DNA–gelatin mixture) preparation, (ii) array printing, and (iii) reverse transfection of spotted arrays into Hek293T cells.

3.1. Probe Preparation: Gelatin–DNA Method

In the gelatin method, DNA samples dissolved in gelatin solution are first arrayed on the glass slides, and, subsequently the transfection reagent is added to all the samples just before transfection. To prepare each gelatin–DNA sample for printing, in a 1.5-ml sterile tube or a 96-well plate, each purified plasmid DNA is diluted 10 times, with 0.2% gelatin solution, to a final DNA concentration of 0.04–0.07 μg/μl. Higher dilutions might also be used; however, the final concentration of gelatin has to remain between 0.2 and 0.17% (*see* **Note 4**). After dilution, the DNA–gelatin samples are mixed and stored at 4°C before printing.

3.2. Probe Preparation: Lipid–DNA Method

In the lipid method, the lipid-based transfection reagent is premixed with the DNA before printing. In our study, we used this approach to successfully transfect Chr.21 ORF plasmids whose transfection efficiencies appeared to be low using the gelatin method (*see* **Note 5**). The protocol comprises the following steps:

1. In a 1.5-ml tube, add 1–2 μg DNA to 15 μl DNA-condensation buffer (Buffer EC from Effectene Kit), in which the filter-sterilized sucrose has been dissolved to a concentration of 0.2–0.4 M.
2. Add 1.5 μl Enhancer solution from the Effectene Kit, mix the tube contents by pipetting up and down five times, and then incubate the mixture at room temperature for 5 min.
3. Add 5 μl Effectene transfection reagent from the Effectene Kit and mix the solution by gentle vortexing. Incubate at room temperature for 10 min (*see* **Note 6**).
4. Add a 1×(24 μl) volume of 0.05% gelatin, remix the solution, and store it at 4°C before printing (*see* **Note 7**).

3.3. Array Printing

Depending on the number of samples to be printed in each test, manual spotting or robotic spotting can be applied. For robotic spotting, both the arrayers utilizing solid contact pins and nanodispensing technique can be used. With either printing method, the DNA probes are printed onto glass slides coated with gamma-amino propyl silane. Alternatively, the slides can be treated with

poly-L-lysine (Sigma). Following printing, the glass slides were air-dried and stored in a vacuum desiccator at room temperature prior to reverse transfection. For long-term use of the slides printed with lipid–DNA samples, storage at 4°C is necessary to maintain the effectiveness of transfection reagents.

3.4. Preparation of Poly-L-Lysine–Coated Glass Slides for Cell Array Use

1. Incubate normal microscopy slides with cleaning solution (70 ml of 1.75 M NaOH, 240 ml ethanol, and 160 ml sterile H_2O) for 2 h at room temperature, followed by three washes with sterile H_2O.
2. Wash the slides with acetone for 5 min and briefly let them air-dry.
3. Immerse the slides in the Vectabond solution for 5 min.
4. Rinse the slides briefly three times with sterile H_2O.
5. Dry the slides in a 37°C oven.
6. Treat the slides with poly-L-lysine solution (20 ml poly-L-lysine, 20 ml PBS, and 160 ml H_2O) in plastic containers at 4°C for 45 min.
7. Wash the slides with H_2O and let them dry in a sterile environment.
8. Incubate the slides at 55°C for 40 min.
9. Keep the slides in the dark in a vacuum desiccator before use.

3.5. Solid Pin-Contact Printing

The spotting procedure is carried out using a robotic arrayer and SMP4 solid pins in a laminar-flow hood (**Fig. 5.2a**). The gelatin- or lipid-prepared DNA samples are transferred into a 384-well plate ("V" shape) before printing. The robot is programmed to transfer the samples to the slides by touching the pins to the slide surface for 25–50 ms (**Fig. 5.2b**). Using SMP4 pins, the printed spots have a diameter of 120 μm. A distance of 400 μm between spots is usually used. The pins are washed thoroughly between each dip into a new well of samples, and the entire printing hood is set to 55% humidity. The thorough wash step and 55% relative humidity environment are important to prevent clogging of samples in the arraying pins. In our study, each Chr.21 gene was spotted at least in triplicate, while GFP and/or HcRed genes were spotted along in each row and column to facilitate the visualization of the printing grid. **Figure 5.2c** shows one spotting grid of dried 9 × 8 spots. The image was taken using a light microscope.

3.6. Printing Using sciFlexarrayer

Compared to solid pin-contact printing, the microdispensing technique is more flexible for printing sample spots with preferential diameters and volumes. The print head of the microdispensing arrayer has a form of nozzle array; once filled with samples, the print head releases a single droplet from each nozzle to the surface

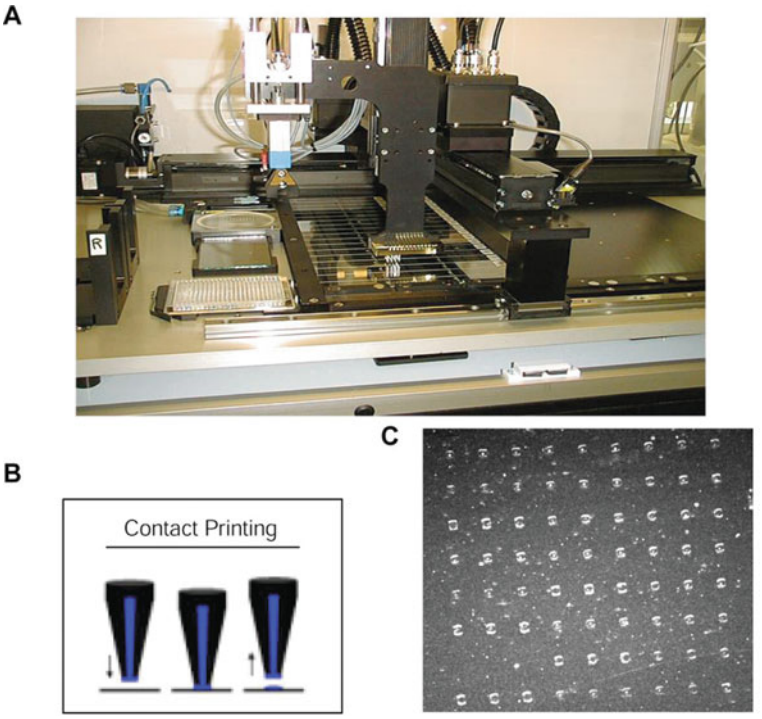

Fig. 5.2. Solid pin-contact printing of cell arrays. The spotting hood used in this study, which contains Virtek Chipwriter robotic arrayer and Telechem's Stealth pins (type SMP4) (**a**). Schematic view of contact printing (**b**). A spotting grid of 9 × 8 spots under light microscopy (**c**). See text for more details.

of the slides without contacting the slides (**Fig. 5.3a**). By adjusting the number of drops that compose the dispensing droplet, samples can be printed with different volumes and spot diameters (**Fig. 5.3b**). In our study, we utilized the sciFlexarrayer S5 piezo dispenser where 2.5 drops contain 1 nl of sample, while 20 drops result in a printing spot of 400 μm in diameter.

3.7. Manual Printing

In some experiments with small numbers of samples, manual printing is an efficient and quick alternative to robotic arrayers. To guide the position of printing, a spotting grid of desired size and distance is drawn on a piece of paper or on a transparent slide. The glass slides are placed on top of the spotting grids, so that the spots can be printed following the grid coordinates. In our study, we usually designed spotting grids of 1.5 × 1.5 mm for each square. The ready-to-print DNA samples were spotted at the center of each square without surpassing the lines, so that they were well separated from the adjacent spots. An example of a printing grid with 19×10 spots is shown in **Fig. 5.4**.

The spotting procedure is carried out under a sterile cell culture hood. Guided by the spotting grid, the samples are printed by quickly touching the long pipette tips filled with 1 μl sample

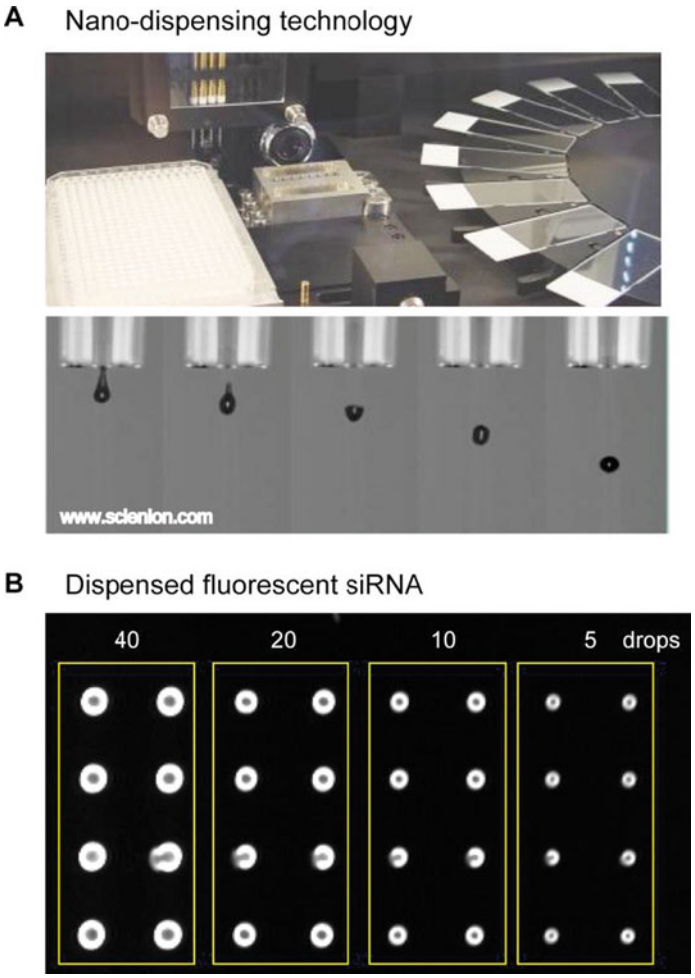

Fig. 5.3. Dispensing printing of cell arrays using a sciFlexarrayer. (**a**) The spotting hood used in this study and a dispensing process from a single print head (www.scienion.com). (**b**) Four spotting grids of 2×4 spots of rhodamine-labeled siRNA. With different numbers of spotting "drops," arrays were produced with different sample volumes and diameters.

on the surface of the cell array slide (**Fig. 5.4**). By using this type of tip, each spot contains 10–15 nl of the samples, and a batch of slides can be spotted using the same tip for each sample multiple times.

3.8. Reverse Transfection

In this step, HEK293T cells are added on top of the slides printed with gelatin- or lipid-treated DNA for the reverse transfection (*see* **Note 8**). When stored appropriately (*see* **Section 3.3.**), the "gelatin-DNA" slides can be used within one month after printing whereas we normally used the "lipid-DNA" slides within one week for efficient reverse transfection.

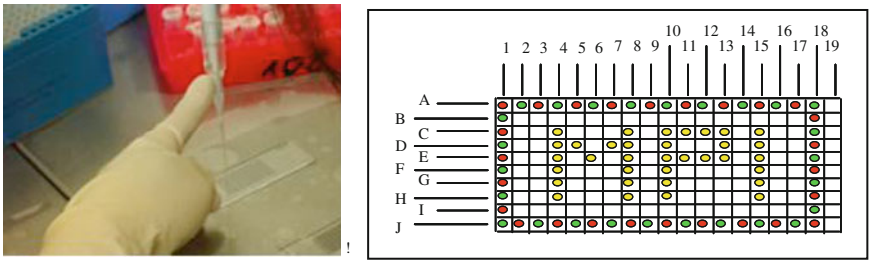

Fig. 5.4. Manual printing of cell arrays. Sample solutions were spotted by quickly touching the long pipette tips (SAFE-SEAL tips PREMIUM XL, Biozym) to the surface of the cell array slide (*left*), which was laid on top of a printing grid (*right*).

3.8.1. Cell Preparation for Reverse Transfection

Approximately 24 h before transfection, cells are split and plated into new culture dishes. We plated 10×10^6 HEK293T cells in 10 ml media in a 100 × 20-mm dish. Alternatively, 5×10^6 HEK293T cells could be cultured for 2 days before transfection. In both cases, cells are actively growing at a nearly confluent density when harvested. Immediately before reverse transfection, the cells are harvested according to a routine protocol. The harvested cells are counted and diluted in a 50-ml conical tube (Falcon) to reach a desired density; to cover one printed slide (76 × 26 × 1 mm) in one well of a QuadriPerm chamber, 3.5×10^6 HEK293T cells should be aliquoted in 8 ml culture media. The cells are mixed thoroughly before use. In case of delays in the transfection, the cells can be kept in the CO_2 incubator for up to 40 min. In this case, the cells should always be re-suspended by pipetting or inverting the tube a few times immediately before adding them to slides.

3.8.2. Reverse Transfection of Lipid–DNA Slides

Slides printed with lipid–DNA samples are ready for transfection without additional treatment with transfection reagents. Because this type of slide is normally stored at 4°C, it is important to adjust the slides back to room temperature before taking them out of the vacuum desiccator. Under a tissue culture hood, the slides are put into each well of a QuadriPerm plate, and the cells are gently added on top of each slide along with the areas without spots. Without agitation, the QuadriPerm plate is carefully transferred into a normal 37°C, 5% CO_2, humidified incubator for the desired culturing period.

3.8.3. Reverse Transfection of Gelatin–DNA Slides

Slides printed with gelatin–DNA samples have to be treated with transfection reagents before adding the cells. Effectene Transfection Reagent Kit containing EC buffer, Enhancer, and Effectene was used for the transfection of slides printed with Chr21ORF-expression plasmids. We used a ratio of EC buffer:Enhancer:Effectene of 150:16:25. In a 1.5-ml microcentrifuge tube, 16 μl Enhancer is added to 150 μl EC buffer and

incubated for 5 min at room temperature (*see* **Note 6**). Then, 25 μl Effectene transfection reagent is added and mixed by slight vortexing for 3–4 s (setting 4 on Vortex Genie 2). A volume of 190 μl of the transfection reagent mixture should be enough to treat one printed slide with the help of the HybriWell Sealing system. The procedure for HybriWell usage is as follows:

1. Peel off the adhesive protection from the HybriWell and lay the HybriWell in a clean square dish with the adhesive side facing up.
2. Using a 200-μl pipette tip, move all the transfection mix (~191 μl) to the center of the HybriWell, and then slowly put one gelatin–DNA printed slide on the top of the HybriWell and let the transfection reagent evenly distribute over the slide. Alternatively, the slide can be attached to the HybriWell, and then the transfection mix can be pipetted through one of the ports of the HybriWell to cover the slide.
3. Incubate the array with the transfection reagent for 20 min before aspirating the reagents by vacuuming or pipetting.
4. Pull off the HybriWell using a thin-tipped forceps or fingers, and place the slide into one well of a QuardriPERM plate.

The addition of cells and culturing of slides are the same as for lipid–DNA slides.

3.9. Immunofluorescent Labeling of His_6-Tagged Recombinant Proteins

Antibodies against the His_6 epitope are used to label the expressed proteins with a His_6 tag at the N-terminus. To assess the performance of antibodies from different manufactures, His_6-tagged eGFP (enhanced green fluorescent protein) can be expressed on cell arrays, followed by anti-His antibody labeling with a red fluorochrome. The labeling performance of antibodies would be evaluated based on the overlap between the red signal and the GFP signal. We screened seven antibodies in this way (**Table 5.4**), and Penta•His Alexa Fluor antibodies gave the most sensitive and specific labelling

Table 5.4
Immunofluorescent labeling performance of seven anti-His antibodies

Antibody name	Tetra•His	Penta•His	RGS•His	Penta•His Alexa555/ Alexa488	Anti-HisG	Anti-His tag
Resource	Qiagen	Qiagen	Qiagen	Qiagen	Invitrogen	DPC Biermann
IF Performance	Unspecific	Unspecific	Low intensity	Specific; sensitive	Unspecific	Unspecific

IF, immunofluorescence labeling.

After the expression of His_6-tagged recombinant proteins, the cells growing on cell arrays are gently washed once with PBS, followed by a 20-min fixation at room temperature with 3.7% paraformaldehyde in the PBS containing 4.0% sucrose. The fixed slides are rinsed for 1–2 min in PBS prior to immunofluorescent labeling. Alternatively, the rinsed slides can be stored at 4°C in PBS for up to 1 week before further processing.

At the time of examination of anti-His antibodies, the fixed slides are processed using the following protocol:

1. Permeabilize the slides for 15 min in 0.1% Triton X-100 in PBS or 0.5% saponin in PBS, followed by rinsing.
2. In a humid chamber, block slides for 1 h with 500 μl blocking solution (5.0% BSA in PBS) per slide.
3. Drain excess blocking solution from the slides and, without rinsing, add 500 μl freshly diluted anti-His antibody. Incubate for 2 h. Another primary antibody that does not cross-react with anti-His antibody may be incubated in this step.
4. Wash slides 3×5 min in PBS.
5. For slides stained with Penta●His Alexa Fluor 555 or 488 antibodies, go directly to Step 6.
6. For slides stained with the anti-His antibodies without fluorochrome conjugation, follow Step 5.
7. Re-block slides for 20 min with blocking solution before adding 500 μl freshly diluted fluorochrome-conjugated secondary antibody (**Table 5.2**). Incubate for 40 min.
8. Wash slides 3 × 5 min in PBS. Let the slides air-dry and mount the slides with ProLong® Gold Antifade reagent following the manufacturer's instructions.
9. Store the labeled slides in the dark at 4°C until examination with fluorescent microscopy or laser scanning. During the entire labeling process, special attention must be paid to protect cells from drying out. Keep the slides in the dark to avoid fluorescence bleaching.

3.10. Cell Organelle Counterstaining

Instead of ectopic expression of control proteins, the in situ components of organelle structures can be used as localization markers. Antibodies and/or dyes that specifically interact with an organelle-specific component have been shown to be effective in accurately identifying the subcellular localization of single proteins. However, it has not yet been applied to large-scale characterizations.

In our study, we developed a high-throughput co-localization method for many organelles on cell arrays. Organelle-specific antibodies or dyes from different suppliers were screened and their performing conditions optimized. In total, nine reagents were found to provide sensitive and specific organelle

Table 5.5
Organelle markers used for co-localization study on cell array

Organelle	Marker	Counterstaining method	Supplier
Successful markers			
Nucleus	DAPI	1	Sigma
F-actin	Phalloidin (rhodamine-conjugated)	2	Molecular Probes
Mitochondria	Prohibitin antibody (rabbit)	3	Abcam
Peroxisome	Catalase antibody (rabbit)	3	Abcam
ER	PDI (mouse)	4	Stressgen
Golgi	Adaptin-γ (mouse)	4	BD Biosciences
Lysosome	LAMP2 (mouse)	4	H4B4, Developmental Studies Hybridoma Bank
Microtubule	α-Tubulin (mouse)	4	Sigma
Intermediate filament	Vimentin (mouse)	4	Affinity BioReagents
Failed markers			
Golgi	Lectin GS-II		Molecular Probes
ER	Calreticulin antibody (rabbit)		Abcam

labeling (**Table 5.5**). They were subsequently counterstained with Penta•His AlexaFluor antibodies for a co-localization study of Chr.21 proteins.

3.10.1. Counterstaining Method 1

The blue fluorescent DAPI stain is used to label nuclear double-stranded DNA (dsDNA). For each cell array slide, DAPI is always added after all the other stains. Immediately before the PBS wash, the DAPI working solution (300 nM) is diluted from the DAPI–dimethylformamide (DMF) stock solution (prepared following the manufacturer's instructions) and added onto cell arrays to incubate on the cells for 5 min. After three PBS washes, the slides are mounted as described above.

3.10.2. Counterstaining Method 2

Phalloidin, a bicyclic peptide, has been used to specifically stain F actin (7). For co-localization of Chr.21 proteins with F actin, a working solution of rhodamine–phalloidin (0.5 μg/ml) is prepared together with mouse Penta•His Alexa 488 antibody (2.5 μg/ml) with antibody dilution solution. Following the protocols as described in **Section 3.5**, **Step 1**, the cell array slides are fixed, permeabilized, and blocked. The incubation of rhodamine–phalloidin and Penta•His Alexa 488 antibody is performed at room temperature for 2 h, followed by DAPI staining, final washing, and mounting.

3.10.3. Counterstaining Method 3

Prohibitins are ubiquitous, abundant, and evolutionarily strongly conserved proteins located in the inner membrane of mitochondria (8, 9). They appear to be reliable markers of mitochondria in many applications. Catalase is the classical marker for peroxisomes and is the most abundant protein within peroxisomes (10).

In counterstaining method 3, cell arrays are fixed with 100% methanol (might contain 2% formaldehyde) at –20°C for 10 min, followed by three PBS washes. Without permeabilization, the cells are directly treated with blocking solution prior to incubation with primary antibodies. Anti-prohibitin and anti-catalase antibodies are diluted to their working concentrations of 5 and 10 μg/ml, respectively, together with Penta•His Alexa 555 or 488 antibody (2.5 μg/ml). Primary antibody incubation, washing, and re-blocking of the cell arrays are conducted under the same conditions as described in **Section 3.2**, **Step 1**. Staining with secondary antibodies is performed with Alexa488-conjugated donkey anti-rabbit IgG antibody (~6 μg/ml) or Cy^3-conjugated mouse anti-rabbit IgG antibody (~5 μg/ml) depending on which Alexa Fluor or His antibody was used. The conditions of DAPI staining and mounting of the cell arrays are the same as above.

It should be mentioned that the His-antibody staining method described in **Section 3.2**, **Step 1** is not optimal for anti-prohibitin labeling. Different fixatives have been found to influence the staining performance of the prohibitin antibody. Labeling of prohibitin following formaldehyde–PBS fixation leads to high background, whereas staining in the presence of a methanol-based fixative is strong and specific. Methanol fixative, however, does not improve the staining performance of the rabbit antibody against calreticulin, an ER-specific protein

3.10.4. Counterstaining Method 4

PDI (protein disulfide isomerase), adaptin-γ, LAMP2 (lysosome-associated membrane glycoprotein 2), α-tubulin, and vimentin are specifically localized in the ER lumen, the vesicles of the Golgi complex, the membrane of lysosomes and endosomes, the microtubules, and the intermediate filaments, respectively (11–15).

Mouse antibodies against these organelle-marker proteins (**Table 5.5**) are specific when used alone. The counterstaining of these mouse antibodies with mouse Penta•His Alexa Fluor antibodies, however, must be performed separately, before His-antibody staining, to avoid cross-reaction.

Treatment of cell arrays for immunofluorescent labeling with mouse organelle-specific antibodies is performed following the conditions described in **Section 3.2**, **Step 1**, but without the use of anti-His antibody. Successful working solutions of the antibodies are 4 μg/ml for anti-PDI, 5 μg/ml for anti-Adaptin-γ, 1.5 μg/ml for anti-LAMP2, 8.5 μg/ml for anti-α-tubulin, and

a 1:30 dilution for the anti-vimentin antibodies. The antibodies are incubated for more than 2 h at room temperature or for overnight at 4°C. Secondary antibody labeling is performed with Alexa488- or Alexa568-conjugated goat anti-mouse IgG antibody (3–6 μg/ml). Subsequently, the excess secondary antibodies are removed by washing thoroughly with PBS 4×5 min. To block the remaining IgG-binding sites on the secondary antibody, the cell array is incubated for 1 h at room temperature with 20% normal mouse serum. After draining the excess serum, a Penta•His Alexa 555 or Alexa 488 antibody whose fluorescence color is different from the secondary antibody is added to detect the His_6-tagged recombinant proteins. After incubating for 2 h at room temperature, the cell arrays are subjected to the DAPI staining, final washing, and mounting.

3.11. Image Acquisition and Analysis

We used the BioCCD scanning system to observe transfected cell clusters throughout the entire cell array. To identify specific localization sites of proteins, confocal microscopy was utilized. Through the application of organelle-specific markers, the localization of a protein can be precisely determined based on the merged fluorescence color resulting from the overlap of protein and organelle stains. The application of this "organelle-colocalized cell array" allows for the determination of the localizations of up to 1,000 recombinant proteins in a single experiment. It also permits the observation of all possible location sites for every studied protein, which, in some cases, reflects the dynamic protein-sorting and translocation behavior inside the cells, thus providing more information about its function. Furthermore, organelle labeling permits a detailed investigation of cellular morphological alterations as a result of the expression of exogenous proteins. Changes in cellular morphology (including organelle phenotypes) between transfected and non-transfected cells can be easily distinguished. Moreover, aberrant cellular phenotypes, together with the protein localization features, might provide important clues about the cellular functions of the proteins as well as their regulatory mechanisms.

4. Notes

1. In this study, we tagged the recombinant proteins with a small His_6 (6-aa) epitope at the N-terminus for the simultaneous immunohistological detection of the expressed proteins on cell arrays. Other small peptides, such as FLAG (8-aa) and Myc (11-aa) tags, can be used in the cloning/tagging strategy. The following protocols for cell

array and co-localization studies stay the same as we have described here, except with the replacement of the anti-His antibody with ones corresponding to the new epitopes. The use of auto-fluorescent proteins (e.g., GFP and its spectral derivates) as fusion tags can facilitate the visualization of protein expression and localization in living cells. However, presence of a large tag (~28 kDa for GFP alone) may influence the native localization of test proteins. For example, GFP fusion has been found to result in protein mislocalization due to alterations in the folding of the protein or to masking of the targeting signal peptide (16, 17).

2. The quality of plasmid purification also has an impact on the transfection efficiency in cell microarrays. To reduce the cytotoxicity introduced by the plasmids, a high quality of plasmid preparation reagents should be used. We generally use Qiagen's endotoxin-free maxi-preparation kit and Miniprep kit for large- and small-scale plasmid preparations, respectively.
3. The issue of which end of the recombinant protein the fusion tag should be inserted has always been raised in protein localization studies. A common preference is to use a C-terminal tag or, if possible, both N- and C-terminal tags. This is because N-terminal fusion of GFP has been found, in some cases, to mask the targeting signals of mitochondrial and plasma membrane proteins (18). However, misdirection of ER and peroxisomal proteins has also been described in proteins with a C-terminal GFP tag (19, 20). In both cases, the localization artifacts should be considered to result from the GFP tag itself in addition to its masking or disruption of the signal peptide. GFP alone has preferential localization in the nucleus and cytoplasm and its large size may interfere with the process of protein targeting, which might happen at both the N-terminus (e.g., signal peptide cleavage) and the C-terminus (e.g., palmitoylation or farnesylation) (21, 22) in a single protein. In our study, we used small epitopes to retain the physiological function of tagged proteins, and the localization results from N-terminal His_6-tags were almost completely confirmed with C-terminal Myc tag. However, for those clones that failed to be detected using N-terminal tags, changing the fusion terminus may help reveal their localization behaviors.
4. The concentrations of plasmid and gelatin in the DNA–gelatin mixture that are spotted on the glass slide are another key for successful reverse transfection on cell microarrays. The final concentration of gelatin solution must be between 0.2 and 0.18%, whereas the final concentration of plasmid DNA should be over 50 ng/μl. Consequently, the

plasmid in the undiluted stock solution should reach at least 0.8 μg/μl.

5. Pre-mixing the plasmid DNA with transfection reagents (the lipid method) before spotting generally provides better transfection efficiency on cell array than the gelatin method. However, the former requires the use of more transfection reagents as well as more preparation steps. The lipid–DNA method was used in our study to transfect a few Chr.21ORF plasmids whose transfection efficiencies appeared low using the gelatin method.
6. Similar to normal transfection, the ratio of nucleic acids to transfection reagents and the incubation time are also critical to transfection efficiency on cell arrays, and they have to be optimized for each cell line. Our experience clearly indicates that HEK293T cells render higher transfection efficiency over HEK293, both of which are better than HeLa.
7. Slides printed with lipid–DNA samples are ready for transfection without additional treatment with transfection reagents. Since this type of slide is normally stored at 4°C, it is particularly important to pre-warm the slides back to room temperature before removing them from the vacuum desiccator.
8. In the reverse transfection of cell arrays, special attention should be paid to the amount of cells used. The cells must be sufficient to grow as a monolayer covering every nucleic acid spot throughout the slide. On the other hand, the number of cells should not be too high to avoid cell death due to overgrowth. Compared to HEK293T cells, much fewer HeLa cells should be loaded on each cell array; to cover one printed slide (76 × 26 × 1 mm) in one well of a QuadriPerm chamber (Greiner), 1.0×10^6 HeLa cells in 8 ml culture media should be plated.

References

1. Hu, Y. H., Vanhecke, D., Lehrach, H., Janitz, M. (2005) High-throughput subcellular protein localization using cell arrays. *Biochem Soc Trans* 33, 1407–1408.
2. Cheng, X., Guerasimova, A., Manke, T., Rosenstiel, P., Haas, S., Warnatz, H. J., Querfurth, R., Nietfeld, W., Vanhecke, D., Lehrach, H., Yaspo, M. L., Janitz, M. (2010) Screening of human gene promoter activities using transfected-cell arrays. *Gene* 450, 48–54.
3. Hu, Y. H., Warnatz, H. J., Vanhecke, D., Wagner, F., Fiebitz, A., Thamm, S., Kahlem, P., Lehrach, H., Yaspo, M. L., Janitz, M. (2006) Cell array-based intracellular localization screening reveals novel functional features of human chromosome 21 proteins. *BMC Genomics* 7, 155.
4. Hu, Y., Lehrach, H., Janitz, M. (2010) Apoptosis screening of human chromosome 21 proteins reveals novel cell death regulators. *Mol Biol Rep*, 37:3381–3387.
5. Vanhecke, D., Janitz, M. (2005) Functional genomics using high-throughput RNA interference. *Drug Discov Today* 10, 205–212.
6. Ziauddin, J., Sabatini, D. M. (2001) Microarrays of cells expressing defined cDNAs. *Nature* 411, 107–110.
7. Wieland, T., Govindan, V. M. (1974) Phallotoxins bind to actins. *FEBS Lett* 46, 351–353.

8. Ikonen, E., Fiedler, K., Parton, R. G., Simons, K. (1995) Prohibitin, an antiproliferative protein, is localized to mitochondria. *FEBS Lett* 358, 273–277.
9. Nijtmans, L. G., de Jong, L., Artal Sanz, M., Coates, P. J., Berden, J. A., Back, J. W., Muijsers, A. O., van der Spek, H., Grivell, L. A. (2000) Prohibitins act as a membrane-bound chaperone for the stabilization of mitochondrial proteins. *Embo J* 19, 2444–2451.
10. Bendayan, M., Reddy, J. K. (1982) Immunocytochemical localization of catalase and heat-labile enoyl-CoA hydratase in the livers of normal and peroxisome proliferator-treated rats. *Lab Invest* 47, 364–369.
11. Cumming, R., Burgoyne, R. D., Lytton, N. A. (1984) Immunofluorescence distribution of alpha tubulin, beta tubulin and microtubule-associated protein 2 during in vitro maturation of cerebellar granule cell neurones. *Neuroscience* 12, 775–782.
12. Franke, W. W., Schmid, E., Winter, S., Osborn, M., Weber, K. (1979) Widespread occurrence of intermediate-sized filaments of the vimentin-type in cultured cells from diverse vertebrates. *Exp Cell Res* 123, 25–46.
13. Gough, N. R., Fambrough, D. M. (1997) Different steady state subcellular distributions of the three splice variants of lysosome-associated membrane protein LAMP-2 are determined largely by the COOH-terminal amino acid residue. *J Cell Biol* 137, 1161–1169.
14. Noiva, R., Lennarz, W. J. (1992) Protein disulfide isomerase. A multifunctional protein resident in the lumen of the endoplasmic reticulum. *J Biol Chem* 267, 3553–3556.
15. Robinson, M. S. (1990) Cloning and expression of gamma-adaptin, a component of clathrin-coated vesicles associated with the golgi apparatus. *J Cell Biol* 111, 2319–2326.
16. Brosius, U., Dehmel, T., Gartner, J. (2002) Two different targeting signals direct human peroxisomal membrane protein 22 to peroxisomes. *J Biol Chem* 277, 774–784.
17. Pouli, A. E., Kennedy, H. J., Schofield, J. G., Rutter, G. A. (1998) Insulin targeting to the regulated secretory pathway after fusion with green fluorescent protein and firefly luciferase. *Biochem J* 331, 669–675.
18. Wiemann, S., Arlt, D., Huber, W., Wellenreuther, R., Schleeger, S., Mehrle, A., Bechtel, S., Sauermann, M., Korf, U., Pepperkok, R., Sultmann, H., Poustka, A. (2004) From ORFeome to biology: a functional genomics pipeline. *Genome Res* 14, 2136–2144.
19. Huh, W. K., Falvo, J. V., Gerke, L. C., Carroll, A. S., Howson, R. W., Weissman, J. S., O'Shea, E. K. (2003) Global analysis of protein localization in budding yeast. *Nature* 425, 686–691.
20. Wiemann, S., Bechtel, S., Bannasch, D., Pepperkok, R., Poustka, A. (2003) The german cDNA network: cDNAs, functional genomics and proteomics. *J Struct Funct Genomics* 4, 87–96.
21. Davis, T. N. (2004) Protein localization in proteomics. *Curr Opin Chem Biol* 8, 49–53.
22. Ogawa, H., Inouye, S., Tsuji, F. I., Yasuda, K., Umesono, K. (1995) Localization, trafficking, and temperature-dependence of the aequorea green fluorescent protein in cultured vertebrate cells. *Proc Natl Acad Sci USA* 92, 11899–11903.

Chapter 6

Cell Arrays for the Measurement of Organelle Dynamics in Living Cells

Holger Erfle, Tautvydas Lisauskas, Christoph Claas, Jürgen Reymann, and Vytaute Starkuviene

Abstract

The Golgi complex is the central organelle in the secretory membrane trafficking and its organization strongly depends upon the flow of coming and leaving material. The principles of cargo transfer to, through, and away from the Golgi complex were investigated in numerous studies. However, the knowledge of how the Golgi complex responses to changes in diverse trafficking events (e.g., ER exit block) on a molecular level is far from being complete. In order to identify regulatory molecules playing a role in the dynamic organization of the Golgi complex, we established a fluorescent microscopy-based quantitative assay to measure rates of the Golgi redistribution and assembly after addition and washout of BFA, respectively. At first, we tested our system under the condition of over-expression of GFP-tagged proteins. We measured their influence upon BFA-induced effects in a format, suitable for large-scale studies in living cell, namely cell arrays. The approach can be applied for large-scale RNA interference studies as well as for chemical screening.

Key words: Reverse transfection, cell arrays, live-cell imaging, fluorescent screening microscopy, Golgi complex, brefeldin A.

1. Introduction

The Golgi complex in mammalian cells typically consists of stacks of three to eight membrane-bound cisternae, which are laterally fused to each other to form the Golgi ribbon. Every Golgi stack displays a polarized organization, which is reflected by differential enrichment of Golgi-resident proteins, like KDEL receptor or glycosyl transferases, just to mention a few (1). Besides serving as a signaling platform and being involved in post-translational

E. Palmer (ed.), *Cell-Based Microarrays*, Methods in Molecular Biology 706,
DOI 10.1007/978-1-61737-970-3_6,

modification, the Golgi complex is the central secretory organelle within the cell. Cargo is constantly delivered from the endoplasmic reticulum (ER), and vesicles targeted to the endosomal/lysosomal system and to the plasma membrane (PM) are constantly leaving the Golgi complex. It is still not clear how the Golgi complex can maintain its defined structure at a steady state in spite of this highly dynamic nature. To answer that, a number of studies were carried out by applying drugs that interfere with various aspects of the Golgi structure and function, e.g., nocodazole, H89, or brefeldin A (BFA). However, all the studies largely concentrated on investigation of mechanistic aspects of Golgi maintenance and ER to Golgi trafficking. In addition, they were performed in a low-throughput format; therefore, regulatory factors involved remain largely unknown. Therefore, there is a vital need for live cell analysis of the Golgi complex dynamics with high resolution in a medium- to high-throughput form to identify and characterize factors critical for the Golgi complex formation and maintenance (2).

In the last years, fluorescent microscopy-based functional analysis has proved to be one of the most useful tools to analyze proteins and their complexes acting in diverse cellular processes. However, the substantial part of completed and on-going large-scale studies was carried out in fixed cells. Endpoint assays of RNA interference (RNAi) or cDNA over-expression might suffer from the significant disadvantage that phenotypes collected could be secondary; therefore, such assays may lead to misinterpretation of results. Live cell time-resolved screens enable such situations to be avoided, and also produce information on how phenotypes change over time (3).

Live-cell time-lapse experiments usually generate tremendous amounts of data which increase requirements for data handling and automated computational methods to analyze results. Besides that, constraints of experiments generally increase a lot for live cell imaging if comparing with fixed cells, because a maximum number of different experiments have to be imaged in parallel and/or in a very much restricted time window. Therefore, independently from the microscope set-up (e.g., wide field, confocal), the device has to fulfill certain technical criteria, most importantly, to posses sufficient data acquisition speed for high-throughput experiments (4). Furthermore, the experimental format plays an important role in order to improve spatial and temporal resolution. Here, cell arrays show a considerable advantage compared to multi-well plates due to their capability for real parallel treatment of different experiments and minimized physical separation between different experiments. Particularly rewarding are assays in living cells allowing to maximally exploit those unique features of the cell-array technology.

2. Materials

2.1. Golgi Complex Redistribution Assay

1. Assay is performed in NRK (normal rat kidney; ATCC CRL-6509) cells stably expressing GalT–CFP (galactosyltransferase-tagged to CFP) for labeling of the Golgi complex (*see* **Note 1**).
2. Growth medium: DMEM (GIBCO/Invitrogen) containing 5% fetal bovine serum, 1% non-essential amino acids (GIBCO/Invitrogen), 2 mM glutamine, 100 U/ml penicillin, and 100 μg–ml streptomycin.
3. Imaging medium: MEM (Sigma-Aldrich, Missouri, USA) pH 7.2–7.4 buffered with 30 mM HEPES and containing 5% fetal bovine serum, 1% non-essential amino acids (GIBCO/Invitrogen), 2 mM glutamine. Prepared imaging medium can be stored for a month.
4. Nucleus staining: Hoechst 33342 (Sigma-Aldrich) diluted to 0.3 μg/ml final concentration in the imaging medium.
5. Brefeldin A (Calbiochem/Merck) diluted to 5 μg/ml final concentration and cycloheximide (Sigma-Aldrich) diluted to 0.1 mg/ml final concentration in Imaging medium. 1 mg/ml stock solution of BFA is prepared in methanol and stored at –20°C for 2 months.
6. Probe substrates for the assay: LabTek 1-well and eight-well chamber slides (further LabTek) (Nalge Nunc) consisting of borosilicate coverglass (0.16–0.19 mm thick) with 9.4 cm^2 and 0.8 cm^2 of culture area per well, respectively.
7. Liquid transfection: plasmids encoding cDNA-YFP, Lipofectamine 2000 (Invitrogen), OptiMEM I + GlutaMAX I (Invitrogen).

2.2. Fabrication of Over-Expression Cell Arrays

1. Plasmids encoding cDNA-YFP.
2. Lipofectamine 2000 (Invitrogen).
3. Sucrose (USB, Cleveland, USA).
4. OptiMEM I + GlutaMAX I (Invitrogen).
5. Drying gels, orange—heavy-metal free (Sigma-Aldrich).
6. Gelatin (Sigma-Aldrich).
7. Human fibronectin (Sigma-Aldrich).
8. Fabrication of the transfection array is performed via a contact printer (ChipWriter "Pro," Bio-Rad Laboratories, California, USA) featuring solid pins for spots with diameters of 400 μm.

2.3. Imaging on an Automated Wide-Field Screening Microscope

Image acquisition is performed with a Scan^R system (www.olympus.com), but it can be done on any other inverted automated screening fluorescence microscope. The major parts of Scan^R system are as follows:

1. The inverse microscopy stand IX81, equipped with a mercury (Hg)+xenon (Xe) lamp light source MT20E. The microscope is equipped with standard filter sets for discriminating among Hoechst 33342, CFP, GFP, YFP, Cy3, and Cy5 in a sequential imaging mode.
2. An automated table (Märzhäuser), which allows the precise movement of the sample.
3. Twelve-bit CCD camera (C8484, Hamamatsu, Munich, Germany).
4. Microscope incubator box with control device allowing temperature, humidity, and CO2 regulation (EMBLEM Technology transfer, Heidelberg, Germany).
5. Scan^R acquisition software (version: 2.1.0.16) controlling all components of the system.

2.4. Automated Data Evaluation

We have measured the change of the Golgi-complex-specific fluorescence over time as a readout of the assays. For this, a special algorithm in MatLab environment was used (*see* **Section 3.5**).

3. Methods

We have described here a fluorescent-microscopy-based assay to quantify the Golgi complex redistribution to the ER and assembly after the addition and washout of BFA, respectively. BFA was first described to have an influence on the Golgi complex integrity more than two decades ago (5). Since then, it is frequently used in the research of the Golgi complex dynamics and ER to Golgi trafficking mechanism. Most likely, BFA is interfering with the function of nucleotide exchange factors, containing Sec7 domain (e.g., GBF-1). That prevents activation of Arf GTPase, and, as a consequence, Golgi resident proteins collapse into the ER within minutes (6). BFA treatment of cells might help to develop models of the Golgi complex formation and determine what detailed functions might be served by various Golgi matrix proteins and enzymes (7). Here, we use addition and washout of BFA to identify proteins having a regulatory role in the ER to Golgi trafficking when over-expressed.

Visualization of fast cellular events in living cells in a high or medium scale still presents a technical challenge. Multiple

technical requirements have to be considered and combined to achieve a reasonable resolution in time. It is likely, that one of the most effective methods for reducing data acquisition times is by high-grade parallelized excitation and detection of different fluorophores. By this, time-consuming filter change can be eliminated. In addition, the properties of fluorophores are essential as the reduction of the exposure times contributes considerably to the overall length of experiments. Tremendous influence on large-scale data acquisition is the auto-focussing procedure, especially for screens in live cells. Here, some of the strong features of the cell array technology play a crucial role, namely, the homogeneous surface properties and the small distances between different experiments (e.g., 1,125 μm) allowing an accurate and fast extrapolation of focus positions (8). Consequently, that significantly reduces auto-focusing times far below 1 s per target position. In experiments, which allow creating a focus map prior to data acquisition, auto-focussing is not a limiting component any longer (9); therefore, even such a fast process as the Golgi complex redistribution could be harnessed for a large-scale analysis.

3.1. Preparation and Fabrication of cDNA Over-Expression Cell Arrays

cDNA transfection arrays are designed and produced as described in (10). Fabrication of the array on LabTeks is performed as follows:

3.1.1. Preparation of the Transfection Solution for Cell Array

1. 0.4 M OptiMEM/sucrose: dissolve 1.37 g sucrose in OptiMEM, total volume of mixture should be 10 ml.
2. Gelatine preparation: add 0.2 g gelatine in 100 ml water (*see* **Note 2**), place into water bath pre-heated to 56°C for 20 min. Cool down gelatine to room temperature (RT), then filter with sterile filter (0.45 μm).
3. Add 1 μl of fibronectin to 100 μl gelatine.
4. Transfection mixture: mix 4.0 μl OptiMEM/sucrose with 3.0 μl Lipofectamine 2000 and incubate for 15 min at RT. Add 2.0 μl cDNA (concentration of 500 ng/μl) and incubate for 15 min at RT. Add 7.0 μl fibronectin/gelatin mixture. Spin shortly in centrifuge at 1,000 rpm.

3.1.2. Dispensing of the Transfection Solution on LabTeks and Storage of the Ready-to-Transfect Substrates

1. Adjust the number of pins in the contact printer. We routinely use eight solid pins PTS 600. The resulting spot diameter of the solid pins PTS 600 pins on the cell arrays is about 400 μm.
2. Adjust the temperature of the 384-well plate to 12°C to avoid evaporation of the sample.
3. Set the spot-to-spot distance in the contact printer menu with respect to the application in mind. We routinely

use 1,125 μm, which allows spotting of 384 samples per LabTek; however, spot-to-spot distance could be set to 750 or 900 μm depending on the application.

4. Set the dwell time of the pins in the 384-well low-volume plate (time pins stay in the spotting solution) in the contact printer menu to 0.5 s.
5. Set the LabTek dwell time (time pins stay on LabTek) in the contact printer menu to 0.3 s.
6. Carry-out solid pin washing between individual samples. The procedure is set-up in the following way: pins remain in the washing container with water for 10 s at RT. Pins remain in the sonicator container with water for 10 s at RT. Move the pins above the holes of the vacuum drying array of the contact printer and vacuum dry the pins for 10 s at RT.

After printing of the array, keep the LabTeks in a gel-drying box containing 50 g of drying gels for at least 24 h. After drying, the LabTeks can be stored for more than 18 months at RT without losing transfection efficiency.

3.2. Golgi Complex Redistribution Assay

1. Plate 6,500–7,000 NRK GalT–CFP cells/well in the eight-well LabTek containing 300 μl of the growth medium/well and incubate for 24 h at 37°C (*see* **Note 3**).
2. Transfect cells with purified cDNAs using Lipofectamine 2000. We have used 96-well plate transfection protocol provided by the manufactures. Incubate transfected cells for 18–24 h before the assay.
3. Turn on the microscope incubation box, set temperature to 37°C at least 3 h before imaging.
4. Prepare fresh imaging medium and pre-warm it to 37°C before applying to cells.
5. Incubate cells for 15 min at 37°C with nucleus stain diluted in the imaging medium. Remove medium with the stain and add 200 μl of imaging medium to each well.
6. Prepare BFA and cycloheximide mixture in the imaging medium (200 μl/well). Final concentration after addition to cells should be 5 μg/ml for BFA and 0.1 mg/ml for cycloheximide.
7. To image redistribution of the Golgi complex, set-up three channels depending on the fluorophore. Namely, use excitation wavelength of 360–370 nm, emission wavelength of 460 nm to image nuclei stained with Hoechst 33342, excitation wavelength of 430–424 nm, emission wavelength of 470–524 nm to image GalT–CFP, and excitation

wavelength of 500–520 nm, emission wavelength of 535–630 nm to image cDNA–YFP over-expressed.

8. Adjust image acquisition settings, like exposure time and intensity of excitation light for each and every fluorophore separately (*see* **Note 4**). Use camera settings without binning.
9. Set time lapse for the assay: acquisition every 1 min for 30 cycles (*see* **Note 5**).
10. Run the first round without addition of BFA and cycloheximide, and then pause the run.
11. Add 200 μl of BFA and cycloheximide mixture to each well you want to image. Run imaging (*see* **Note 6**).

3.3. Golgi Complex Assembly Assay

1. Steps 1–8 are identical to that described in **Section 3.2**.
2. Add BFA and cycloheximide mixture to each well you want to image and incubate cells for 30 min.
3. Set time-lapse for the assay: acquisition every 10 min for 12–15 cycles (*see* **Note 5**).
4. Remove media with BFA, wash cells once with pre-warmed growth medium. Add 400 μl of growth medium with cycloheximide (0.1 mg/ml concentration) to each well and run imaging.

3.4. Golgi Complex Redistribution and Assembly Assays on Cell Arrays

1. Plate NRK cells at densities of 2.5×10^5 in the 1-well LabTek with the spotted cDNAs and incubate for 24 h. Three milliliter of growth medium is sufficient.
2. All the other steps are as described in **Section 3.2** and **3.3**, except different volumes of solutions used when working in eight-well substrates. Namely, 1 ml of imaging medium should be added after cell nucleus staining in 1-well LabTek.

3.5. Quantification of the Golgi Complex Dynamics

The assay is based on measuring how fluorescence intensity of the Golgi resident GalT–CFP protein changes over time after the BFA addition. Analysis of the process is based on single cell detection, tracking (nuclei based) over time, and measuring of changes in GalT–CFP-labeled structures. Also it is necessary to discriminate between cDNA-transfected and non-transfected cells automatically.

For measurement of changes in the Golgi complex, many features should be taken into account. It is proposed that the most reliable measure is texture measure (11). Also taken into account should be that not all cells show effect of brefeldin A, around 20% of the cell population show no response to treatment of

brefeldin A. Formation of tubules due to the effects of brefeldin A also may require additional steps in image analysis.

4. Notes

1. The assays are not limited to NRK cells—virtually any type of cells suitable for microscopy could be used. Also, Golgi complex dynamics could be measured by measuring other GFP tagged Golgi enzymes, for example, GalNAc-T2, ManII.
2. Water in our text refers to 18.2 MΩ × cm pure water prepared by TKA 08.2207 UV-TOC/UF.
3. Number of cells for plating should be adjusted depending on cell line and their growth rate. At the time of imaging, cells should be confluent by not more than 85%, as it is necessary for better cell separation in the following image analysis steps.
4. Images must not contain saturated pixels. To prevent a sample from photo bleaching over the length of the whole experiment, it is better to minimize the excitation light intensity.
5. One-minute interval is a reasonable compromise to capture changes occurring at the Golgi complex upon addition of BFA and to enable at least a middle-sized screen to be performed. As the Golgi complex assembly is a much slower process than redistribution, one could increase acquisition time interval 10-fold without loss of the data, but decrease the effects of photo-toxicity.
6. Addition of BFA and cycloheximide increases background level; this may lead to worse auto-focusing accuracy and also may create difficulties for image analysis, such as recognition of the objects.

Acknowledgments

The authors would like to acknowledge funding within the Forsys-ViroQuant consortium, Project no. 0313923, as well as by the Federal Ministry of Education and Research (BMBF). The ViroQuant-CellNetworks RNAi Screening core facility is supported by CellNetworks—Cluster of Excellence (EXC81). NRK GalT–CFP cells were provided by Prof. A. Mironov, Consorzio Mario Negri Sud, Italy and cDNAs-YFP by Dr. S. Wiemann, DKFZ, Heidelberg.

References

1. Pfeffer, S. R. (2007) Unsolved mysteries in membrane traffic. *Annu Rev Biochem* 76, 629–645.
2. Marsh, B. J., Howell, K. E. (2002) The mammalian golgi – complex debates. *Nat Rev Mol Cell Biol* 3(10), 789–795.
3. Walter, T., Held, M., Neumann, B., Hériché, J. K., Conrad, C., Pepperkok, R., Ellenberg, J. (2010) Automatic identification and clustering of chromosome phenotypes in a genome wide RNAi screen by time-lapse imaging. *J Struct Biol* 170(1), 1–9.
4. Pepperkok, R., Ellenberg, J. (2006) High-throughput fluorescence microscopy for systems biology. *Nat Rev Mol Cell Biol* 7(9), 690–696.
5. Fujiwara, T., Oda, K., Yokota, S., Takatsuki, A., Ikehara, Y. (1988) Brefeldin A causes disassembly of the golgi complex and accumulation of secretory proteins in the endoplasmic reticulum. *J Biol Chem* 263(34), 18545–18552.
6. Peyroche, A., Antonny, B., Robineau, S., Acker, J., Cherfils, J., Jackson, C. L. (1999) Brefeldin A acts to stabilize an abortive ARF-GDP-sec7 domain protein complex: involvement of specific residues of the sec7 domain. *Mol Cell* 3(3), 275–285.
7. Mardones, G. A., Snyder, C. M., Howell, K. E. (2006) Cis-golgi matrix proteins move directly to endoplasmic reticulum exit sites by association with tubules. *Mol Biol Cell* 17(1), 525–538.
8. Conrad, C., Erfle, H., Warnat, P., Daigle, N., Lörch, T., Ellenberg, J., Pepperkok, R., Eils, R. (2004) Automatic identification of subcellular phenotypes on human cell arrays. *Genome Res* 14(6), 1130–1136.
9. Neumann, B., et al. (2006) High-throughput RNAi screening by time-lapse imaging of live human cells. *Nature Methods* 3, 385–390.
10. Erfle, H., Neumann, B., Liebel, U., Rogers, P., Held, M., Walter, T., Ellengerb, J., Pepperkok, R. (2007) Reverse transfection on cell arrays for high content screening microscopy. *Nat Protocols* 2, 392–399.
11. Pan, H., Yu, J., Zhang, L., Carpenter, A., Zhu, H., Li, L., Ma, D., Yuan, J. (2008) A novel small molecule regulator of guanine nucleotide exchange activity of the ADP-ribosylation factor and golgi membrane trafficking. *J Biol Chem* 283(45), 31087–31096.

Chapter 7

High-Throughput Immunofluorescence Microscopy Using Yeast Spheroplast Cell-Based Microarrays

Wei Niu, G. Traver Hart, and Edward M. Marcotte

Abstract

We have described a protocol for performing high-throughput immunofluorescence microscopy on microarrays of yeast cells. This approach employs immunostaining of spheroplasted yeast cells printed as high-density cell microarrays, followed by imaging using automated microscopy. A yeast spheroplast microarray can contain more than 5,000 printed spots, each containing cells from a given yeast strain, and is thus suitable for genome-wide screens focusing on single cell phenotypes, such as systematic localization or co-localization studies or genetic assays for genes affecting probed targets. We demonstrate the use of yeast spheroplast microarrays to probe microtubule and spindle defects across a collection of yeast strains harboring tetracycline-down-regulatable alleles of essential genes.

Key words: Yeast, immunofluorescence, high-throughput microscopy, cell microarrays, microtubule.

1. Introduction

DNA microarrays and mass spectrometry, among other approaches, have proved to be powerful tools for direct assay of gene function on a genome-wide scale (1, 2). However, such approaches often do not monitor gene and protein behavior in intact cells nor do they assay behavior at the single cell level (3). Nonetheless, it is often desirable to measure single cell phenotypes, and high-throughput microscopy offers a viable strategy for such assays, especially when used in combination with available libraries of genetically distinct cells. To aid in performing such assays, we have described an extension of the spotted cell

E. Palmer (ed.), *Cell-Based Microarrays*, Methods in Molecular Biology 706,
DOI 10.1007/978-1-61737-970-3_7,

microarray platform (4) to perform high-throughput immunofluorescence assays on yeast cells. This approach, dubbed yeast spheroplast microarrays, enables analysis of localization phenotypes of probes of interest (e.g., any target of an affinity reagent such as an antibody) in thousands of genetically distinct cells in parallel.

Yeast spheroplast microarrays have several advantages compared with high-throughput assays in 96- or 384-well plates. First, the high capacity of the arrays (up to ~5,000 spots per array) minimizes the use of expensive reagents to screen a library of cells by limiting the use of antibodies or dyes to single microscope slides. Second, the high density of samples in the arrays increases data acquisition speed by automated microscopy. Third, yeast spheroplast microarrays provide a platform for highly parallel and reproducible large-scale screens. More than a hundred cell microarrays can be manufactured from the same sample sources under the same conditions, and microarrays can be stored at –80°C at least for a month without apparent loss of immunostaining signals. As each slide can in principle be probed with a different antibody, this allows many independent imaging assays to be performed on cells drawn from the same biological samples.

Performing such high-throughput immunofluorescence experiments in yeast requires spheroplasting the cells to allow antibody access to intracellular contents. One of the primary limitations of high-throughput immunofluorescence imaging of yeast cells is the difficulty associated with uniformly spheroplasting cells in a strain collection using a single spheroplasting condition, especially given that optimal treatment times can vary with genetic background. Therefore, spheroplast conditions must be optimized by testing the time of zymolyase treatment when manufacturing arrays from different yeast cell libraries.

To enable such experiments, we present here a protocol for high-throughput spheroplasting of yeast cells and construction and imaging of spheroplast cell microarrays (*see* **Fig. 7.1** for an overview of the protocol). As a demonstration of the construction and utility of such arrays, yeast spheroplast chips were built from the *TetO7* promoter collection covering 75% of essential genes (5), then probed with anti-alpha tubulin antibody to examine the effects on the organization of microtubule and spindle when essential genes were downregulated (**Fig. 7.2**).

Yeast microtubule organization depends strongly on cell cycle progression (6, 7). In wild-type G1-phase cells, microtubules form star-like cytoplasmic arrays radiating from the microtubule organizing center (**Fig. 7.3a**). During S/G2 phase, cytoplasmic astral microtubules reorient towards the bud tip and penetrate the bud (**Fig. 7.3b**). When cells enter mitosis, microtubules rearrange into a bipolar spindle positioned through the bud neck. In anaphase, cytoplasmic microtubules shorten, the spindle

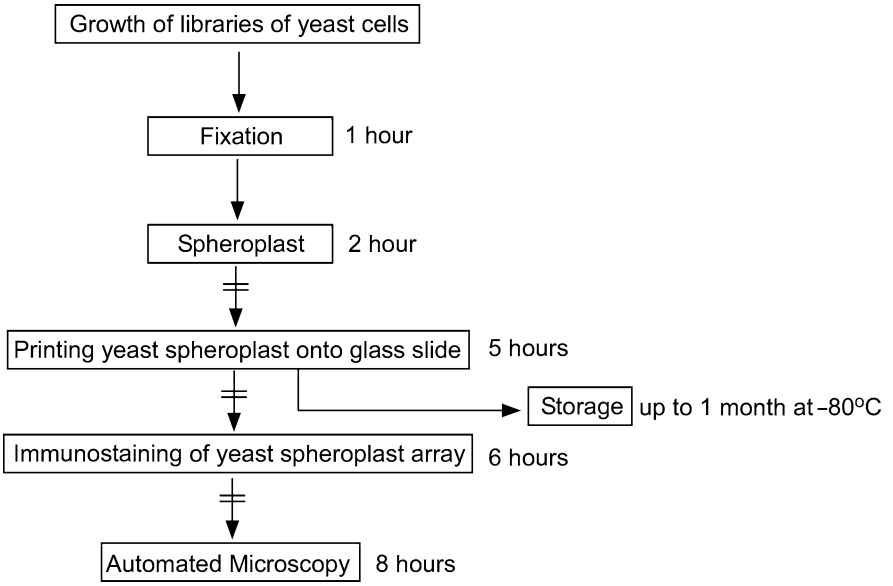

Fig. 7.1. Work flow of the yeast spheroplast microarray protocol. Yeast cells are cultured, fixed, and spheroplasted in 96-well plates, e.g., using an automated liquid handling robot. Subsequently, they are robotically printed onto poly-L-lysine microscope slides using a slotted steel pin-based DNA microarray robot. The resulting slides each contain ~5,000 spots. Each slide can be stored at –80°C or can be probed with a specific antibody immediately after printing. Images are acquired through automated microscopy. The different steps of the protocol are indicated in *boxes* by *arrows*. The approximate time required for each step is indicated near the *box*. Steps at which the protocol can be paused are indicated in the diagram by pairs of *short lines* across the *arrows*. Times indicated for each step are approximate and will depend upon the precise equipment used for the experiment.

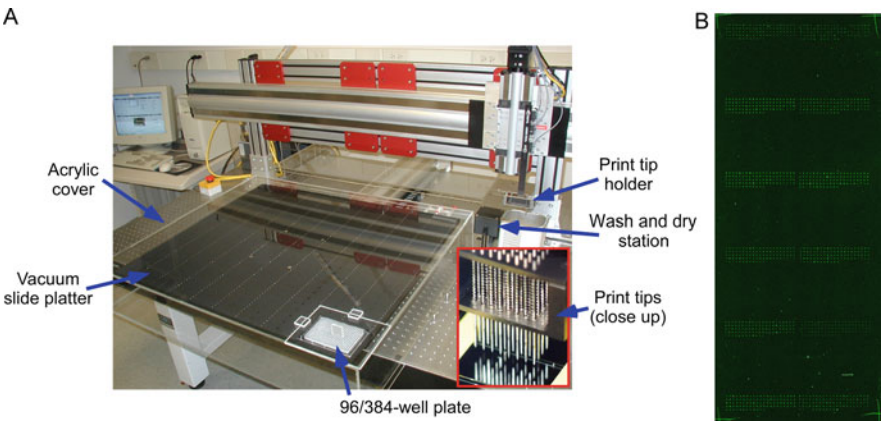

Fig. 7.2. A microarray printing robot suitable for printing yeast spheroplast microarrays, shown alongside an example microarray (**a**). A Stanford-style Newport DNA microarray print robot with 12 pins directly delivers yeast spheroplasts from 96-well plate onto slides (**a**) (4). A yeast spheroplast array carrying ~700 yeast *Tet07*-promoter strains (spot diameter, 200 μm; spot-to-spot distance, 410 μm) is shown in (**b**).

elongates, and sister chromosomes are segregated (**Fig. 7.3c**). When cytokinesis is completed, the spindle disassembles (**Fig. 7.3d**).

In the example spheroplast array, abnormal microtubule structures could be observed in cells with knockdown of genes

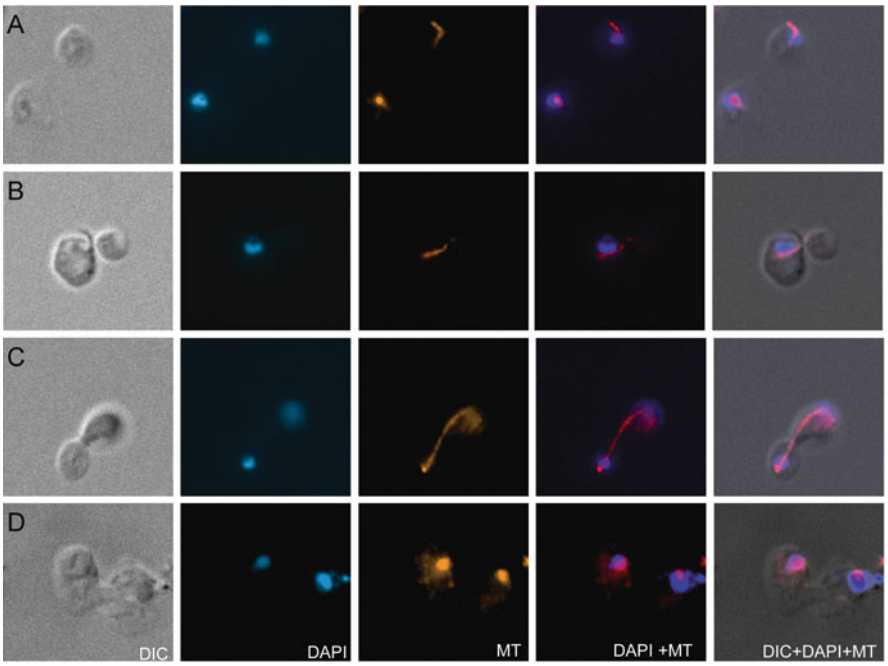

Fig. 7.3. Examples of microtubule and spindle morphology in different yeast cell cycle stages from (**a**) to (**d**) show G1 phase cells, S/G2 phase cells, anaphase cells, and completed cytokinesis, respectively. Nuclei and microtubules are depicted.

whose mutations are known to cause defective spindle formation. For example, Spc97 and Spc98 are two major components of the microtubule nucleating Tub4 complex, involved in microtubule nucleation and mitotic spindle organization (8). Downregulation of *SPC97* and *SPC98* resulted in short spindles, elongated cytoplasmic microtubules, and defective

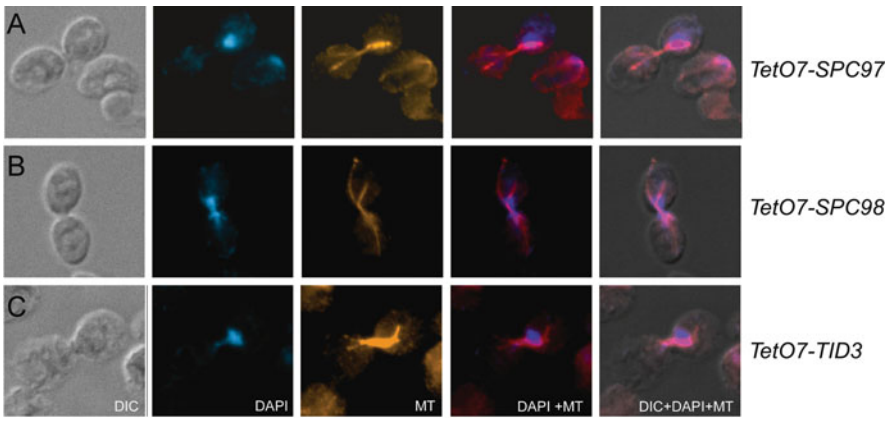

Fig. 7.4. Example images for *TetO7* promoter strains exhibiting defective microtubule and spindle structure (**a**, **b**). Downregulation of *SPC97* and *SPC98* resulted in short spindles and elongated cytoplasmic microtubules (**c**). Downregulation of *TID3* caused defective spindle elongation and uneven nuclear division.

chromosome segregation, thus showing a defect resembling that of the corresponding temperature-sensitive mutants (**Fig. 7.4a**,**b**). Similarly, Tid3 is a component of the kinetochore-associated Ndc80 complex, involved in chromosome segregation and microtubule nucleation (9, 10). Downregulation of *TID3* caused defects in spindle elongation and nuclear division (**Fig. 7.4c**). Thus, the potential can be seen of spheroplast chips for high-throughput immunofluorescence imaging-based genetic screens in yeast.

2. Materials

2.1. Yeast Cell Growth and Fixation

1. Yeast strains: for the example array shown here, we used the yeast TetO7-promoter strain collection (5) (Open Biosystems).
2. Growth medium: YPED medium (1% yeast extract, 2% peptone, and 2% D-dextrose) supplemented with 200 μg/ml doxycycline.
3. 37% Formaldehyde.
4. 1× PBS buffer: 8 g NaCl, 0.2 g KCl, 1.44 g Na_2HPO_4, and 0.24 g KH_2PO_4 in 800 ml of distilled H_2O. Adjust pH to 7.4 with HCl. Add H_2O to 1 l.
5. Spheroplast buffer: 1.2 M sorbitol, 0.1 M KH_2PO_4, pH 7.5.

2.2. Zymolyase Treatment

1. Zymolyase solution: 200 μl Spheroplast buffer supplemented with 0.025 mg/ml zymolyase 20T (Seikagaku corporation) and 0.4 μl β-mercaptoethanol.

2.3. Preparation of Poly-L-Lysine Glass Slides

1. Glass slide wash solution**:** dissolve 33 g NaOH pellets in 133 ml H_2O, add additional NaOH pellets until solution is saturated, and then add 200 ml 95% EtOH.
2. Poly-L-lysine solution**:** 250 ml H_2O, 35 ml 1× PBS (filtered), 50 ml poly-L-lysine.
3. Glass slide dish.
4. Glass slide rack.

2.4. Spheroplast Microarray Printing

1. DNA microarray printing robot. Here, we use a Stanford-style Newport printer.
2. Printer pins. Here, we use conically tapered 1/16 inch diameter stainless steel printing tips with 0.0015 inch slots (Majer Precision Engineering).
3. 0.5× SSC.

2.5. Storage and Recovery of Yeast Spheroplast Microarrays

1. 95% Ethanol.

2.6. Immunostaining of Yeast Spheroplast Microarrays

1. Methanol, –20°C.
2. Acetone, –20°C.
3. Blocking buffer: 3% BSA in 1× PBS.
4. Primary antibody: Anti-bovine α-tubulin, mouse monoclonal antibody, and 4 μg/ml in blocking buffer.
5. Secondary antibody: Texas-red conjugated goat anti mouse IgG (H+L), 4 μg/ml in blocking buffer.
6. VECTASHIELD hard set mounting medium (Vector Laboratories, Inc) with DAPI.
7. Clear nail polish.
8. Staining jars.

2.7. Automated Imaging

1. Automated fluorescence microscope.

3. Methods

3.1. Yeast Cell Growth and Fixation

1. Grow or treat cells in 96-well plates in 170 μl proper medium.
2. Fix cells immediately after growth or treatment in proper growth medium with 1/10 volume 37% formaldehyde for 1 h at 30°C.
3. Wash cells with 1× PBS buffer twice and resuspend cells in 200 μl spheroplast buffer.
4. At this point, cells can be stored at 4°C overnight or spheroplasted immediately as in **Section 3.2**.

3.2. Zymolyase Treatment

1. Spin down cells and resuspend cells in 200 μl zymolyase solution (*see* **Note 1**).
2. Incubate cells for 2 h at 30°C. This is a critical step and should be monitored closely. *See* **Fig. 7.5** for images of the desired degree of spheroplasting.
3. Centrifuge cells at low speeds (<3,000 rpm) and wash cells twice with spheroplast buffer, and resuspend cells in 200 μl spheroplast buffer.

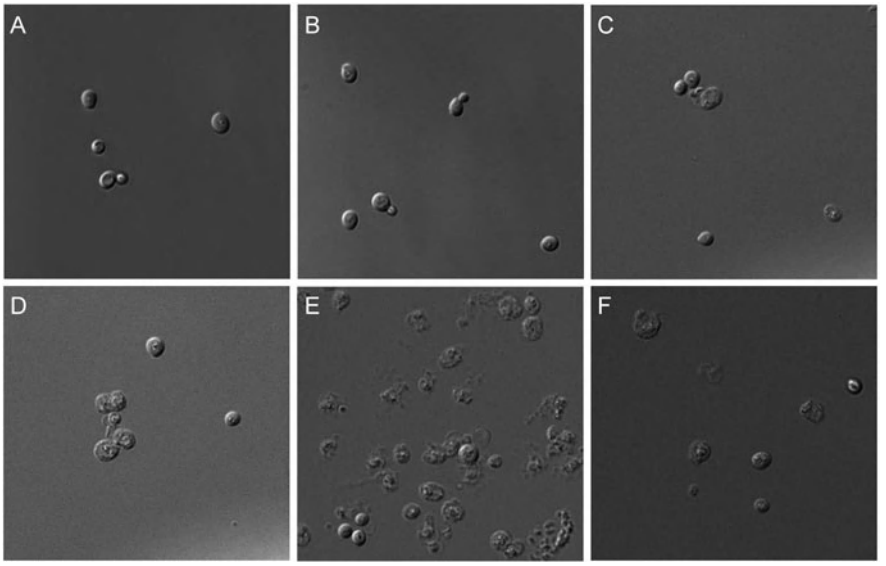

Fig. 7.5. Examples of morphology changes of yeast cells treated with zymolyase to differing extents. Cells should be a *dark*, translucent *gray* after an appropriate degree of digestion (**d**). (11). *Bright cells* are insufficiently digested (**a**–**c**) (11). "Ghost cells" (*pale gray* with little any internal structure) have been over-digested (**e**, **f**) (11). Spheroplasting protocols for cells typically employ a relatively high concentration of zymolyase and short digestion times (less than 30 min). However, given that yeast spheroplast microarrays are designed for large-scale experiments usually analyzing hundreds or thousands strains at a time, 30 min digestion times are impractical and unforgiving for small errors in timing. We therefore employed lower concentrations of zymolyase and longer digestion times in order to get an appropriate degree of digestion. The optimal concentration for the Tet07 strain collection in our example assay was 0.025 mg/ml; the digestion time was 2 h (**d**).

4. At this point, spheroplasted cells can be stored at 4°C overnight or printed immediately as in **Section 3.4** (*see* **Note 2**).

3.3. Preparation of Poly-L -Lysine Glass Slides (Described for 30 Slides)

1. Rinse slide dishes completely with H_2O in a plastic basin four times to wash away any dust and debris that might be on the slides (*see* **Note 3**).
2. Place racks in glass slide dishes and pour slide wash solution over slides and cover. Shake gently for 2 h (*see* **Note 4**).
3. Rinse each rack with tap-distilled water two times, making sure to rinse both surfaces of each slide.
4. Rinse the racks with double distilled H_2O at least two times. Make sure that you have removed all of the NaOH.
5. Place one rack of slides into glass slide dishes, draining briefly, and pour poly-L-lysine solution to cover each set of slides. Shake gently for 30 min.
6. Rinse each rack with distilled H_2O twice in a plastic basin by removing poly-L-lysine from slides.

7. Place racks on top of 2 folded over paper towels in a tabletop centrifuge, and spin at 600 rpm at room temperature for 5 min to dry.
8. Store slides in a clean plastic box at room temperature.

3.4. Spheroplast Microarray Printing

In principle, any slotted pin-based DNA microarray printer can be used. We present specific protocols for the Stanford-style Newport printer, using Arraymaker control software.

1. Depending on the array printer, it may be necessary to set the print depth to be appropriate for 96-well plates prior to loading a plate in the plate holder (*see* **Note 5**).
2. Use 12 pins, skipping a pin in each direction. Pins are placed in hole numbers 2, 4, 10, 12, 18, 20, 26, 28, 34, 36, 42, and 44 (*see* **Note 6**).
3. Position poly-L-lysine-coated slides on the printing platter, taping in position if necessary.
4. Fill sonicating water bath with 0.5×SSC.
5. For plate alignment, due to the variability in well volumes, align printer pins so that the liquid level is just below the start of the beveled portion of the printing tip.
6. Align the slide position as typical for DNA microarray printing.
7. Set wash time at 6,000 ms, dry time at 8,000 ms, load time at 1,000 ms, the spot-to-spot distance as 410 μm. Use "slow pickup."
8. Test print by using a test plate with the wild-type samples before the large-scale printing, and check the cell counts under a microscope (*see* **Note 7**).
9. Start the formal print runs once the test print results are satisfying.
10. When the print is complete, tape slides into a swinging bucket plate centrifuge (max: 5 slides/bucket) or use custom-made plastic flat slide holders, and spin flat at 1,500–2,000 rpm for 5 min.

3.5. Storage and Recovery of Yeast Spheroplast Microarrays

1. Store spheroplast chips at 4°C for overnight or at –80°C for long-term storage (**Fig. 7.6**) (*see* **Note 8**).
2. To recover a slide after storage at –80°C, fill a 50 ml Falcon tube with 95% EtOH. Dunk slide into the tube immediately upon taking slide out of the freezer (*see* **Note 9**).
3. Take the slide out quickly and put it into a clean and dry 50-ml Falcon tube, and then dry the slide by spinning in an empty 50-ml tube without cap at 600–700 rpm for 5 min.

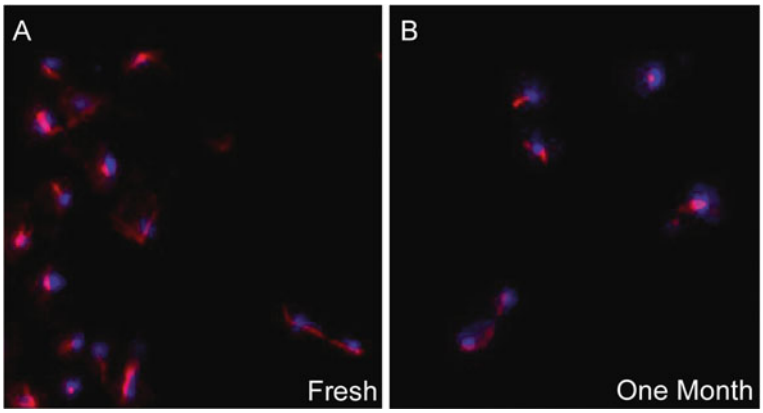

Fig. 7.6. Spheroplast microarrays can be stored at least a month at –80°C without substantial effects on cellular morphology or subcellular structure, as shown here for microtubule structure. Compared to fresh chips (**a**), chips stored at –80°C still maintain intact microtubule structures after one month (**b**). Nuclei and microtubules are depicted.

3.6. Immunostaining of Yeast Spheroplast Microarrays

1. Permeabilize cells in cold methanol for 6 min and then in cold acetone for 30 s. Air-dry slides completely.
2. Wash slides for 5 min with 1× PBS.
3. Place ~200 μl blocking buffer on the slide. Trim a piece of parafilm to the size of the slide and gently lay over the sample. Incubate for 30 min at 30°C in a sealed humidity chamber (*see* **Note 10**).
4. Carefully remove the parafilm and add ~200 μl primary antibody onto the slide. For instance, the anti-bovine α-tubulin mouse monoclonal antibody was used as the primary antibody in the current protocol (Invitrogen, cat. no. A-11126). Incubate for 2 h at 30°C.
5. Wash the slide three times in staining jars with 1× PBS, 5 min each time.
6. Add ~200 μl secondary antibody onto the slides. Incubate for 2 h at 30°C and in the dark (*see* **Note 11**).
7. Wash the slide three times in staining jars with 1× PBS, 5 min each time.
8. Add ~60 μl VECTASHIELD hard-set mounting medium and cover with cover slip.
9. Let the mounting medium dry out for 15 min at room temperature or overnight at 4°C. Seal the slides with clear nail polish.
10. Store the slides at 4°C and protect the slides from light. Immunostained yeast spheroplast microarrays can be stored at 4°C for at least a month with no apparent loss of signal.

3.7. Automated Imaging

In principle, any automated fluorescent microscope can be used to capture cell chip images. Here, we have presented a protocol specific to the Nikon TE2000 inverted epifluorescence microscope with NIS Elements controller software.

1. Turn on the microscope and all components. Initialize the stage. With a dummy slide, calibrate the stage and slide mounting bracket to ensure a flat focal plane across the sample area on the slide. This can be accomplished by marking one side of the slide with reference marks in the corners of the slide (using, for example, a fine-point Sharpie marker), navigating to each mark, and adjusting the calibration screws in the mounting plate until all reference spots can be viewed clearly at the desired magnification by translating X and Y without adjusting focus.
2. Edit the create_block_coordinates macro script (*see* **Note 12**) to reflect the block size on the printed microarray. Block size is the number of rows and columns of spots printed by a single pin on the array. Also specify the spot pitch—the distance between the printed spots in the array construction (in this protocol, 410 μm was used in lines 24 and 25 of the script).
3. Mount the slide and manually scan to the first printed spot in the first block. Focus on the spot in DIC at the desired magnification. 60× or greater magnification is recommended.
4. Execute the create_block_coordinates macro. An ND Experiment file will be created that specifies the coordinates of all spots in the current block.
5. In the ND Experiment dialog box, specify the desired immunofluorescence wavelengths to be captured. Also specify whether to autofocus on every spot. This should be unnecessary if the stage and slide mounting bracket are well calibrated (*see* **Section 3.7**, Step 1). Finally, specify the output file.
6. Execute the ND Experiment. The microscope will image the current block.
7. Repeat Steps 3–6 for each block. A 12-pin print will have 12 blocks.

4. Notes

1. The spheroplast buffer with zymolyase and β-mercaptoethanol should be prepared fresh before use.

2. Note that yeast cells without cell walls are quite fragile, and in general spheroplasted cells should be handled carefully and centrifuged at low speeds.
3. We recommend wearing powder-free gloves at all times, as talcum powder will stick to slides and leave visible debris in the resulting images.
4. This wash removes residual oil and debris from slides. The wash solution should be prepared fresh before use.
5. On Stanford-style printers optimized for DNA microarray printing, this step is important, because 96-well plates are often taller than 384-well plates. If the vertical printing depth (Z) is not set high enough, the printing pins will hit the 96-well plate bottom.
6. If using the Stanford-style arrayer and Arraymaker software, be sure to use the 48-tip printing designation in the Arraymaker software.
7. Ideally, there should be ~20–30 cells per spot. If cell count is low, consider resuspending cells in smaller volumes.
8. Empirically, we find that spheroplast arrays are fine if stored at 4°C for a few days, but for longer periods, it is better to store them at –80°C. Storage times up to 1 month have been tested.
9. This step is to prevent condensation on the slide. Condensation will smear the spots, cause potential cross-contamination, and make it very difficult to grade the spots on the slide.
10. It is important to not let the slides dry out from this step on.
11. Keep slides in the dark from this point on to minimize photobleaching of fluors.
12. The create_block_coordinates script referenced in protocol **Section 3.7**, Step 2-on, suitable for use with NIS Elements microscope controller software (specifically tested on NIS Elements AR (Advanced Research) v3.0.)

```
//Automatic Spot Coordinate calculation for a spotted
  cell microarray
//Program moves in NORMAL PRINT PATTERN
//User inputs x,y,z at first, last spot
//Program calculates x,y,z of every spot
//by Traver Hart, 1/22/07

// BE SURE STAGE IS INITIALIZED BEFORE RUNNING THIS
   MACRO

char Debug[1024];
```

```
int main()
{

    double dYSpotBegin,dXSpotBegin, dZSpotBegin;
    double dYSpotEnd,dXSpotEnd, dZSpotTwo, dZSpotThree;
    double dYOffset,dXOffset,dyTemp,dxTemp, dZOffset,
     dZYOffset, dZXOffset, dzTemp;
    int i,j;
    int numRows, sectorWidth;

    sectorWidth = 21; // (y direction)
    numRows = 21;     // (x direction)

    //Set distance between spots - specified as 410
      microns in arrayer
    dXOffset=410;
    dYOffset=410;


    Int_Question("Automated Print Block ND
     Initialization","Please move to the TOP
    LEFT spot (should be position 1,1 of block).","OK"
      ,"","","",1,1);
    StgGetPos(&dXSpotBegin,&dYSpotBegin,&dZSpotBegin);

  dzTemp = dZSpotBegin;

     for(i=0;i<numRows;++i)
        {
          for(j=0;j<sectorWidth;++j)
          {
               dxTemp=(dXSpotBegin - (dXOffset*i) );
               dyTemp=(dYSpotBegin - (dYOffset*j) );

               ND_AppendMultipointPoint(dxTemp,dyTemp,
                 dzTemp,"sample");
           }


         }

         _ND_CreateAndRunExperiment();
}
```

Acknowledgments

This work was supported by grants from the N.S.F., N.I.H., and Welch (F-1515) and Packard Foundations to E.M.M.

References

1. Lockhart, D. J., Winzeler, E. A. (2000) Genomics, gene expression and DNA arrays. *Nature* 405, 827–836.
2. Aebersold, R., Mann, M. (2003) Mass spectrometry-based proteomics. *Nature* 422, 198–207.
3. Levsky, J. M., Shenoy, S. M., Pezo, R. C., Singer, R. H. (2002) Single-cell gene expression profiling. *Science* 297, 836–840.
4. Narayanaswamy, R., Niu, W., Scouras, A. D., Hart, G. T., Davies, J., Ellington, A. D., Iyer, V. R., Marcotte, E. M. (2006) Systematic profiling of cellular phenotypes with spotted cell microarrays reveals mating-pheromone response genes. *Genome Biol* 7, R6.
5. Davierwala, A. P., Haynes, J., Li, Z., Brost, R. L., Robinson, M. D., Yu, L., Mnaimneh, S., Ding, H., Zhu, H., Chen, Y., et al. (2005) The synthetic genetic interaction spectrum of essential genes. *Nat Genet* 37, 1147–1152.
6. Winsor, B., Schiebel, E. (1997) Review: an overview of the Saccharomyces cerevisiae microtubule and microfilament cytoskeleton. *Yeast* 13, 399–434.
7. Kilmartin, J. V., Adams, A. E. (1984) Structural rearrangements of tubulin and actin during the cell cycle of the yeast saccharomyces. *J Cell Biol* 98, 922–933.
8. Knop, M., Pereira, G., Schiebel, E. (1999) Microtubule organization by the budding yeast spindle pole body. *Biol Cell* 91, 291–304.
9. Zheng, L., Chen, Y., Lee, W. H. (1999) Hec1p, an evolutionarily conserved coiled-coil protein, modulates chromosome segregation through interaction with SMC proteins. *Mol Cell Biol* 19, 5417–5428.
10. Wigge, P. A., Kilmartin, J. V. (2001) The ndc80p complex from Saccharomyces cerevisiae contains conserved centromere components and has a function in chromosome segregation. *J Cell Biol* 152, 349–360.
11. Burke, D., Dawson, D., Stearns, T. (2000) *Methods in Yeast Genetics.* Cold Spring Harbor Laboratory Press, Cold Spring Harbor, NY.

Chapter 8

Cell-Based Microarrays of Infectious Adenovirus Encoding Short Hairpin RNA (shRNA)

Hansjürgen Volkmer and Frank Weise

Abstract

Genome-wide screening procedures have developed into a useful tool for assigning new functions to known proteins or for identifying new interplayers in cell metabolism, especially under pathological conditions. Since primary cells reflect the physiological situation more closely than transformed cell lines, their employment in such screenings is highly desirable. A difficulty to overcome – besides the shortage in cell supply – is that primary cells are less amenable to classical methods of genetic manipulation such as lipofection or electroporation. By using adenovirus as the vehicle for genetic manipulation, efficient transfer of genetic information can be achieved without drastic effects on cell viability, and by using a microarray format even small amounts of cells suffice to perform a screen.

Key words: Adenovirus, shRNA, knock-down, immunofluorescence microscopy.

1. Introduction

Microarrays of different viruses have been employed in functional genomics studies (1, 2), including adenovirus (3, 4). These viral microarrays represent a significant extension of the initial microarray concept, in which DNA, and later siRNA, were immobilised (5, 6), as they opened the way to tackle cells sensitive to the harsh methods of classical genetic manipulation such as lipofection or electroporation. Many primary cells display a significant drop in viability when exposed to these methods, which excludes assaying the cellular response to the specific genetic change in these most interesting types of cells.

E. Palmer (ed.), *Cell-Based Microarrays*, Methods in Molecular Biology 706,
DOI 10.1007/978-1-61737-970-3_8,

The genetic manipulation that has recently experienced the strongest increase in experimental usage is the employment of small interfering RNA (siRNA) for specific gene knockdown. The occurrence of siRNA was initially discovered as a natural way of RNA silencing in nematodes (7), and it was quickly adapted to be employed as a genetic tool in eukaryotic cells (8). Notably, by the development of short hairpin RNA (shRNA), the way was paved for the intracellular generation of siRNA from a DNA molecule transferred by a vector (9), such as a virus.

Although this chapter focuses on gene knockdown mediated by viral transfer of shRNA-encoding DNA, alternative cassettes for the overexpression of genes can likewise be transferred.

The following protocol describes how to generate a reverse transduction array by non-covalently immobilising adenovirus onto a microscopic slide, allowing for optical analysis of the cellular response by immunofluorescence microscopy. Thus, the chapter is written in the expectation that the reader has adenovirus to start with. To illustrate the scope of the possible application of this technique, an example is given demonstrating the employment of this technique to study the cellular response upon downregulation of gene expression mediated by adenoviral transfer of the corresponding shRNA-encoding sequence.

2. Materials

2.1. Preparation of Array Support

1. Microscopic glass slides, pre-coated with poly-L-lysine (Poly-Prep slides, Sigma-Aldrich, St. Louis, MO).
2. Protran™ nitrocellulose membrane (Whatman, GE Healthcare, Waukesha, WI) is dissolved at 2.5 mg/ml in methanol and stored at room temperature.

2.2. Arraying Adenovirus

1. Sterile, non-pyrogenic polystyrene petri dishes (100 mm× 20 mm, Corning Inc., Corning, NY); use one per slide.
2. Phosphate buffered saline (Dulbecco's PBS; PAA, Pasching, Austria).
3. Handheld microarrayer (e.g. MicroCaster, Whatman, GE Healthcare, Waukesha, WI).
4. 70% Ethanol (cell culture grade).

2.3. Blocking Cell Adhesion Outside of the Spots and Seeding the Cells

1. Stabilguard (Surmodics, Eden Prairie, MN).
2. Trypsin–EDTA (PAA, Pasching, Austria) for suspending adherent cells.

2.4. Immunostaining

1. Paraformaldehyde (Merck): prepare a 4% (w/v) solution in PBS and aliquot in portions of 10 ml. Store at –20°C and use a fresh aliquot for each experiment.
2. PBS/NaN_3: Prepare a 1% (w/v) stock solution of NaN_3 (Sigma-Aldrich) in PBS (*see* **Note 1**). Store at room temperature. Dilute to a final concentration of 0.05% before use.
3. Permeabilisation solution: 0.25% (v/v) Triton X-100 (Sigma-Aldrich) in PBS.
4. Nuclear stain: prepare a stock solution of 1 mg/ml DAPI (4,6-diamidino-2-phenylindole; Roche) in sterile ddH_2O (or alternatively 500 μg/ml Hoechst dye 33342 (Sigma-Aldrich) or 500 μg/ml Hoechst dye 33258 (Polysciences Inc., Warrington, PA, USA)). Dilute 1:100 for working solution.
5. Mounting medium: fluorescence mounting medium (Dako North America, Carpinteria, CA).
6. Conventional nail varnish to seal the slides.

3. Methods

Adenovirus must be handled under biosafety level 2 conditions. Make sure that only experienced and authorised personnel conduct the following experiments, taking into account the respective safety precautions.

Although the infection efficiency depends on the cell type under study, with the procedure described, commonly about 50–90% of the cells are infected. To discriminate infected from non-infected cells, it is helpful to co-express a fluorescent marker such as EGFP by including a suitable expression cassette in the adenoviral genome.

This protocol assumes the employment of a handheld microarrayer, which allows the precise arraying of up to 768 viral spots. Alternatively, a micropipette can be used to allocate the viruses, with a concomitant decrease in the number of spots that can be arrayed.

For better identification of the viral spots, it is recommended to block cell adhesion outside the viral spots, so that the array of virus translates into an array of cells. A schematic view of the procedure is given in **Fig. 8.1**.

3.1. Preparation of Array Support

1. The following steps are best carried out under a fume cupboard: a slide carrier is filled with nitrocellulose solution. The pre-coated microscopic slides are dipped into the carrier so

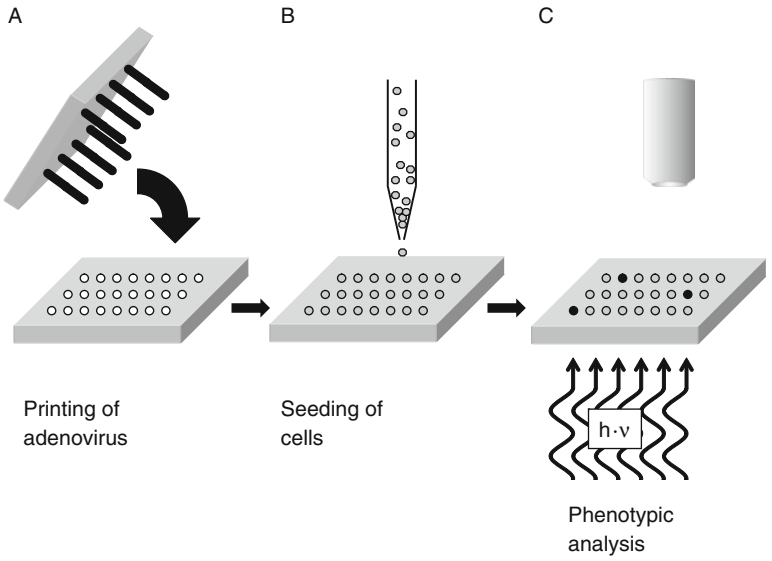

Fig. 8.1. Schematic view of the arraying process. (**a**) Adenovirus encoding shRNA are immobilised in an array on a microscopic slide. (**b**) Cells are seeded onto the adenoviral array. If the slide is properly blocked, cells can only become adherent to the adenoviral spots, simplifying the localisation of individual spots later on. (**c**) The cells become transduced by the immobilised virus, and the cellular response to the shRNA-mediated knockdown can be analysed by optical methods (adapted from 4 under a Creative Commons licence).

that they become entirely covered by the nitrocellulose solution. After 40 , the slide carrier is removed from the nitrocellulose solution and left under the hood until the methanol has evaporated (*see* **Note 2**).

2. Recollect the slides from the slide carrier and sterilise by UV irradiation (90 s). The slides are subsequently stored at room temperature in a sterile container (*see* **Note 3**).

3.2. Arraying Adenovirus

1. Use high-titre virus suspensions (>1×108 infectious units/ml). Carry out all the arraying steps according to biosafety 2 level regulations and under a laminar air flow bench. The virus suspension is pipetted into a suitable reservoir, e.g. the cavities of a 96-well plate (*see* **Note 4**).
2. Take as many of the prepared slides as needed and place them into petri dishes, one per dish.
3. Remove a prepared slide form the dish and place it into the support of the arrayer. Dip the microarrayer into the virus suspension and print the suspension according to the manufacturer's instructions. Using the same adenovirus, the printing procedure can be repeated as many times as required.

4. Before switching to another adenovirus, carefully bathe the needles in 70% ethanol for approximately 10 s. For this purpose, again a 96-well plate serves well. Let the needles dry under the laminar air flow bench.
5. After arraying one slide, remove it from the arrayer's support and place it back into its petri dish. Add some sterile water to the petri dish to humidify the chamber, avoiding any spill-over onto the microscopic slide. Put on the lid and seal tightly with laboratory film (e.g. parafilm). Store at 4°C overnight before further use (*see* **Note 5**).
6. Once the last virus has been printed, carefully bathe the needles of the arrayer first in 70% ethanol, and then bath in the disinfectant recommended by your authorities for virus inactivation for the time recommended. Usually, disinfection overnight with the air flow switched off and the front window pane shut is convenient. After disinfection, rinse the needles with water.

3.3. Blocking Cell Adhesion Outside of the Spots and Seeding the Cells

1. Carry out the following steps according to biosafety 2 level regulations. Place the petri dishes with the viral arrays under a laminar air flow bench. Remove the water from the dish. Rinse the slide carefully with sterile PBS by slowly pipetting PBS onto the slide until its surface is covered by the liquid. Do not pipette directly onto the array, and avoid spill-over into the dish.
2. Remove the PBS by carefully sucking it into a pipette. Discard as biosafety 2 level waste.
3. Carefully pipette Stabilguard onto the slide. Do not pipette directly onto the array, and avoid spill-over into the dish. Put the lid on and leave standing for 45 min.
4. Prepare the cells for seeding. In case of adherent cells, suspend the cells by trypsinisation. Remove the cell culture medium, rinse the cells once with Dulbecco's PBS and add trypsin–EDTA. Put the cells back into the incubator. Depending on the cell type, adherent cells become detached within 5–15 min. Count the cells. Use approximately $0.5–1.0\times10^6$ cells in the appropriate culture medium for each petri dish, in a volume of 800 µl (*see* **Note 6**).
5. Remove the Stabilguard by carefully sucking it into a pipette. Discard as biosafety 2 level waste.
6. Rinse the slide carefully with sterile PBS (700 µl) by slowly pipetting PBS onto the slide. Do not pipette directly onto the array, and avoid spill-over into the dish.
7. Remove the PBS by carefully sucking it into a pipette. Discard as biosafety 2 level waste.

8. In case a liquid connection between the surface of the slide and the dish has formed, carefully remove any spill-over and sweep dry using tissue paper, as otherwise the medium with the cells to be applied next will flow from the slide into the dish. Carefully pipette the cell suspension onto the slide. Do not pipette directly onto the array.
9. To humidify the chamber, add some medium at the edge of the dish, carefully avoiding contact with the slide. Put the lid on and transfer the dish to an incubator set at the appropriate temperature and CO_2 concentration for cultivating the cells, and leave incubating overnight (*see* **Note 7**).
10. On the next morning, carefully add 10 ml of medium to the dish until the slide is completely submerged, and continue incubation.

An example of cells seeded onto the viral spots is given in **Fig. 8.2**, demonstrating the successful viral infection by the expression of green fluorescent protein and red fluorescent protein, respectively.

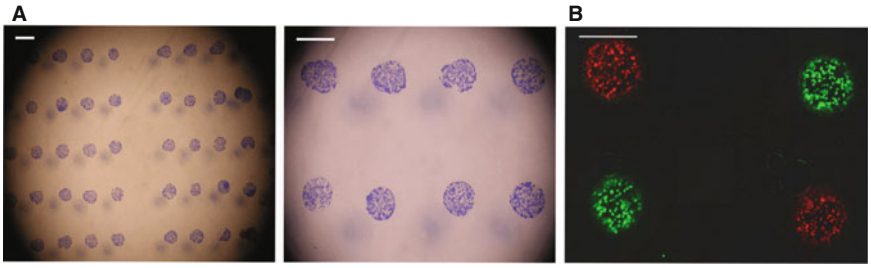

Fig. 8.2. Example of cells seeded on an adenoviral array. (**a**) HeLa cells have been seeded onto an array of adenovirus blocked by Stabilguard. The cells have been visualised by Coommassie staining. Note that cells have only become adherent on the actual viral spots. Two different magnifications are given. (**b**) An array of adenovirus alternately carrying the gene for a green fluorescent protein or for a red fluorescent protein has been printed. The effectivity of the infection of U-2 OS cells is demonstrated by fluorescence microscopy, as upon viral infection the genes are expressed by the cells, rendering them fluorescent. Scale bars: 100 μm (reproduced from 4 under a Creative Commons licence).

3.4. Immunofluorescence Microscopy

Depending on the kinetics of the shRNA expression and the turnover of the protein, the expression of which you aim to knockdown, it takes about 3–5 days for the knock down effect to become manifest at the protein level.

1. Carry out the following steps according to biosafety 2 level regulations. Place the petri dishes with the viral arrays under a laminar air flow bench. Remove the cell culture medium and discard as biosafety 2 level waste.

2. Rinse the slide carefully twice with sterile PBS by slowly pipetting PBS into the dish until the slide becomes covered by the liquid. Do not pipette directly onto the slide, as otherwise cells might become detached due to the mechanical stress. Remove the PBS by carefully sucking it into a pipette. Discard as biosafety 2 level waste.
3. For fixation, add 4% formaldehyde and leave at room temperature for 15 min.
4. Rinse the slide carefully twice with sterile PBS/NaN_3 by slowly pipetting PBS/NaN_3 into the dish until the slide becomes covered by the liquid. Do not pipette directly onto the slide.
5. To detect epitopes located in the cytoplasm or in organelles, permeabilise the cells by applying the permeabilisation solution for 15 min at room temperature.
6. Proceed with the immunolabelling using the appropriate primary and secondary antibodies according to your standard protocol.
7. After immunolabelling, rinse the slide carefully twice with sterile PBS/NaN_3 by slowly pipetting PBS/NaN_3 into the dish until the slide becomes covered by the liquid. Do not pipette directly onto the slide. Add the nuclear stain to the first rinsing step (in a 1:100 dilution from the stock) and leave for 5 min.
8. Remove PBS/NaN_3 and then add one drop of mounting medium onto the slide. Take a cover slip and put it onto the slide with one narrow end, forming an angle of approximately 45° between slide and cover slip, whilst still holding the other, upper end of the cover slip. Slowly lower the upper end to let the cover slip glide onto the drop, carefully avoiding the formation of air bubbles. A pair of foreceps is helpful for controlled lowering of the cover slip. Allow the mounting medium to solidify for approximately 3 h at room temperature. Store the slides protected from light.
9. Use conventional nail varnish so seal the sample, and allow at least 30 min for the varnish to dry.

An example of a functional read-out of a knock-down experiment is given in **Fig. 8.3**: Adenovirus harbouring an expression cassette for a single shRNA directed against the PDZ-binding kinase (PBK) was used to infect human umbilical vein endothelial cells (HUVEC). The induction of apoptosis due to the knock-down of PBK expression was analysed by immunodetection of activated caspase-3. Activation of caspase-3 is an early committed step on the pathway to programmed cell death. For better identification of infected cells, the adenovirus contained an expression cassette for green fluorescent protein.

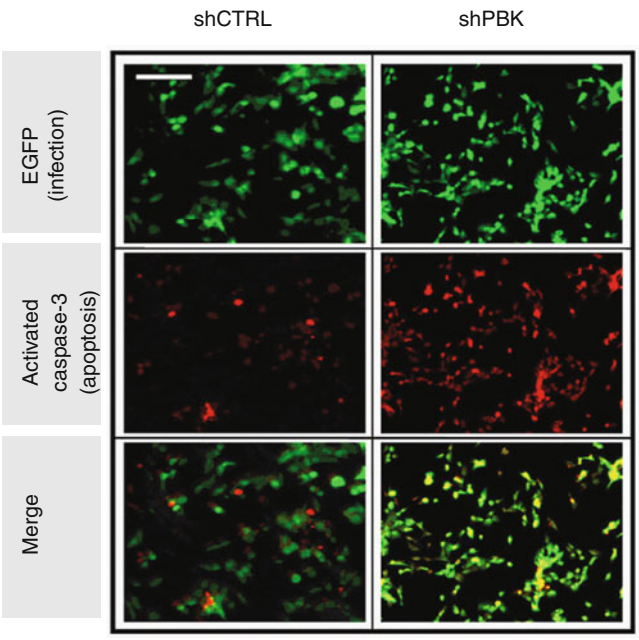

Fig. 8.3. Functional readout of an shRNA-mediated knockdown of the expression of a protein kinase: adenovirus encoding either an shRNA directed against the kinase PBK ("shPBK") or a control shRNA ("shCTRL") was arrayed. Human umbilical vein endothelial cells were seeded onto the array. Three days after infection, the cells were fixed and immunostained for activated caspase-3. In the *top row*, infected cells show up brightly due to fluorescence mediated by the infection of EGFP-encoding virus. In the *centre row*, *fluorescence* indicates the presence of activated caspase-3. A merger of both images is given in the *bottom row*. Note the increase in brightness from the *top row* to the *bottom row* in the case of the cells infected with virus carrying a knock-down sequence directed against PBK, due to the detection of activated caspase-3. In contrast, there is no apparent change in brightness in the case of cells infected with virus carrying the shCTRL sequence, as only activated caspase-3 is detectable in only but a few cells. Scale bar: 20 μm (reproduced from 4 under a Creative Commons licence).

4. Notes

1. NaN_3 prevents the growth of bacteria and fungi by inhibiting the bacterial and mitochondrial electron transport chain. Consequently, NaN_3 is toxic, and so handle with the necessary precautions and wear personal protective equipment. Under acidic conditions, volatile HN_3 becomes released; so, make sure to dissolve NaN_3 only in buffered liquids with a pH >7.0. Do not dissolve in ddH_2O, as ddH_2O tends to be slightly acidic!
2. The nitrocellulose solution can be re-used two or three times. As methanol is volatile, the nitrocellulose solution should be stored in a tight container; otherwise the

nitrocellulose concentration will increase over time. Wear gloves when handling the slides in order to avoid fingerprints. In general for the following steps, take the same measure of care as in conventional eukaryotic cell culture. Make sure to use cell culture grade chemicals to avoid contamination by pyrogens.

3. Ensure the sterility of the slide storage container. Avoid touching the surface onto which the virus is to be arrayed, as the nitrocellulose film deposited on the slide becomes easily detached by mechanical stress. Thus, the slides are best kept in containers with racks that prevent slide-to-slide contact.
4. The MicroCaster microarrayer is suitable to print an array of 32×24 spots, i.e. 768 spots in total. This device is designed in such a way that eight spots are printed at a time. Thus, the virus supension to be arrayed has to be offered in a suitable reservoir, allowing the user to dip in the needles of the arrayer (e.g. a 96-well plate). The print volume is in the order of approximately 20–70 nl, it will vary slightly from spot to spot. For a first-time user, it might be helpful to spike the virus suspension with fluorescently labelled protein (e.g. Cy3-BSA; Invitrogen, Carlsbad, CA) for visual inspection of the quality of the printing process.
5. Alternatively, the adenoviral spots can be stored at 4°C for up to 2 weeks without significant loss of infectivity.
6. There is a variety of trypsinisation agents on the market. Use the one you normally employ to passage your cells. Do not directly add trypsinised cells to the slide, as trypsin might interfere with viral stability and infectivity: After trypsinisation and counting, take $0.5–1.0 \times 10^6$ cells and top-up with cell culture medium to 800 µl before adding to the slide. This protocol is designed for the employment of adherent cells. Cells in suspension will likewise sediment onto the slide, but the number of cells required for full coverage of the viral spots might vary.
7. Be careful not to tilt the petri dishes, especially during transport and when stacking them on top of another in an incubator, as otherwise you might spill the liquid inside.

Acknowledgments

The authors would like to thank Thomas Joos for initial suggestions for the adenovirus array design, Uta Rheinweiler and Angelika Oehmig for the experiments in miniaturising adenovirus

generation and printing, and Ursula Härle for technical assistance. This work was supported by BMBF grant 0313180A/B/C.

References

1. Bailey, S. N., Ali, S. M., Carpenter, A. E., Higgins, C. O., Sabatini, D. M. (2006) Microarrays of lentiviruses for gene function screens in immortalized and primary cells. *Nat Methods* 3, 117–122.
2. Carbone, R., Giorgetti, L., Zanardi, A., Marangi, I., Chierici, E., Bongiorno, G., et al. (2007) Retroviral microarray-based platform on nanostructured TiO_2 for functional genomics and drug discovery. *Biomaterials* 28, 2244–2253.
3. Michiels, F., van Es, H., van Rompaey, L., Merchiers, P., Francken, B., Pittois, K., et al. (2002) Arrayed adenoviral expression libraries for functional screening. *Nat Biotechnol* 20, 1154–1157.
4. Oehmig, A., Klotzbücher, A., Thomas, M., Weise, F., Hagner, U., Brundiers, R., et al. (2008) A novel reverse transduction adenoviral array for the functional analysis of shRNA libraries. *BMC Genomics* 9, 441–453.
5. Ziauddin, J., Sabatini, D. M. (2001) Microarrays of cells expressing defined cDNAs. *Nature* 411, 107–110.
6. Mousses, S., Caplen, N. J., Cornelison, R., Weaver, D., Basik, M., Hautaniemi, S., et al. (2003) RNAi microarray analysis in cultured mammalian cells. *Genome Res* 13, 2341–2347.
7. Fire, A., Xu, S., Montgomery, M. K., Kostas, S. A., Driver, S. E., Mello, C. C. (1998) Potent and specific genetic interference by double-stranded RNA in caenorhabditis elegans. *Nature* 391, 806–811.
8. Elbashir, S. M., Harborth, J., Lendeckel, W., Yalcin, A., Weber, K., Tuschl, T. (2001) Duplexes of 21-nucleotide RNAs mediate RNA interference in cultured mammalian cells. *Nature* 411, 494–498.
9. Brummelkamp, T. R., Bernards, R., Agami, R. (2002) A system for stable expression of short interfering RNAs in mammalian cells. *Science* 296, 550–553.

Chapter 9

Reverse Transfected Cell Microarrays in Infectious Disease Research

Andreas Konrad, Ramona Jochmann, Elisabeth Kuhn, Elisabeth Naschberger, Priya Chudasama, and Michael Stürzl

Abstract

Several human pathogenic viruses encode large genomes with often more than 100 genes. Viral pathogenicity is determined by carefully orchestrated co-operative activities of several different viral genes which trigger the phenotypic functions of the infected cells. Systematic analyses of these complex interactions require high-throughput transfection technology. Here we have provided a laboratory manual for the reverse transfected cell microarray (RTCM; alternative name: cell chip) as a high-throughput transfection procedure, which has been successfully applied for the systematic analyses of single and combination effects of genes encoded by the human herpesvirus-8 on the NF-kappaB signal transduction pathway. In order to quantitatively determine the effects of viral genes in transfected cells, protocols for the use of GFP as an indicator gene and for indirect immunofluorescence staining of cellular target proteins have been included. RTCM provides a useful methodological approach to investigate systematically combination effects of viral genes on cellular functions.

Key words: Transfection, high-throughput, microarray, cell chip, human herpesvirus-8, KSHV.

1. Introduction

Several human pathogenic viruses encode large genomes with often more than 100 genes. This specifically applies for the families of herpesviridae and poxviridae carrying double-stranded linear DNA genomes with 125–230 kb and 130–360 kb, respectively (1, 2). The interaction of these viruses with eukaryotic cells is a key determinant of their pathogenicity. This complex interaction is not due to single gene effects but occurs over the course

E. Palmer (ed.), *Cell-Based Microarrays*, Methods in Molecular Biology 706,
DOI 10.1007/978-1-61737-970-3_9,

of carefully orchestrated co-operative activities of several different viral genes, which trigger the phenotypic functions of the infected cells.

Gene functions are commonly investigated by transfection experiments. The gene of interest is inserted into appropriate expression plasmids and introduced into the target cell. Subsequently, the effect of the ectopically expressed gene on different cell functions can be investigated. Analyses of all single gene effects of one of the viruses mentioned above requires several dozen and up to a 100 transfection experiments. However, already the consideration of only pairwise combination effects results in several thousands of transfections which are necessary for a systematic analysis. This requires novel high-throughput transfection approaches.

Ongoing research programs aim to increase the speed of gene function analysis in mammalian cells by (i) miniaturization of assays, (ii) automation of experimental processes, and (iii) improvement and automation of data recording and management [for a review *see* (3)]. With the goal to carry out many different tests in parallel on a reduced cost basis, experiments are usually carried out by robots in a 96-well or 384-well format.

In 2001, Ziauddin and Sabatini succeeded in scaling down high-throughput gene function analysis to the microarray level (4). Different cDNA expression plasmids were spotted onto slides using a microarray robot (**Fig. 9.1a**). The dried slides were exposed to a transfection reagent, placed in a culture dish, and covered with adherent mammalian cells in medium. Alternatively, DNA and transfection reagent can be mixed at once and applied directly onto the slide (4). Both methods create microarrays of simultaneously transfected cell clusters with different plasmids in distinct and defined areas in a lawn of cells (**Fig. 9.1b**). The process of creating a microarray of clusters of transfected cells was called transfected cell microarray. The transfection method was named reverse transfection, because, in contrast to conventional transfection protocols, DNA was "seeded" first and the cells were added subsequently. Reverse transfected cell microarrays (RTCM), also called "cell chip analyses", allow the parallel performance of several hundred to thousand transfection experiments in eukaryotic cells on a single glass slide. Co-transfections of appropriate reporter plasmids can be used to establish quantitative measures of gene effects on signaling pathways.

RTCM technology has been most commonly used to overexpress proteins in order to study protein localization, interaction of proteins with binding factors, and the effects of the respective proteins on the cell's phenotype (4–9). In addition, gene silencing experiments were conducted by transfecting synthetic siRNAs or various vectors expressing short hairpin (sh)RNA (10, 11). In the meantime, RTCM technology has been established

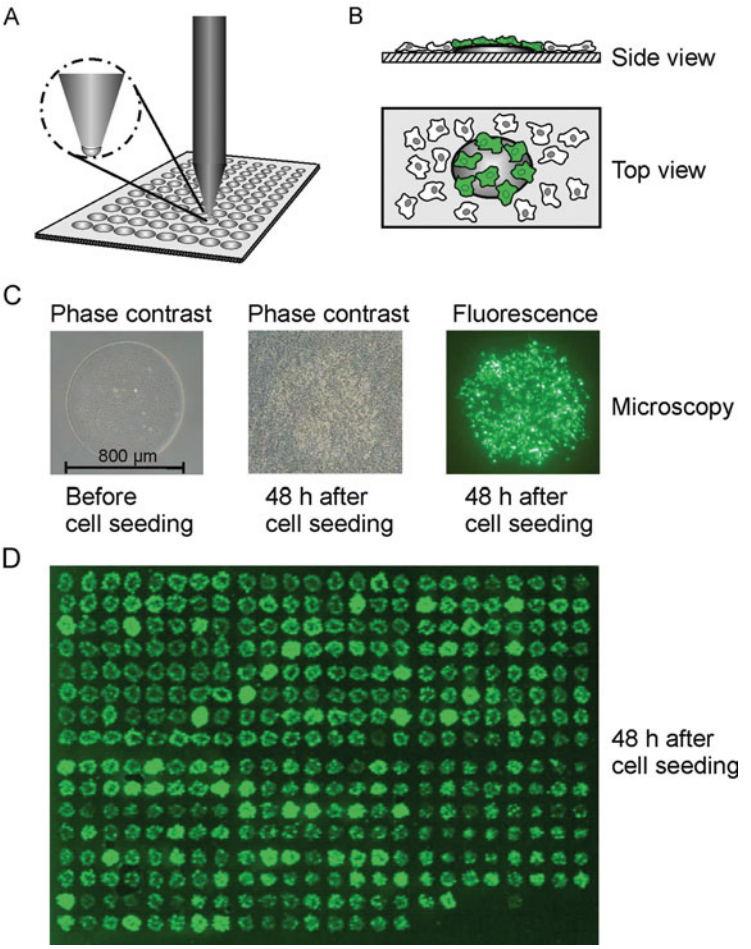

Fig. 9.1. Reverse transfected cell microarray to determine signaling activity of over-expressed HHV-8 proteins. (**a**) Transfection mixtures containing a reporter plasmid expressing GFP under the control of a signal transduction pathway sensitive promoter (e.g., NF-kappaB) in combination with one or two different plasmids expressing the HHV-8-encoded genes are spotted onto a microarray slide. (**b**) Subsequently, the slide is overlaid with HEK 293T cells, which leads to transfection of the cells growing directly on the printed spots. GFP-expression indicates activation of the respective signaling pathway. (**c**) Phase-contrast pictures of the transfection spot without cells (*left*) and 48 h after cell seeding (*middle*). Epifluorescent detection of GFP expression in the cells on the respective transfection spot (*right*). (**d**) Representative laser scanning photograph of a reverse transfected cell array with 371 transfection spots. The figure is partly reproduced with permission from Stürzl et al. (29).

by several different laboratories worldwide using different conditions, cell types, and approaches to detect gene effects on the cells' phenotypes [for a review *see* (3)].

In our laboratory, RTCM is used to systematically analyze single and combination effects of all genes encoded by the human herpesvirus-8 (HHV-8), also called Kaposi's sarcoma-associated herpesvirus (KSHV), on cellular signal transduction pathways.

HHV-8 is the etiological agent of Kaposi's sarcoma (KS) and of two rare lymphoproliferative disorders, primary effusion lymphoma (PEL) and multicentric Castleman's disease (12, 13). Activation of NF-kappaB is crucial for the development and progression of HHV-8-associated diseases. It protects HHV-8-

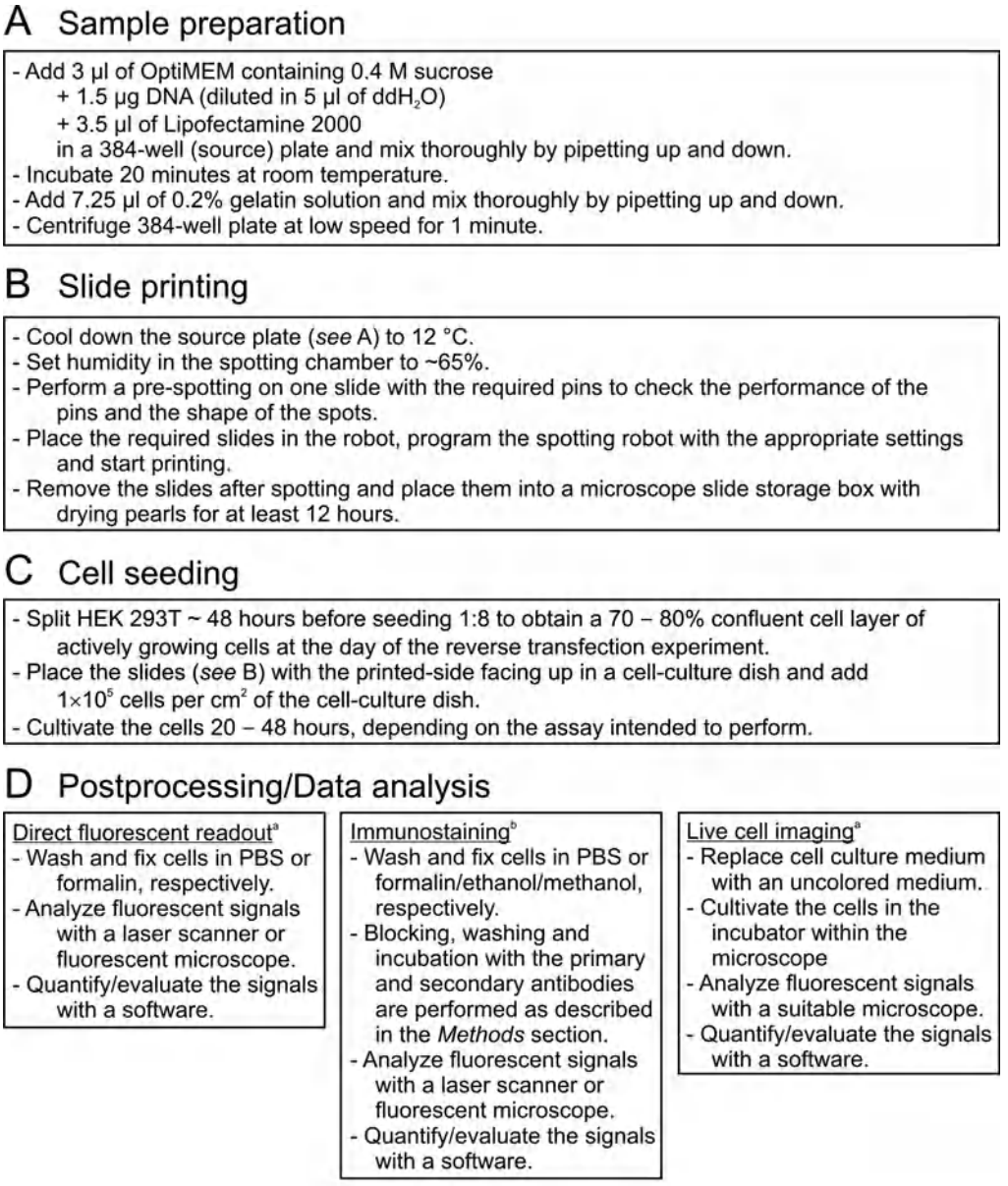

Fig. 9.2. Overview of the RTCM procedure in HEK 293T cells. The method is divided into four parts: (**a**) sample preparation, (**b**) slide printing, (**c**) cell seeding, and (**d**) postprocessing/data analysis. [a]The transfected indicator plasmid expresses a fluorescent reporter protein. [b]Staining of protein(s) of interest is performed with an fluorescently labeled secondary antibody.

infected cells against apoptosis (14, 15) and maintains the latent viral life cycle (16, 17). HHV-8 encodes at least 86 genes (18, 19). Of these, only few have been studied for their impact on NF-kappaB signaling. We used RTCM as an unbiased systems biology approach to analyze systematically the effects of all HHV-8 single genes and of a selection of 21 genes in pairwise combinations on the NF-kappaB signaling pathway (20). By this approach, the open reading frame (ORF) 75 was detected as a new HHV-8-encoded activator of NF-kappaB (20). Additionally, known HHV-8-encoded activators and inhibitors of NF-kappaB were confirmed, showing the reliability of the method.

In order to determine the effects of HHV-8-encoded genes on NF-kappaB activation, we used an indicator plasmid expressing GFP under the control of an NF-kappaB-sensitive consensus promoter. In this setup, the expression of GFP provided a quantitative measure of the respective gene effects on NF-kappaB activation. To date, RTCM has been employed for different applications, such as screening for modulators of different signal transduction pathways (reporter assays, as described here) (20–24), investigation of ligand–receptor binding (4, 6), determination of interaction partners (mammalian two-hybrid) (25), localization studies of previously uncharacterized proteins (by co-staining of organelle-specific markers) (7, 8), identification of pro-apoptotic genes (either by TUNEL analysis or by detection of apoptotic bodies) (9, 26), and analyses of gene effects on proteasomal function (27), on secretory pathways (28), and on cell morphology (5). In most cases, these assays were either based on the detection of the expression of a fluorescent indicator gene as described above or of cellular indicator gene products *via* indirect immunofluorescence staining.

This chapter provides a laboratory protocol for the reverse transfection of plasmids in HEK 293T cells. GFP induction assay and indirect immunofluorescence are exemplarily given as methods to determine quantitatively gene effects in transfected cells. A short summary of the procedure is given in **Fig. 9.2**.

2. Materials

2.1. Sample Preparation

1. 0.2% (w/v) gelatin solution is freshly prepared (*see* **Note 1**) by dissolving the gelatin powder (type B from bovine skin, cell-culture tested; Sigma-Aldrich, Munich, Germany) for 20 min at 60°C in double-distilled water (ddH_2O). The gelatin solution is filtered through a 0.45-μm cellulose–acetate sterile filter after it has cooled down to room temperature.

2. Sucrose (Merck, Darmstadt, Germany) is added to Opti-MEM (Invitrogen, Karlsruhe, Germany) to a final concentration of 0.4 M. Prepare the solution fresh and filter it sterile as described above.
3. Different batches of Lipofectamine 2000 (Invitrogen) should be tested to obtain best transfection efficiency and the same batch should be used for the whole screening project.
4. Plasmids are isolated in an endotoxin free or reduced manner and are adjusted to a concentration of 1.0 μg/μl in Tris–EDTA (TE) buffer (e.g., EndoFree Plasmid Maxi Kit, Qiagen, Hilden, Germany).
5. 384-well plates (flat bottom; Nunc, Thermo Fisher Scientific, Langenselbold, Germany).
6. Centrifuge for 384-well plates (e.g., Hettich Rotina 35R, rotor #1713, Tuttlingen, Germany).

2.2. Slide Printing

1. Gamma-amino-propyl silane (GAPS) II coated slides (Corning) (*see* **Note 2**).
2. Contact microarray printer/robot for spotting, containing a cooling device for the source plate a humidity control, and an ultrasonic water bath for the pins (e.g., VersArray ChipWriter Pro Bio-Rad, Munich, Germany) (*see* **Note 3**).
3. Solid microarray pins: e.g., PTS600 pins (600 μm diameter, Anopoli, Eichgraben, Austria) (*see* **Note 4**).
4. Phase-contrast microscope to control the spot shape after pre-spotting (e.g., Axiovert25, Zeiss, Göttingen, Germany).
5. Microscope slide storage box and drying pearls (Neolab, Heidelberg, Germany).

2.3. Cell Seeding

1. Human embryonic kidney (HEK) 293T cells (ATCC no. CRL-11268).
2. Dulbecco's modified eagle medium (DMEM) (PAA, Pasching, Austria) supplemented with 10% fetal calf serum (Biochrom, Berlin, Germany), 100 U/ml penicillin, and 100 μg/ml streptomycin (both from PAA).
3. Neubauer chamber or automatic cell counter for counting the cells (e.g., Casy1, Casy Cell Counter, Innovatis, Reutlingen, Germany).
4. Cell-culture dishes for reverse transfection (*see* **Note 5**).

2.4. Postprocessing/Data Analysis

1. Coplin/staining jars (e.g., Hellendhal type, Noviglio, Italy).
2. Phosphate buffered saline, 1× (PBS, Biochrom).
3. Formalin solution, neutral buffered, 4% (Sigma-Aldrich).

4. Microscope cover slips (size depends on the printed area of the slides; e.g., 24×60 mm, Menzel-Gläser, Braunschweig, Germany).
5. Fluorescent mounting medium (Dako, Hamburg, Germany).
6. Fluorescence scanner (Fuji FLA-5000 laser scanner, Fujifilm, Düsseldorf, Germany).
7. Quantification software (e.g., AIDA software package, Straubenhardt, Germany).
8. Fluorescence microscope (e.g., Leica, DMRBE, Wetzlar, Germany).
9. For immunofluorescence staining, tris-buffered saline (TBS, 50 mM Tris–HCl pH 7.6, 150 mM NaCl), saponin (Sigma), DAPI (Invitrogen), and goat-normal-serum (GNS, Dianova, Hamburg, Germany) are additionally required.

3. Methods

3.1. Sample Preparation

1. Transfer 3 μl of OptiMEM containing 0.4 M sucrose and 3.5 μl of ddH_2O per well in a 384-well plate (source plate). Add 1.5 μg DNA to each well of the respective plasmid (=1.5 μl, *see* Step 4, **Section 2.1**, and *see* **Note 6**). Add 3.5 μl of Lipofectamine 2000 to each well and mix thoroughly by pipetting up and down (*see* **Note 7**).
2. Incubate at room temperature for 20 min.
3. Add 7.25 μl of a 0.2% (w/v) gelatin solution to each well and mix thoroughly by pipetting up and down (*see* **Note 7**).
4. The 384-well plate is centrifuged at low speed (< 100×*g*) for 1 min to remove air bubbles in the solution and to level the sample surface (proceed directly to "Slide printing").
5. The total volume is 18.75 μl containing 0.08 μg/μl DNA, 0.077% gelatin, and 18.7% Lipofectamine 2000. Up to 150 spots of one sample can be printed with this solution.

3.2. Slide Printing

1. Cool down the source plate in the microarray robot to 12°C to avoid evaporation while printing.
2. Set humidity in the spotting chamber to ~65%.
3. Clean pins with 70% ethanol and place them in the correct position in the print head of the microarray robot.
4. Define the appropriate settings in the software program to define the spotting parameters (*see* **Note 8**).
5. Place the slides in the microarray robot and start printing (*see* **Note 9**).

6. Store and dry printed slides for at least 12 h in a microscope slide storage box with drying pearls before they are used for reverse transfection (*see* **Note 10**).

3.3. Cell Seeding

1. Place the slides with the printed-side facing up in a sterile cell-culture dish.
2. Trypsinize actively growing cells, resuspend them in an appropriate volume of medium, and ensure to obtain a single cell suspension. (Pipette the cell suspension gently 10 times up and down. Avoid foam formation.)
3. Determine cell number.
4. 1×10^5 HEK 293T cells per cm^2 are seeded for reverse transfection (*see* **Note 11**).
5. Pour/dispense the cell suspension carefully over the slide(s). Do not pipette directly on the spotted area.
6. Cultivate the cells under normal growth conditions (37°C, 8.5% CO_2) for 40–48 h until confluence (*see* **Note 12**).

3.4. Postprocessing/Data Analysis

1. Remove the medium completely but gently from the cell-culture dish. Ideally, remove the medium directly in the incubator without moving the dish.
2. Take out the slides from the cell-culture dish and wash them gently in a coplin jar with PBS for 2 min at room temperature.
3. Let the slides air-dry completely.
4. Fix the cells on the slides in a coplin jar using formalin for 15–20 min at room temperature (*see* **Note 13**).
5. Wash the slides in a coplin jar with PBS for 2 min at room temperature and proceed directly with Step 14, **Section 3.4**, when using fluorescent proteins as a direct readout. For immunofluorescence staining, wash the slides in a coplin jar with TBS at room temperature for 2 min and proceed with Step 6, **Section 3.4**.
6. Permeabilize cells with 0.1% saponin in TBS for 20 min at room temperature.
7. Block unspecific binding sites with 10% GNS in TBS for 10 min at room temperature.
8. Incubate cells with the first antibody diluted in 5% GNS in TBS (*see* **Note 14**).
9. Gently wash the slides two times with TBS for 2 min at room temperature.
10. Incubate cells in the dark for 45 min with the secondary antibody diluted in 5% GNS in TBS (*see* **Note 15**).

11. Gently wash the slides two times with TBS for 2 min at room temperature.
12. Counterstain the cell nuclei with DAPI (1 μg/ml in ddH_2O, Invitrogen) for 10 min in the dark at room temperature.
13. Gently wash the slides two times with TBS for 2 min at room temperature.
14. Let the slides dry for a few minutes, and mount the slides with fluorescence mounting medium and a cover slip of the appropriate size. Let the mounting medium solidify for more than 30 min.
15. For long-term storage, the edges of the cover slip may be sealed with nail polish to prevent forming of air pockets.
16. Clean lower side of the slides carefully with 70% ethanol.
17. Analyze the slides/signals with a fluorescence microscope or a fluorescence scanner (*see* **Note 16**).
18. Quantify the resulting signals using a quantification software.

4. Notes

1. Optimal DNA, sucrose, and gelatin concentration, slide surface/type of slides, and transfection reagent should be tested for every cell type and application.
2. As an alternative to GAPS-coated slides, also "normal" microscope glass slides (e.g., superfrost, Thermo Fisher Scientific) can be used for most applications.
3. To avoid cross-contamination, the pins should be washed and sonicated between spotting of different samples.
4. Using smaller tip pins (diameter <600 μm), the number of spots per slide can be increased. However, this will result in fewer transfected cells per spot and correspondingly lower signal intensity.
5. Examples for cell culture dishes suitable for reverse transfection: four-well square multi-dishes (quadriPERM, GreinerBio-One, Frickenhausen, Germany) for four slides; 10×10-cm petri dish (Integrid, BD Biosciences, Heidelberg, Germany) for three slides in one dish; "10-cm dish" (diameter of 8.6 cm) (Thermo Fisher Scientific) for one slide. *See* **Note 11** for the amount of cells for the different cell-culture dishes.

6. For pathway activation analysis of single genes, 0.5 μg reporter plasmid ("indicator"), 0.5 μg of expression plasmid 1 ("effector"), and 0.5 μg of an empty vector were used. For the pairwise activation analysis of two genes, 0.5 μg indicator plasmid, 0.5 μg of effector plasmid no.1, and 0.5 μg of effector plasmid no.2 were used. For pathway inhibition analysis of single genes, 0.5 μg indicator plasmid, 0.5 μg of a known activating plasmid, and 0.5 μg of a potential inhibitor plasmid were used.
7. Mixing should be conducted similarly for each sample by pipetting up and down for a constant number of cycles.
8. The use of the above-mentioned settings creates spots with a size of ~800 μm in diameter (**Fig. 9.1c**). In this case, the spot center-to-center distance should be ≥ 1,120 μm (**Fig. 9.1d**). These settings allow a maximum of 384 spots in duplicates per slide (768 total spots per slide).
9. It is recommended to perform a pre-spotting before starting the proper/final spotting program. To this goal, spot the first samples 8–16 times on a separate slide. Check the shape of the spots under the microscope and repeat the pre-spotting until all of the spots are uniformly shaped.
10. Printed slides can be stored several months in a microscope slide storage box containing drying pearls at room temperature.
11. All parameters are given for HEK 293T cells and a 40–48 h incubation time until the cells reach confluency. Seed 2.3×10^6 cells in 8 ml medium for each well of a four-well square multi-dish; seed 1.0×10^7 cells in 25–30 ml of medium for a 10×10 cm dish; seed 5.7×10^6 cells in 12–15 ml medium for a 10-cm dish.
12. The indicated parameters are for HEK 293T cells and cultivation until a confluent cell layer is achieved. For live cell imaging, slides can be directly transferred to a suitable microscope already 20 h after cell seeding. For this application, it is necessary to replace the medium with a cell-culture medium without phenol red.
13. The cells can also be fixed with 100% ethanol or methanol for 5–10 min at –20°C depending on the primary antibody used for immunostaining. When using ethanol/methanol as fixation, the permeabilization (Step 6, **Section 3.4**) is not required.
14. Example of Myc-tag immunostaining: incubate the slides with mouse anti-Myc-tag monoclonal antibody (9B11, Cell Signaling, Danvers, MA, USA, 1:5,000) diluted in 5% GNS in TBS for 2 h at room temperature. For one slide, 500–1,000 μl of antibody solution is sufficient.

15. Incubate the respective secondary antibody [e.g., goat-anti-mouse IgG AlexaFluor488-conjugated antibody (Invitrogen)] diluted 1:500 in 5% GNS in TBS for 45 min at room temperature in the dark. For one slide, 500–1,000 μl of antibody solution is sufficient.
16. Scanner settings were as follows: use an 473-nm excitation laser (blue) and Y510 filter (long pass blue) for GFP- and AlexaFluor488 signals and an 532-nm excitation laser (green) with the BPG1 filter (green, 570DF20) for RFP- and AlexaFluor546 signals. A resolution of 25 μm is sufficient for spot signal evaluation. If you want to detect changes of the cell morphology or protein localization at the single cell level, a fluorescence microscope or a scanner with a resolution higher than 5 μm is required.

Acknowledgments

This work was supported by grants of the Deutsche Forschungsgemeinschaft (DFG-SPP 1130, DFG-GK 1071, and DFG 317/2-1) and of the Interdisciplinary Center for Clinical Research (IZKF) of the University Medical Center Erlangen to MS and by a habilitation grant (Habilitationsstipendium, ELAN-Förderprogramm) of the University Medical Center Erlangen to RJ.

References

1. Roizman, B., Baines, J. (1991) The diversity and unity of herpesviridae. *Comp Immunol Microbiol Infect Dis* 14, 63–79.
2. Lefkowitz, E. J., Wang, C., Upton, C. (2006) Poxviruses: past, present and future. *Virus Res* 117, 105–118.
3. Stürzl, M., Konrad, A., Sander, G., Wies, E., Neipel, F., Naschberger, E., Reipschläger, S., Gonin-Laurent, N., Horch, R. E., Kneser, U., Hohenberger, W., Erfle, H., and Thurau, M. (2008) High throughput screening of gene functions in mammalian cells using reversely transfected cell arrays: review and protocol. *Comb Chem High Throughput Screen* 11, 159–172.
4. Ziauddin, J., Sabatini, D. M. (2001) Microarrays of cells expressing defined cDNAs. *Nature* 411, 107–110.
5. Conrad, C., Erfle, H., Warnat, P., Daigle, N., Lorch, T., Ellenberg, J., Pepperkok, R., Eils, R. (2004) Automatic identification of subcellular phenotypes on human cell arrays. *Genome Res* 14, 1130–1136.
6. Delehanty, J. B., Shaffer, K. M., Lin, B. (2004) Transfected cell microarrays for the expression of membrane-displayed single-chain antibodies. *Anal Chem* 76, 7323–7328.
7. Hodges, E., Redelius, J. S., Wu, W., Höög, C. (2005) Accelerated discovery of novel protein function in cultured human cells. *Mol Cell Proteomics* 4, 1319–1327.
8. Hu, Y. H., Warnatz, H. J., Vanhecke, D., Wagner, F., Fiebitz, A., Thamm, S., Kahlem, P., Lehrach, H., Yaspo, M. L., Janitz, M. (2006) Cell array-based intracellular localization screening reveals novel functional features of human chromosome 21 proteins. *BMC Genomics* 7, 155.

9. Mannherz, O., Mertens, D., Hahn, M., Lichter, P. (2006) Functional screening for proapoptotic genes by reverse transfection cell array technology. *Genomics* 87, 665–672.
10. Neumann, B., Held, M., Liebel, U., Erfle, H., Rogers, P., Pepperkok, R., Ellenberg, J. (2006) High-throughput RNAi screening by time-lapse imaging of live human cells. *Nat Methods* 3, 385–390.
11. Vanhecke, D., Janitz, M. (2005) Functional genomics using high-throughput RNA interference. *Drug Discov Today* 10, 205–212.
12. Ensoli, B., Stürzl, M., Monini, P. (2001) Reactivation and role of HHV-8 in Kaposi's sarcoma initiation. *Adv Cancer Res* 81, 161–200.
13. Stürzl, M., Zietz, C., Monini, P., Ensoli, B. (2001) Human herpesvirus-8 and kaposi's sarcoma: relationship with the multistep concept of tumorigenesis. *Adv Cancer Res* 81, 125–159.
14. Keller, S. A., Schattner, E. J., Cesarman, E. (2000) Inhibition of NF-kappaB induces apoptosis of KSHV-infected primary effusion lymphoma cells. *Blood* 96, 2537–2542.
15. Thurau, M., Marquardt, G., Gonin-Laurent, N., Weinlander, K., Naschberger, E., Jochmann, R., Alkharsah, K. R., Schulz, T. F., Thome, M., Neipel, F., Stürzl, M. (2009) Viral inhibitor of apoptosis vFLIP/K13 protects endothelial cells against superoxide-induced cell death. *J Virol* 83, 598–611.
16. Brown, H. J., Song, M. J., Deng, H., Wu, T. T., Cheng, G., Sun, R. (2003) NF-kappaB inhibits gammaherpesvirus lytic replication. *J Virol* 77, 8532–8540.
17. Ye, F. C., Zhou, F. C., Xie, J. P., Kang, T., Greene, W., Kuhne, K., Lei, X. F., Li, Q. H., Gao, S. J. (2008) Kaposi's sarcoma-associated herpesvirus latent gene vFLIP inhibits viral lytic replication through NF-kappaB-mediated suppression of the AP-1 pathway: a novel mechanism of virus control of latency. *J Virol* 82, 4235–4249.
18. Neipel, F., Albrecht, J. C., Fleckenstein, B. (1997) Cell-homologous genes in the Kaposi's sarcoma-associated rhadinovirus human herpesvirus 8: determinants of its pathogenicity? *J Virol* 71, 4187–4192.
19. Russo, J. J., Bohenzky, R. A., Chien, M. C., Chen, J., Yan, M., Maddalena, D., Parry, J. P., Peruzzi, D., Edelman, I. S., Chang, Y., and Moore, P. S. (1996) Nucleotide sequence of the kaposi sarcoma-associated herpesvirus (HHV8). *Proc Natl Acad Sci USA* 93, 14862–14867.
20. Konrad, A., Wies, E., Thurau, M., Marquardt, G., Naschberger, E., Hentschel, S., Jochmann, R., Schulz, T. F., Erfle, H., Brors, B., Lausen, B., Neipel, F., and Stürzl, M. (2009) A systems biology approach to identify the combination effects of human herpesvirus 8 genes on NF-kappaB activation. *J Virol* 83, 2563–2574.
21. Redmond, T. M., Ren, X., Kubish, G., Atkins, S., Low, S., Uhler, M. D. (2004) Microarray transfection analysis of transcriptional regulation by cAMP-dependent protein kinase. *Mol Cell Proteomics* 3, 770–779.
22. Tian, L., Wang, P., Guo, J., Wang, X., Deng, W., Zhang, C., Fu, D., Gao, X., Shi, T., Ma, D. (2007) Screening for novel human genes associated with CRE pathway activation with cell microarray. *Genomics* 90, 28–34.
23. Webb, B. L., Diaz, B., Martin, G. S., Lai, F. (2003) A reporter system for reverse transfection cell arrays. *J Biomol Screen* 8, 620–623.
24. Yamauchi, F., Okada, M., Kato, K., Jakt, L. M., Iwata, H. (2007) Array-based functional screening for genes that regulate vascular endothelial differentiation of flk1-positive progenitors derived from embryonic stem cells. *Biochim Biophys Acta* 1770, 1085–1097.
25. Fiebitz, A., Nyarsik, L., Haendler, B., Hu, Y. H., Wagner, F., Thamm, S., Lehrach, H., Janitz, M., Vanhecke, D. (2008) High-throughput mammalian two-hybrid screening for protein-protein interactions using transfected cell arrays. *BMC Genomics* 9, 68.
26. Palmer, E. L., Miller, A. D., Freeman, T. C. (2006) Identification and characterisation of human apoptosis inducing proteins using cell-based transfection microarrays and expression analysis. *BMC Genomics* 7, 145.
27. Silva, J. M., Mizuno, H., Brady, A., Lucito, R., Hannon, G. J. (2004) RNA interference microarrays: high-throughput loss-of-function genetics in mammalian cells. *Proc Natl Acad Sci USA* 101, 6548–6552.
28. Simpson, J. C., Cetin, C., Erfle, H., Joggerst, B., Liebel, U., Ellenberg, J., Pepperkok, R. (2007) An RNAi screening platform to identify secretion machinery in mammalian cells. *J Biotechnol* 129, 352–365.
29. Stürzl, M., Konrad, A., Alkharsah, K. R., Jochmann, R., Thurau, M., Marquardt, G., and Schulz, T. F. (2009) The contribution of systems biology and reverse genetics to the understanding of Kaposi's sarcoma-associated herpesvirus pathogenesis in endothelial cells. *Thrombosis and Haemostasis* 102(6), 1117–1134.

Chapter 10

Transfected Cell Microarrays for the Expression of Membrane-Displayed Single-Chain Antibodies

Baochuan Lin and James B. Delehanty

Abstract

Transfected cell microarrays, arrays of cells expressing defined cDNAs, are promising technologies that can enable the functional analysis of many proteins in parallel. This technique has been adapted for the comparative functional analysis of single-chain antibodies (scFvs) and to facilitate the screening and characterization of these antibodies for their use in diagnostic and therapeutic applications. In this method, membrane-targeting expression vectors encoding scFvs are mixed with transfection reagents and are deposited at high density onto a microscope slide. Adherent mammalian cells are subsequently added to the printed array. Upon attachment to the substrate, the cells take up the plasmid DNA and express the particular protein encoded at each location. The result is an array whose features are micrometer-sized clusters of cells expressing defined genes. This approach provides for the high-throughput functional analysis of many different proteins in parallel and can be considerably more informative and cost-effective relative to more traditional protein expression techniques.

Key words: Transfected cell microarray, single-chain antibody (scFv), reverses transfection, high-throughput functional analysis, immunoglobulin, fusion protein.

1. Introduction

The human genome project has fostered the development of high-throughput methodologies to obtain and analyze nucleic acid sequence information. DNA microarrays, collections of hundreds to thousands of nucleic acid probes immobilized on a solid support, have been a key technology to emerge from this effort. The spatial separation of the immobilized DNA probes allows for the interrogation of large numbers of targeted complementary nucleic acid sequences simultaneously. A variety of microarray formats has been developed for gene expression

E. Palmer (ed.), *Cell-Based Microarrays*, Methods in Molecular Biology 706,
DOI 10.1007/978-1-61737-970-3_10,

profiling, genetic polymorphism analysis, and microbe detection and diagnosis. Building on the principle of DNA microarrays, transfected cell microarrays, arrays of cells expressing defined cDNAs, have emerged as a methodology for analyzing gene function within the context of mammalian cells (1, 2). A transfected cell microarray is composed of "cDNAs" in the form of plasmids deposited at high density onto a microscope slide, where each spot can carry either one or a collection of different cDNAs and adherent mammalian cells that are subsequently added to the printed array. The cells internalize the plasmid DNA upon contact with the deposited DNAs on the spots and subsequently express the specific plasmid-encoded protein(s) at each location. The result is an array whose features are micrometer-sized clusters of cells expressing defined genes at a high-spatial density (1–3).

Single-chain antibodies (scFvs), also called single-chain variable fragments, are recombinant fusion proteins constructed by joining together the heavy- and light-chain variable regions of immunoglobulins with a flexible peptide linker. The scFv proteins (approximately one-sixth the molecular weight of the parent immunoglobulin) retain the specificity of the original immunoglobulins and, because the antigen-binding domain is expressed as a single peptide, it can be easily produced and genetically manipulated through recombinant DNA techniques. This has led to an increased interest in their use in diagnostic and therapeutic applications (4, 5). Concomitant with the development of using scFvs as diagnostics tools and therapeutic agents has emerged the need for a high-throughput means to assess the binding activity of scFvs and other recombinant fragments as they are displayed on the surface of mammalian cells. Transfected cell microarrays expressing membrane-displayed single-chain antibodies can address this need. In the method presented herein, a membrane-targeting expression vector, pDisplay (Invitrogen Life Technologies, Carlsbad, CA) was used to express scFvs as a fusion with a C-terminal myc-epitope tag and a PDGF receptor transmembrane domain (PDGFR-TM) (**Fig. 10.1a**). The plasmids encoding the scFvs were then mixed with a transfection reagent in a fixed ratio to obtain optimal transfection efficiency and they were subsequently printed onto microarray slides using a non-contact microarray printer. Adherent cells were then added to the printed arrays. After allowing sufficient time for expression of the scFvs, their expression on the cell surface was monitored. In this chapter, we have used well-characterized anti-fluorescein scFv 4-4-20 and its mutants to demonstrate the utility of the microarray format to determine the expression levels of the different clones and to characterize their differential binding affinities for the fluorescein ligand.

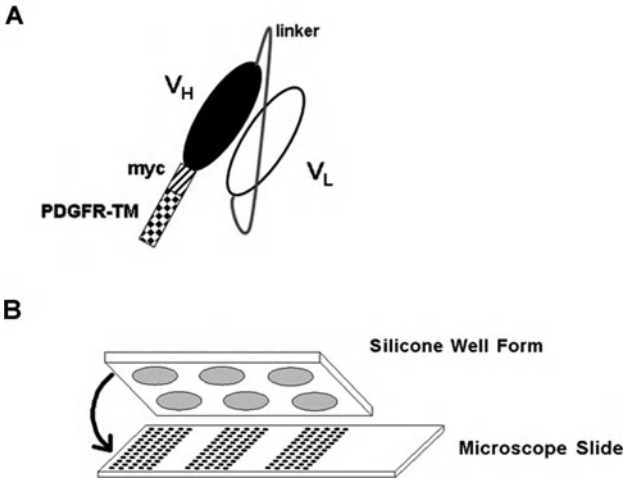

Fig. 10.1. 4-4-20 scFv and transfected cell array microarray format. (**a**) In the 4-4-20 scFv format, the light-chain variable (V_L) and heavy-chain variable (V_H) domains are joined by a 25-residue amino acid linker. The scFv is expressed as a fusion with a C-terminal myc-epitope tag for detection and a PDGF receptor transmembrane domain (PDGFR-TM). (**b**) In the transfected cell microarray, scFv plasmid DNA is mixed with transfection reagent and deposited in a gelatin/sucrose printing buffer onto the surface of a glass slide. A multiple-well silicon form is then aligned onto the printed array. The addition of cells to the array results in the transfection of cells in spatially discrete spots. Reproduced with permission from the ACS (3).

2. Materials

2.1. Control Plasmid

1. pDsRed2-Nuc expression vector (which expresses the fluorescent protein DsRed2 within the nucleus of transfected mammalian cells by virtue of its fusion with a nuclear localization signal from SV40 virus) was obtained from BD Biosciences (Palo Alto, CA). The plasmid was stored at –20°C for up to 6 months or –80°C for several years.
2. LB kanamycin plates: 0.01% (w/v) tryptone, 0.005% (w/v) yeast extract, 0.005% (w/v) NaCl, 0.015% (w/v) agarose, and 50 μg/ml kanamycin. The plates were stored at 4°C for up to 3 months.
3. LB kanamycin broth: 0.01% (w/v) tryptone, 0.005% (w/v) yeast extract, 0.005% (w/v) NaCl, and 50 μg/ml kanamycin. The broth was stored at 4°C for up to 3 months.
4. QIAGEN Plasmid Midi kit (Qiagen) or PureYield Plasmid Midiprep System (Promega Corp.) was stored at room temperature for up to 12 months (*see* **Note 1**).

2.2. Cloning of Anti-fluorescein Single-Chain Antibodies

1. pDisplay vector was obtained from Invitrogen Life Technologies. The plasmid was stored at –20°C for up to 6 months or –80°C for several years.
2. *Pfu* Turbo DNA polymerase (2.5 U/μl) (Stratagene) and 10× *Pfu* DNA polymerase reaction buffer were stored at –20°C for up to 6 months (*see* **Note 2**).
3. 10 mM dNTPs (Invitrogen) were stored in 100 μl aliquots at –20°C for up to 6 months (*see* **Note 3**).
4. PCR primers obtained from Operon Biotechnologies Inc. were dissolved in TE buffer to a stock concentration of 100 μM and stored at –80°C for up to 1 year. Working solutions (1–10 μM) were prepared by diluting the stock into nuclease-free H_2O and stored at –20°C for up to 6 months (*see* **Note 3**).
5. PCR reaction buffer: 20 mM Tris–HCl (pH 8.8), 2 mM $MgSO_4$, 10 mM KCl, 10 mM $(NH_4)_2SO_4$, 0.1% Triton® X-100, 0.1 mg/ml BSA, 200 μM of dNTPs, and 200 nM each of sense and antisense primers.
6. MasterPure™ DNA purification kit (Epicentre Biotechnologies, Madison, WI) was stored at room temperature for up to 12 months (*see* **Note 4**).
7. The restriction endonucleases, *AccI*, *EcoRI*, *SfiI*, and *SalI*, were obtained from New England BioLabs (NEB) and stored at –20°C for up to 6 months (*see* **Note 3**).
8. Calf intestinal alkaline phosphatase (10 U/μL, NEB) was stored at –20°C for up to 6 months (*see* **Note 5**).
9. T4 DNA ligase (1 U/μL) and 5× ligation buffer (Invitrogen) were stored at –20°C for up to 6 months (*see* **Note 6**).
10. Ligation reaction buffer contains 50 mM Tris–HCl (pH 7.6), 10 mM $MgCl_2$, 1 mM ATP, 1 mM DTT, and 5% (w/v) polyethylene glycol-8000.
11. DH5α competent cells (Invitrogen) were stored in 50 μl aliquots at –80°C for up to 6 months (*see* **Note 3**).
12. LB kanamycin plates: 0.01% (w/v) tryptone, 0.005% (w/v) yeast extract, 0.005% (w/v) NaCl, 0.015% (w/v) agarose, and 50 μg/ml kanamycin. The plates were stored at 4°C for up to 3 months.
13. LB kanamycin broth: 0.01% (w/v) tryptone, 0.005% (w/v) yeast extract, 0.005% (w/v) NaCl, and 50 μg/ml kanamycin. The broth was stored at 4°C for up to 3 months.
14. LB ampicillin plates: 0.01% (w/v) tryptone, 0.005% (w/v) yeast extract, 0.005% (w/v) NaCl, 0.015% (w/v) agarose,

and 100 μg/ml ampicillin. The plates were stored at 4°C for up to 3 months.

15. LB ampicillin broth: 0.01% (w/v) tryptone, 0.005% (w/v) yeast extract, 0.005% (w/v) NaCl, 0 and 100 μg/ml ampicillin. The broth was stored at 4°C for up to 3 months.
16. QIAprep spin miniprep kit and QIAGEN Plasmid Midi kit (Qiagen) or PureYield Plasmid Midiprep System (Promega Corp.) were stored at room temperature for up to 12 months.
17. Glycerol solution: 65% glycerol, 0.1 M $MgSO_4$, and 25 mM Tris–HCl (pH 8.0). The glycerol solution was autoclaved and stored at room temperature for up to 12 months.

2.3. Site-Directed Mutagenesis

1. QuickChange® Site-Directed Mutagenesis Kit (Stratagene), containing *Pfu* Turbo DNA polymerase (2.5 U/μl), 10× reaction buffer, Dpn I digestion enzyme, oligonucleotide control primers, dNTP, and pUC18 control plasmid, was stored at –20°C for up to 6 months.
2. PCR primers (Operon Biotechnologies Inc.) were dissolved in TE buffer to a stock concentration of 100 μM and stored at –80°C for up to 1 year. Working solutions (1–10 μM) were prepared by diluting the stock into nuclease-free H_2O and stored at –20°C for up to 6 months (*see* **Note 3**).
3. XL1-Blue supercompetent cells (Stratagene), part of the QuickChange® Site-Directed Mutagenesis Kit, were stored in 50 μl aliquots at –80°C for up to 6 months (*see* **Note 3**).
4. NZY broth: 0.01% (w/v) NZ amine (casein hydrolysate), 0.005% (w/v) yeast extract, 0.005% (w/v) NaCl, 12.5 mM each of $MgCl_2$ and $MgSO_4$, and 0.4% (w/v) glucose. The broth can be stored at room temperature for up to 6 months.
5. QIAprep spin miniprep kit (Qiagen) was stored at room temperature for up to 12 months.
6. LB ampicillin plates: 0.01% (w/v) tryptone, 0.005% (w/v) yeast extract, 0.005% (w/v) NaCl, 0.015% (w/v) agarose, and 100 μg/ml ampicillin. The plates were stored at 4°C for up to 3 months.
7. LB ampicillin broth: 0.01% (w/v) tryptone, 0.005% (w/v) yeast extract, 0.005% (w/v) NaCl, 0 and 100 μg/ml ampicillin. The broth was stored at 4°C for up to 3 months.
8. QIAGEN Plasmid Midi kit (Qiagen) or PureYield Plasmid Midiprep System (Promega Corp.) was stored at room temperature for up to 12 months.

9. Glycerol solution: 65% glycerol, 0.1 M $MgSO_4$, and 25 mM Tris–HCl (pH 8.0). The solution was autoclaved and stored at room temperature for up to 12 months.

2.4. Sample Preparation and Microarray Fabrication

1. Effectene transfection reagent (Qiagen), a non-liposomal lipid reagent for DNA transfection (supplied with EC buffer and enhancer reagent), was stored at 4°C for up to 12 months.
2. 2× Transfection printing buffer: 0.2% gelatin and 0.2 M sucrose in MilliQ water. The solution was stored at 4°C for up to 6 months.
3. 0.2% Tween 20 (Sigma-Aldrich, St. Louis, MO) was stored in 100 μl aliquots at –20°C for up to 6 months.
4. GAPS II microscope slides (3-aminopropyl triethoxysilane slides) were obtained from Corning (Acton, MA) and stored dessicated at room temperature for up to 12 months.

2.5. Cell Culture and Microarray Transfection

1. Frozen stocks of human embryonic kidney (HEK 293T/17) cells (ATCC, Manassas, VA) at low-passage number (typically below four) were stored in liquid nitrogen.
2. Dulbecco's modified eagle's medium—high glucose (DMEM, high glucose) (Invitrogen) can be stored at 4°C for up to 6 months.
3. Fetal bovine serum (FBS, ATCC) was stored at –20°C for up to 12 months or –80°C for up to 24 months.
4. Complete growth media: DMEM, high glucose, 3.7 mM L-glutamine, 17 mM sodium bicarbonate, 1 mM sodium pyruvate, 1% antibiotic/antimycotic (v/v), 10% fetal bovine serum. The media can be stored at 4°C for up to 3 months.
5. Phosphate-buffered saline (PBS): 137 mM NaCl, 3 mM KCl, 10 mM phosphate, pH 7.4. The buffer was stored at room temperature for up to 6 months (*see* **Note 3**).
6. Trypsin solution: 0.2% trypsin/0.03 M EDTA in PBS.
7. Press-to-seal silicon adhesive well forms were obtained from Schleicher and Schuell (Keene, NH) and stored at room temperature.

2.6. Assays for Protein Expression

1. Fluorescein-5-isothiocyanate, isomer I (FITC)-conjugated anti-myc epitope polyclonal antibody (Novus Biologicals, Littleton, CO) was stored at 4°C for up to 6 months.
2. Phosphate-buffered saline (PBS): 137 mM NaCl, 3 mM KCl, 10 mM phosphate, pH 7.4. The buffer was stored at room temperature for up to 6 months (*see* **Note 3**).
3. Four percent paraformaldehyde in PBS (PFA/PBS, pH 7.4) was prepared by dissolving 4 g of paraformaldehyde in PBS

while stirring and heating. Once dissolved, the solution can be stored at 4°C for several weeks.

4. Vectashield mounting medium containing DAPI (4′,6-diamidino-2-phenylindole) (1.5 μg/ml) (Vector Laboratories, Burlingame, CA) was stored at 4°C in the dark for up to 3 months.

2.7. Assay for Fluorescein Binding Acitivity

1. FluoReporter FITC protein labeling kit (Molecular Probes) was stored at 4°C shielded from light for up to 6 months.
2. 1 M sodium bicarbonate buffer pH9: dissolve 0.84 g of $NaHCO_3$ in 9 ml deionized water. Adjust the pH to 9 with NaOH and add water to a final volume of 10 ml. The solution should be stored at 4°C and used within 1 week.
3. Phosphate-buffered saline (PBS): 137 mM NaCl, 3 mM KCl, 10 mM phosphate, pH 7.4. The buffer was stored at room temperature for up to 6 months (*see* **Note 3**).
4. Four percent paraformaldehyde in PBS (PFA/PBS, pH 7.4) was prepared by dissolving 4 g of paraformaldehyde in PBS while stirring and heating. Once dissolved, the solution can be stored at 4°C for several weeks.
5. Vectashield mounting medium containing DAPI (4′,6-diamidino-2-phenylindole) (1.5 μg/ml) (Vector Laboratories, Burlingame, CA) was stored at 4°C in the dark for up to 3 months.

2.8. Image Collection and Data Analysis

1. Nikon E800 Eclipse fluorescence microscope equipped with fluorescein and rhodamine filters.
2. MCID Analysis image analysis software version 7 (Imaging Research Inc., Ontario, Canada).

2.9. Improvement of Cellular Adhesion on Microarrays

1. Lyophilized fibronectin was reconstituted to 1 mg/ml in cell-culture-grade PBS.
2. Working stock of fibronectin in PBS (25 μg/ml) was prepared by diluting the 1 mg/ml stock to 25 μg/ml. The solution was stored as 500-μl aliquots at –20°C for 3–6 months.

3. Methods

The successful expression of membrane-displayed single-chain antibodies on cell-based microarrays depends primarily on two main factors. First, the nucleic acids encoding the single-chain antibodies must be cloned into an appropriate expression plasmid that directs their expression upon the surface of the cellular

membrane. Second, the expression plasmids must be deposited onto the microarray at high density with the optimal amount of transfection reagent to mediate efficient cellular internalization upon the addition of adherent cells to the array.

3.1. Control Plasmid—pDsRed2-Nuc Expression Vector

The plasmid pDsRed2-Nuc expression vector which expresses the fluorescent protein DsRed2 within the nucleus of transfected mammalian cells by virtue of its fusion with a nuclear localization signal from SV40 virus was used as control.

1. The plasmid was transformed into DH5α competent cells and grown overnight at 37°C on LB kanamcyin plates.
2. Single colony was selected from the LB kanamycin plate and grown overnight in 250 ml LB kanamycin broth.
3. Large-scale plasmid preparation was performed using the QIAGEN Plasmid Midi kit or PureYield Plasmid Midiprep System according to the manufacturer's protocols.
4. The plasmid was quantified by measuring the OD at 260/280 nm and was stored at –20°C for up to 12 months or at –80°C for several years (*see* **Note 1**).

3.2. Cloning of Anti-fluorescein Single-Chain Antibodies

A membrane-targeting vector (pDisplay) was used to express anti-fluorescein single-chain antibodies upon the surface of the cellular membrane.

1. The pDisplay vector was transformed into DH5α competent cells and grown overnight at 37°C on LB kanamycin plates.
2. Single colony was selected from the LB kanamycin plates and grown overnight in 250 ml LB kanamycin broth.
3. Large-scale plasmid preparation was performed using the QIAGEN Plasmid Midi kit or PureYield Plasmid Midiprep System according to the manufacturer's protocols.
4. The plasmid was quantified by measuring the OD at 260/280 nm and was stored at –20°C for up to 12 months or at –80°C for several years (*see* **Note 1**).
5. The coding region of the 4-4-20 anti-fluorescein antibody was amplified from the vector pRS316 prepro/MBP/4-4-20/Aga2 (a gift from Dr. Robert Siegel) using primers containing an *SfiI* restriction site (sense primer) and a *SalI* restriction site (antisense primer) (**Table 10.1**) (*see* **Note 7**).
6. The PCR reactions were performed in 50 μl volumes using 1 U of *PfuTurbo* DNA polymerase with 10 ng of pRS316 prepro/MBP/4-4-20/Aga2 template.
7. The amplification reaction was carried out in a Peltier Thermal Cycler-PTC225 with preliminary denaturation at 94°C for 3 min followed by 5 cycles of 94°C for 30 s, 44°C for 30 s, 72°C for 45 s, then followed by 35 cycles of 94°C for 30 s, 60°C for 45 s, and a final extension at 72°C for 10 min.

Table 10.1
Primers used for the cloning and site-directed mutagenesis of 4-4-20 scFv

Primer name	Sequence (5'→3')
scFV-SfiI	ATC GGC CCA GCC GGC CGA CGT CGT TAT GAC T
scFV-SalI	TTA GTC GAC TGA GGA GAC GGT GAC TGA GGT
FITC-stopmycBACK	GAA GAG GAT CTG TAA TAA AAT GCT GTG GGC
FITC-stopmycFOR	GCC CAC AGC ATT TTA TTA CAG ATC CTC TTC
HisL27dLysBACK	GTC AGA GCC TTG TAA AGA GTA ATG GAA ACA CCT ATT TAC
HisL27dLysFOR	GTA AAT AGG TGT TTC CAT TAC TCT TTA CAA GGC TCT GAC
HisL27dAlaBACK	GTC AGA GCC TTG TAG CCA GTA ATG GAA ACA CCT ATT TAC
HisL27dAlaFOR	GTA AAT AGG TGT TTC CAT TAC TGG CTA CAA GGC TCT GAC
TyrL32PheBACK	CAG TAA TGG AAA CAC CTT TTT ACG TTG GTA CCT G
TyrL32PheFOR	CAG GTA CCA ACG TAA AAA GGT GTT TCC ATT ACT G
ArgL34LysBACK	GGA AAC ACC TAT TTA AAA TGG TAC CTG CAG AAG CCA GG
ArgL34LysFOR	CCT GGC TTC TGC AGG TAC CAT TTT AAA TAG GTG TTT CC
ArgL34HisBACK	GGA AAC ACC TAT TTA CAT TGG TAC CTG CAG AAG CCA GG
ArgL34HisFOR	CCT GGC TTC TGC AGG TAC CAA TGT AAA TAG GTG TTT CC
ArgL34AlaBACK	GGA AAC ACC TAT TTA GCT TGG TAC CTG CAG AAG CCA GG
ArgL34AlaFOR	CCT GGC TTC TGC AGG TAC CAA GCT AAA TAG GTG TTT CC
TrpL96TyrBACK	CAA AGT ACA CAT GTT CCG TAT ACG TTC GGT GGA GGC
TrpL96TyrFOR	GCC TCC ACC GAA CGT ATA CGG AAC ATG TGT ACT TTG
TrpL96PheBACK	CAA AGT ACA CAT GTT CCG TTC ACG TTC GGT GGA GGC
TrpL96PheFOR	GCC TCC ACC GAA CGT GAA CGG AAC ATG TGT ACT TTG
TrpH33TyrBACK	CAC TTT TAG TGA CTA CTA TAT GAA CTG GGT CCG C
TrpH33TyrFOR	GCG GAC CCA GTT CAT ATA GTA GTC ACT AAA AGT G
TrpH33PheBACK	CAC TTT TAG TGA CTA CTT TAT GAA CTG GGT CCG C
TrpH33PheFOR	GCG GAC CCA GTT CAT AAA GTA GTC ACT AAA AGT G

8. The PCR products were cleaned up with MasterPure™ DNA purification kit (*see* **Note 4**) and subsequently digested with *SalI* at 37°C for 7 h in 50 μl reaction volume. The *SalI*-digested PCR product was ethanol precipitated and digested with *SfiI* at 50°C overnight in a 50 μl reaction volume followed by ethanol precipitation and resuspension in 30 μl of nuclease-free water.
9. 5 μg of pDisplay vector was digested with *SalI* in 100 μl reaction volume at 37°C overnight. The *SalI*-digested vector was ethanol precipitated and digested with *SfiI* at 50°C overnight in 100 μl reaction volume. The *SfiI*- and *SalI*-digested vectors were incubated with 10 U of calf intestinal phosphatase overnight at 37°C. The dephosphorylated vector was cleaned with MasterPure™ DNA purification kit (*see* **Note 5**).

10. The digested, cleaned PCR products (7 μl) were ligated to 50 ng of pDisplay vector also digested with *SfiI* and *SalI* with 1U T4 DNA ligase in a 10 μl reaction volume containing 1x ligation buffer for 1 h at room temperature.
11. 1 μl of the ligation mixture was mixed with 50 μl DH5α competent cells and incubated on ice for 30 min. The cells were then subjected to heat-shock at 42°C for 45 s and then placed on ice for 2 min. An aliquot of SOC medium (0.45 ml) was added and the cells were incubated at 37°C for 1 h with shaking (225 rpm). A portion of the cells (200 μl) were spread onto LB ampicillin plates and incubated overnight at 37°C.
12. Five to ten colonies were selected from the LB plates and grown overnight in 5 ml LB ampicillin broth.
13. The plasmids were purified using the QIAprep spin miniprep kit following the manufacturer's protocol.
14. The purified plasmids were digested with *EcoRI* and *AccI* to confirm the presence of the 4-4-20 anti-fluorescein coding sequence and were subsequently sequenced for further confirmation.
15. Glycerol stocks of the clones were prepared by mixing 0.5 ml of the fresh overnight-culture with 0.5 ml of glycerol solution and snap-freezing the mixture in an ethanol-dry ice bath. Stocks could be stored at –80°C for years.

3.3. Site-Directed Mutagenesis

Site-directed mutagenesis of the 4-4-20 anti-fluorescein construct was performed using the QuikChange® Site-Directed Mutagenesis Kit. Complementary oligonucleotides containing the desired mutation were listed in **Table 10.1**.

1. Mutation-introducing PCR reactions were performed in 50 μl volumes with 2.5 U of *Pfu* Turbo DNA polymerase and 50 ng of pDisplay/4-4-20 anti-fluorescein plasmid as template.
2. The amplification reaction was carried out in a Peltier Thermal Cycler-PTC225 with preliminary denaturation at 94°C for 30 s followed by 18 cycles of 95°C for 30 s, 55°C for 1 min, and 68°C for 6 min 10 s (*see* **Note 8**).
3. The PCR products were digested with 10 U of *Dpn* I at 37°C for 1 h.
4. An aliquot (1 μl) of the digested PCR products was incubated with 50 μl XL1-Blue super-competent cells on ice in a pre-chilled 14-ml BD Falcon polypropylene round-bottomed tube for 20 min. The cells were then heat-shocked at 42°C for 45 s. After incubating the heat-shocked cells on ice for 2 min, 0.5 ml of NZY medium (pre-warm to 42°C)

was added to the cells. The cells were incubated at 37°C for 1 h with shaking (225 rpm). 250 μl of the cells were spread onto LB ampicillin plates and incubated overnight at 37°C.

5. Two to three colonies were selected from the LB ampicillin plates and grown overnight in 5 ml LB ampicillin broth for plasmid miniprep.
6. The QIAprep spin miniprep kit was used to purify the plasmids from the colonies following the manufacturer's protocol (*see* **Note 1**).
7. The purified plasmids were digested with *EcoRI* and *AccI* to ensure that they contained insert of the appropriate size.
8. The presence of the desired mutation was confirmed by sequencing. Glycerol stocks of the clones were made by mixing 0.5 ml of the fresh overnight-culture with 0.5 ml of glycerol solution and snap-freezing in ethanol-dry ice bath followed by storage at –80°C for years.
9. Large-scale preparation of the plasmids (wild type and mutants) were performed using the QIAGEN Plasmid Midi kit or PureYield Plasmid Midiprep System according to the manufacturer's protocols and quantified by measuring OD at 260/280 nm. The plasmids were stored at –20°C for up to 6 months or –80°C for several years (*see* **Note 1**).

3.4. Sample Preparation and Microarray Fabrication

All microarrays were printed using a BioChip Arrayer I non-contact microarray instrument (Perkin-Elmer Life Sciences, Boston, MA) housed in an environmentally isolated chamber with a relative humidity of 35–45% at room temperature.

1. Plasmid DNA was prepared as a DNA-transfection reagent complex prior to printing. Samples (composed of DNA, EC buffer, Enhancer reagent, and Effectene transfection reagent) were prepared to a final volume of 25 μl in a 96-well medium-binding plate for printing. Plasmids encoding the wild-type pDisplay/4-4-20 anti-fluorescein scFv and its corresponding binding site mutants were diluted to 2.0 μg/ml with EC buffer in individual wells of the plate.
2. Enhancer reagent was added to each well at a ratio of 6:1 (μl reagent/μg plasmid) and incubated for 5 min at room temperature.
3. Effectene transfection reagent was then added to each well at the same 6:1 ratio (μl reagent/μg plasmid) and the mixtures were incubated at room temperature for 20 min.
4. An equal volume (25 μl) of 2× transfection printing buffer was added to the 25 μl DNA:transfection reagent mixture such that each well contained final concentrations of 0.1% gelatin and 0.1 M sucrose.

5. The arrayer was programmed to deliver solutions to the surface of GAPS II microscope slides at 1.5 nl per spot at a spacing of 650 μm between spots (*see* **Note 9**).
6. The samples were deposited in horizontal rows across the surface of the slides for later alignment with the wells of a silicon well form (**Fig. 10.1b**).
7. A row of spots encoding the red fluorescent protein DsRed2 was deposited as an internal control to monitor the transfection efficiency.
8. The slides were stored at 4°C in a desiccator until ready to use (typically within 1–2 days).

3.5. Cell Culture and Microarray Transfection

1. HEK 293T/17 cells were cultured in complete growth medium and incubated at 37°C in a 5% CO_2 atmosphere tissue culture incubator.
2. For transfection, cells were trypsinized using trypsin solution. The trypsinized cells were pooled and adjusted to a final concentration of $\sim 2.5 \times 10^5$ cells/ml in complete growth media.
3. The printed slides were equilibrated to room temperature and a press-to-seal silicon well form was affixed to each slide such that the rows of arrayed spots were centered in the wells (**Fig. 10.1b**).
4. An aliquot (150 μl) of trypsinized cells was added to each well of the slide and the cells were allowed to attach to the printed spots. The cells were incubated on the arrays for 24–48 h to allow for plasmid internalization and protein expression.

3.6. Assay for Protein Expression

The expression levels of the cell membrane-displayed scFvs were assessed using immunocytochemistry using an anti-myc polyclonal antibody directed against the myc tag on the expressed scFv protein.

1. The anti-myc antibody was diluted to a final concentration of 5 μg/ml in complete growth medium and incubated on the cell arrays for 1 h.
2. Following the incubation period, the medium was removed followed by the removal of the silicon well form.
3. The slides were then rinsed with PBS that was pre-warmed to 37°C for 10 s and then fixed in 4% paraformaldehyde in PBS for 30 min at room temperature.
4. After fixing, the slides were rinsed with PBS at room temperature twice.
5. The slides were then mounted with two drops of Vectashield mounting medium containing DAPI and covered with a No.

1 coverslip. The edges of the coverslip were sealed with nail polish to prevent drying of the sample.

3.7. Assay for Fluorescein Binding Activity

The microarrays were used to characterize the relative binding affinities of the wild-type 4-4-20 scFv and its corresponding mutants. The native antibody binds fluorescein with an equilibrium dissociation constant of $2.0\pm0.2\times10^{-10}$ M (6) while the scFv form has an affinity that is within two- to threefold that of the native binding site. The mutation of W96 in the scFv light chain to phenylalanine ((L) W96F) causes a 170-fold decrease in the affinity of the scFv for fluorescein. The mutation of (L) R34 to either lysine ((L) R34K) or histidine ((L) R34H) decreases the affinity of the binding site by 415- and 750-fold, respectively (6–8). These binding data are summarized in **Table 10.2**.

1. Prepare fluorescein–BSA conjugate using the FluoReporter FITC protein labeling kit according to the manufacturer's instruction. Add 200 μl of BSA (0.5–1 mg/ml) to a reaction tube and then 20 μl of 1 M of sodium bicarbonate buffer to the tube. Warm DMSO and reaction dye to room temperature. Prepare 10 mg/ml reactive dye stock solution by adding 50 μl of DMSO and the reactive dye. Add 2.4–4.8 μl of reaction dye to the reaction tube while stirring, and stir the reaction at room temperature for 1 h shielding from light. Prepare the spin column by removing the top cap and the bottom closure and allow the column buffer to drain from the column by gravity. Place the spin column in a 2-ml collection tube and spin for 3 min at $1{,}100\times g$ using a swing bucket rotor. Discard the buffer and place the spin column back to the collection tube. Add the labeled proteins to the tube and allow the solution to absorb into the gel bed. Centrifuge the column for 5 min at $1{,}100\times g$ to collect the fluorescein–BSA conjugate (*see* **Note 10**).

Table 10.2
Binding constants of anti-fluorescein scFv 4-4-20 and mutants

Clone designation	K_a (M^{-1})[a] (soluble)	K_d (M)[b] (soluble)	K_d (M)[c] apparent (cell array)
Wild type	$4.9\pm0.5\times10^{9}$	$2.0\pm0.2\times10^{-10}$	$1.9\pm0.3\times10^{-9}$
(L) W96F	$2.9\pm1.3\times10^{7}$	$3.4\pm1.6\times10^{-8}$	$5.8\pm1.3\times10^{-8}$
(L) R34K	$1.2\pm0.2\times10^{7}$	$8.3\pm1.2\times10^{-8}$	$1.1\pm0.2\times10^{-7}$
(L) R34H	$6.6\pm1.8\times10^{6}$	$1.5\pm0.4\times10^{-7}$	$8.0\pm2.0\times10^{-7}$

[a] K_a values are reported in (6, 7).
[b] K_d values were determined from the identity $K_d = 1/K_a$.
[c] Apparent K_d values were determined from the microarray data shown in **Fig. 10.2**.

2. On a single microscope slide, replicate arrays of cells expressing the wild-type scFv 4-4-20 and the mutants (L) W96F, (L) R34H, and (L) R34K were constructed by depositing replicate spots of plasmid DNA and allowing the cells to express the scFvs for 24 h.
3. The binding activities of the cell-surface-expressed scFvs on the microarrays were assessed using a fluorescein–BSA conjugate. The conjugate consisted of BSA functionalized with 8–10 fluorescyl ligands. This configuration allowed for the binding of the fluorescyl ligand into the binding pocket of the scFv while leaving a sufficient number of fluorescyl ligands available to confirm binding via fluorescence.
4. The fluorescein–BSA conjugate was diluted to the effective working concentration in complete growth medium and incubated on the array for 1 h at 37°C.
5. After the 1-h incubation period, the culture media were removed and the silicon form was removed from the slide.
6. The slides were rinsed for 10 s with PBS that was prewarmed to 37°C and then fixed in 4% paraformaldehyde in PBS for 30 min at room temperature.
7. After fixation, the slides were rinsed twice with PBS.
8. The slides were then mounted with two drops of Vectashield mounting medium containing DAPI and covered with coverslips and sealed with nail polish.
9. The resulting fluorescence pattern obtained is shown in **Fig. 10.2a** and the binding curves determined from the microarrays are shown in **Fig. 10.2b**.
10. The relative rankings of the affinities of the scFvs as determined from the microarrays were in good agreement with the published values and were only slightly lower than those reported for the soluble versions of the antibodies (*see* **Table 10.2**).

3.8. Image Collection and Data Analysis

1. Individual images of transfected cell spots were collected using a Nikon E800 Eclipse fluorescence microscope equipped with fluorescein and rhodamine filters.
2. Within each array area, control spots were included to determine the transfection efficiency within each array as described elsewhere (9). Briefly, within each control spot, the number of transfected cells was determined by totaling the number of cells expressing the red fluorescent protein, DsRed2, within the nucleus. The total number of cells was determined by counting the number of DAPI-stained nuclei. The transfection efficiency was determined as the number of transfected cells (red) divided by the number of total cells (blue).

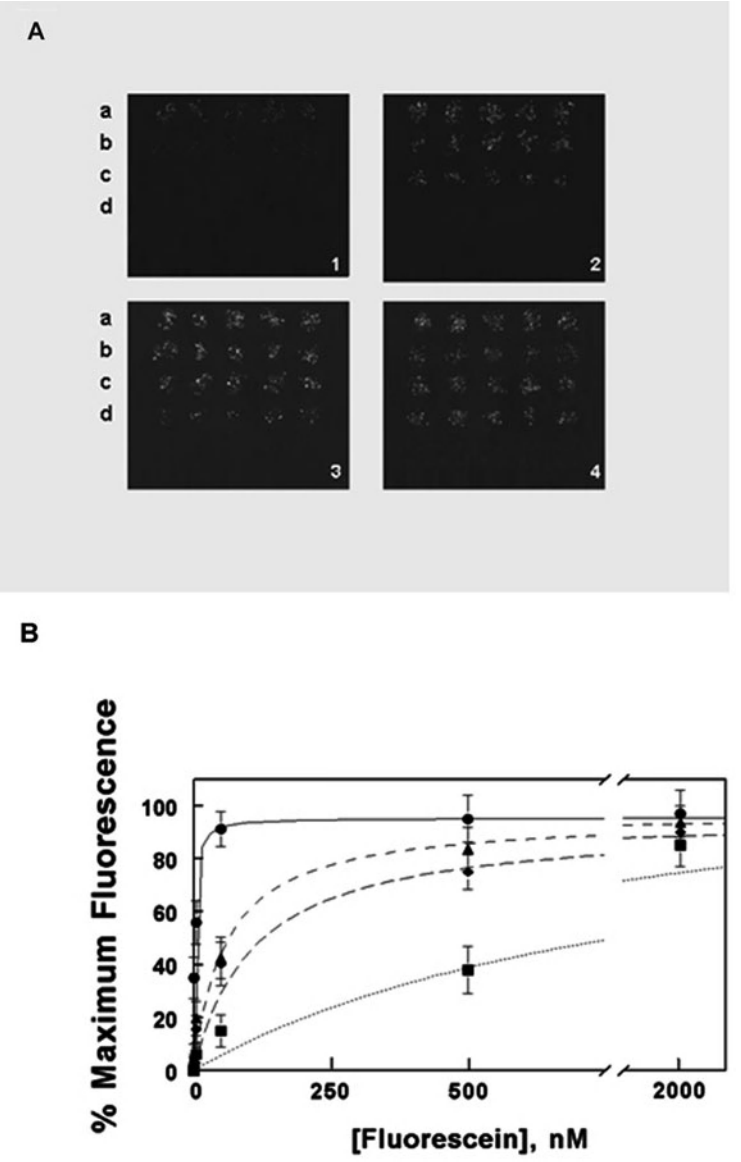

Fig. 10.2. Determination of cell-surface displayed scFv affinity using transfected cell microarray. (**a**) Replicate spots of plasmid DNA encoding the (*a*) wild-type scFv 4-4-20 and the mutants (*b*) (L) W96F, (*c*) (L) R34K, and (*d*) (L) R34H were deposited as described in the text. After the addition of cells and a 24-h expression period, the arrays were incubated with a fluorescein–BSA conjugate at the following concentrations: (*1*) 0.5, (*2*) 50, (*3*) 500, and (*4*) 2,000 nM. (**b**) Dose–response curves for the binding interaction of expressed 4-4-20 scFv with fluorescein–BSA. Each data point is the mean±SEM of 10 replicate spots taken from slides prepared in duplicate. A one-site ligand-binding equation was used to determine the best line through the points, and the results are plotted as percent of maximum fluorescence. Symbols represent the following: (●) wild-type, (▲) (L) W96F, (♦) (L) R34K, and (■) (L) R34H. Reproduced with permission from the ACS (3).

3. For quantification of the relative expression level of membrane-displayed scFvs, images of cell clusters consisting of 80–100 cells were collected and the fluorescence intensities of each image were determined using MCID Analysis image analysis software version 7.
4. The fluorescence signal for each image was determined as the product of the average pixel intensity times the total number of pixels within the image minus the fluorescence intensity of the background.
5. For the dissociation constants, the fluorescence intensity values were determined at each fluorescein concentration and transformed into a corresponding value of percent maximum fluorescence relative to the fluorescence value corresponding to a saturating concentration of fluorescein.
6. The percent maximum fluorescence was plotted versus the fluorescein concentration, and the dissociation constant was determined from the following equation:

$$\%\ \text{maximum fluorescence} = X/(X + K_{\mathrm{d}})$$

where X represents the fluorescein concentration and K_{d} represents the apparent dissociation constant.

3.9. Improvement of Cellular Adhesion on Microarrays

1. One common technical hurdle often experienced with cellular microarrays is the loss of cells due to poor adhesion to the microscope slide surface. While the extent of this problem varies with the particular cell line being used, we demonstrate here how the incorporation of an appropriate cell adhesion molecule during array construction can significantly improve the adhesion of cells to the microarray.
2. Passive adsorption of the cell adhesion molecule, fibronectin, onto the surface of GAPS II slides prior to the plasmid DNA deposition and its inclusion in the gelatin/sucrose printing buffer dramatically improves the adhesion of HEK 293T/17 cells to GAPSII slides while having no deleterious effect on transfection efficiency.
3. GAPSII slides were coated with fibronectin overnight at 37°C, washed with distilled water, and dried under a stream of nitrogen. 9×9 microarrays of plasmid DNA encoding the red fluorescent protein DsRed2-Nuc were printed in gelatin/sucrose printing buffer prior to the addition of HEK 293T/17 cells. In comparison to slides without fibronectin coating, slides coated with fibronectin exhibited superior retention of cells after processing of the slides (**Fig. 10.3**).
4. The addition of fibronectin to the printing buffer, while improving cellular adhesion, has no deleterious effect on the transfection efficiency (**Fig. 10.4**).

4. Notes

1. Other plasmid isolation kits can also be used for this step.
2. Other high-fidelity DNA polymerase can also be used to generate PCR products. Good laboratory practice (e.g., use

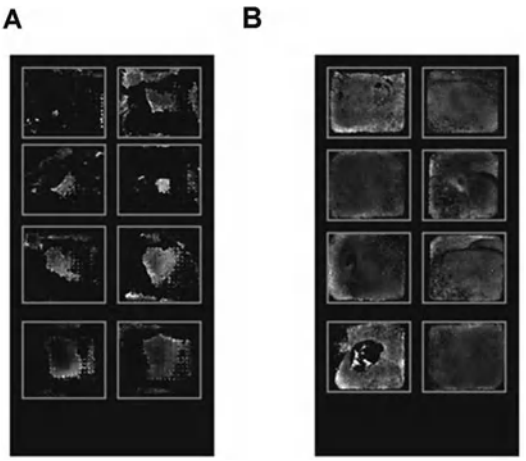

Fig. 10.3. Fibronectin improves cellular adhesion of HEK 293T/17 cells on well-based reverse transfection microarrays. GAPSII were used as supplied (**a**) or were coated with 25 μg/ml fibronectin prior to printing of microarrays (**b**). Subsequently, eight separate 9×9 microarrays were printed onto the surface. After deposition and culture of cells, the arrays were processed and stained with DAPI to visualize all cells retained within the wells. Slides coated with fibronectin exhibited superior retention of cells after processing of the slides.

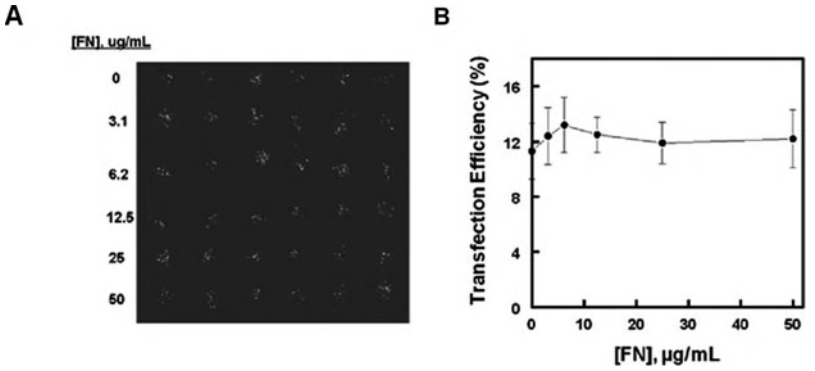

Fig. 10.4. Fibronectin-improved cell adhesion on two microarray printing platforms. Microarrays for reverse transfection were printed using a non-contact printer (BioChip Arrayer). 6×6 microarrays in which each spot contained 30 pg of a plasmid encoding a nuclear-localizing red fluorescent protein (DsRed2-nuc) were printed onto the surface of GAPSII slides coated with fibronectin. Fibronectin (FN) was also included in the printing buffer at the concentrations indicated. HEK 293T/17 cells were added and cultured for 24 h prior to fixing and staining with DAPI. The quantification of the transfection efficiency as a function of fibronectin concentration is shown.

of filtered pipette tips, gloves, and a UV-irradiated PCR hood) is necessary to prevent contamination issue in the PCR reactions.

3. Competent cells, dNTPs, PCR primers, restriction endonucleases, and PBS from other commercial suppliers can also be used.
4. Other PCR purification kits can also be used for cleaning up PCR products.
5. Other phosphatases (e.g., antarctic phosphatase) can also be used. Some alkaline phosphatases can be heat-inactivated without the need to purify the dephosphorylated vector.
6. T4 DNA ligase is unstable on ice for long periods of time. It is best to keep the enzyme at –20°C until ready for use and return it to –20°C immediately after use. Ligation buffer contains ATP and DTT which can be degraded by repeat freezing and thawing and will reduce the ligation efficiency. It is best to store the ligation buffer in small, single-use aliquots.
7. When designing oligonucleotide primers with linker sequences, it is necessary to consider using cloning sites on the vector that will generate the right orientation of the coding sequence.
8. The extension time is based on the size of the plasmid used according to the manufacturer's recommendation.
9. For all printing operations, a rinse step was performed between each sample aspiration/dispense cycle. The tips were rinsed with 0.2% Tween-20 liberally in a sonicating bath followed by a final rinse with distilled water.
10. The conjugate can be prepared in advance and stored at 4°C in the dark for up to 3 months.

References

1. Wu, R. Z., Bailey, S. N., Sabatini, D. M. (2002) Cell-biological applications of transfected-cell microarrays. *Trends Cell Biol* 12, 485–488.
2. Ziauddin, J., Sabatini, D. M. (2001) Microarrays of cells expressing defined cDNAs. *Nature* 411, 107–110.
3. Delehanty, J. B., Shaffer, K. M., Lin, B. (2004) Transfected cell microarrays for the expression of membrane-displayed single-chain antibodies. *Anal Chem* 76, 7323–7328.
4. Blazek, D., Celer, V. (2003) The production and application of single-chain antibody fragments. *Folia Microbiologica* 48, 687–698.
5. Weisser, N. E., Hall, J. C. (2009) Applications of single-chain variable fragment antibodies in therapeutics and diagnostics. *Biotechnology Adv* 27, 502–520.
6. Denzin, L. K., Whitlow, M., Voss, E. W., Jr. (1991) Single-chain site-specific mutations of fluorescein-amino acid contact residues in high affinity monoclonal antibody 4-4-20. *J Biol Chem* 266, 14095–14103.

7. Denzin, L. K., Gulliver, G. A., Voss, E. W., Jr. (1993) Mutational analysis of active site contact residues in anti-fluorescein monoclonal antibody 4-4-20. *Mol Immunol* 30, 1331–1345.
8. Herron, J. N., He, X. M., Mason, M. L., Voss, E. W., Edmundson, A. B. (1989) Three-dimensional structure of a fluorescein-fab complex crystallized in 2-methyl-2,4-pentanediol. *Proteins* 5, 271–280.
9. Delehanty, J. B., Shaffer, K. M., Lin, B. (2004) A comparison of microscope slide substrates for use in transfected cell microarrays. *Biosens Bioelectron* 20, 773–779.

Chapter 11

Blood Cell Capture on Antibody Microarrays and Monitoring of the Cell Capture Using Surface Plasmon Resonance Imaging

Yoann Roupioz, Sarah Milgram, André Roget, and Thierry Livache

Abstract

Blood is a tremendous source of data for diagnostic purposes. Thanks to the qualitative and quantitative analysis of the different cell types carried into the blood stream. To that end, cell capture of several cell types at different locations on a microarray is an interesting alternative to classical techniques run 'in solution' as it allows simultaneous characterization of several cells on a single device. In this chapter, we have described a method based on the production of antibody microarrays specific to two different cell types: B and T lymphocytes. We have also described the real-time monitoring of the cell capture on the microarray using surface plasmon resonance imaging (SPRi).

Key words: Antibody microarrays, blood cell, cell capture, electrochemical functionalization, surface plasmon resonance imaging, pyrrole.

1. Introduction

Many technological progresses made during the last decades rendered possible the fabrication of microsystems and microdevices on a micrometric scale. As these developments can now be used at the size of eukaryotic cells, a large repertoire of applications have been made to study individual cells on biochips (1). Among all the biological fluids routinely processed in laboratories, blood is a major sample as it carries both biomedically relevant molecules (hormones, sugars, and drugs etc.) and non-adherent circulating cells. Because these cells are involved in a large variety of biological phenomena, their characterization on microsystems is a

E. Palmer (ed.), *Cell-Based Microarrays*, Methods in Molecular Biology 706,
DOI 10.1007/978-1-61737-970-3_11,

major issue (2). These analyses can be very challenging as blood carries several cell types (erythrocytes, leukocytes, and platelets etc.) present at very different concentrations and also because the biologically relevant data are often obtained by looking at small sub-type cellular populations ($CD4^+$ T lymphocytes and $CD8^+$ T lymphocytes for HIV-infected patients for instance).

Some cell populations might be sorted using their following intrinsic physical properties: differences in size (pore size controlled filtration), density (centrifugation), and dielectric susceptibility (dielectrophoresis). Although these approaches might be convenient for some specific analyses, they cannot be suitable for the characterization/sorting of cells from the same family (or sub-family), such as B versus T lymphocytes. To that end, one can exploit the chemical diversity of biomolecules decorating the outer membrane of the cells. Indeed, impressive efforts have been made to identify biomolecules highly specific to either a cell type or a transitory differentiation state. Hundreds of such "biomarkers" have been mapped and specific antibodies have been raised to recognize and bind these antigens. The fluorescence-assisted cell sorting (FACS) technology is based on this approach and is one of the most powerful techniques for sorting millions of cells. This affinity-based approach has also been adapted to microarrays by grafting cell-type-specific antibodies onto a surface and flowing blood cells on it (3). To that end, the electrochemical polymerization of pyrrole and pyrrole-modified proteins has been shown to be suitable for arraying antibodies on gold-covered glass slides. Such antibody microarrays have been shown to be powerful devices for cell-type-specific capture and optical microscopy-based readout (4), or surface plasmon resonance imaging (5). This latter technique allows the label-free analysis thus saving time and reagents by comparison to end-point alternative techniques.

2. Materials

2.1. Synthesis of N*-Hydroxy-Succinimidyl-6-(1H-pyrrole-1-yl) Hexanamide (Pyrrole–NHS)*

1. 2,5-Dimethoxytetrahydrofuran, mixture of *cis* and *trans* isomers 98% (Sigma-Aldrich).
2. 99+ % 6-aminocaproic acid (Acros Organics).
3. 99.8% 1, 4 dioxane anhydrous (Sigma-Aldrich).
4. Acetic acid puriss (Fluka).
5. 98% *N*-Hydroxysuccinimide (Sigma-Aldrich).
6. *N*, *N′*-Dicyclohexylcarbodiimide (Fluka).
7. *N*, *N*-Dimethylformamide (DMF) for analysis (Carlo Erba).

8. Dichloromethane (CH_2Cl_2) (SdS).
9. Ethyl alcohol anhydrous (EtOH) for analysis (Carlo Erba).
10. 99.9% D Chloroform-d stabilized with 0.5 wt silver foil (Sigma-Aldrich).
11. Silicagel PF_{254} containing $CaSO_4$ for preparative layer chromatography.

2.2. Coupling of Pyrrole–NHS on Immunoglobulin G (IgG)

1. IgG type antibody reacting with specific cells for immunofluorescent and/or immunohistochemical staining (BD Biosciences), 0.5 mg/ml in storage buffer (usually PBS-containing sodium azide). Store at 4°C.
2. 1 mM Pyrrole–NHS in DMSO (synthesis as described in **Section 3.1**). Store at 4°C.
3. Phosphate buffer (PBS) (Sigma Aldrich): 8 mM Na_2HPO_4, 1.5 mM KH_2PO_4, 2.7 mM KCl, 138 mM NaCl, pH 7.4. Store at 4°C.
4. Vivaspin 0.5-ml centrifugal filter units with 30,000 MWCO polyether sulfone membrane (Sartorius Stedim).
5. Storage and spotting buffer: 50 mM NaH_2PO_4, 50 mM NaCl, 10% (w/v) glycerol; final pH adjusted to 6.8 with a NaOH solution. Store at 4°C (–20°C for conservation longer than 2 weeks).

2.3. Electrochemical Arraying of Pyrrole–IgG on Biochips

1. Chips: high-index glass prisms coated with a 50-nm-thick layer of gold (Genoptics).
2. Piranha solution: 1/3 (v/v) of H_2O_2 30% and 2/3 (v/v) H_2SO_4. Care must be taken as this reaction is highly exothermic and reacts strongly with carboneous materials. It can burn the skin from both the heat produced and the reaction of the chemicals with the skin.
3. ≥98% Dodecanethiol (Sigma Aldrich).
4. Ethyl alcohol anhydrous (EtOH) for analysis (Carlo Erba).
5. 1 M Pyrrole in acetonitrile (Tokyo Kasei, Japan). Store at –20°C in a dark bottle to minimize pyrrole oxidation.
6. 6 μM Pyrrole–IgG conjugate (prepared as described in **Section 3.2**).
7. The microarrayer required for immobilizing IgG on the chip is available commercially (Genoptics). It mainly consists of a stainless steel needle (260 μm internal diameter) which is filled with the solution (6 μl) containing the antibody to be grafted and which can be moved to a defined location on the chip. An electrical pulse between the needle (counter electrode) and the gold surface of the chip (working electrode) induces the electrochemical oxidation of pyrrole monomers in

polypyrrole solid film and its deposition on the gold surface.

8. Sodium azide (NaN_3) (Sigma Aldrich).

2.4. Lymphocyte Preparation and Capture on the Antibody Microarray Using SPR Imaging

1. Working buffer (buffer flowed on the microarray): RPMI-1640 medium (Sigma Aldrich), 10 mM HEPES *N*-(2-hydroxyethyl)piperazine-*N*′-(2-ethanesulfonic acid). Store at 4°C for 1 month in sterile conditions.
2. 0.4% Aqueous trypan blue solution (Sigma Aldrich).
3. Saturation buffer: 10% (v/v) fetal bovine serum (FBS; Sigma-Aldrich) in RPMI-1640 medium.
4. The SPRi apparatus is a SPRi lab (Genoptics, Orsay, France). The prism is inserted in the apparatus and is covered by a biocompatible flow cell (10–120 µl volume, stainless steel or PEEK). A LED light source (660 nm) illuminates the prism and a CCD camera monitors the ligand–probe interactions. Data are analyzed with dedicated software (SPRi view).

3. Methods

3.1. Synthesis of N-hydroxy-succinimidyl-6-(1H-pyrrole-1-yl) hexanamide (Pyrrole–NHS)

1. A mixture of 2,5-dimethoxytetrahydrofuran (0.49 mol, 65 ml), 6-aminocaproic acid (0.43 mol, 56 g), acetic acid (450 ml), and dioxane 600 ml is heated under reflux for 4 h and stirred at room temperature overnight (6).
2. Remove the volatiles under reduced pressure. The residue is co-evaporated in ethanol (2×100 ml) to eliminate acetic acid.
3. Dissolve the residue in 500 ml of dichloromethane. This organic solution is washed with 2×250 ml of water and evaporated until dry.

Product 1 (**Fig. 11.1**) is obtained with a yield of 82% after purification by flash chromatography on a silicagel (600 g) column

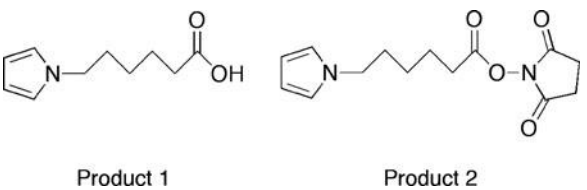

Product 1 Product 2

Fig. 11.1. Pyrrolated derivatives used for the electrochemical grafting of biomolecules. The carboxylic conjugate (product 1) was synthesized from dimethoxytetrahydrofuran before coupling to an activated ester (product 2) suitable for conjugation with primary amines.

with a discontinuous gradient of ethanol in CH_2Cl_2. After deposition in the minimum amount of CH_2Cl_2, the elution starts with CH_2Cl_2 (500 ml), then CH_2Cl_2/EtOH: 98/2 (300 ml), CH_2Cl_2/EtOH: 95/5 (400 ml), and finally CH_2Cl_2/EtOH: 90/10 to elute the product. Product 1 is obtained after evaporation of the solvents as a brownish oil.

M. S. product 1 (m/z) = 182.1 (M^+).
1H-NMR product 1 (200 MHz;$CDCl_3$) δ(ppm):1.72 (m, 6H, $-CH_2-(CH_2)_3-CH_2-$); 2.34 (t, 2H, $-CH_2-COOH$); 3.87 (t, 2H, CH_2-N); 6.13 (dd, 2H, 3-H and 4-H pyrrole); 6.64 (dd, 2H, 2-H and 5-H pyrrole).

4. Product 1 (144 mmol, 26.05 g), *N*-hydroxysuccinimide (144 mmol, 16.56 g), and *N*, *N′*-dicyclohexylcarbodiimide (159 mmol, 32.75 g) are dissolved in DMF (1 l) and stirred overnight at room temperature.
5. Eliminate the white precipitate of *N*,*N′*-dicyclohexyl-urea by filtration on a sinter glass.
6. Remove the solvent by evaporation on a rotavapor. Product 2 can be used without further purification. Alternatively it can be purified on a silicagel column in the same way than product 1 (elution CH_2Cl_2/EtOH 95/5).

   M. S. product 2 (m/z) = 279.3 (**Fig. 11.1**)
   1H-NMR product 2 (200 MHz;$CDCl_3$) δ(ppm):1.72 (m, 6H, $-CH_2-(CH_2)3-CH_2-$); 2.33 (t, 2H, $-CH_2-CO$); 2.88 (tt, 4H, CH_2 of NHS); 3.87 (t, 2H, CH_2-N); 6.13 (dd, 2H, 3-H and 4-H pyrrole); 6.64 (dd, 2H, 2-H and 5-H pyrrole).

3.2. Coupling of Pyrrole–NHS on Immunoglobulin G (IgG)

The coupling of pyrrole–NHS on IgG is based on the covalent coupling of activated ester on amine function of proteins. Each IgG is provided at 0.5 mg/ml in PBS containing sodium azide (*see* **Note 1**).

1. Sodium azide is removed before initialization of the coupling reaction. For this, IgG (300 µl) are purified by ultracentrifugation using filter units with 30,000 MWCO membranes. After washing of the membrane with 200 µl of PBS, 200 µl of IgG is loaded on the filter and concentrated by ultracentrifugation at 15,000×*g* for 15 min at 4°C. IgG are then washed with 200 µl of PBS and centrifuged twice. Eventually, purified IgG are collected in 200 µl of PBS. The concentration of purified IgG is quantified using a spectrophotometer and 280-nm absorbance (molar extinction coefficient 210,000 M/cm).
2. Prepare the reacting solution by mixing 200 µl of 3.3 µM IgG (corresponding to 0.5 mg/ml) with 70 µl of 0.1 mM

pyrrole–NHS and adjust to 400 µl final volume with PBS buffer. The molar ratio of IgG/pyrrole–NHS is 10.

3. Incubate overnight at 4°C in the dark to minimize pyrrole oxidation.
4. Purify pyrrole-modified IgG by removing the excess of unreacted pyrrole–NHS by ultracentrifugation on a 30,000 MWCO membrane. Wash IgG with PBS and centrifuge it three times. Then collect the conjugated IgG by adding 100 µl of storage buffer. After UV titration, adjust the volume with storage buffer to 6 µM final concentration of modified IgG. Pyrrole–IgG conjugate is stable at 4°C up to 2 months at this low concentration.

3.3. Electrochemical Arraying of Pyrrole–IgG on Biochips

Before spotting, the gold layer of the chip is striped and functionalized with dodecanethiol self-assembled monolayers (SAM) (*see* **Note 2**).

1. Incubate the chip in Piranha solution (1/3 (v/v) H_2O_2 30%, 2/3 (v/V) H_2SO_4) for 20 min. Care must be taken as this reaction is highly exothermic and reacts strongly with carboneous materials. It can burn the skin from both the heat produced and the reaction of the chemicals with the skin.
2. Rinse the chip with deionized water and absolute EtOH and dry it with argon or air jet.
3. Incubate the chip for 2 h in a 10-mM dodecanethiol solution prepared by diluting 60 µl of stock solution in 25 ml of absolute EtOH.
4. Wash the chip with water and EtOH and dry it with argon or air jet. The chip can be stored dry at 4°C.
5. Prepare a 100-mM pyrrole solution by diluting 5 µl of the 1 M stock solution in dry acetonitrile with 45 µl of spotting buffer.
6. Prepare the spotting solution in a 96-microwell plate by mixing 10 µl of the 6 µM pyrrole–IgG conjugate solution with 6 µl of the 100-mM pyrrole solution and complete with spotting buffer to a final volume of 30 µl. Final concentration for pyrrole–IgG and free pyrrole is 2 µM and 20 mM, respectively (*see* **Note 3**). Be careful to ensure a good homogenization of the spotting solution without introducing air bubbles (*see* **Note 4**).
7. Load the multiwell plate containing the spotting solutions in the microarrayer and carry out the electrochemical arraying on the chip (**Fig. 11.2**). The electrochemical conditions consist of a 2 V difference of potential for 100 ms (*see* **Note 5**) on defined areas of the gold-covered glass prism.

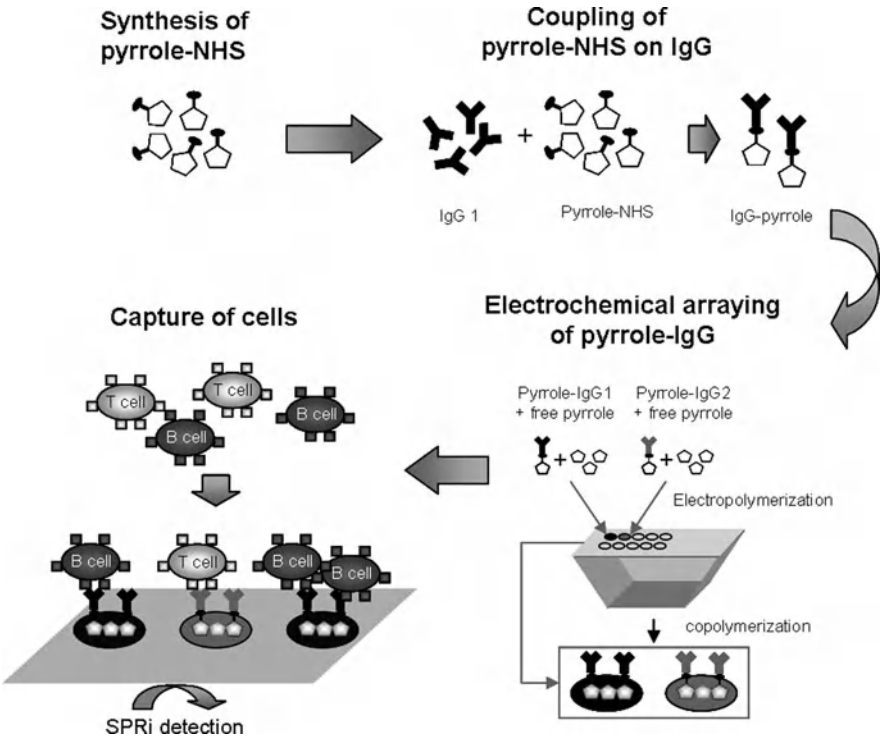

Fig. 11.2. General scheme of the different experimental steps leading to the production of antibody microarray specific to B and T lymphocytes and the specific capture of this two cell types.

8. When all IgG spots have been spotted (*see* **Note 6**), the chip is removed from the microarrayer, rinsed with water, and stored at 4°C in PBS containing 15 mM sodium azide.

3.4. Lymphocyte Sample Preparation and Capture on the Antibody Microarray Using SPR Imaging

Lymphocytes are provided in suspension in their culture medium (*see* **Note 7**).

1. Numbering of the viable blood cells. Mix 50 µl of trypan blue solution with 150 µl of cell suspension (*see* **Note 8**). Only dead cells will be stained in blue. Count blue cells and total cells using a Malassez cell or an automatic cell counter and determine the total number of viable cells in the initial cell suspension (*see* **Note 9**).
2. Centrifuge the cell suspension for 5 min at 300×*g* and gently re-suspend the pellet in RPMI-1640 medium containing 10 mM of HEPES buffer (*see* **Note 10**) to have a final cellular density of 5.10^6 cells/ml, leading to a density of 76,000 cells/cm^2 after sedimentation and capture on the biochip (*see* **Note 11**). Cell suspensions have to be prepared just before the capture on biochip.
3. Start SPR apparatus (*see* **Note 12**). The conditions are the following (**Fig. 11.3**):

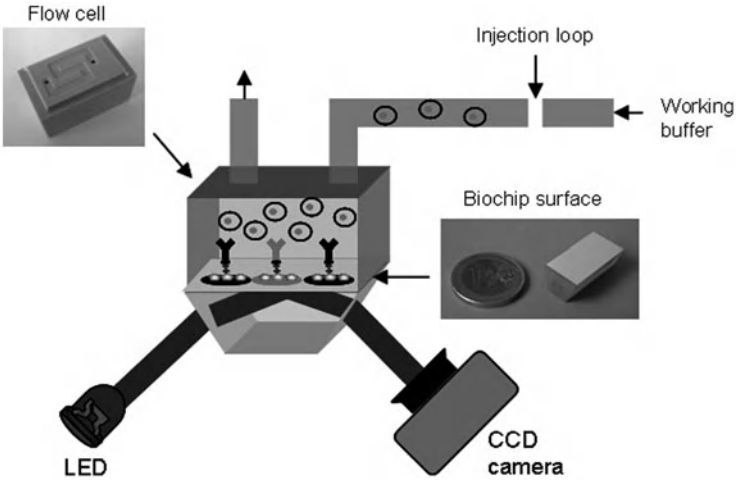

Fig. 11.3. Scheme of the SPR imaging setup.

- Flow cell with a section of 150 μm (thickness) by 0.2 cm (width) (*see* **Note 13**).
- Working buffer: RPMI-1640 medium containing 10 mM HEPES.
- Volume of injection loop = 100 μl.
- Dead volume of the injection tubing (from the injection loop to the SPR imager) = 400 μl.
- Flow rate = 50 μl/min.

4. Eliminate all the air bubbles present in the tubing (*see* **Note 14**).
5. Insert the chip in the SPR imager (*see* **Note 15**) and monitor the reflectivity variations.
6. Saturate the chip by injecting RPMI-1640 complemented by 10% (v/v) of fetal bovine serum (FBS). This saturation solution is particularly adapted to the study of complex sample like cells suspension.
7. After 30 min, rinse the chip by increasing the flow rate up to 200 μl/min during 10 min. The chip is ready to sample injection.
8. Carry out the cells capture on the micro arraying chip (**Fig. 11.2**). Inject the cellular sample with a flow rate of 200 μl/min for 2 min and then decrease the flow rate to 10 μl/min during 15 min (*see* **Note 16**). Rinse to flush unbound cells for 10 min by increasing the flow rate up to 200 μl/min. Captured cells appear on SPR images just 1 or 2 min after the decreasing of flow rate.

9. Several successive injections could be realized but no regeneration of chip is possible. Reactivity of chip decreases with the number of injections, due to saturation of the IgG-specific binding sites on the chip (**Fig. 11.4**).

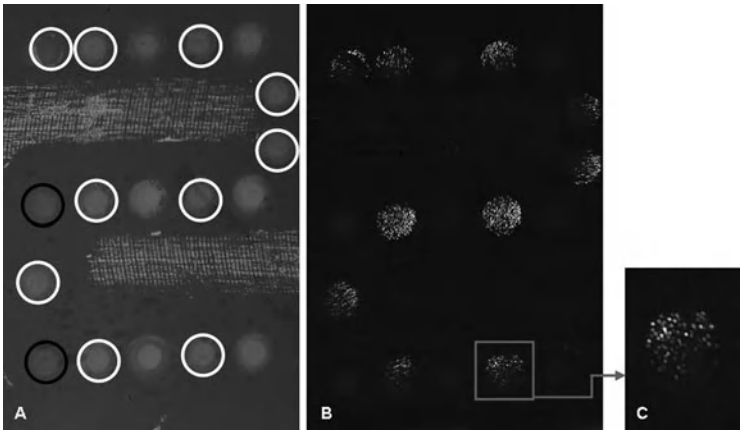

Fig. 11.4. (**a**) SPR image of the chip at the beginning of capture experiment. The *black circled spots* are functionalized with polypyrrole without protein, the *white circled spots* are functionalized with anti-CD71 IgG specific to F10 B-cell hybridoma, and other spots are functionalized with irrelevant IgG. Each *spot* is about 500 μm in diameter. (**b**) SPR image after capture of cells on specific spots (initial image was subtracted and used as the background level). (**c**) Zoom of one specific spot after cells capture. Individual captured cells are clearly distinguishable as discrete objects.

4. Notes

1. Several IgG have been tested for coupling with pyrrole–NHS. Tests were performed with success for pyrrole modification of IgG anti-CD19, anti-CD180, anti-IAb, anti-CD90, anti-CD3e, anti-CD71, and also for some antigens specific to adherent cells.
2. Dodecanethiol is chosen for its hydrophobic properties. It favors a clear definition of spot outlines and limits unspecific fixation of cells on the gold surface. However, such cell lines can show incompatibility with this hydrophobic treatment. Other more hydrophilic thiols like PEG-SH can replace dodecanethiol. The compatibility between cells and SAMs has to be checked for all cell lines studied.
3. Different final IgG concentrations have to be prepared to determine the optimum concentration leading to the highest number of cell–biochip interactions. The coupling yield as the antibody–antigen affinity could differ from one

IgG to another. Moreover, the cell type can also influence the cell capture, in part due to the variation of biomarkers expression from one cell type to another. In all cases, a 20 mM final concentration of pyrrole is required.

4. The presence of air bubbles in the sampling needle acts as an insulating layer and prevents a correct electropolymerization.
5. These conditions lead to a 2–5-nm thick polypyrrole film. Different pulse durations can be tested (50, 100, 200 ms) to optimize the electrodeposition. It is worth noting that too long an electrical pulse and/or too high a voltage could lead to a thicker polypyrrole film and thus decrease SPR sensitivity readout.
6. It is recommended to array the spots in triplicates to improve the reliability of the results. To quantify the background level, control spots including irrelevant IgG and spots polypyrrole without protein have to be performed.
7. Different cells were tested for this process: mouse B- or T-cell hybridoma lines or primary splenocytes. Cellular samples can be composed of one or several cell types.
8. Before each cell sampling, the mother cell suspension has to be properly homogenized by gently pippeting up and down the cells.
9. The Malassez grid delineates 1 μl of suspension. If N is the total number of cells counted in the Malassez grid and m the number of trypan-blue-stained cells counted in the Malassez grid, then the total number of living cells in the sample is $(N–m) \times 3/2 \times 1{,}000$ V, where V is the volume of cells sample in ml.
10. RPMI-1640 medium was chosen for its optical stability during SPRi analysis. Addition of 10 mM HEPES buffer is necessary to ensure a good stability of pH during the analysis performed in absence of a CO_2-enriched atmosphere. If other culture medium is necessary, it is preferable to test its stability during the SPRi analysis.
11. The optimum cellular density leading to the highest cell capture ratios on the biochip is dependant on both the cellular types and SPR flow cell characteristics. A better way to express cellular density is the number of cells by square centimetre of biochip in contact with cells. The optimum density for specific capture of B- or T-cells hybridoma was set at 76,000 cells/cm^2 versus 140,000 cells/cm^2 for mouse splenocytes that are smaller cells.
12. Capture of cells could also be observed by optical microscopy. However, SPRi allows the real-time

monitoring of cells microarray interaction, whatever may be the sample clearness or transparency.

13. Several types of flow cell are commercially available (Genoptics, Orsay, France). Be careful about the biocompatibility of materials composing the flow cell and all the fluidic systems. PEEK is recommended for its high biocompatibility properties.
14. It is recommended to de-gas the working buffers by incorporating a de-gasser in the flow circuit before the injection loop.
15. After IgG grafting on the surface, keep it wet. Drying could considerably damage IgG grafted on the chip and make them non-functional.
16. During the first step of injection, the flow rate is kept at a high level (200 μl/min) to allow a very quick delivery of cells to the flow cell and in order to avoid cell adsorption in the tubing and cellular aggregate formation. The duration of delivery has to be calculated according to the injection tubing size. For a 400-μl injection tubing, the optimum duration of delivery is 2 min. In the second step, 10 μl/min of flow rate was shown to allow the optimum B- or T-cells hybridoma capture using a flow cell with 0.2 × 0.015 cm section. The optimum flow rate is dependent on both the flow cell section and the cellular type. The optimum flow has to be assayed in your own conditions.

References

1. El-Ali, J., Sorger, P. K., Jensen, K. F. (2006) Cells on chips. *Nature* 442(7101), 403–411.
2. Toner, M., Irimia, D. (2005) Blood-on-a-chip. *Annu Rev Biomed Eng* 7, 77–103.
3. Belov, L., de la Vega, O., dos Remedios, C. G., Mulligan, S. P., Christopherson, R. I. (2001) Immunophenotyping of leukemias using a cluster of differentiation antibody microarray. *Cancer Res* 61(11), 4483–4489.
4. Roupioz, Y., Berthet-Duroure, N., Leichle, T., Pourciel, J. B., Mailley, P., Cortes, S., Villiers, M. B., Marche, P. N., Livache, T., Nicu, L. (2009) Individual blood-cell capture and 2d organization on microarrays. *Small* 5(13), 1493–1497.
5. Suraniti, E., Sollier, E., Calemczuk, R., Livache, T., Marche, P. N., Villiers, M. B., Roupioz, Y. (2007) Real-time detection of lymphocytes binding on an antibody chip using SPR imaging. *Lab Chip* 7(9), 1206–1208.
6. Grosjean, L., Cherif, B., Mercey, E., Roget, A., Levy, Y., Marche, P. N., Villiers, M. B., Livache, T. (2005) A polypyrrole protein microarray for antibody-antigen interaction studies using a label-free detection process. *Anal Biochem* 347(2), 193–200.

Chapter 12

Immobilized Culture and Transfection Microarray of Non-adherent Cells

Satoshi Yamaguchi, Erika Matsunuma, and Teruyuki Nagamune

Abstract

Cell-based microarrays are promising tools for high-throughput functional analysis of gene products, but their application has been limited to adherent cells due to the difficulty in immobilization of non-adherent cells. Herein, we have introduced our techniques that can rapidly and strongly immobilize non-adherent cells and can allow the transfection of non-adherent cells with plasmid cDNA and small interfering RNA (siRNA) at a defined position on substrates with poly(ethylene-glycol)-lipid-modified surface.

Key words: Non-adherent cells, cell immobilization, transfection microarray, reverse transfection, PEG-lipid.

1. Introduction

Microarrays of living cells are promising tools for high-throughput functional analysis of gene products. Most of such cell microarrays are based on the transfection microarray that was first reported by Sabatini's group in 2001 (1). In this report, the cDNA plasmids were printed at the defined position on gelatin-coated glass slides, and then mammalian cells were cultured on these glass slides. Cells growing on printed areas took up the DNA, and as a result, many spots of living cells transfected with defined cDNA were formed on the glass slide. This unique transfection technique was named as "reverse transfection" and was applied for the introduction of various kinds of nucleic acids or vectors such as siRNA (2, 3) and lentivirus vectors

E. Palmer (ed.), *Cell-Based Microarrays*, Methods in Molecular Biology 706,
DOI 10.1007/978-1-61737-970-3_12,

(4), and furthermore, small synthetic molecule into living cells (5). On the other hand, by using the glass slides micropatterned with various bioactive molecules such as proteins, carbohydrates, peptides, and synthetic polymers, cell-based functional screenings were performed (6–9). In these systems, the effects of cell–biomolecule interaction on cell behavior were characterized in a high-throughput manner. Thus, a wide variety of cell microarrays have been developed, and some of them were practically used in a drug discovery and toxicity test.

All the conventional cell microarrays utilize the adhesive properties of adherent cells for immobilization of cells on nucleic acid- or biomolecule-arrayed slides as described above. In addition, the strong adherence of cells on the defined area prevented cross-contamination between closely spaced cell spots on glass slides. Therefore, there is the major limitation that conventional cell microarray techniques cannot be applied to non-adherent cells. Non-adherent cells such as blood cells (especially immunocytes), some cancer cells, and stem cells are widely important in biological and medical fields. At present, the cell-based high-throughput screening method for these non-adherent cells has been rarely reported, except for a few methods using microwells (10, 11) and is needed for selection of antibody, drug screening for hematological disease, and so on. Thus, it is important to expand the range of application of cell microarray techniques to non-adherent cells.

To apply cell microarray technique to non-adherent cells, we developed a new cell immobilization method using the cell membrane anchoring reagents consisting of poly(ethylene-glycol)-lipid (PEG-lipid), which was jointly developed with NOF corporation (Tokyo, Japan) and named as biocompatible anchor for membrane (BAM) (12). BAM consists of the following three distinct units: (i) a hydrophobic oleyl group, (ii) a hydrophilic PEG chain, and (iii) an amino-reactive *N*-hydroxysuccimide (NHS) ester group (**Fig. 12.1a**). In our cell immobilization method, a protein-coated glass slide was modified with BAM via the amide-coupling reaction between the amine groups of protein surface and the NHS ester group of BAM. Non-adherent cells can be immobilized on the BAM-coated glass slide through insertion of the oleyl moiety of BAM within the cell membrane (**Fig. 12.1b**). We demonstrated that various non-adherent cells such as Jurkat, Daudi, mouse ES and 32D, and adherent cells such as HEK293 and NIH/3T3 can be immobilized (**Fig. 12.1c**) and proliferate normally on the BAM-coated slide. Furthermore, using this cell immobilization technique, we developed a gene transfection microarray for non-adherent cells (13). In our method, plasmid DNAs were deposited in defined areas on BAM-modified glass

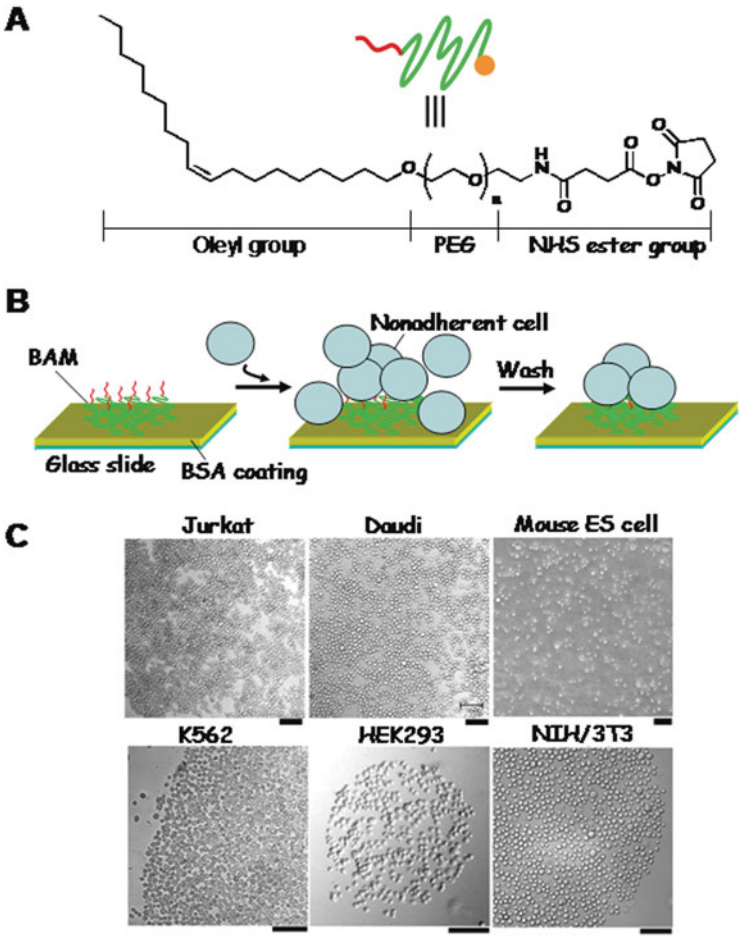

Fig. 12.1. Immobilization of non-adherent cells on a BAM-modified surface. (**a**) The chemical structure of BAM. (**b**) The schematic illustration of cell immobilization on a BAM-coated glass slide. (**c**) The microscopic images of various immobilized cells. All scale bars indicate 100 μm.

slides and transferred into the non-adherent cells that were immobilized by the cell-adhesive moiety of BAM (**Fig. 12.2**). This method allowed the gene transfection of non-adherent cells without cross-contamination between DNA spots on glass slides (13). In addition, small interfering RNA (siRNA) was also introduced into non-adherent cells using the same format. In this chapter, we have explained in detail our procedure for immobilization of non-adherent cells on the BAM-modified glass slide (3–1) and performing reverse transfection of non-adherent cells on this BAM-modified slide (3–2). These techniques make it possible to screen the gene related to targeted phenotypes of non-adherent cells on a microchip.

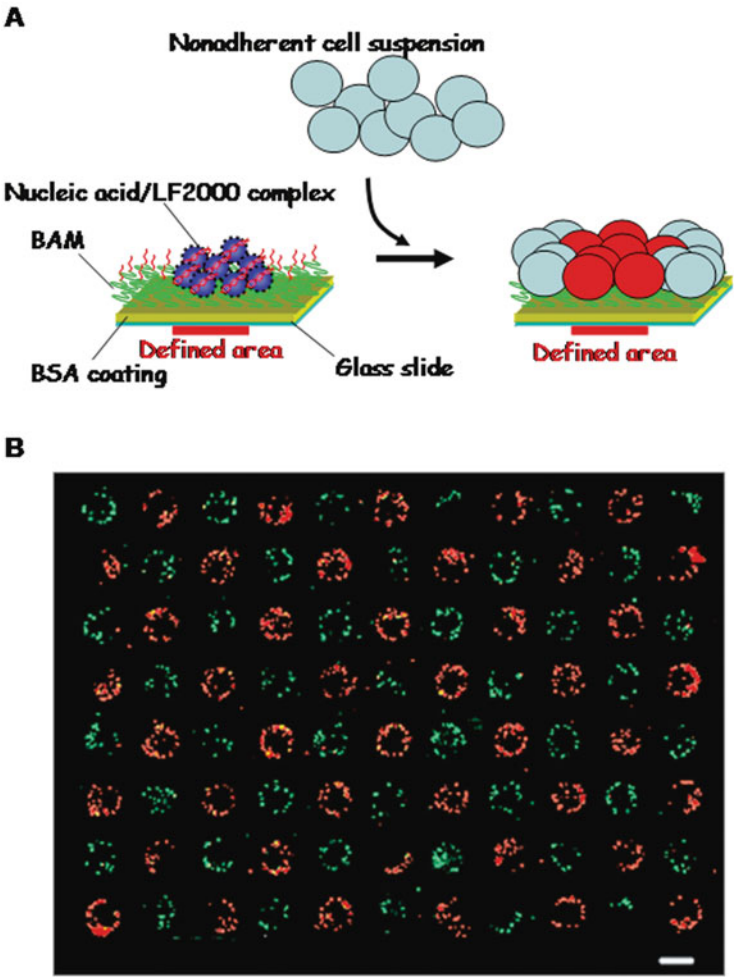

Fig. 12.2. Reverse transfection of non-adherent cells on a BAM-modified surface. (**a**) The schematic illustration of reverse transfection of the non-adherent cells immobilized on a BAM-coated glass slide. (**b**) The fluorescent-microscopic images of cell microarray transfected with EGFP-expression plasmid and DsRed-expression plasmid. The scale bar indicates 500 μm.

2. Materials

2.1. Immobilization of Non-adherent Cells on BAM-Modified Surface

1. PBS buffer: PBS buffer can be prepared either by purchasing a commercially available one or by dissolving proper salts according to general procedures. PBS buffer must be sterilized before use.
2. 1% BSA solution: bovine serum albumin (BSA), fatty-acid-free powder, must be used. 1% BSA is dissolved in PBS

and is filter-sterilized. BSA solution must be prepared just before use.

3. 100 μM BAM solution: The commercially available equivalent of BAM can be purchased from NOF Corporation with the product name SUNBRIGHT OE-060CS (MW 8000). First, 10 mM BAM in dry DMSO is prepared. Here, distilled DMSO can be prepared either by obtaining a commercially available one or by distilling according to general procedures. This BAM solution in DMSO is stable below –20°C. The repeated freeze/thaw of this BAM solution in the air hydrolyzes the NHS ester moiety of BAM and decreases the reactivity. Next, 100 μM BAM in PBS is prepared by diluting 10 mM BAM in DMSO with PBS just before use. This BAM solution in PBS should not be stored because of rapid hydrolysis of BAM in PBS.

2.2. Reverse Transfection of Non-adherent Cells on BAM-Modified Surface

Transfection mixture solution: in case of cDNA plasmid, the transfection mixture solution is prepared by mixing cDNA plasmid (1–4 μg), Lipofectamine^{TM} 2000 (abbreviated as LF2000) (Invitrogen) (2 μl), RPMI 1640 medium (8 μl), and Milli-Q water (28 μl). This solution is pre-incubated for 10 min at room temperature before spotting onto the BAM-modified surface. In the case of siRNA, siRNA (0.3 μg), LF2000 (1 μl), RPMI 1640 medium (2 μl), and Milli-Q water (6 μl) are mixed, and pre-incubated for 30 min at room temperature.

3. Methods

3.1. Immobilization of Non-adherent Cells on BAM-Modified Surface

1. The surface of substrates such as glass slides, glass-bottomed culture dishes, and polystyrene culture dishes is treated with 1% BSA in PBS at room temperature for more than 16 h.
2. After washing with Milli-Q® water for more than three times, the surface is completely air-dried in a clean bench.
3. The surface is treated with 100 μM BAM in PBS for 10–30 min at room temperature (*see* **Note 1**).
4. After washing with Milli-Q® water for more than three times, non-adherent cells suspended in PBS (3×10^6 cells/cm^2) are dropped on the surface and left for approximately 5 min at room temperature (*see* **Note 2**).
5. The cell-immobilized surface is gently washed with PBS one time to remove non-immobilized cells (*see* **Note 3**).

3.2. Reverse Transfection of Non-adherent Cells on BAM-Modified Surface

1. The BAM-modified surface is prepared as described above and air-dried on a clean bench.
2. Aliquots (1 μl) of transfection mixture solutions including nucleic acids such as cDNA plasmid and siRNA, lipofection reagent, and medium are manually spotted on the BAM-modified surface (*see* **Note 4**).
3. The surfaces are air-dried at room temperature for 30 min on a clean bench (*see* **Note 5**).
4. Non-adherent cells suspended in serum-free RPMI 1640 medium (5×10^5 cells/cm^2) are transferred onto the surface and incubated for approximately 10 min at room temperature.
5. The cell-immobilized surface is gently washed with PBS one time to remove non-immobilized cells (*see* **Note 3**).
6. The cells immobilized on the substrate are incubated under general culture conditions using media either with or without serum (*see* **Note 6**).
7. Each cell spot on the defined nucleic-acid-printed area is evaluated according to the intended use.

4. Notes

1. BAM in PBS solution must be prepared just before use. When the BAM solution was left at room temperature for a long time (more than 1 h), the amount of immobilized cells decreased probably because the NHS ester moiety of BAM hydrolyzes in PBS solution.
2. Non-adherent cells must be suspended in serum-free media or buffers. If cell suspension includes serum, the immobilization of cell is suppressed by serum probably because albumin in serum strongly binds to the oleyl moiety of BAM and prevents its insertion into cell membranes.
3. After immobilizing adherent cells, the wash operation must be gentle. If not gentle, the immobilized cells are detached from the substrates. Do not drop PBS directly on the immobilized cells. PBS must be poured along the wall of dishes. If a glass slide is used, it should be treated in a dish with the correct size. When the poured PBS is removed from the dish, PBS is gently aspirated by putting the end of pipette on the corner of the dish.
4. The diameter of the spots is approximately 1.5 mm. To prepare high-density and uniformly sized spots, a commercially

available ink-jet printer can be employed. For example, when 20 nl of transfection mixture solutions was microprinted onto the BAM-modified surface by using an ink-jet printer (from Cartesian Technologies, Irvine, USA), all the spots were about 500 μm in diameter.

5. The dried nucleic-acid-printed surfaces can be stored at 4°C in the presence of a desiccating agent for up to 8 months.
6. The culture dish with the immobilized cells must not be shaken. Particularly, in the case that a medium with serum is used, the immobilized cells are easy to be detached from the surface.

References

1. Ziauddin, J., Sabatini, D. M. (2001) Microarrays of cells expressing defined cDNA. *Nature* 411, 107–110.
2. Wheeler, D. B., Bailey, S. N., Guertin, D. A., Carpenter, A. E., Higgins, C. O., Sabatini, D. M. (2004) RNAi living-cell microarrays for loss-of-function screens in Drosophila melanogaster cells. *Nat Method* 1, 127–132.
3. Wheeler, D. B., Carpenter, A. E., Sabatini, D. M. (2005) Cell microarrays and RNA interference chip away at gene function. *Nat Gene* 37, S25–S30.
4. Bailey, S. N., Ali, S. M., Carpenter, A. E., Higgins, C. O., Sabatini, D. M. (2006) Microarrays of lentiviruses for gene function screens in immortalized and primary cells. *Nat Method* 3, 117–122.
5. Bailey, S. N., Sabatini, D. M., Stockwell, B. R. (2004) Microarrays of small molecules embedded in biodegradable polymers for use in mammalian cell-based screens. *Proc Natl Acad Sci* 101, 16144–16149.
6. Anderson, D. G., Levenberg, S., Langer, R. (2004) Nanoliter-scale synthesis of arrayed biomaterials and application to human embryonic stem cells. *Nat Biotechnol* 7, 863–866.
7. Disney, M. D., Seeberger, P. H. (2004) The use of carbohydrate microarrays to study carbohydrate-cell interactions and to detect pathogen. *Chem Biol* 11, 1701–1711.
8. Okochi, M., Nakanishi, M., Kato, R., Kobayashi, T., Honda, H. (2006) High-throughput screening of cell death inducible short peptides from TNF-related apoptosis-inducing ligand sequence. *FEBS Lett* 580, 885–889.
9. Kato, K., Sato, H., Iwata, H. (2005) Immobilization of histidine-tagged recombinant proteins onto micropatterned surfaces for cell-based functional assays. *Langmuir* 21, 7071–7075.
10. Yamamura, S., Kishi, H., Tokimitsu, Y., Kondo, S., Honda, R., Rao, S. R., Omori, M., Tamiya, E., Muraguchi, A. (2005) Single-cell microarray for analyzing cellular response. *Anal Chem* 77, 8050–8056.
11. Love, J. C., Ronan, J. L., Grotenbreg, G. M., van der Veen, A. G., Ploegh, H. L. (2006) A microengraving method for rapid selection of single cells producing antigen-specific antibodies. *Nat Biotechnol* 24, 703–707.
12. Kato, K., Umezawa, K., Funeriu, D. P., Miyake, M., Miyake, J., Nagamune, T. (2003) Immobilized culture of nonadherent cells on an oleyl poly(ethylene glycol) ether-modified surface. *BioTechniques* 35, 1014–1021.
13. Kato, K., Umezawa, K., Miyake, M., Miyake, J., Nagamune, T. (2004) Transfection microarray of nonadherent cells on an oleyl poly(ethylene glycol) ether-modified glass slide. *BioTechniques* 37, 444–452.

Chapter 13

Plasma Polymer and PEG-Based Coatings for DNA, Protein and Cell Microarrays

Andrew L. Hook, Nicolas H. Voelcker, and Helmut Thissen

Abstract

DNA, protein and cell microarrays are increasingly used in a multitude of bioassays. All of these arrays require substrates that are suitable for the immobilisation and display of arrayed probe molecules whilst at the same time resisting non-specific interactions of biomolecules with the substrate in areas between printed spots. To meet these conflicting requirements, three different approaches have been developed, all of which were based on low-fouling, high-density poly(ethylene glycol) (PEG) background coatings. In the first approach, the coating was based on allylamine plasma polymerisation (ALAPP) and the subsequent high-density grafting of PEG, followed by the generation of a surface chemical pattern using laser ablation. In the second approach, a photoreactive polymer was printed on the same ALAPP–PEG background. The third approach was based on ALAPP deposition followed by the formation of a multifunctional layer by spin coating a PEG-based polymer that also displayed epoxy groups. The successful demonstration of DNA, protein and cell microarrays has been achieved on each of these coatings.

Key words: Patterned substrates, plasma polymerisation, PEG, laser ablation, contact printing, ink-jet printing, microarrays.

1. Introduction

Microarray technology has been successfully deployed in many diverse research areas including genomics, gene profiling, materials development, living cell assays and pharmaceutics screening assays (1–5). Typically, these microarrays are formed by depositing nanolitre volumes of solutions onto addressable locations of a substrate using a contact or ink-jet printer. The substrates used can vary considerably, but typically consist of a glass slide with a coating that supports the adsorption or attachment of the arrayed

E. Palmer (ed.), *Cell-Based Microarrays*, Methods in Molecular Biology 706,
DOI 10.1007/978-1-61737-970-3_13,

material. Once formed, arrays are routinely subjected to bioassays to assess the extent of binding of specific proteins, DNA and oligonucleotide strands, living cells and other biomolecules such as polysaccharides. For most microarray applications, a low-fouling background is desirable to minimise non-specific adsorption of biomolecules in-between printed spots. However, this requirement is in conflict with the need to adsorb or covalently attach arrayed molecules and requires advanced substrate coating architectures to be realised. This can be achieved by the creation of a patterned substrate containing adhesive regions (that support the adsorption of biomolecules and living cells) as well as low-fouling regions. For this purpose a substrate has been developed whereby an allylamine plasma polymer (ALAPP) coating is generated by plasma polymerisation followed by subsequent high-density grafting of a poly(ethylene glycol) (PEG) layer. Plasma polymerisation is able to produce thin, adherent, pin-hole-free coatings onto almost any substrate, and by judicious choice of a monomer, the chemistry of the coating can be tailored to a specific application (6). ALAPP has been shown to support the adsorption or immobilisation of DNA, protein and cells (7–11). In contrast, high-density PEG coatings are well known for their ability to resist biomolecular adsorption (12). This platform was initially developed for the effective control of protein adsorption, cell attachment and even tissue outgrowth (13). However, more recently, this coating platform has been extended to the formation of DNA, protein and transfected cell microarrays (TCM) (7, 9, 14–18).

Three predominant methods were employed. The first was achieved by the use of laser ablation to remove portions of the PEG top-layer, thereby re-exposing the underlying ALAPP layer and, thus, producing a surface that contains two surface chemistries: one that supports biomolecular adsorption and the other that is low fouling (13). In the second approach, the biomolecules themselves were chemically altered to contain a photoactive crosslinker that could be activated to form a covalent linkage to the surface (16). Thus, if printed onto a non-fouling substrate, such as PEG, activation of the crosslinker ensured that the biomolecules were affixed to the surface whilst maintaining a low-fouling background. For example, this process was used to create a surface pattern by printing a polymer that is supportive for biomolecular adsorption, such as collagen or poly(L-lysine) (PLL) on a PEG-coated substrate. The layer of polymer then acted as an adhesive surface onto which other biomolecules were printed. The advantage of this approach is the facile alignment of the surface pattern with the formation of a DNA or protein microarray and the ability to achieve surface patterning and array formation in a single print run. In the third approach, ALAPP was used as a substrate to attach a crosslinked, spin-coated, multifunctional layer containing both PEG and epoxy functional groups.

Here, a PEG methacrylate (PEGMA) was copolymerised with glycidyl methacrylate (GMA). The amine-reactive epoxy groups of the GMA ensured the crosslinking of the spin-coated polymer layer, the covalent immobilisation on the amine functional group presenting ALAPP surface and the ability to covalently link arrayed biomolecules to the surface (17). The epoxy group could also be deactivated, resulting in non-adhesive PEG regions, suitable as a background surface for subsequent bioassays. All three of these methods are illustrated in **Fig. 13.1**.

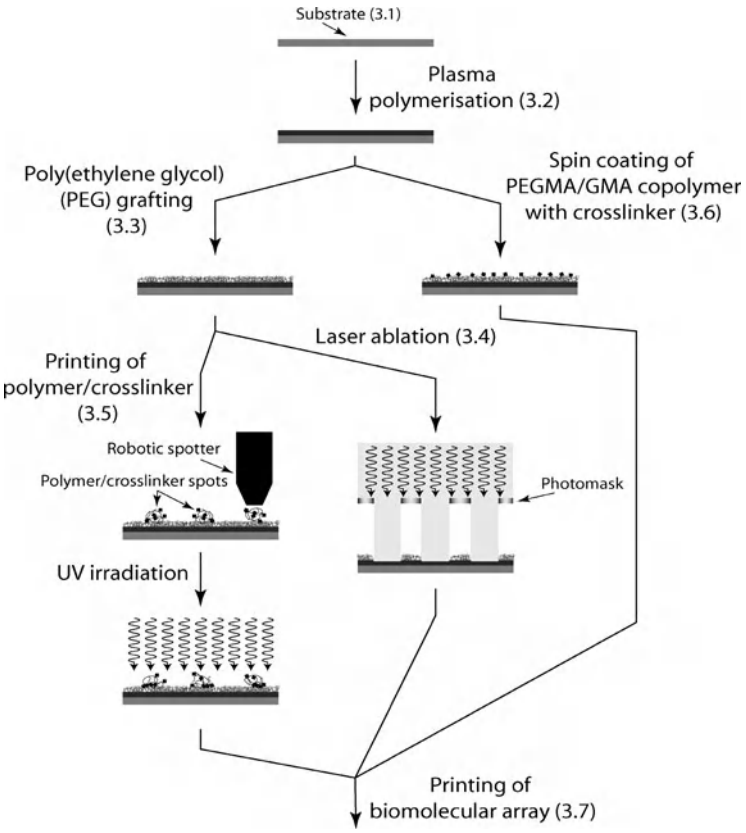

Fig. 13.1. Schematic representation of the three patterning methods used to create a platform for biomolecule arrays. Crosslinkers are represented by a *gray square*. Schematic not drawn to scale. The section number describing each step has been given.

2. Materials

2.1. Substrate Preparation

1. 5% RBS (RBS-35, Pierce, Rockford, IL, USA) surfactant solution prepared in 95% ethanol and stored at room temperature (*see* **Note 1**).

2.2. Plasma Polymerisation

1. Allylamine stored at 4°C (>98% purity, Sigma).
2. Substrate surfaces, surfactant cleaned and dried.

2.3. PEG Grafting for Laser Ablation

1. Monomethoxy poly(ethylene glycol) aldehyde (PEG) stored at –20°C (5000 MW, Shearwater polymers).
2. 0.1 M NaOH.
3. 0.1 M NaH_2PO_4 (pH 7.4).
4. K_2SO_4 (Aldrich).
5. $NaCNBH_3$ (Aldrich).

2.4. Surface Patterning by Printing a Photoreactive Polymer

1. *N*-succinimidyl-5-azido-2-nitrobenzoate stored at –20°C (*N*SANB) (Fluka).
2. A biomolecule or polymer containing amine functional groups (e.g. poly(L-lysine), Sigma, MW 70000) to be grafted to the surface (*see* **Note 2**).
3. ALAPP–PEG-coated substrates.

2.5. Formation of the Multifunctional Layer

1. Poly(ethylene glycol) methacrylate (PEGMA) (MW 475, Sigma).
2. Glycidyl methacrylate (GMA) (Sigma).
3. Dioxane, water-free (BDH Chemicals).
4. Azobisisobutyronitrile (AIBN) (Sigma).
5. Bis(2-aminoethyl) polyethylene glycol (MW 3400, Fluka).
6. Fresh ALAPP-coated substrates.
7. 0.1 M NaH_2PO_4 (pH 7.4).

3. Methods

3.1. Substrate Preparation

The deposition of polymer layers using plasma polymerisation has previously been reviewed in detail (6). A key advantage of this approach is its substrate independence, that is, coatings with nearly identical physical and chemical properties can be generated on entirely different substrates, rendering this approach highly engineering-friendly. However, in order for the coating to remain attached, it is important to thoroughly clean the substrate before deposition of the plasma polymer layer. The cleaning procedure will vary depending on the substrate. Here, a procedure commonly used for cleaning glass and silicon substrates is described (19).

1. Substrates are placed in a glass beaker, completely covered by a surfactant solution and sonicated for 30 min.
2. The surfactant solution is removed and the substrates are rinsed 10 times with MilliQ^{TM} ultra pure water (resistivity of 18.2 MΩ.cm). They are then dried under a stream of nitrogen or in a laminar flow hood.
3. If silicon wafer substrates are used (*see* **Note 3**), the samples are subsequently placed in a sealed vessel and irradiated for 30 min under UV light to achieve a stable oxide top-layer.

3.2. Plasma Polymerisation

Plasma polymerisation is achieved by the ionisation of molecules in the gas phase to generate a plasma. The plasma is able to ablate material from the surface (an effect routinely used for cleaning of surfaces), but at the appropriate power, radicals can be generated to instigate the polymerisation and deposition of a thin coating onto a substrate. The conditions at which this deposition occurs are dependent on the dimensions of the plasma chamber used. As such, the conditions described for the creation of ALAPP are specific to the reactors used; however, the principles outlined can be translated to any system.

1. The plasma reactor consists of two circular electrodes separated by 125 mm in a cylindrical reactor being 350 mm high with a diameter of 170 mm held vertically (20). Allylamine gas is introduced through the top of the reactor and removed through the bottom of the reactor by a vacuum pump such that there is a constant flow of monomer through the chamber. The allylamine reservoir is kept on ice in a glass round-bottomed flask (*see* **Note 4**).
2. The cleaned substrates are placed on the bottom electrode (*see* **Note 5**).
3. The chamber is pumped down to >0.01 mbar using a vacuum pump. A valve on the line to the monomer reservoir is used to regulate the monomer flow (*see* **Note 6**). The valve is gradually opened until the pressure in the chamber increased to 0.200 mbar.
4. At this point, the frequency generator is turned on to apply a radio frequency between the two electrodes at a frequency of 200 kHz and a power of 20 W for a duration of 25 s (*see* **Note 7**).

3.3. PEG Grafting for Laser Ablation and for Printing a Photoreactive Polymer

1. Initially, the grafting solution is prepared. 1.1 mg of K_2SO_4 is added to a 90-mm Petri dish.
2. 10 ml of phosphate buffer, freshly made by adding 0.1 M NaOH to 50 ml of 0.1 M NaH_2PO_4 until a pH of 6.2 is achieved, is added. At this stage, not all of the salt will

dissolve; however, this will happen once the temperature of the solution is increased.

3. 30 mg of $NaCNBH_3$ and 25 mg of PEG are added to the solution and dissolved by gentle shaking. $NaCNBH_3$ is a strong reducing agent and is toxic and corrosive. It should be handled with due care. The grafting solution is now complete.
4. Freshly ALAPP-coated samples are then added to the grafting solution and incubated at 60°C (in an oven or in a water bath) for 16 h under occasional shaking. ALAPP-coated samples should be added as soon as possible after taking them out of the plasma polymerisation reactor to maximise the availability of functional groups (*see* **Note 8**). A schematic of the chemical reaction occurring in this step is shown in **Fig. 13.2**.
5. After grafting is complete, the grafting solution is removed and the samples rinsed 10 times with ultra pure water. They are then dried under a stream of nitrogen or in a laminar flow hood.

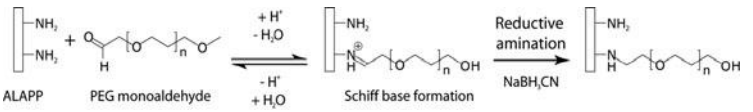

Fig. 13.2. Schematic of the chemical grafting of a PEG monoaldehyde molecule to an ALAPP-coated surface.

3.4. Surface Pattern by Laser Ablation

The advantage of laser ablation is the ability to generate many different geometries in varied arrangements in a controlled and highly resolved manner. Furthermore, the pattern generation is very quick.

1. For best results, this methodology is conducted in a clean room.
2. ALAPP–PEG-coated samples are placed on the stage (*see* **Note 9**) of a suitable laser ablation apparatus (*see* **Note 10**).
3. PEG-grafted ALAPP samples on silicon substrates are ablated at an energy density of 60 mJ/cm^2 and four pulses of 20 ns duration per area to form a spatially patterned substrate (*see* **Note 11**).

3.5. Surface Pattern by Printing a Photoreactive Polymer

The key advantage of this method is the ability to form a pattern and print an array in the same apparatus. This negates the need to align the surface pattern generated by laser ablation or another patterning method with the printed pattern deposited in the array printer.

1. Initially, a 1 mg/ml *N*SANB solution is prepared in MilliQ^{TM} ultra pure water (*see* **Note 12**). This is close to the saturation point for *N*SANB in water (*see* **Note 13**).
2. The *N*SANB solution is then diluted 1:1 with a 4 mg/ml solution of the polymer to be used for creation of the surface pattern resulting in a solution containing 1.6 mM *N*SANB and 0.029 mM polymer (*see* **Note 14**). The actual concentration of the polymer solution may vary depending on which polymer is used. The concentration given is optimised for use with PLL (MW 70000).
3. The solution is incubated for 10 min at 37°C. A schematic depicting the chemistry involved with this process is shown in **Fig. 13.3**.

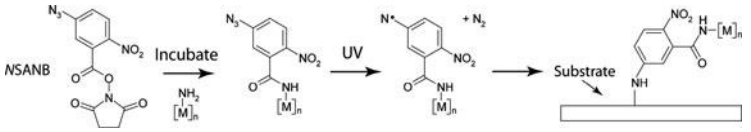

Fig. 13.3. Schematic of the use of *N*SANB for crosslinking a polymer to a substrate. The same reaction also leads to crosslinking within the printed polymer.

4. The polymer–*N*SANB solution is then pipetted into a source plate and placed into the printer for the formation of a microarray (*see* **Note 15**).
5. The PEG-coated substrate is placed in the array printer (*see* **Note 16**).
6. The *N*SANB-functionalised polymer is printed in the desired pattern using standard arraying methodologies. The water solubility of the polymers used means that washing can be done with MilliQ^{TM} ultra pure water.
7. The sample is then irradiated with UV for 10 min (*see* **Note 17**).

3.6. Formation of Multifunctional Layer

1. 20% (w/v) monomer solutions containing either PEGMA or GMA are prepared in dioxane and chromatographed through a glass column filled with inhibitor remover.
2. The monomer solutions are then combined in a PEGMA/GMA ratio of 1:1 (v/v). The structures of the two monomers used are shown in **Fig. 13.4**. The thermal initiator AIBN is then dissolved in the PEGMA/GMA solution at a ratio of 1 mg of AIBN to 2 ml of monomer solution.
3. The solution is purged with nitrogen for 15 min and then sealed and placed into a 60°C oven for 16 h. The solution is then used in subsequent experiments after cooling to room temperature.

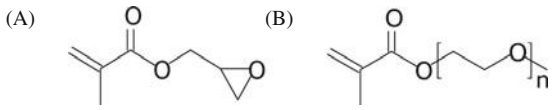

Fig. 13.4. Schematic of the two monomers used in the formation of a multifunctional polymer coating; (**a**) GMA; (**b**) PEGMA.

4. The PEGMA/GMA solution is diluted with dioxane to a 2.5% (w/v) solution, and 0.2% (w/v) bis(2-aminoethyl) polyethylene glycol is added and dissolved just before the spin-coating step to act as a crosslinker.
5. Freshly prepared ALAPP-coated glass slides are then placed on a spin coater and completely covered with the solution containing the crosslinker using a glass pipette. The substrates are then spin-coated at 5,000 rpm for 30 s.
6. The resulting films are stored for 2 h at room temperature in a laminar flow cabinet and finally for 16 h in a vacuum chamber in order to remove the remaining solvent and to allow for crosslinking to occur.
7. The slides are then removed from the vacuum chamber, washed in 0.1 M NaH_2PO_4 at 37°C for 2 h, washed with MilliQ^{TM} ultra pure water, and dried in a spin dryer before printing.

3.7. Formation of a Microarray

Once prepared, the different ALAPP/PEG substrates are immediately ready for array formation. The substrates are applicable for all conventional arrayers and no further preparation is required before printing. As discussed previously, care should be taken to ensure that biomolecular microarrays align with the surface chemical patterns on the substrates. This is not necessary for the multifunctional polymer coating.

4. Notes

1. The surfactant solution can be prepared in large quantities ahead of time. It is important to use a high-quality surfactant such as RBS 35.
2. The choice of a biomolecule or polymer for patterning by printing onto ALAPP–PEG-coated substrates is not limited to amine-containing species. Several alternatives to *N*SANB are commercially available (e.g. Pierce) that feature a photoreactive group at one end and a reactive functional group at the other end of the molecule. Alternatively, amine groups may be generated on the biomolecule

or polymer prior to reaction with *N*SANB. Various organic and bioconjugate chemistry strategies can be employed to convert functional groups to amines.

3. Due to the formation of an oxide layer on silicon-based materials, it is necessary to UV-irradiate the substrates prior to plasma polymer deposition in order to produce a consistent top-layer. The use of a sealed vessel is important in this case in order to generate and maintain an O_3-containing atmosphere. This procedure is not necessary on other substrate materials such as polymers.
4. The monomer, in this case, must be cooled to lower the vapour pressure to a manageable level. Other monomers with very low vapour pressures may be heated when used in a plasma polymerisation process.
5. Care should be taken to clearly mark which side has been coated. One approach to achieve this on rectangular glass substrates (i.e. glass slides) is to scratch or cut off the top right hand corner. This enables the slide to always be orientated correctly.
6. Maintaining an appropriate monomer flow through the chamber is imperative to a successful plasma deposition as this parameter greatly alters the power from the excitation source per monomer unit. If the flow rate is too high, then too many monomer units will be present and the monomer will not ionise sufficiently to achieve polymerisation. If on the other hand, the flow rate is too low, then each monomer unit will receive too much power and will fracture, removing chemical functionalities that one may wish to preserve in the resultant film. Moreover, the plasma could shift from the deposition regime to the ablation regime.
7. The length of the application of the plasma determines the deposition time, which is approximately proportional to the thickness of the film.
8. The critical element to creating a low-fouling PEG layer is an appropriate high density. There are two key aspects of this experiment that must be adequately considered in order to achieve this. Firstly, the grafting needs to be done at 'cloud point' whereupon the salt concentration is suitably high such that the PEG molecules become highly collapsed. They can then be grafted at a higher density, and when subsequently exposed to a solution with a reduced salt content the PEG molecules will swell, which improves the exclusion properties of the layer. Secondly, the PEG molecules are grafted to the surface via the amine groups present on the ALAPP layer. The ALAPP layer is highly

susceptible to oxidation and other ageing phenomena, mainly due to atmospheric oxygen, after re-exposure to air. Thus, it is important to transfer the newly coated substrates to the grafting solution as soon as possible. In order to achieve this, the grafting solution should be prepared prior to the plasma polymer layer deposition so that the grafting can commence as soon as the sample is removed from the reactor.

9. A key aspect to the successful formation of a patterned substrate that can be used for microarray applications is the generation of a pattern that can be subsequently aligned with the array produced by an array printer. Great care, thus, should be taken to ensure guide marks are in place so that the pattern generated by laser ablation occurs at a predictable location that can easily be found and aligned with.
10. In previous work, ablation experiments were conducted using a 248-nm KrF excimer laser Series 8000 (Exitech Limited, UK) equipped with a Lambda Physik LPX210i laser source. The square beam was passed through a chrome-on-quartz mask pattern and a 1:10 demagnification lens, resulting in a 1.5-mm diameter field with a resolution of 0.8 μm. The beam delivery system contained beam shaping and homogenisation optics to create a uniform, square beam at the plane of a mask held on an open frame CNC-controlled X–Y stage set. However alternative laser ablation units, including those not using a mask in the laser beam, would be equally suitable.
11. It is important to tune the energy density and the number of pulses such that the top PEG layer is removed but the ALAPP layer is not completely removed.
12. The *N*SANB solution is extremely sensitive to UV light and must be prepared fresh before each experiment and handled, up to its UV activation, in a dark room. A weak red light source may be used in the room.
13. Heating the *N*SANB solution to 40°C can assist in the complete dissolution of the *N*SANB.
14. The concentration of this solution will depend on the polymer used. When using PLL, which is amenable to the process and adhesive, a 2 mg/ml solution is adequate. The spots generated by this solution should be assessed to ensure that a complete and even coating has been generated. There is no reason why the polymer cannot be substituted for other biomolecules such as proteins. However, for formation of a surface pattern that can be used subsequently for DNA, protein and cell microarrays, a polymer

that offers a stable and predictable surface chemistry is desirable.

15. Typically a contact printer with a solid (not a slitted) pin has been used for this methodology. There is no reason why this methodology could not be adapted to an ink-jet printer or other printing techniques (e.g. soft lithography).
16. Most printers are designed to accommodate standard glass slides, and for this reason, this is the easiest substrate to handle for this preparation.
17. Depending on the stability of the resultant-grafted layer and the target assay, it may be necessary to introduce an additional washing step prior to formation of a biomolecular array on top of the surface pattern in order to remove any weakly bound *N*SANB-functionalised molecules. This is achieved by removing the sample from the printer and rinsing with MilliQ^{TM} ultra pure water 10 times. Care should be taken to ensure that the sample is placed directly where it was initially positioned to preserve the alignment of the surface pattern with any subsequent biomolecular microarrays.

References

1. Meloni, R., Khalfallah, O., Biguet, N. F. (2004) DNA microarrays and pharmacogenomics. *Pharmacol Res* 49, 303–308.
2. Forster, T., Roy, D., Ghazal, P. (2003) Experiments using microarray technology: limitations and standard operating procedures. *J Endocrinol* 178, 195–204.
3. Kumar, A., Goel, G., Fehrenbach, E., Puniya, A. K., Singh, K. (2005) Microarrays: the technology, analysis and application. *Eng Life Sci* 5, 215–222.
4. Hook, A. L., Anderson, D. G., Langer, R., Williams, P., Davies, M. C., Alexander, M. R. (2010) High throughput methods applied in biomaterial development and discovery. *Biomaterials* 31, 187–198.
5. Hook, A. L., Voelcker, N., Thissen, H. (2009) Patterned and switchable surfaces for biomolecular manipulation. *Acta Biomaterialia* 5, 2350–2370.
6. Yasuda, H. (1985) *Plasma Polymerization*. Academic Press, Orlando, FL.
7. Cole, M. A., Voelcker, N. H., Thissen, H. (2007) Electro-induced protein deposition on low-fouling surfaces. *Smart Mater Struct* 16, 2222–2228.
8. Hook, A. L., Thissen, H., Quinton, J., Voelcker, N. H. (2008) Comparison of the binding mode of plasmid DNA to allylamine plasma polymer and poly(ethylene glycol) surfaces. *Surf Sci* 602, 1883–1891.
9. Thissen, H., Johnson, G., Hartley, P. G., Kingshott, P., Griesser, H. J. (2006) Two-dimensional patterning of thin coatings for the control of tissue outgrowth. *Biomaterials* 27, 35–43.
10. Hamerli, P., Weigel, T., Groth, T., Paul, D. (2003) Surface properties of and cell adhesion onto allylamine-plasma-coated polyethyleneterephthalate membranes. *Biomaterials* 24, 3989–3999.
11. Zhang, Z., Chen, Q., Knoll, W., Foerch, R., Holcomb, R., Roitman, D. (2003) Plasma polymer film structure and DNA probe immobilization. *Macromolecules* 36, 7689–7694.
12. Kingshott, P., Thissen, H., Griesser, H. J. (2002) Effects of cloud-point grafting, chain length, and density of PEG layers on competitive adsorption of ocular proteins. *Biomaterials* 23, 2043–2056.
13. Thissen, H., Hayes, J. P., Kingshott, P., Johnson, G., Harvey, E. C., Griesser, H. J. (2002) Nanometer thickness laser ablation for spatial control of cell attachment. *Smart Mater Struct* 11, 792–799.
14. Hook, A. L., Creasey, R., Hayes, J. P., Thissen, H., Voelcker, N. H.

(2009) Laser based patterning of transfected cell microarrays. *Biofabrication* 1, 045003–045012.
15. Hook, A. L., Thissen, H., Hayes, J. P., Voelcker, N. H. (2005) Spatially controlled electro-stimulated DNA adsorption and desorption for biochip applications. *Biosens Bioelectron* 21, 2137–2145.
16. Hook, A. L., Thissen, H., Voelcker, N. H. (2009) Advanced substrate fabrication for cell microarrays. *Biomacromolecules* 10, 573–579.
17. Kurkuri, M. D., Driever, C., Johnson, G., McFarland, G., Thissen, H., Voelcker, N. H. (2009) Multifunctional polymer coatings for cell microarray applications. *Biomacromolecules* 10, 1163–1172.
18. Szili, E., Thissen, H., Hayes, J. P., Voelcker, N. (2004) A biochip platform for cell transfection assays. *Biosens Bioelectron* 19, 1395–1400.
19. Maurdev, G., Gee, M. L., Meagher, L. (2002) Controlling the adsorbed conformation and desorption of polyelectrolyte with added surfactant via the adsorption mechanism: a direct force measurement study. *Langmuir* 18, 9401–9408.
20. Griesser, H. J. (1989) Small-scale reactor for plasma processing of moving substrate web. *Vacuum* 39, 485–488.

Chapter 14

Polymer Microarrays for Cellular High-Content Screening

Salvatore Pernagallo and Juan J. Diaz-Mochon

Abstract

Polymer microarrays as platforms for cell-based assays are presented, offering a unique approach to high-throughput cellular analysis. These high-throughput (HT) platforms are used for the screening of new materials with the purpose of first finding substrates upon which a specific cell line would adhere and second to gain a rapid understanding of the interactions between cells and biomaterials. Arrays presented here are fabricated using pre-synthesised polymers by contact printing via a robotic microarrayer. These large arrays of polymers are then incubated with cell cultures and the results obtained are used to significantly help the design of synthetic biomaterials, implant surfaces and tissue-engineering scaffolds by finding correlations between their chemical structure and their biological performance. The flexibility of polymer microarrays analysis not only greatly refines our knowledge of multitude of cell-biomaterial interactions but could also be used in biocompatibility assessments as novel biomarkers.

Key words: Polymer microarrays, mouse fibrosarcoma cells (L929), K562 cells, scanning electron microscopy (SEM), high-throughput screening (HTS), cell-based assays.

1. Introduction

The development of biomaterials for the biomedical field, especially in the case of polymers, represents a major opportunity to improve quality of life (1). For this reason, great quantities of resource have been spent with the intention of synthesising and improving biocompatible materials (2). However, the nature of the interactions between a polymer and its biological environment is highly complex. For example, due to the multiplicity of the cell-surface components (lipid bilayer, membrane proteins, glycoproteins and small molecules), the principles of immobilisation of cells on a surface are more difficult to predict than that of the

E. Palmer (ed.), *Cell-Based Microarrays*, Methods in Molecular Biology 706,
DOI 10.1007/978-1-61737-970-3_14,

immobilisation of single biomolecules. In fact, cell–biomaterial interactions should be considered as the result of a range of co-operative and dynamic non-covalent interactions between these components and a given substrate. Surface characteristics, such as hydrophobicity, roughness and charge, and chemical composition, are all known to play key roles in regulating the response of cells that interact with biomaterials (3). It is impossible to theoretically predict cellular response, and thus every time a new material is generated, it is vital to test its biocompatibility using cells with which it will come into contact. Traditional methods of screening, identifying and testing of new polymers are slow; yet over recent years, the field of automated and parallel screening of polymers has grown enormously. The use of a high-throughput approach, such as polymer microarrays, to allow the rapid screening of chemically diverse polymers offers an important tool for finding correlations between the design and performance of such materials (4, 5). The system of polymer microarrays has had, and will continue to have, a massive impact on the study and development of new biomaterials with diverse applications.

2. Materials

2.1. Polymer Microarray Preparation

1. Aminoalkylsilane poly-prep slides (Sigma-Aldrich).
2. Agarose type I-B.
3. 1-Methyl-2-pyrrolidinone (NMP).
4. 384-Well polypropylene microplate.
5. Robotic microarrayer: QArray Mini (Genetix).
6. Polymer libraries synthesised via radical polymerisation on a mmol scale (6–8).

2.2. Cell Culture

1. Dulbecco's modified eagle medium (DMEM) supplemented with 10% foetal bovine serum (FBS), L-glutamine (4 mM) and antibiotics (penicillin and streptomycin, 100 units/ml).
2. RPMI 1640 medium supplemented with 10% FBS, L-glutamine (4 mM) and antibiotics (penicillin and streptomycin, 100 units/ml).
3. 1 × Phosphate-buffered saline (1 l) (1 × PBS buffer): 8 g of NaCl, 0.20 g of KCl, 1.44 g of Na_2HPO_4 and 0.24 g of KH_2PO_4 dissolved in 800 ml of deionised H_2O, filter through Millipore filter. Adjust the pH to 7.4 with HCl or NaOH. Add Millipore filter distilled H_2O to 1 l.
4. Trypsin solution: 0.050% w/v trypsin, 0.20% w/v EDTA in PBS.

2.3. Cell Fixing and Staining

1. 4% (w/v) formaldehyde in PBS.
2. Isotonic solution: 8.1 g/l NaCl, 0.2 g/l KCl.
3. Hoechst-33342 solution: 1 μg/ml in PBS.
4. CellTracker Green™ (CTG): 5 μM in PBS.
5. Alexa Fluor® 568 phalloidin: 0.2 μM in 1% in PBS containing 1% FBS.

2.4. High-Content Screening

Image capture and analyses are carried out using a platform, based on a Nikon 50i fluorescence fluorescent microscope (×20 objective) equipped with an X–Y–Z stage, device equipped with the Pathfinder™ (IMSTAR) having a mercury lamp as light source. It allows the automated capture of single images (0.46 mm^2) for each polymer spot with a resolution of 0.58 μm.

The filters used are as follows:

1. DAPI filter set: excitation D350/50×; emission D460/50 m.
2. FITC filter set: excitation HQ480/40×; emission HQ535/50 m.
3. Cy3 filter set: excitation HQ535/50×; emission HQ610/75 m.

2.5. SEM Binding Assay

1. Spin coater (Speedlines Technologies).
2. 24-mm diameter glass coverslips.
3. Tetrahydrofuran (THF).
4. 0.2 M stock solution of cacodylate buffer (250 ml) (pH 7.4): combine 20.15 g sodium cacodylate trihydrate (MW = 214), 0.1 ml HCl and 250 ml of deionised H_2O, filter through Millipore filter.
5. Fixing solution: 2.5% glutaraldehyde in 0.1 M cacodylate buffer (pH 7.4).
6. Post-fixing solution: 1% osmium tetroxide aqueous solution.
7. Philips XL30CP scanning electron microscope at 30 kV in a secondary electron imaging mode.

3. Methods

The Bradley research group has developed a novel approach to fabricate arrays of different materials by contact printing preformed polymers onto cytophobic (agarose-coated) slides (*see* **Note 1**) to generate well-defined polymer microarrays (9). Before

printing, each library member is dissolved in a common, non-volatile solvent (NMP) (*see* **Note 2**). A number of printing parameters, such as inking and printing time, were optimised in this process to ensure uniformity of polymer spot within the array (**Fig. 14.1a**). Since each library member is synthesised on a scale that allowed characterisation prior to array fabrication, there is full confidence in any structure-activity relationship generated while allowing immediate scale-up following polymer identification. Several cell types, from immortalised cell lines, primary cells, to stem cells can be studied. In general terms, cell types can be categorised as either adherent or suspension cells; so two different protocols have to be followed (9–12).

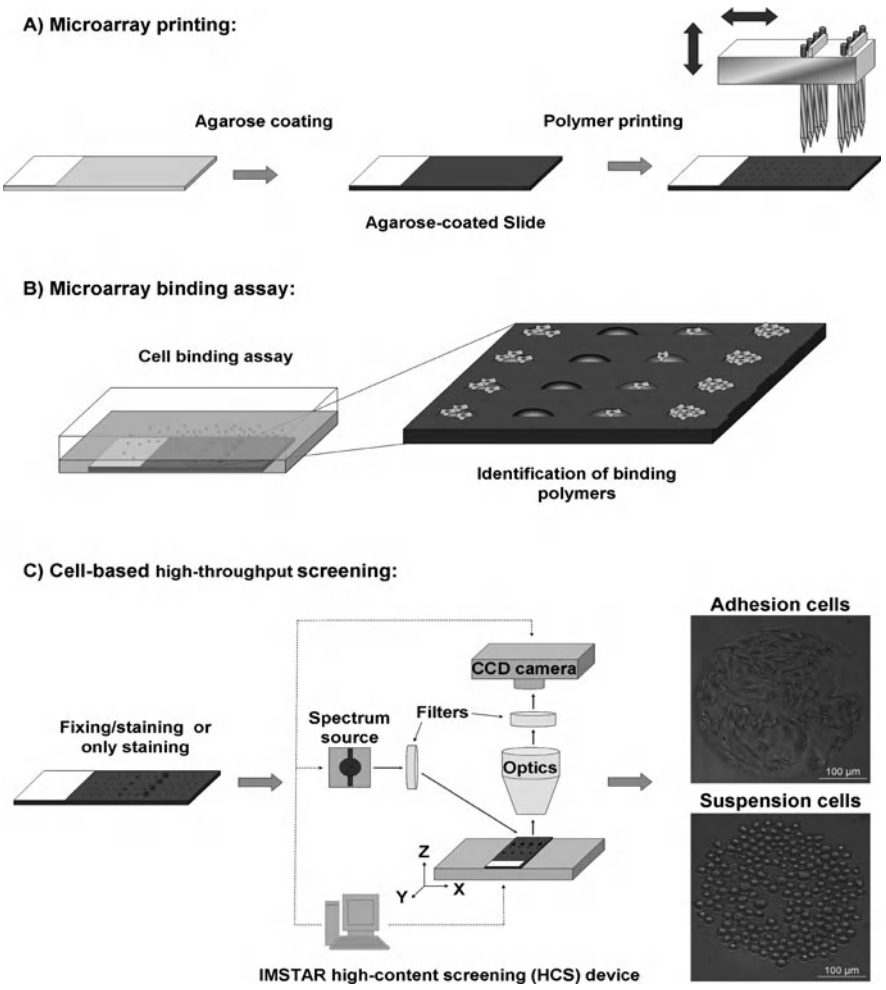

Fig. 14.1. General protocol for the identification of substrates for cell-polymer binding studies: (**a**) polymer microarray preparation; (**b**) microarray binding assay; (**c**) cell-based high-throughput screening.

3.1. Polymer Microarray Preparation

1. Every polymer of the libraries is characterised using analytical methods such as gel permeable chromatography, differential scanning colorimetry and fourier transform infrared (13, 14).
2. Polymers are dissolved at 1% w/v in NMP.
3. The solutions are placed into a 384-well microplate prior to printing.
4. Coating glass slides with agarose is achieved by dip-coating the aminoalkylsilane slides in a 1% w/v solution of agarose type-I B at 65°C followed by removal of the coating on the bottom side. After drying overnight at room temperature, the coated slides are stored at room temperature or used immediately for printing (15).
5. The robot used is the QArray Mini. The solutions are deposited by contact printing using 150 mm solid pins. Each polymer solution is printed as four identical spots and each spot is formed by a minimum of five contact printings to give a microarray with up to 2,048 spots per slide (*see* **Note 3**).
6. The solvent is removed by drying under vacuum at (24 h at 42°C/200 mbar).
7. The slides are sterilised in a biosafety cabinet by exposure to UV irradiation for 20 min prior to use.

3.2. Cell-Based Microarrays – Adherent Cells

To carry out experiments using adherent cells, mouse fibrosarcoma cell line, L929 (*see* **Note 4**) was chosen. Cells were incubated with a polymer microarray for 48 and 72 h (**Fig. 14.1b**). In order to study the biocompatibility of the polymer support, cells are stained with CTG, an indicator of cell viability (16), 1 h before fixing. Subsequently, the cells are fixed, and cell nuclei and cytoskeleton are stained with Hoechst-33342 and Alexa Fluor® 568 phalloidin respectively. Cell-permeable Hoechst-33342 is an adenine–thymine-specific dye that binds to the minor groove of DNA and is used to enable the counting of cells (17). Alexa Fluor® 568 phalloidin is a fluorescent bicyclic peptide with high affinity for F-actin, which is an important component of the cytoskeleton, and is used to study cell morphology (18). Each array position is then captured using three fluorescent channels (DAPI, FITC and Cy3 filter sets) and brightfield illumination, giving rise to four images per position (**Fig. 14.1c**). Cell number, biocompatibility and morphology of each polymer member are determined in an automated manner using Pathfinder™. Cell morphology is further analysed by confocal microscopy (**Fig. 14.2**).

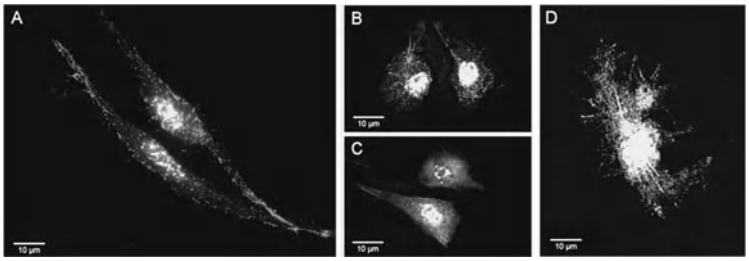

Fig. 14.2. Confocal images of L929 cells on polymer microarrays. Cells are imaged under excitation at 555/28 and 360/40 nm using a DeltaVision RT microscope (×63 objective) and then merged: (**a**) PU-87; (**b**) PU-133; (**c**) PU-161 and (**d**) PU-107.

3.3. Cell Adhesion, Biocompatibility and Morphology Studies

1. L929 cells are washed with PBS, detached with 0.050% w/v trypsin, 0.20% w/v EDTA in PBS, counted and diluted with DMEM-complete media to a final concentration of 10^5 cells/ml.
2. Six millilitre of this dilution is gently added onto two polymer microarrays contained in a sterile four-well plate and incubated for different periods of time (48 and 72 h).
3. Polymer microarrays are washed twice in PBS and incubated with CTG at 37°C and 5% CO_2 for 15 min and then gently washed.
4. Cells are fixed with *p*-formaldehyde solution at room temperature (RT) for 15 min.
5. Incubate with Hoechst-33342 for 15 min at RT.
6. Incubate with Alexa Fluor® 568 phalloidin for 15 min at RT.
7. The polymer microarray slides are then rinsed in deionised water and air-dried before scanning.
8. Image capture and analyses are carried out using a high-content screening (HCS).
9. Cell morphology studies are performed on the polymer microarray by a DeltaVision RT microscope (×63 objective) using DAPI and rhodamine channels, after 72 h (**Fig. 14.2**).

3.4. Cell-Based Microarrays – Suspension Cells

Cellular binding of suspension cells onto polymer microarrays is achieved *via* the analysis of polymer microarrays using K562 cells (*see* **Note 5**). This method measures not only polymer-binding capacities but also cellular proliferation (19).

In order to quantify both cellular adhesion and proliferation, the average number of cells and the standard deviation are determined at three different incubation times (24, 48 and 72 h) on three separate polymer microarrays (**Fig. 14.3**). Through the analysis of the arrays, it is then possible to profile different materials. The images are automatically processed by Pathfinder™ (**Fig. 14.3b**) by counting cell nuclei which are stained with Hoechst 33342.

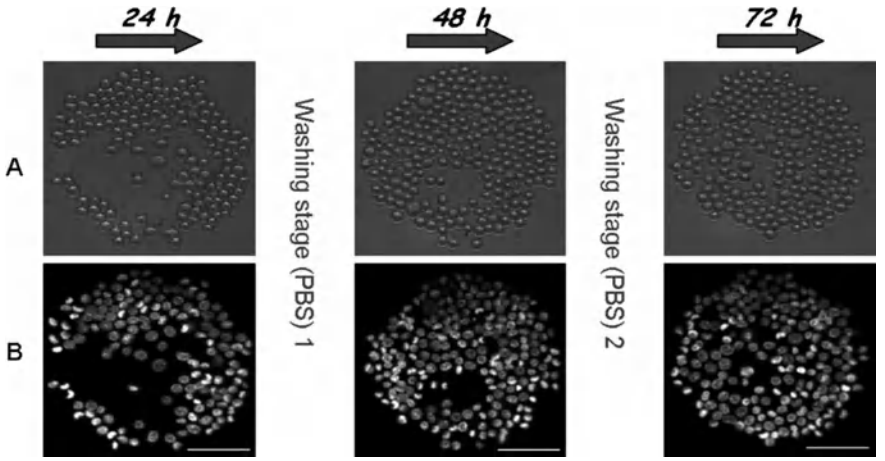

Fig. 14.3. Parallel analysis of polymer cellular binding and proliferation on a representative spot (PA-374): (**a**) Brightfield images; (**b**) DAPI channel. Scale bar 100 μm.

1. K562 cells are washed with PBS, counted and diluted with RPMI-complete media to a final concentration of 10^5 cells per ml.
2. An aliquot of 6 ml of this dilution is gently added to the three polymer microarrays contained in a four-well plate and incubated for 24, 48 or 72 h.
3. The polymer microarray is washed with PBS (*see* **Note 6**) and then incubated for 30 min with fresh RPMI serum-free media supplemented with Hoechst 33342.
4. The polymer microarray slides are then rinsed in an isotonic solution and immersed in this solution to facilitate K562 live cell analysis.
5. Image capture and analyses are carried out using HCS. Live automatic scanning is achieved by ×20 objective (in an immersion manner), using fluorescent (DAPI filter set) and brightfield channels of the polymer spots (**Fig. 14.3**).

3.5. SEM Binding Assay

SEM studies are undertaken so that the effect of the different polymers on the cells could be assessed. This allows a better understanding of the effect that polymers produce on suspension cells adhered on them (**Fig. 14.4**).

1. Hit polymers selected from cell-based polymer microarray experiments are dissolved at 2.0% w/v in THF.
2. 200 ml of the polymer solutions (2.0% w/v in THF) are placed onto the coverslips and spin-coated for 2 s at 2,000 rpm.
3. The solvent is removed by drying under vacuum (12 h at 42°C/200 mbar).

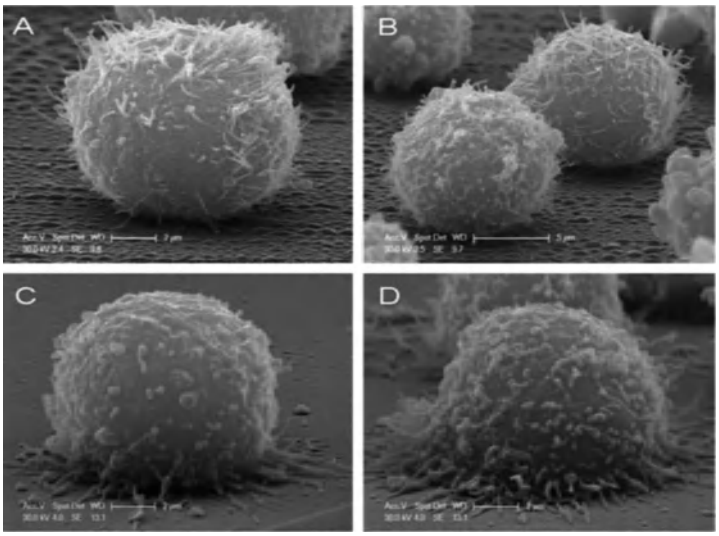

Fig. 14.4. Scanning electron micrographs. (**a**, **b**) Control K562 cells after 24 h; (**c**) cells grown on a selected polymer after 24 h; (**d**) cells grown on a selected polymer after 72 h.

4. The glass coverslips are sterilised in a biosafety cabinet by exposure to UV irradiation for 20 min prior to use.
5. K562 cells are washed with PBS, counted and diluted with RPMI-complete media to a final concentration of 10^5 cells/ml.
6. An aliquot of 1 ml of this dilution is gently seeded to the polymer-coated glass coverslips contained in a 12-well plate and incubated for 24 or 72 h.
7. K562 cells are fixed at RT for 2 h (*see* **Note 7**).
8. All samples are post-fixed with osmium tetroxide for 1 h at room temperature, dehydrated through graded ethanol (50, 70, 90 and 100%), critical point-dried in CO_2 and gold coated by sputtering.
9. The samples are examined with a scanning electron microscope (**Fig. 14.4**).

4. Notes

1. Several functionalised and gold-coated glass slides were investigated for this application, most of which provide a suitable surface for polymer printing, and could be readily sterilised under UV irradiation, but unfortunately did not prevent cellular adhesion. The following substrates were

prepared and tested: C18-functionalised slides, aluminium slides and perfluoroalkylthiol-modified slides. The best results were obtained by dip-coating aminoalkylsilane slides with a thin film of agarose type I-B. Importantly agarose is readily sterilised by UV irradiation and does not dissolve in most organic solvents (9).

2. NMP is selected on the basis that the majority (> 95%) of the polymer library is soluble in this solvent and that it allowed uniform spots to be printed.
3. The typical spot diameter is 300 mm (±20 mm) with a volume of about 7 nl which is equivalent to about 70 pg of polymer.
4. Mouse connective tissue cells (fibroblast cells (L929)) are cells of interest in biomedical research since fibroblasts provide a structural framework (stroma) for many tissues and play a critical role in wound healing (20).
5. K562 cells are a suspension cell line derived from a chronic myelogenous leukaemia patient. This cell line does not normally undergo the same adhesion process as anchorage-dependent cells and, therefore, is especially appropriate for the study of cell adhesion over long periods of time (21).
6. Each polymer microarray is washed at each time-point in order to remove the cells which had not adhered to the polymer.
7. As controls, K562 cells are collected, centrifuged for 5 min ($300 \times g$ at 20°C) and fixed in suspension at RT for 2 h. After washing twice with 0.1 M cacodylate buffer, the cells were seeded on coverslips coated with a selected polymer for 24 h.

Acknowledgments

The authors thank Professor Mark Bradley for being the pioneer of cell-based polymer microarray technologies, Hitoshi Mizomoto and Jeff Thaburet for their work on synthesising polymers, Guilhem Tourniaire for starting developing cell-based polymer microarrays and Asier Uniciti-Broceta for his work on morphologies studies.

References

1. Langer, R. (2009) The evolution of biomaterials. *Nat Mater* 8, 444–445.
2. Williams, D. F. (2009) On the nature of biomaterials. *Biomaterials* 30, 5897–5909.
3. Lecuit, T., Lenne, P. F. (2007) Cell surface mechanics and the control of cell shape, tissue patterns and morphogenesis. *Nat Rev Mol Cell Biol* 8, 633–644.

4. Michael, A. R. M., Richard, H., Ulrich, S. S. (2004) Combinatorial methods, automated synthesis and high-throughput screening in polymer research: the evolution continues. *Macromol Rapid Commun* 25, 21–33.
5. Hook, A. L., et al. (2010) High throughput methods applied in biomaterial development and discovery. *Biomaterials* 31, 187–198.
6. Mizomoto, H. (2004) The synthesis and screening of polymer libraries using a high throughput approach. Ph.D. Thesis: University of Southampton, Southampton, UK.
7. Jose, A. J. (2005) Synthesis and Screening of biocompatible polymer using a multiparallel approach. Ph.D. Thesis: University of Southampton, Southampton, UK.
8. Thaburet, J. F. O., Mizomoto, H., Bradley, M. (2004) High-throughput evaluation of the wettability of polymer libraries. *Macromol Rapid Commun* 25, 366–370.
9. Tourniaire, G., et al. (2006) Polymer microarrays for cellular adhesion. *Chem Commun* 20, 2118–2120.
10. Pernagallo, S., et al. (2008) Deciphering cellular morphology and biocompatibility using polymer microarrays. *Biomed Mater* 3, 034112.
11. Pernagallo, S., Diaz-Mochon, J. J., Bradley, M. (2009) A cooperative polymer-DNA microarray approach to biomaterial investigation. *Lab Chip* 9, 397–403.
12. Unciti-Broceta, A., et al. (2008) Combining nebulization-mediated transfection and polymer microarrays for the rapid determination of optimal transfection substrates. *J Comb Chem* 10, 179–184.
13. Tourniaire, G., Diaz-Mochon, J. J., Bradley, M. (2009) Fingerprinting polymer microarrays. *Comb Chem High Throughput Screen* 12, 690–696.
14. Thaburet, J. F. O., Mizomoto, H., Bradley, M. (2004) High-throughput evaluation of the wettability of polymer libraries. *Macromol Rapid Commun* 25, 366–370.
15. Roth, E., et al. (2004) Ink-jet printing for high-throughput cell patterning. *Biomaterials* 25, 3707–3715.
16. Pucci, F., et al. (2009) Survival of benthic foraminifera under hypoxic conditions: results of an experimental study using the CEllTRACKER green method. *Mar Poll Bull* 59, 336–351.
17. Singh, S., Dwarakanath, B. S., Mathew, T. L. (2004) DNA ligand hoechst-33342 enhances UV induced cytotoxicity in human glioma cell lines. *J Photochem Photobiol B* 77, 45–54.
18. Cooper, J. A. (1987) Effects of cytochalasin and phalloidin on actin. *J Cell Biol* 105, 1473–1478.
19. Wang, J. H., Hung, C. H., Young, T. H. (2006) Proliferation and differentiation of neural stem cells on lysine-alanine sequential polymer substrates. *Biomaterials* 27, 3441–3450.
20. Chang, H. Y., et al. (2002) Diversity, topographic differentiation, and positional memory in human fibroblasts. *Proc Natl Acad Sci USA* 99, 12877–12882.
21. Leif, C. A., Kenneth, N., Carl, G. G. (1979) K562 – a human erythroleukemic cell line. *Int J Cancer* 23, 143–147.

Chapter 15

High-Throughput Analyses of Gene Functions on a Cell Chip by Electroporation

Koichi Kato and Hiroo Iwata

Abstract

Genome-wide functional annotation of genes is one of the major challenges in current biology. Such investigation requires a high-throughput methodology for efficient and parallel overexpression or silencing of multiplexed genes in living cells. The transfection method described here employs an electric pulse and a cell-chip technology, and provides the possibility of analyzing gene functions in a high-throughput manner.

Key words: Electroporation, microarray, gene transfer, plasmid DNA, small-interfering RNA, poly(ethyleneimine), green fluorescent protein, self-assembled monolayer, functional genomics.

1. Introduction

Manipulation of gene expression in living organisms provides significant information on gene functions. To date, various kinds of methods have been developed for investigations of genes by gain-of-function studies using plasmid DNA or loss-of-function using small interfering RNAs (siRNAs). In these studies, transfection microarrays have been developed for the high-throughput transfection of nucleic acids into living mammalian cells.

The Human Genome Project completed in 2003 provided us with the complete sequence of the 3 billion DNA subunits in the human genome (1). As a result, the number of human genes was estimated to be 20,000–25,000 (2). Accordingly the next challenge is to interpret the function of human genes genome-wide. This would be possible by a large-scale functional genomics study

E. Palmer (ed.), *Cell-Based Microarrays*, Methods in Molecular Biology 706,
DOI 10.1007/978-1-61737-970-3_15,

in which individual genes are overexpressed or silenced in living cells. For this challenge, we need a novel method that allows efficient transfection of a large panel of plasmids or siRNAs separately into cells in a high-throughput manner.

Transfection microarrays have been developed by several research groups (3–10). In this technology, a panel of plasmids or siRNAs is arrayed on a small chip and then cells are directly plated onto the array for transfection. In many cases, transfection is promoted by complexing nucleic acids with a cationic lipid enhancer. However, the efficiency of transfection is limited and, more importantly, transfection cannot be temporally controlled. The method (11–17) that uses electric pulses to trigger the transfection of plasmids or siRNAs permits more efficient and temporally controlled transfection on a chip.

This chapter introduces the method for electroporation of cells with plasmids or siRNAs on a micropatterned electrode chip. Protocols are described for overexpression of enhanced green fluorescent protein (EGFP) and silencing of endogeneous EGFP gene by siRNA. These examples help establish an experimental setup for the parallel transfer of multiplexed plasmids or siRNAs. The protocols described here assume the use of specific apparatuses that we have used (thermal evaporator, ultraviolet lamp, fluorescence microscope, imaging software, etc.), but are not restricted to them if similar experimental conditions can be achieved.

2. Materials

2.1. Plasmids and siRNAs

1. pEGFP-C1 and pd2EGFP-N1 (both from Clontech Laboratories, Palo Alto, CA) that code EGFP and destabilized EGFP, respectively, under the control of a cytomegalovirus promoter (*see* **Note 1**).
2. Synthetic siRNA specific for EGFP (EGFP–siRNA): sense: 5′-GCAAGCUACCCUGAAGUUCAU-3′, antisense: 5′-GAACUUCAGGGUCAGCUUGCC G-3′ (Qiagen, Hilden, Germany). Non-specific siRNA (control–siRNA): sense: 5′-UUCUCCGAACGUGUCACGUdTdT-3′, antisense: 5′-ACGUGACACGUUCGGAGAAdTdT-3′ (Qiagen). The control–siRNA is used as a negative control.

2.2. Cell Culture

1. Human embryonic kidney cells (HEK293) can be obtained from, for example, Health Science Research Resources Bank, Tokyo, Japan (*see* **Note 2**).
2. HEK293 cells stably transformed with pd2EGFP-N1 (*see* **Note 3**).

3. Minimal essential medium (MEM) (Invitrogen) supplemented with 10% heat-inactivated fetal bovine serum (FBS), 100 U/ml penicillin, and 0.1 mg/ml streptomycin.

2.3. Preparation of Plasmid- or siRNA-Loaded Electrodes

1. Glass plate (24 mm × 26 mm × 1.5 mm) (Matsunami Glass Ind., Ltd, Osaka, Japan). Standard glass slides cut into the above size are also suitable.
2. Piranha solution (concentrated sulfuric acid: 30% hydrogen peroxide solution = 7:3 by volume) (*see* **Note 4**).
3. Thermal evaporator (V-KS200, Osaka Vacuum Instruments, Osaka, Japan) used for depositing a thin layer of chromium and gold onto glass plates.
4. 1-Hexadecanethiol (Tokyo Kasei Kogyo Co., Tokyo, Japan) dissolved in ethanol to a concentration of 1 mM. The solution should be made fresh as required.
5. Methoxypoly(ethylene glycol) thiol (SUNBRIGHT ME-050SH, Mw = 5,000, NOF Corp., Tokyo, Japan) dissolved in a 1:6 mixture of water and ethanol. The solution should be made fresh as required.
5. Quartz-based chromium photomask with an array of tiny windows.
6. Ultra-high-pressure mercury lamp (500 W, Optical Modulex SX-UI500HQ, Ushio, Inc., Osaka, Japan).
7. 11-Mercaptoundecanoic acid (Aldrich Chemical Co.) dissolved in ethanol to a concentration of 1 mM. The solution should be made fresh as required.
8. Branched poly(ethyleneimine) (PEI) (Aldrich) with an average molecular weight of 800–2,000. PEI is dissolved in phosphate buffered saline (PBS) to a concentration of 1% (w/v). The solution is adjusted to pH 7.4 with HCl solution and stored at 4°C.

2.4. Determination of Loaded Plasmid and siRNA

1. Rhodamine-conjugated plasmid DNA (pGeneGrip^{TM} Rhodamine/GFP, Gene Therapy Systems, Inc., San Diego, CA).
2. EGFP–siRNA conjugated with rhodamine at the 3′ end (EGFP–siRNA–Rho): sense: 5′-GCAAGCUGACCCUGAAGUUCAU-3′, antisense: 5′-GAACUUCAGGGUCAGCUUGCCG-3′ (Qiagen).
3. Fluorescence microscope (MZ FLIII fluorescence stereomicroscope, Leica) equipped with a cooled-CCD camera (ORCA-ER, Hamamatsu Photonics K.K., Shizuoka, Japan).
4. AQUALite digital imaging software (Hamamatsu Photonics).

3. Electroporation

1. Electroporation setup (**Fig. 15.1**) connected to a pulse generator (ElectroSquare-Porator T820, BTX, San Diego, CA or Gene Pulser Xcell, Bio-Rad, Hercules, CA).
2. Standard cell-culture facility with CO_2 incubator, laminar flow clean bench, autoclave, centrifuge, etc.
4. 70% Ethanol solution for disinfecting.
5. Sterilized and cooled PBS.
6. Inverted fluorescence microscope (BX-51, Olympus, Tokyo, Japan).

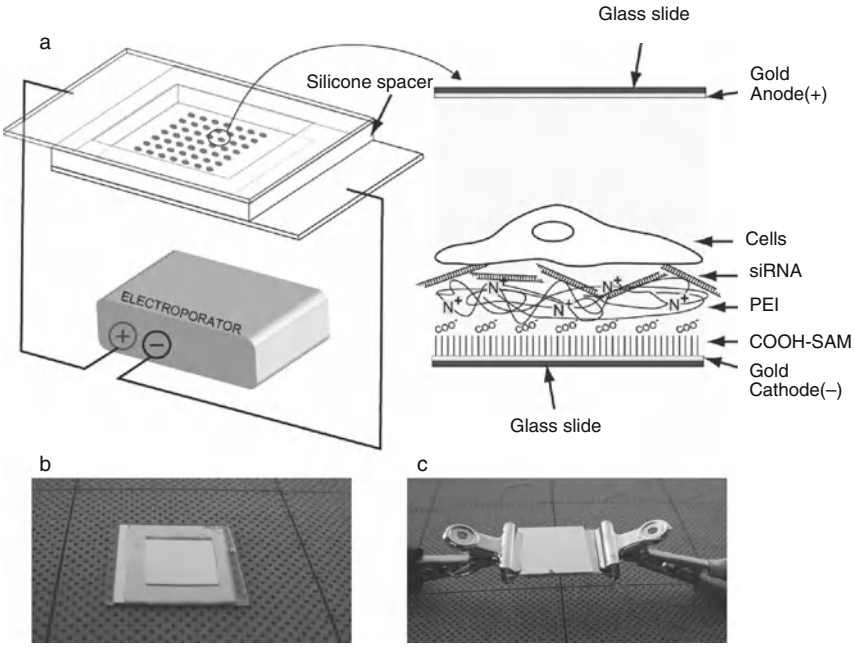

Fig. 15.1. (**a**) Schematic drawings of the electroporation setup. Drawings are not to scale. Photographs of (**b**) a basement electrode with a silicone frame and (**c**) basement and upper electrode connected to a pulse generator. Reproduced from Fujimoto et al. (16) with permission from Springer ©2008.

4. Methods

4.1. Preparation of Plasmid- or siRNA-Loaded Electrodes

1. A glass plate is treated with a Piranha solution at room temperature for 5 min to remove impurities. The cleaned glass plate is thoroughly washed with deionized water and

2-propanol, and dried under a stream of nitrogen gas (*see* **Note 5**).

2. A thin primer layer of chromium (thickness: 1 nm) is deposited onto the glass surface, and then a gold layer (thickness: 19 nm) is further deposited on top of the chromium layer in a continuous process using a thermal evaporator operated at a pressure of 3–4 $\times$ 10^{-4} Pa (*see* **Note 6**).
3. Immediately after deposition, the plate is immersed in 1 mM 1-hexadecanethiol solution at room temperature for 24 h to form a self-assembled monolayer (SAM) of the alkanethiol on the gold-evaporated glass plate. Alternatively, methoxypoly(ethylene glycol) thiol is used for the preparation of a cell-repelling SAM. The plate is then washed with ethanol and water, and dried under a stream of nitrogen gas.
4. The photomask is overlaid onto the surface of the SAM, and then the monolayer surface is irradiated by UV light through the photomask from a ultra-high-pressure mercury lamp at a distance of 20 cm under atmospheric condition for 2 h. The irradiated plate is then washed with ethanol and water to remove photo-cleaved alkanethiols (*see* **Note 7**).
5. Immediately after the above procedure, the plate is immersed in 1 mM 11-mercaptoundecanoic acid solution at room temperature for 3 h to form a COOH-terminated SAM within the gold spots. Then the glass plate is washed with ethanol to remove unreacted alkanethiols (*see* **Note 8**).
6. An aliquot of PEI solution is manually applied to the carboxylic acid-terminated spots ($\sim$0.2 μl per spot) and the solution is kept for 30 min at room temperature to electrostatically adsorb PEI to the spots. Then, the plate is washed with water to remove weakly adsorbed PEI, disinfected with 70% ethanol and air-dried in a sterile laminar flow hood (*see* **Note 9**).
7. A sterilized solution of plasmid or siRNA (50 μg/ml) in PBS (pH 7.4) is applied to the cationic polymer-modified spots and allows for the adsorption of plasmid or siRNA for 2 h at room temperature. The resulting plasmid- or siRNA-loaded glass plate is extensively washed with PBS and used for later experiments without drying (*see* **Note 10**).

4.2. Determination of Loaded Plasmid and siRNA

1. To determine the amount of plasmid loaded on the electrode surface, pGeneGrip^{TM} rhodamine/GFP is loaded by the same procedure as described above but in the dark, and visualized with a fluorescence microscope equipped

with a cooled-CCD camera. In the case of siRNA-loaded electrodes, EGFP–siRNA–Rho is used.

2. Fluorescence intensity is determined on a plasmid- or siRNA-loaded spot using the imaging software and converted to their loading amounts using calibration curves that are obtained by depositing the plasmid or siRNA of known amounts on the PEI-adsorbed gold surface (*see* **Note 11**).

4.3. Electroporation

1. A sterilized silicone frame (**Fig. 15.1a**) is attached to the plasmid- or siRNA-loaded electrode to confine the cell-culture region.
2. A suspension of HEK293 cells is transferred within the silicone frame at a density of 45,000 cells/cm^2 for plasmid-loaded electrode or 60,000 cells/cm^2 for the siRNA-loaded electrode.
3. The plate is placed in a polystyrene cell-culture dish. MEM containing 10% FBS, 100 U/ml penicillin, and 0.1 mg/ml streptomycin is added to cover the entire surface of the plate. Then, cells are cultured at 37°C under 5% CO_2 atmosphere normally for 24 h to allow for the attachment of cells to the electrode surface (*see* **Note 12**).
4. The plate with cells is carefully washed with PBS, and the inner space of the silicone frame is filled with cold PBS.
5. A counter electrode (gold-evaporated glass plate; **Fig. 15.1**) is placed on the frame with the gold surface down at a distance of 0.5–2 mm (*see* **Note 13**) above the plasmid-loaded electrode. Lower (cathode) and upper (anode) electrodes are connected to a pulse generator.
6. Cells are treated with a single electric pulse at a field strength of 75–260 V/cm for a duration of 10 ms (*see* **Note 14**).
7. After 10-min incubation at room temperature, PBS is replaced with MEM containing 10% FBS, 100 U/ml penicillin, and 0.1 mg/ml streptomycin. Then the cells are further cultured at 37°C under 5% CO_2 atmosphere.
8. Cells are observed 48 h after electroporation using a fluorescence microscope to assess the expression/silencing of EGFP. As an example, photographs of cell chips that display EGFP-expressing cells are shown in **Fig. 15.2** for plasmids and **Fig. 15.3** for siRNAs.
9. For a quantitative study, fluorescent intensity of EGFP is determined for every spot using digital imaging software such as AQUA-Lite (Hamamatsu Photonics).

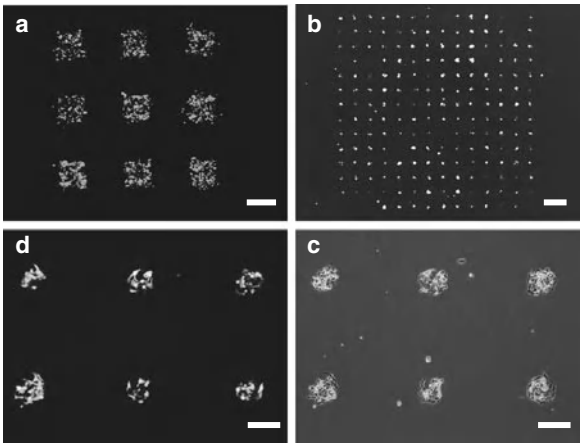

Fig. 15.2. Electroporation of pEGFP-C1 plasmid into HEK293 cells. Cells were seeded on the plasmid-arrayed electrode, cultured for 24 h, and then treated with a single electric pulse at a field strength of 75 V/cm for 10 ms duration. Fluorescence images were acquired 48 h after electric pulsing. (**a**) Fluorescence image showing EGFP expression in the restricted regions of HEK293 cells 48 h after electric pulsing. Note that cells are adhered to the entire surface of the electrode, while fluorescently active cells are observed only in the plasmid loaded square islands. (**b**) Fluorescence image of HEK293 cells transfected on the electrode with a plasmid-loaded island array prepared using the poly(ethylene glycol)-tethering alkanethiol .(**c**) Higher magnification image of (**b**). (**d**) Phase-contrast image of (**c**). Note that cells adhere only on the islands but not on the surrounding regions. Scale bar: (**a**, **b**) 1 mm; (**c**, **d**) 200 μm. Reproduced from Yamauchi et al. (11) with permission from Oxford University Press ©2004.

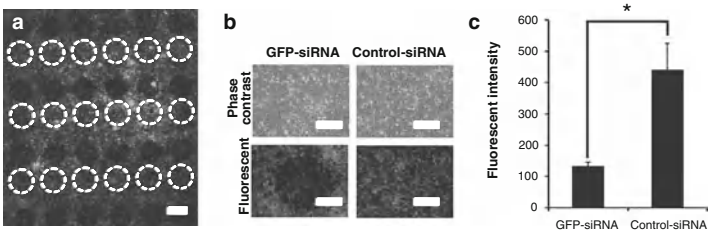

Fig. 15.3. Electroporation of siRNAs into dsEGFP–HEK cells. (**a**) Low-magnification fluorescence image of d2EGFP-HEK cells electroporated on the microarray that displayed 42 spots arrayed in a 6 × 7 matrix. The image was recorded 48 h after electric pulsing at 240 V/cm for 10 ms. GFPsiRNA was loaded to spots (*dark spots*) on odd lines from the *top*; control–siRNA (highlighted with *dashed circles*) was loaded on even lines. (**b**) Higher magnification image of cells in (**a**). Phase-contrast and fluorescence microphotographs are shown for d2EGFP-HEK cells electroporated on the spots with (*left*) GFP–siRNA and (*right*) control–siRNA. Scale bar: (**a**) 1 mm and (**b**) 500 μm. (**c**) Fluorescence intensity of d2EGFP-HEK cells electroporated on the spots with GFP–siRNA and control–siRNA. The fluorescence intensities were determined 48 h after electroporation. The data are expressed as mean ± standard deviation for 12 spots on two independent microarrays. An *asterisk* indicates statistical significance ($p<0.05$) by Student's *t*-test. Reproduced from Fujimoto et al. (16) with permission from Springer ©2008.

5. Notes

1. The plasmids are expanded in *Escherichia coli* and purified using, for example, EndoFree Plasmid Maxi Kit (Qiagen, Hilden, Germany) according to the manufacturer's instruction. The plasmids are dissolved in 10 mM Tris–HCl buffer (pH 8.0) containing 0.1 mM ethylenediamine-*N,N,N′*,N′-tetraacetic acid (EDTA) and stored at –20°C until use.
2. HEK293 cells are routinely maintained in MEM supplemented with 10% FBS, 100 U/ml penicillin, and 0.1 mg/ml streptomycin at 37°C under a 5% CO_2 atmosphere.
3. HEK293 cells stably transformed with pd2EGFP-N1 (d2EGFP-HEK) are obtained by standard lipofection and subsequent selection in the presence of geneticin.
4. It is a hazardous solution and must be handled with care.
5. This chapter assumes the use of gold electrode as a platform for the preparation of transfection microarrays. A transparent electrode made of indium-tin-oxide (ITO) can be used as an alternative substrate (12). In this case, the layer-by-layer assembly of PEI and plasmid DNA is efficient for stable loading and efficient transfection.
6. The thickness of chromium and gold layers can be monitored using a quartz crystal microbalance sensor (Inficon, Leybold AG, Köln, Germany) equipped in a sample chamber.
7. A holder for a glass plate and a photomask helps prevent dislocation of the photomask during UV irradiation. This process produces an array of spots presenting a pristine gold surface. We routinely prepare an array of circular spots with a diameter of 1 mm, to which more than 2,000 cells can adhere. The spot size can be easily reduced down to, for instance, 0.2 mm by changing the design of a photomask, but it must be taken into consideration that too few number of cells affects the reliability of data obtained from a single spot.
8. This process produces an array of spots presenting carboxylic acid-terminated SAM which is surrounded by the methyl-terminated SAM.
9. PEI can be replaced with highly cationic amidoamine dendrimers for the enhancement of electroporation efficiency (15). Modification of PEI-adsorbed surface with carboxylated carbon nanotubes also enhances electroporation efficiency (13).

10. Transfection efficiency is greatly impaired by storage of the plasmid-loaded electrode, due to water evaporation from arrayed plasmids. The addition of monosaccharide (glucose, fructose), disaccharide (trehalose, sucrose), or trisaccharide (raffinose) to a concentration of 10% (w/v) serves to retain transfection efficiency at a reasonably high level after storage for up to 30 days at −20°C (17).
11. In a typical case, loading amounts reach 0.1–0.5 $\mu g/cm^2$ for plasmid DNA and 0.01–0.03 $\mu g/cm^2$ for siRNA.
12. At the moment of electroporation, confluency of 70–80% is recommended. Plasmids are released only when an electric pulse is applied. Depending on the specific purpose, a culture period before electric pulsing can be prolonged up to 72 h without considerable reduction in transfection efficiency.
13. A glass plate with a gold layer (200 nm in thickness) without SAM is used as a counter electrode. Use sterilized tweezers to handle electrodes. The distance between upper and lower electrodes should be optimized for the specific experimental setup.
14. An electric field strength has great influence on transfection efficiency and should be optimized for specific cases.

Acknowledgments

The part of this work was supported by Grants-in-Aid for Scientific Research (No. 15310090), Ministry of Education, Culture, Sports, Science and Technology (MEXT) and Kobe Cluster, the Knowledge-Based Cluster Creation Project, MEXT.

References

1. International Human Genome Sequencing Consortium (2001) Initial sequencing and analysis of the human genome. *Nature* 409, 860–921.
2. Tyers, M., Mann, M. (2003) From genomics to proteomics. *Nature* 422, 193–197.
3. Ziauddin, J., Sabatini, D. M. (2001) Microarrays of cells expressing defined cDNAs. *Nature* 411, 107–110.
4. Kumar, R., Conklin, D. S., Mittal, V. (2003) High-throughput selection of effective RNAi probes for gene silencing. *Genome Res* 13, 2333–2340.
5. Mousses, S., Caplen, N., Cornelison, R., Weaver, D., Basik, M., Hautaniemi, S., Elkahloun, A. G., Lotufo, R. A., Choudary, E. R., Suh, E., Kallioniemi, O. (2003) RNAi microarray analysis in cultured mammalian cells. *Genome Res* 13, 2341–2347.
6. Yamauchi, F., Kato, K., Iwata, H. (2004) Micropatterned, self-assembled monolayers for fabrication of transfected cell microarrays. *Biochim Biophys Acta* 1672, 138–147.
7. Yoshikawa, T., Uchimura, E., Kishi, M., Funeriu, D. P., Miyake, M., Miyake, J. (2004) Transfection microarray of human

mesenchymal stem cells and on-chip siRNA gene knockdown. *J Control Release* 96, 227–232.
8. Fujimoto, H., Yoshizako, S., Kato, K., Iwata, H. (2006) Fabrication of cell-based microarrays using micropatterned alkanethiol monolayers for the parallel silencing of specific genes by small-interfering RNA. *Bioconjug Chem* 17, 1404–1410.
9. Fujimoto, H., Kato, K., Iwata, H. (2008) Use of microarrays in transfection of mammalian cells with dicer-digested small interfering RNAs. *Anal Biochem* 374, 417–422.
10. Yamauchi, F., Okada, M., Kato, K., Martin, J. L., Iwata, H. (2007) Array-based functional screening for genes that regulate vascular endothelial differentiation of flk1-positive progenitors derived from embryonic stem cells. *Biochim Biophys Acta* 1770, 1085–1097.
11. Yamauchi, F., Kato, K., Iwata, H. (2004) Spatially and temporally controlled electroporation of adherent cells on plasmid DNA-loaded electrode. *Nucleic Acids Res* 32, e187.
12. Yamauchi, F., Kato, K., Iwata, H. (2005) Layer-by-layer assembly of poly(ethyleneimine) and plasmid DNA onto transparent indium-tin oxide electrodes for temporally- and spatially-specific gene transfer. *Langmuir* 21, 8360–8367.
13. Inoue, Y., Fujimoto, H., Ogino, T., Iwata, H. (2008) Site-specific gene transfer with high efficiency onto a carbon nanotube-loaded electrode. *J R Soc Interface* 5, 909–918.
14. Njatawidjaja, E., Iwata, H. (2008) Gene delivery to cells on a miniaturized multiwell plate for high-throughput gene function analysis. *Anal Bioanal Chem* 392, 405–408.
15. Koda, S., Inoue, Y., Iwata, H. (2008) Gene transfection into adherent cells using electroporation on a dendrimer-modified gold electrode. *Langmuir* 24, 13525–13531.
16. Fujimoto, H., Kato, K., Iwata, H. (2008) Electroporation microarray for parallel transfer of small interfering RNA into mammalian cells. *Anal Bioanal Chem* 392, 1309–1316.
17. Fujimoto, H., Kato, K., Iwata, H. (2009) Prolonged durability of electroporation microarrays as a result of addition of saccharides to nucleic acids. *Anal Bioanal Chem* 393, 607–614.

Chapter 16

Microfluidic Image Cytometry

Ken-ichiro Kamei, Jing Sun, Hsian-Rong Tseng, and Robert Damoiseaux

Abstract

Cell-based arrays offer powerful tools for genomics/proteomics and drug discovery, and are widely applicable for most cell lines. However, it is challenging to apply cell-based arrays for in vitro diagnosis due to limited amount of patient samples. Here, we utilized and demonstrated microfluidic image cytometry (MIC), capable of quantitative, single-cell profiling of multiple signaling molecules using only 300–3,000 cells from clinical brain tumor specimens for in vitro molecular diagnosis. First, we characterized the PI3K/AKT/mTOR pathway, which is often over-activated in the brain tumors, in U87 brain tumor cell lines by measuring EGFR, PTEN, pAKT, and pS6 with a MIC platform, and applied this measurement to clinical brain tumor specimens. In conjunction with statistical analysis, we were able to characterize extensive inter- and intra-tumoral molecular heterogeneity.

Key words: Microfluidic image cytometry, molecular diagnosis, glioblastoma, Pi3k signaling pathway, immunofluorescence, biostatistics.

1. Introduction

Cell-based arrays consist of printed siRNA and cDNA in an expression vector or even lentiviruses which are then overlaid with cells. The cells take up the material and the array of manipulated cells can be then used for experiments to study gene function or even for drug discovery. Cell-based arrays have the capability to overcome some of the biggest limitations one frequently encounters in research: sample size, economy, and to some extent throughput. As with other functional genomics techniques, high content screening (HCS) (1–4) is typically the readout of choice, since it is possible to acquire data on a per-cell basis which is

E. Palmer (ed.), *Cell-Based Microarrays*, Methods in Molecular Biology 706,
DOI 10.1007/978-1-61737-970-3_16,

vital in this case as only a few hundred—or fewer—cells per array member are present.

For most applications, much more cell material is available than cell-based arrays require, with one exception: personalized medicine. Here, extremely small sample sizes—typically gained from tumors—are rather the rule than the exception. In fact, the sample size is so small that traditional cell-based arrays which rely on plating tens of thousands of cells on top of the array cannot be used. This excludes potentially life-saving testing of anticancer drugs on patient samples. However, by marrying cell-based array technology and microfluidics, it is possible to generate a novel kind of platform called microfluidic image cytometry (MIC) (5, 6), which enables cell-based experiments on a sub-microliter scale using only electric hand-held pipetters and other laboratory readily available items. The resulting platform offers advantages in specimen economy, reduced reagent consumption, improved reproducibility and sensitivity, and multi-parameter measurement capabilities using HCS, self-organizing maps, and thus signaling pathway analysis. In this chapter, we will focus on the problem of how to apply microfluidic cell-based arrays to clinical samples. We will cover how MIC chips are constructed, optimization of immunohistochemistry, use of the MIC arrays, and mining of the resulting data using self-organizing maps. We will use clinical brain tumor samples as a real-life example and show the advantages of using microfluidic arrays compared to traditional techniques such as western blotting.

2. Materials

2.1. Fabrication of a Cell-Array Chip

1. Poly(dimethylsiloxane) (PDMS) precursors (Sylgard 184, Dow Corning).
2. Poly-L-lysine (PLL)-coated glass slide (Polysciences, Inc., Philadelphia, PA).
3. PDMS Mixer (Phoenix Equipment Inc., Rochester, NY).
4. Spin coater (Laurell Technologies Corp., North Wales, PA).

2.2. Human Tumor Specimen Preparation

1. DMEM/F12 (Invitrogen).
2. Percoll (GE Healthcare) is diluted with a HEPES buffer (0.2 M HEPES, 0.8 M NaCl, and 1 M glycerol).
3. 40-μm single-cell strainer (BD Falcon).
4. Matrix 12-channel electronic multi-channel pipette, 0.5–12.5 μl (Thermo Fisher Scientific).

2.3. On-Chip Cell Culture

1. Human glioblastoma cell line U87-MG (American Type Culture Collection).
2. U87 isogenic cell lines (7) (U87-PTEN, U87-EGFR, U87-PTEN EGFR).
3. Dulbecco's modified eagle's medium (DMEM) (Invitrogen).
4. Penicillin/streptomycin (PS, MP Biomedicals, Solon, OH).
5. Culture medium: DMEM supplemented with 10% FBS (Lonza) and 1% PS.
6. TrypLE Express (Invitrogen).

2.4. On-Chip Immunocytochemistry (ICC)

1. 4% PFA fix solution: 16% paraformaldehyde (PFA, Electron Microscopy Sciences, Hatfield, PA) is diluted with PBS. Store at 4°C.
2. *N*-doceyl-β-maltoside (DDM): (Pierce, Rockford, IL) dissolve in ddH_2O at 5% as stock solution. Store at –20°C.
3. Normal goat serum (NGS, Jackson ImmunoResearch, West Grove, PA). Store at 4°C.
4. Blocking solution: 10% NGS, 3% bovine serum albumin (BSA) Sigma-Aldrich, 0.1% DDM in PBS. Store at 4°C.
5. 4′,6-diamidino-2-phenylindole, dihydrochloride (DAPI) (Invitrogen): dissolve at 300 nM in PBS. Store at –20°C.
6. Antibodies: PE-conjugated anti-PTEN (BD Biosciences), anti-epidermal growth factor receptor (EGFR, BD Pharmingen), Alexa Fluor 647-conjugated anti-pAKT (Cell Signaling Technology), and Alexa Fluor 488-conjugated anti-pS6 (Cell Signaling Technology). Anti-EGFR is conjugated with LiCOR/HiLyte Fluor 750 labeling kit (Dojindo Molecular Technologies, Inc., Rockville, MD) following manufacturer's protocol.
7. Antibody cocktail: 2.8 μg/ml anti-EGFR labeled with LiCor/HiLyte Fluor 750, 0.63 μg/ml PE-conjugated anti-PTEN, 1.25 μg/ml Alexa Fluor 647-conjugated anti-pAKT, and 3.8 μg/ml Alexa Fluor 488-conjugated anti-pS6 are diluted with blocking solution for on-chip immunocytochemistry.

2.5. Image Acquisition and Processing

1. For image acquisition, the chip is placed onto a Nikon-TE-2000 inverted fluorescence microscope (Nikon, Melville, NY) with a charge-coupled device (CCD) camera (Cascade II, Photomatrix, Tucson, AZ), X-cite 120 mercury lamp (EXFO, Ontario, Canada), automated stage (Applied Scientific Instrumentation, Eugene, OR), objective lens (Plan Fluor 10X/0.30 Ph1 DL, Nikon), and

filters for five fluorescent channels (W1 (UV excitation, UV-2A, Chroma Technology, Bellows Falls, VT), W2 (Blue excitation, B-2E/C, Chroma Technology), W3 (Green excitation, TRITC, Chroma Technology), W4 (Orange excitation, HYQ-CY5, Chroma Technology), and W5 (Red excitation, LI-COR, Lincoln, NE)). The microscope is placed in a dark room thus preventing light exposure. MetaMorph (Version 7.5.6.0, Molecular Devices, Sunnyvale, CA) is used for microscope control, image acquisition, and processing.

2.6. Optimization and Validation of the MIC Technology Using Brain Tumor Cell-Line Models

1. RIPA buffer (Cell Signaling).
2. BCA protein assay kit (Bio-Rad, Hercules, CA).
3. Enhanced chemiluminescence (ECL) kit (Amersham Bioscience, Piscataway, NJ).
4. Rapamycin (Sigma-Aldrich).
5. Epidermal growth factor (EGF) Sigma-Aldrich.

2.7. Training of Self-organizing Maps (SOMs)

1. *R* (Open source software, http://www.r-project.org/).

3. Methods

The production of miniaturized microfluidic arrays consisting of a plastic upper and a microscopic slide on the lower part is a multi-step process. The first step is the fabrication of the plastic part: the plastic precursors are mixed in the correct ratio and the resulting solution is poured into a mold which has been photolythographically produced. Since cleanliness is essential, the plastic part and the glass slide must be cleaned in oxygen plasma. After this, an adhesive is applied to the plastic and the array can be assembled. The surface of the glass can also be modified with matrigel, for example, to enable culture of human embryonic stem cells. The use of the array is relatively simple. In the case of a tumor sample, the raw material is pre-processed by a pathologist and then dissociated in the lab, first by blade, and then enzymatically. The resulting cell suspension is then applied to the chip using a hand-held pipetter. The cells will attach to the glass part of the array. It is important to change the media on a regular basis, potentially once a day, since the volume of the array is very small, and the media will be depleted more quickly in microfluidic arrays than under standard cell-culture conditions. After the predetermined incubation time, the microfluidic array can be immunohistochemically processed and stained for marker proteins. Finally,

the array is read using a high-content screening system and image analysis software is used to produce single cell measurements. The resulting measurements are used to generate self-organizing maps and for principal component analysis.

3.1. Design and Fabrication of the Cell-Array Chips

A cell-array chip (**Fig. 16.1**) consists of 24 (3 × 8) cell-culture chambers, each with dimensions of 8 μm (l) × 1 μm (w) × 120 μm (h) for a total volume of 960 nl. The cell-array chip is fabricated by directly attaching a polydimethylsiloxane (PDMS)-based microfluidic component onto a commercial poly-L-lysine (PLL)-coated glass slide.

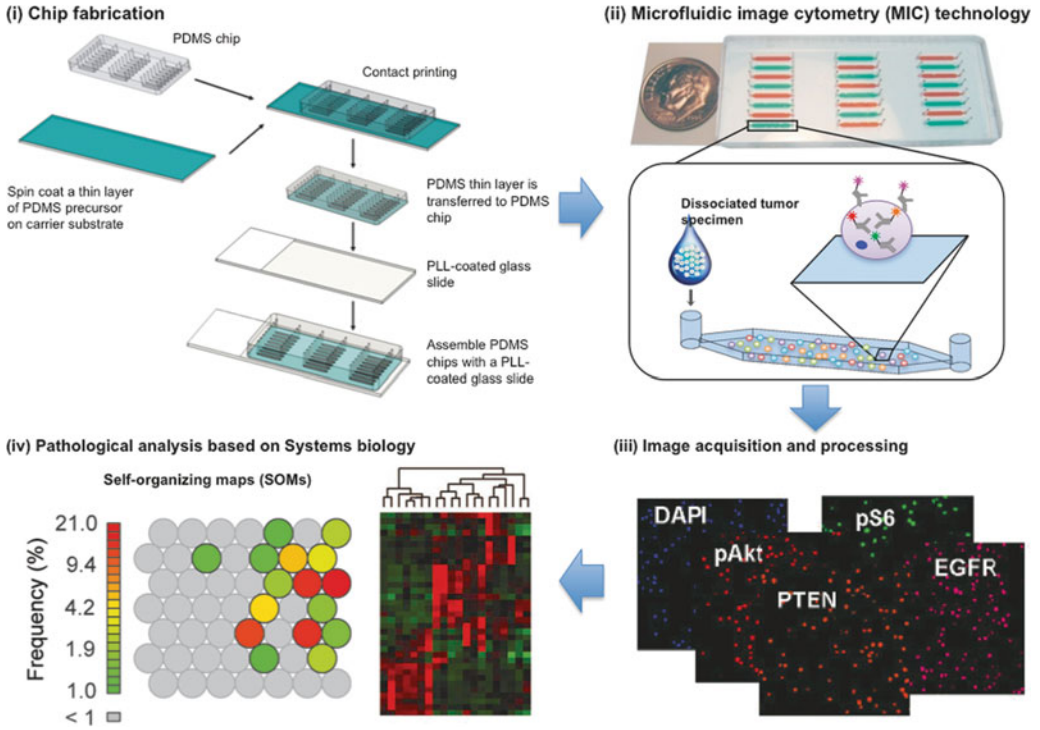

Fig. 16.1. Illustration of the microfluidic image cytometry (MIC) technology combined with a pathology analysis in conjunction with systems biology of clinical brain tumor specimens. (**a**) Fabrication process of a PDMS-based microfluidic cell array. (**b**) A microfluidic cell array chip for accommodating dissociated tumor specimens and performing immunocytochemistry (ICC) and (**c**) image acquisition and cytometry analysis by fluorescent microscopy to quantitatively measure multiple signaling molecules in individual cells. (**d**) Systems pathology analysis using self-organizing maps (SOMs) and hierarchical clustering.

1. The PDMS-based microfluidic component was fabricated using a soft lithography method (8, 9) using a photolithographically fabricated mold. Well-mixed PDMS precursors (Sylgard 184, A:B = 10:1 weight ratio) were poured onto a negative silicon wafer mold of the microchannel patterns. After vacuum degassing and curing at 80°C overnight, the microfluidic component was peeled off the mold, followed by introduction of holes using a hole puncher with pipette

tip size-matched diameters at the ends of the resulting microchannels.

2. To attach the microfluidic component to a PLL-coated glass slide, we prepared a 1–3-μm-thick adhesive PDMS layer by spin-coating a 1:4 mixture of toluene and PDMS precursors (Sylgard 184, A:B = 5:1 weight ratio) onto a glass substrate. Then, the PDMS microfluidic component was put on the PDMS-coated a glass substrate to transfer this adhesive PDMS layer onto the PDMS microfluidic component. This PDMS-based microfluidic component with the adhesive layer was attached onto a PLL-coated glass slide. The assembled chip was then baked in a vacuum oven at 80°C for 24 h.

3.2. Human Tumor Specimen Preparation

1. Patient tumors were brought directly from neurosurgery suites upon resection and placed on ice for rapid portioning by the attending neuropathologist.
2. Tumor portions were washed with PBS, minced to less than 0.5 mm in a diameter with a scalpel blade, and placed in TrypLE enzyme for 15 min at 37°C. TrypLE supernatant was removed and replaced with DMEM/F12 and triturated with three successively smaller bore Pasteur pipettes.
3. To remove cellular debris and red blood cells (RBCs) from tumor specimens, a Percoll purification procedure was used. First, Percoll was mixed with a HEPES buffer at a 9:1 ratio and then mixed this Percoll solution with an equal volume of cells suspended in DMEM/F12. Second, the cell suspension was centrifuged at 1,000×*g* for 5 min. The pellet containing RBCs was discarded, and the supernatant was mixed with the Percoll solution at a 1:2 ratio, followed by centrifugation at 3,000×*g* for 5 min. Third, the pellet containing cellular debris was discarded and the supernatant was diluted with DMEM/F12. Phenotypic comparison of Percoll-purified cell populations under a microscope with unpurified specimens was made to verify that only RBCs and debris were removed during this process.

3.3. On-Chip Cell Culture

The cell culture steps outlined here are identical for standard cell lines as well as primary tissue samples. For simplicity's sake, we outline here the process for standard cell-culture samples only.

1. All liquid/buffer exchanges for on-chip experiments were done using an electrical pipette that regulated dispensing rates and thus protected the cells from shear forces.
2. Prior to cell culture, the cell array chips were sterilized by exposure to UV light for 15 min.
3. U87-MG (America Type Culture Collection, Manassas, VA) and U87 isogenic cell lines (7) (U87-PTEN,

U87-EGFR, U87-PTEN EGFR) were maintained in standard culture medium using standard techniques.

4. Cells from tumor specimens were obtained as described in **Section 3.2**.
5. In preparation for loading into microfluidic cell-culture channels, cell-containing plates were washed with PBS twice, and then exposed to TrypLE (Invitrogen) solution at 37°C for 5 min to harvest cells from the dish. Next, cells were collected into a 15-ml falcon tube and centrifuged at 1,000×*g* for 2 min. Obtained cell pellets were resuspended in culture medium and then filtered through a 40-μm single cell strainer.
6. Using an electrical pipette (0.5–12.5 μl, Thermo Fisher Scientific) capable of handling precise volume and flow rates, 2 μl of cell suspension at a density of 250–500 cells/μl was filled into the tip.
7. The tip filled with the cell suspension was gently inserted into the inlet of the cell array chip. At this step, we need to avoid the contamination of air bubbles in the cell-culture chambers. The air bubbles in the chamber cause cell damage.
8. The solution was dispensed into each cell culture channel at 6 μl/s using an electrical pipette.
9. Chips loaded with cells were subjected to a centrifugation (1,000×*g*, 1 min) to facilitate cell attachment (*see* **Note 1**).
10. Chips were then placed in a 10-cm petri dish with 3 ml ddH_2O to maintain humidity and placed in 5% CO_2, 37°C incubator for 15 min prior to on-chip ICC.

3.4. On-Chip Immunocytochemistry (ICC)

1. After cell culturing in the chip, cells were washed with PBS and then fixed with 4 μl of the fix solution for 15 min at room temperature (RT).
2. Following washing with 4 μl of PBS, cells were permeabilized with 4 μl of PBS added with 0.3% Triton X-100 for 15 min at RT.
3. After permeabilization, cells were washed with 4 μl of PBS and then treated with blocking solution for 12 h at 4°C.
4. A cocktail of all fluorophore-conjugated antibodies (2.8 μg/ml anti-EGFR labeled with LiCor/HiLyte Fluor 750, 0.63 μg/ml PE-conjugated anti-PTEN, 1.25 μg/ml Alexa Fluor 647-conjugated anti-pAKT, and 3.8 μg/ml Alexa Fluor 488-conjugated anti-pS6. *see* **Section 2.4**) was freshly prepared by dilution in blocking solution while preventing light exposure and used.
5. 4 μl of antibody cocktail was loaded into each chamber and incubated for 12 h at 4°C.

6. After immunostaining, cells were washed with 4 μl of PBS-T twice for 15 min at RT. This washing step is the most important to avoid high background signal in each staining and obtain reproducible data for further analysis. At this step, we can evaluate the background signals by using the fluorescence microscope. If individual chambers on a chip have higher than average background signals, we can repeat this washing step to reduce the background signal.
7. Cells were treated with 4 μl of DAPI solution (300 nM DAPI) for 30 min at RT followed with PBS rinse prior to HCI.
8. Chips can be stored at 4°C for a week without any signal loss.

3.5. Image Acquisition and Processing

Since the foundation of the microfluidics array is a standard-size microscope slide, various platforms can be used to acquire the images. A standard inverted microscope with fluorescence capabilities and a camera will suffice. The image acquisition process could also be automated with an Image Xpress high-content screening system by simply using the slide adaptor and defining the array as well. For statistical reasons, it is suggested to image each channel on the microfluidics array entirely in order to collect data from the maximal number of cells.

1. For image acquisition, the chip is placed onto a Nikon TE-2000 inverted fluorescence microscope.
2. For image acquisition for quantitative ICC for U87 cell lines, the exposure times are 50 ms for W1 (DAPI), 0.2 s for W2 (pS6), 0.1 s for W3 (PTEN), 2 s for W4 (pAKT), and 10 s for W5 (EGFR) with a 10× objective lens.
3. For tumor specimens, the exposure times were identical except 1 s for PE and 0.5 s for W2 (pS6).
4. Collections of images of five fluorescence channels for signaling nodes (DAPI, EGFR, PTEN, pAKT and pS6) were acquired.
5. Following image acquisition, MetaMorph is used to quantify fluorescent signals in individual cells.
6. The "multi-wavelength cell scoring" module of the MetaMorph software allowed image analysis for scoring cells based on fluorescence images of four fluorophore-labeled antibodies.
7. Background signals in each image were subtracted. First, a lowest signal value in each image was measured. This is the background signal in the image. Second, all fluorescence values of individual pixels in the entire image were subtracted with the background signal value. The new

image which has "0" value as the lowest signal in the image was generated through this procedure.

8. Nuclear images of DAPI staining were segmented to identify all cells in the images.
9. For the remaining four channels (PTEN, pAKT, pS6 and EGFR), a maximum and minimum thresholds of fluorescent intensity for individual channels were set.
10. The cell-segmentation for individual cells was then based on the staining for the four marker proteins.
11. We measured fluorescence intensities in a stained cell area for each fluorescent channels on a per-cell basis.

3.6. Optimization and Validation of the MIC Technology Using Brain Tumor Cell-Line Models

In order to detect proteins or phosphorylation thereof in a primary tissue sample in a reliable manner, it is necessary to optimize the detection, first using controls of which protein contents and phosphorylation state are known. Here, we have used U87 cell lines which have been either engineered to overexpress the target protein or treated with a stimulant in order to activate the desired pathway. The controls can be validated using a western blot.

1. To optimize ICC and microscopy-based cytometry protocols for reproducible quantification of expression/phosphorylation levels of EGFR, PTEN, pAKT, and pS6, first, we prepared sets of negative and positive controls for each signaling protein described below (**Fig. 16.2**).

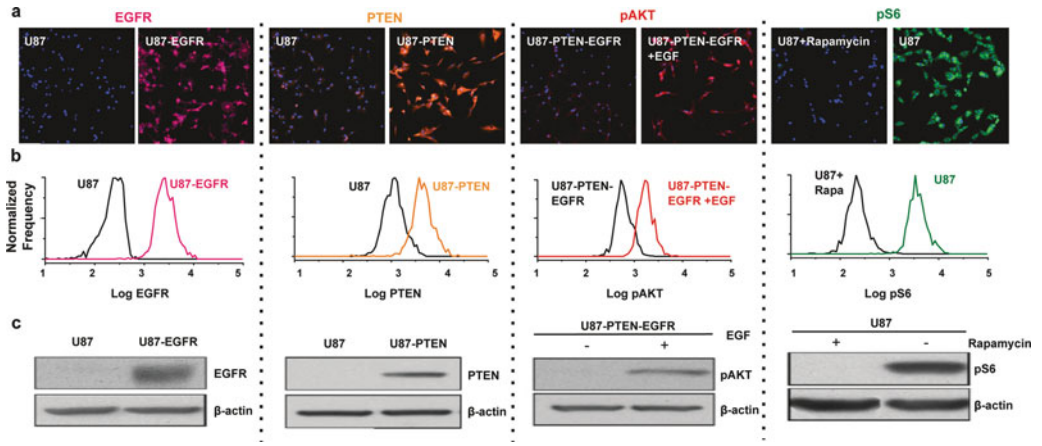

Fig. 16.2. Optimization and validation of the MIC technology using brain tumor cell-line models. Four pairs of controlled cell lines and treatments (U87 vs. U87-EGFR, U87 vs. U87-PTEN, serum-starved U87-PTEN-EGFR vs. EGF-treated U87-PTEN-EGFR, and rapamycin-treated U87 vs. U87) were employed to optimize and determine the dynamic range of the MIC technology to quantify EGFR, PTEN, pAkt, and pS6 levels in individual cells. (**a**) Fluorescent micrographs of immunocytochemically analyzed cells. (**b**) Based on ICC images, immunofluorescent intensities in individual cells are quantified, and then, histograms were generated to determine the dynamic ranges of the MIC measurements. (**c**) The MIC data were validated with Western blotting analysis.

(i) EGFR staining optimization: U87 cells were used as a negative control of EGFR staining due to low expression of EGFR. U87-EGFR cells were used as a positive control due to overexpression of EGFR.

(ii) PTEN staining optimization: U87 cells were used as a negative control of PTEN staining due to no expression of PTEN. U87-PTEN cells were used as a positive control due to overexpression of PTEN.

(iii) pAKT staining optimization: serum-starved U87-PTEN-EGFR cells were used as a negative control due to very low phosphorylation levels of AKT due to serum starvation. EGF-treated U87-PTEN-EGFR cells were used as a positive control due to high phosphorylation levels of AKT due to EGF stimulation.

(iv) pS6 staining optimizaton: rapamycin-treated U87 cells were used as a negative control because rapamycin inhibits phosyphorylation of S6 by mTOR. U87 cells were used as a positive control because of high phosphorylation levels of S6 (*see* **Note 2**).

2. We titrated antibody concentrations of ICC for each signaling protein in the range from 0.05 to 5 μg/ml. After image acquisition, fluorescence signals of each signaling protein in individual cells were quantified, and then fluorescent intensity histograms for the cells were generated.
3. The optimal antibody concentrations for each signaling protein were determined by choosing the antibody concentrations which showed robust reproducibility and the biggest difference of mean values between negative and positive controls.
4. For control purposes, a traditional Western blot was performed. Cells cultured in a 10-cm dish were washed twice with 4 ml of PBS and then lysed with RIPA buffer. After centrifugation to remove the insoluble fractions from cell lysates, the lysates were assayed for protein concentration using the BCA protein assay kit. Twenty μg/ml of proteins was loaded and separated in 10% SDS polyacrylamide gels, then transferred to nitrocellulose membranes, and subjected to immunoblotting. Detection of immunoreactive bands was examined using the ECL kit.

3.7. Training of Self-organizing Maps (SOMs)

SOMs are a two-dimensional representation of a multi-dimensional dataspace. The multi-dimensional dataspace is projected into a two-dimensional plane and objects with similar properties are clustered closely together. This allows for the identification of expression/phosphorylation profile clusters thus allowing the stratification of sub-populations of cells with similar

expression profiles. Thus, it also has applications for evaluating clinical samples and might allow staging of cancers in the future. The use of these self-organizing maps is two-staged: First, a set of data with known properties (our data from the four different U87 cell lines in the presence of serum or rapamycin in duplicate) is used to train the software and allow for proper setup. In the second step, individual samples from the compendium are used to train the SOM subjected to the SOM analysis (*see* **Section 3.8**).

1. Each member of the SOM used here contains the information from four parameters (EGFR, PTEN, pAKT, and pS6) which are ordered into a two-dimensional grid of 7×7 members. The SOMs were created in *R* using the *Kohonen* package (10).
2. Before SOM training, all the measurements were normalized into a frequency. (That is how often a cell with any given combination of signal for each marker protein is present.)
3. For SOM training, "som" function in *Kohonen* package is used for the input dataset.
4. The codebook vectors are then randomly initialized based on the input data and subjected to a training process that involves repeated presentation of the training data to the SOM.
5. Each presented piece of data is assigned to a "winning" (or most similar) grid, and the codebook vector of the winning grid is updated using a weighted average, where the weight is the learning rate α (here 0.05).
6. Because each training process involves random initialization of the codebook vectors and thus distinct map topologies emerge, three SOMs were trained for each dataset, and the resulting maps were examined for qualitative consistency. **Figure 16.3a** shows the resulting SOM grid used for analysis (*see* **Note 3**).

3.8. Using SOMs for Analysis

After the training, the individual samples can then be mapped to the SOM to indicate which portion of the parameter space is occupied by the individual sample.

1. The normalized data for each chamber on the MIC array were subjected singly to the SOM map. The cellular signaling difference among U87 cell lines (U87, U87-EGFR, U87-PTEN, U87-PTEN-EGFR) under two conditions (with serum or rapamycin) using SOM analysis.
2. The resulting fingerprint for each sample is shown in **Fig. 16.3b**.

Results: EGFR and PTEN expression in each cell line did not change between serum and repamycin treatments. Comparing the signaling signatures in U87 cell lines treated with serum or

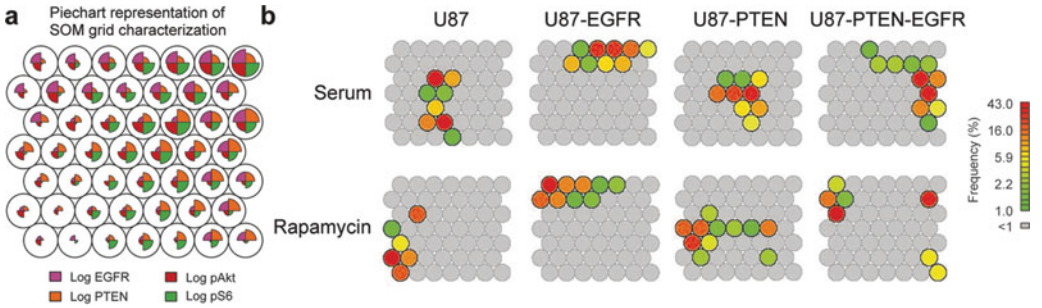

Fig. 16.3. Characterization of U87 cell lines by multi-parameter SOM analysis reveals a diversity of signaling phenotypes. (**a**) Pie chart representation of the code vectors in a 7×7 SOM. Using ~40,000 single-cell four-parameter measurements of EGFR, PTEN, pAkt, and pS6 from U87 cell lines, we trained a SOM analysis brain tumor cell lines. Each grid of the SOM is represented by a vector with characteristic values for EGFR, PTEN, pAkt, and pS6, termed the codebook vector for that grid. To visually represent how these vectors vary over the SOM grid, each grid is divided into quadrants, and the size of the color-coded quadrant represents the intensity of the indicated stain in that grid. (**b**) SOM mappings for U87 cell lines after various treatments. Each dataset of U87 cells under the indicated conditions was mapped onto the SOM. By examination of each map, it is possible to see how each treatment affected the cell lines. For example, rapamycin treatment universally shifted the regions of highest density to the left and lower right-hand corner of the SOM grid, which are the regions with low pS6 expression, as shown in (**a**).

rapamycin, rapamycin treatment usually shifted the regions of highest density to the left and lower right-hand corner of the SOM grid, which are the regions with low S6 phosphorylation, as shown in **Fig. 16.3a**, **b**. We could not observe a big difference in pAKT levels between these treatments, since rapamycin inhibited mTOR which was downstream of pAKT in the pathway. The resulting fingerprints are consistent with the anticipated results.

3.9. Using SOMs to Analyze Patient Samples

We used the same training method for the SOMs as above in order to generate an SOM. We used a total of 19 patient tumor bulk samples and measured the same four marker proteins as above in duplicate. For one sample, we also had a tumor margin sample which we profiled as well.

1. The SOM map was trained using all 19 samples as in **Section 3.7**). The resulting SOM can be seen in **Fig. 16.4a** as a pie chart and in **Fig. 16.4b** as a heatmap.
2. First, we used a tumor containing tumor bulk and surrounding margin.
3. **Figure 16.4a** represents pie charts of the four-parameter vectors characterizing the SOM grid for clinical patient samples. Each grid is represented by a vector with characteristic values for EGFR, PTEN, pAkt, and pS6. **Figure 16.4b** represents heatmaps for individual parameter vectors of SOM grid characteristics.
4. Analyzing (*see* **Section 3.8**) the sample of the patient for which we obtained tumor bulk and margin samples, the SOM analysis revealed that the tumor bulk occupied a

significantly larger number of SOM grids than the margin, indicating greater phenotypic heterogeneity within the tumor bulk (**Fig. 16.4c**). Based on this SOM analysis, we found that the major difference between the tumor and shared regions was higher pS6 levels in the tumor bulk.

5. To further quantify the overlap between the tumor bulk and margin, we designated each SOM grid as bulk, shared, or margin, and compared the percentage of cells mapped to each region. Whereas 86% of margin cells mapped to the shared region, the tumor bulk was divided between the shared and tumor regions (45% and 48%, respectively, **Fig. 16.4d**), suggesting that the tumor bulk contains cells from the tumor margin. Examining the SOM grids that are unique to the tumor, the major difference between the tumor and shared regions was significantly higher pS6 levels in the tumor bulk (*see* **Note 4**).
6. When analyzing various tumor specimens, large diversity of signaling phenotypes is found. **Figure 16.4e** shows SOM mappings of brain tumor specimens of the three different types and homogeneous, heterogeneous, or bimodal distributions. For the bimodal tumor, we plotted a histogram of the single-cell PTEN expression levels to demonstrate the bimodal nature of PTEN expression in this sample, suggesting that two clones or sub-populations differing in PTEN expression co-exist within these tumors. Thus, SOMs can serve as a technique for stratification of multi-parameter, single-cell MIC measurements of clinical brain tumor specimens.

3.10. Summary

In summary, we present microfluidic image cytometry (MIC) as an enabling technology taking cell-based arrays to the next level. We demonstrated that this technology requires about 10–100-fold less material than a standard western blot and allows for HCI analysis in individual cells from solid tumors. This analysis modality allows for pathway analysis of standard cell culture as well as clinical samples. First, using only 300–3,000 cells per chip chamber of the brain tumor cell line U87 and isogenic control cell lines (U87-PTEN, U87-EGFR, and U87-EGFR-PTEN), we validated the MIC platform and data analysis. We characterized the PI3K/AKT/mTOR pathway in these cell lines by measuring EGFR, PTEN, pAKT, pS6 and applied the measurement of the same analytes to clinical brain tumor specimens. Then, we adapted SOM analysis to characterize extensive inter- and intra-tumoral phenotypic heterogeneity. Because of the assay's flexible nature, we envisioned rapid clinical application to other tumor types and/or signaling pathways, as well as intra- and inter-patient comparison of molecular endpoints pre- and post-treatment using

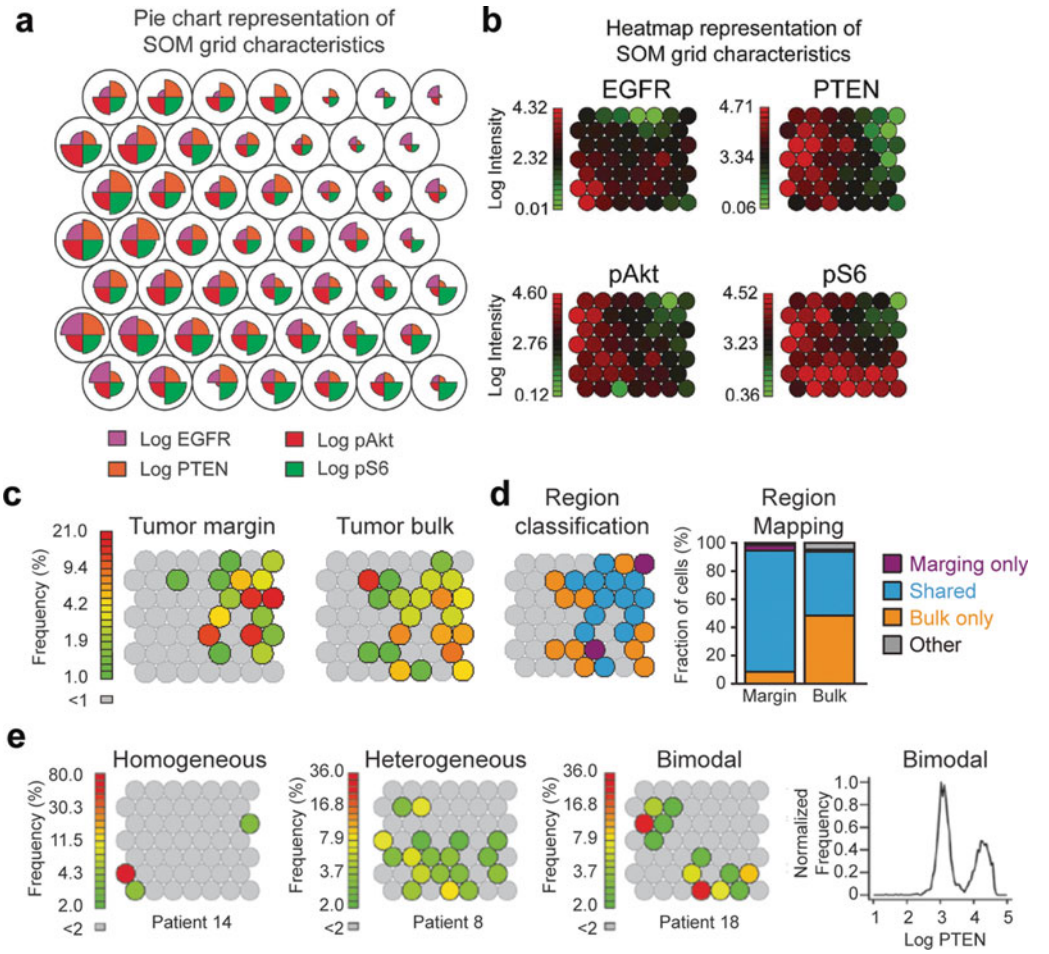

Fig. 16.4. Brain tumor characterization by SOM analysis. (**a**) Pie chart representation of the code vectors in a 7×7 SOM based on patient samples. Each grid of the SOM is represented by a vector with characteristic values for EGFR, PTEN, pAkt, and pS6, termed the codebook vector for that grid. To visually represent how these vectors vary over the SOM grid, each grid is divided into quadrants, and the size of the color-coded quadrant represents the intensity of the indicated stain in that grid. (**b**) Heatmap representation of the four-parameter vectors characterizing the SOM grid. To visualize the codebook vectors of the SOM grid in a different manner, each stain is depicted in an individual map where red and green represent high and low protein expression, respectively, as shown by the scale bar for each map. (**c**) SOM analysis can discriminate between two tissues (tumor bulk and margin) of different pathological state from a single tumor. After MIC analysis, the data were mapped to the SOM in (**a**). By examination of the SOM mappings, the tumor bulk occupies a larger number of grids than the margin, indicating that the MIC measurements from this sample are more heterogeneous. (**d**) Characterization of the tumor bulk-only, shared, and margin-only regions of the tumor bulk and tumor margin SOM mappings (*left*). To assess the degree of overlap between the tumor bulk and margin, grids were characterized as either margin-only, shared, or bulk-only, and (*right*) the percentage of each sample that maps to these regions was calculated. Whereas 86% of cells from the tumor margin map to the shared region of the SOM, only 45% of the tumor bulk cells mapped to this region. The tumor-only region, by contrast, contains 48% of the tumor bulk cells and only 8% of the tumor margin cells, demonstrating the distinct nature of the tumor bulk. (**e**) Characterization of tumor specimens based on signaling phenotypes. SOM mappings of several brain tumor specimens exhibited phenotypes that were either homogeneous, heterogeneous, or bimodal. For the bimodal tumor, we plotted a histogram of the single-cell PTEN expression levels to demonstrate the bimodal nature of PTEN expression in this sample.

fine-needle biopsies. Furthermore, we expected that molecular analysis of in vitro prognostic models such as multi-passage neurosphere cultures will help elucidate the significance of brain tumor stem cells in tumorigenesis. Thus, the MIC platform represents a novel technology for quantitative systems pathology to enable prospective studies integrating in vitro molecular diagnostics, systems analysis of disease, and patient stratification for personalized medicine.

4. Notes

1. For cells from tumor specimens, immediate fixing is preferable rather than culturing in order that no changes in signaling occur. However, this prevents cell spreading and the tumor cells remained morphologically spherical in the microfluidic chip.
2. We used the mTOR inhibitor rapamycin at 20 nM for 2 days. Rapamycin inhibits mTOR activity, which is in upstream of S6 in the signaling pathway. The concentration of rapamycin (or other control molecules) and incubation time need to be determined empirically.
3. We used duplicates of each cell line for two conditions (with serum or rapamycin) for the training procedure. The size of the SOM is determined empirically on the training set. We tested sizes from 4×4 to 10×10 and found that 7×7 was ideal for our application.
4. These observations demonstrate that SOM analysis of MIC measurements can (i) accurately discriminate between tumor bulk and margin and (ii) reproduce our observation that a subset of cells in the tumor bulk exhibits significantly higher mTOR activity than the margin.

Acknowledgments

This work was supported by the NanoSystems Biology Cancer Center (NSBCC), the Eli and Edythe Broad Center of Regenerative Medicine, and the Institute of Molecular Medicine at University of California, Los Angeles. H.R.T. was supported by California Institute of Regenerative Medicine. R.D. was supported by the Johnsson Comprehensive Cancer Center and the California NanoSystems Institute.

References

1. Neumann, B., Held, M., Liebel, U., Erfle, H., Rogers, P., Pepperkok, R., Ellenberg, J. (2006) High-throughput RNAi screening by time-lapse imaging of live human cells. *Nat Methods* 3, 385–390.
2. Perlman, Z. E., Slack, M. D., Feng, Y., Mitchison, T. J., Wu, L. F., Altschuler, S. J. (2004) Multidimensional drug profiling by automated microscopy. *Science* 306, 1194–1198.
3. Tanaka, M., Bateman, R., Rauh, D., Vaisberg, E., Ramachandani, S., Zhang, C., Hansen, K. C., Burlingame, A. L., Trautman, J. K., Shokat, K. M., Adams, C. L. (2005) An unbiased cell morphology-based screen for new, biologically active small molecules. *PLoS Biol* 3, e128.
4. Pelkmans, L., Fava, E., Grabner, H., Hannus, M., Habermann, B., Krausz, E., Zerial, M. (2005) *Nature* 436, 78–86.
5. Kamei, K., Ohashi, M., Gschweng, E., Suh, J., Ho, Q., Yu, Z. T. F., Tang, J., Teitell, M., Clark, A. T., Pyle, A. D., Lee, K.-B., Witte, O. N., Tseng, H.-R. (2010) Microfluidic image cytometry for quantitative single-cell profiling of human pluripotent stem cells in chemically defined conditions. *Lab on a Chip* 10, 1113–1119
6. Sun, J., Masterman-Smith, M., Graham, N. A., Jiao, J., Mottahedeh, J., Ohashi, M., DeJesus, J., Laks, D. R., Panosyan, E., Park, J., Kamei, K., Lee, K.-B. Wang, H., Yu, Z. T.-F., Lu, Y.-T., Shuang, H., Li, K., Liu, M., Zhang, N., Wang, S., Angenieux, B., Samuels, E., Williams, D., Kankatit, V., Nathanson, D., van Dam, M., Phelps, M., Liau, L., Mischel, P. S., Lazareff, J. A., Kornblum, H. I., Wu, H., Yong, W. H., Graeber, T. G., Tseng, H.-R. (2010) A microfluidic platform for systems pathology: multiparameter single-cell signaling measurements of clinical brain tumor specimens. *Cancer Res* 70, 6128–6138.
7. Wang, M. Y., Lu, K. V., Zhu, S., Dia, E. Q., Vivanco, I., Shackleford, G. M., Cavenee, W. K., Mellinghoff, I. K., Cloughesy, T. F., Sawyers, C. L., Mischel, P. S (2006) Mammalian target of rapamycin inhibition promotes response to epidermal growth factor receptor kinase inhibitors in PTEN-deficient and PTEN-intact glioblastoma cells. *Cancer Res* 66, 7864–7869.
8. Brittain, S., Paul, K., Zhao, X. M., Whitesides, G. (1998) Soft lithography and microfabrication. *Physics World* 11, 31–36.
9. Whitesides, G. M., Ostuni, E., Takayama, S., Jiang, X., Ingber, D. E. (2001) Soft lithography in biology and biochemistry. *Annu Rev Biomed Eng* 3, 335–373.
10. Wehrens, R., Buydens, L. M. C. (2007) Self- and super-organizing maps in R: the kohonen package. *J Stat Soft* 21, 1–19.

Subject Index

A

Adenovirus 6, 97–105
ALAPP, *see* Allylamine plasma polymerisation (ALAPP)
Alexa fluor 65–66, 68, 173, 175–176, 193, 197
Alkaline Phosphatase 42, 46, 122, 136
Allylamine 160, 162–163
Allylamine plasma polymerisation (ALAPP) 160–164, 166–168
Antibody 3, 6, 16, 21, 28, 32, 40–41, 56–57, 65–70, 84–85, 88, 91, 110, 114, 116–117, 119, 124, 126, 130–131, 139–149, 152, 193, 197, 200
Array
  antibody 6
  cell 53–71, 73–80, 192, 195–197
  cell-based 5, 7–8, 28, 45, 191–192, 203
  DNA 13–15, 32, 37, 58, 83, 85, 87, 90, 93, 119–120
  polymer 8
  protein 57–59, 160
  transfected-cell 53–71, 107–117, 119–136, 160
  transfection 4, 37, 75, 77
Automate 5, 8, 47, 74, 76, 84–85, 88, 92, 94, 172–173, 175, 193, 198

B

BAM, *see* Biocompatible anchor for membrane (BAM)
Biocompatible anchor for membrane (BAM) 7, 152
Biochip 129, 135, 139, 141–142, 144–145, 147–148
Biostatistics 191
Blood 6, 139–149, 152, 196
Blood cell capture 139–149
Brefeldin A 73–75, 79–80

C

Cell
  adherent 13, 15, 59, 98, 101, 105, 120, 126, 147, 151–157, 175–176
  chip 181–189
  HEK293 . . . . . 15, 182, 186–188
  HEK293T 6, 13–24, 27–40, 60, 63–64, 71
  K562 . . . . . 7, 176–179
  L929 176
  non-adherent 8, 151–157
  suspension 174, 176–177, 179
Cell-based
  array 5, 7–8, 28, 45, 191–192, 203
  assay 173–174, 177–178
Cell imaging
  fixed 59, 74
  live 59, 74
Cell immobilization 152–153
Cell microarray 16, 20–23, 70–71, 84, 107–117, 119–136, 151–152, 154, 159–169
Clone 2, 17, 28–31, 33, 35–39, 45–46, 50, 55–56, 59, 70, 120, 125, 128–129, 134, 203
CMV-AP6 . . . . . 42, 46
Confocal immunofluorescence 53
Co-transfection 13–24, 44, 108
Cross-link 8
Cytometry 191–205
Cytoplasm 70, 84, 86, 103

E

Effectene 15–17, 22–23, 32, 37, 55–56, 60, 64–65, 124, 129
Electrochemical functionalization 140–142, 144–145
Electroporation 7–8, 97, 181–189

F

Fluorescent screening microscopy 73, 76
Functional genomics 54, 97, 181, 191
Fusion protein 5, 120

G

Gelatin 15, 17, 29, 32, 37, 39, 55–56, 59–61, 63–65, 70–71, 75, 77, 111, 113, 115, 121, 124, 129, 134, 151
Gene transfer 181
GFP, *see* Green fluorescent protein (GFP)
Glioblastoma 193
Glycerol . . . 29–30, 32, 35, 51, 123–124, 128–129, 141, 192
Gold 7, 57, 66, 140–141, 144, 147, 178, 183–186, 188–190
Golgi complex 68, 73–80
Graft 140–142, 149, 160, 162–164, 167–168

E. Palmer (ed.), *Cell-Based Microarrays*, Methods in Molecular Biology 706,
DOI 10.1007/978-1-61737-970-3, © Springer Science+Business Media, LLC 2011

Green fluorescent protein (GFP) 3–5, 7, 14–15, 20–21, 23, 28–29, 35, 37–38, 45, 49, 61, 65, 70, 73, 76, 80, 102–103, 109, 111, 182–183, 185, 187
Grid 36–37, 39, 46–47, 49, 61–64, 148, 201–204

H

HHV–8 109–111
High throughput
  functional analysis 151
  microscopy 83
  screen 1, 4, 8, 28, 174
His6-tag 54–55, 59, 65–66, 69–70
HTS, *see* High throughput, screen
Human Herpesvirus–8 109

I

Immobilize 14, 54, 59, 119, 151–157
Immunofluorescence 65, 83–94, 98, 102–104, 111, 113–114
Immunofluorescence microscopy 83–94, 98, 102–104
Immunoglobulin 120, 141, 143–144

K

Kaposi's sarcoma-associated herpesvirus (KSHV) 109–110
Knock-down 103–104
KSHV, *see* Kaposi's sarcoma-associated herpesvirus (KSHV)

L

LacZ 15, 17, 21–22
Laser ablation 160, 162–164, 168
Localisation
  co– 54, 57, 60, 67, 70
  subcellular 53, 66
Luciferase 44–45, 50–51

M

Membrane-display 119–136
MGC collection 27
MIC, *see* Microfluidic image cytometry (MIC)
Microarray
  antibody 139–149
  cell 16, 20–23, 70–71, 84, 93, 107–117, 119–136, 151–152, 154, 159–169
  cell-based 1–8, 13–15, 24, 27–52, 83–94, 97–106, 125, 175–176
  DNA 13, 15, 32, 37, 58, 83, 85, 87, 90, 93, 119–120
  polymer 171–179
  protein 57–59, 160
  transfected-cell 107–117, 119–136, 160
  transfection 4, 13–24, 135, 151–157, 181–182, 188
Microfluidic image cytometry (MIC) 191–205
Microplate 13–24, 172, 175
Microtubule 67–68, 84–87, 91
Molecular diagnosis 205
Mutagenesis 45–46, 50, 123–124, 127–129
Mutant 6, 44–45, 50, 87, 120, 129, 131–133

N

Nitrocellulose 98–100, 104–105, 202
Nucleus 5, 67, 70, 75, 78–79, 121, 126, 132

O

Organelle 4, 54, 60, 66–69, 73–80, 103, 111

P

Patterned substrates 160, 164, 168
PEG
  laser ablation 162–164
  lipid 152
Peroxisome 67–68
Phosphorylation 44, 199–200, 202
Photo
  mask 183, 185, 188
  reactive 162–166
PI3K signaling pathway 191, 203
Pin 16–18, 32, 37, 39, 61–62, 78, 85, 90, 92, 160, 169
Plasma polymerisation 160, 162–164, 167
Plasmid 2, 7–8, 13–15, 17, 22–23, 28–29, 31, 33–39, 42, 46, 55, 60, 65, 70–71, 75, 108–113, 116, 120–123, 125–126, 128–130, 132–136, 151–152, 154–156, 181–189
Poly
  ethyleneimine 183
  -l-lysine 46–47, 55, 61, 87, 89–90, 98, 192, 195
  pyrrole 144, 147–148
Polymer 6–8, 14, 33, 35, 122–123, 126, 128, 135, 140, 148, 152, 159–169, 171–179, 185
Printing
  contact 61–62, 173, 175
  ink-jet 157, 159, 169
PRKG1 . . . . . 44–46, 50
Protein
  kinase 4, 44–45, 104
  localization 53–71, 108, 117

R

Reporter genes 42
Reverse transfection 13–15, 19–20, 22–24, 37, 41, 55, 58–61, 63–65, 71, 108, 111–112, 114–115, 135, 151, 153–156
Robot 32, 37, 45, 55, 58–62, 85, 87, 108, 112–113, 172, 175

S

SAM, *see* Self-assembled monolayer (SAM)
Scanning electron microscopy (SEM) . . 133, 173, 177–178
scFv, *see* Single-chain antibody (ScFv)
Self-assembled monolayer (SAM) 7, 14, 144, 184–185, 188–189
SEM, *see* Scanning electron microscopy (SEM)
short hairpin RNA (shRNA) 4–5, 97–106
shRNA, *see* short hairpin RNA (shRNA)

Single-chain antibody (scFv) 6, 28, 120–121, 127, 129
siRNA, *see* Small-interfering RNA (siRNA)
Small-interfering RNA (siRNA) 1, 4–8, 14, 63, 97–98, 108, 151, 155–156, 181–187, 189, 191
Spindle 5, 84–87
Spot 5, 7, 18, 24, 36–37, 42, 47, 49, 62–63, 71, 77–78, 85, 90, 92–93, 105, 109, 112, 115–117, 120, 130, 132, 135, 147, 156, 173–175, 177, 179, 185–186, 188
Surface-mediated transfection 14, 22
Surface plasmon resonance imaging 139–149

T

Time-lapse 5, 74, 79
Transfected-cell
  array 53–71, 109, 121
  microarray 107–117, 119–136
Transfection 2–8, 13–24, 27–28, 32, 36–39, 41–42, 44–47, 49–51, 54–56, 58–61, 63–65, 70–71, 75, 77–78, 108–109, 111–112, 114–115, 120–121, 124, 126, 129–130, 132, 134–135, 151–157, 181–182, 188–190
Tumor 192–199, 202–205

V

Vector 3, 5, 7, 15, 27–29, 31–32, 34–37, 39, 42, 44–46, 50, 54–55, 58–59, 88, 98, 108, 116, 120–122, 125–128, 136, 151, 191, 201–202, 204
Virus 6, 8, 97–110, 121, 126, 151, 182, 191

Y

Yeast 6, 29, 83–94, 121–123